Investigating the host immune response to population-tailored PPE_MPTR peptides

by
Caitlyne Young

Thesis presented in partial fulfilment of the requirements for the degree of Master of Science in Molecular Biology in the Faculty of Medicine and Health Sciences at Stellenbosch University

Supervisor: Prof. Samantha Leigh Sampson
Co-supervisor: Dr. Nastassja Kriel and Dr. Andre G. Loxton

March 2020

Declaration

By submitting this thesis electronically, I declare that the entirety of the work contained therein is my own, original work, that I am the sole author thereof (save to the extent explicitly otherwise stated), that reproduction and publication thereof by Stellenbosch University will not infringe any third party rights and that I have not previously in its entirety or in part submitted it for obtaining any qualification.

March 2020

Abstract

Tuberculosis (TB), caused by *Mycobacterium tuberculosis*, is one of the top 10 causes of death worldwide, with more than 95% of deaths occurring in low- and middle-income countries. Eradication of TB disease within these countries requires the development of more effective diagnostic tools, anti-TB drugs and vaccines. The host immune response against *M. tuberculosis* is largely governed by $CD4^+$ T-cells, making *M. tuberculosis*-specific antigens that induce strong $CD4^+$ T-cell responses of interest for vaccine studies. The induction of an effective cell-mediated immune response requires activation of $CD4^+$ T-cells following antigen presentation via MHC-II molecules. The human leukocyte antigen (HLA) alleles that encode MHC-II molecules are polymorphic, resulting in thousands of these alleles within a population. The distribution of HLA alleles differs between individuals from different geographical populations; thus, an effective vaccine candidate should include a variety of epitopes that bind numerous HLA alleles. The PPE_MPTR proteins are a sub-family of the PE/PPE proteins, which are encoded by the *pe/ppe* genes. This family occupies approximately 10% of the *M. tuberculosis* H37Rv genome, however the precise role of PE/PPE proteins in *M. tuberculosis* pathogenicity is unclear. Numerous PE/PPE proteins have shown to be highly immunogenic, however little is known regarding the immunogenicity of PPE_MPTR proteins. Previous work in our laboratory made use of a reverse vaccinology workflow which identified 35 PPE_MPTR epitopes predicted to have strong binding affinity for HLA alleles found in African populations. Nineteen epitopes from six PPE_MPTR proteins (PPE_MPTR12, -13, -28, -40, -42 and -62) showed high population coverage in four African populations.

Here we present functional assays performed to assess the immunogenicity of the nineteen epitopes in African populations. We also investigated the potential of these epitopes to distinguish between infected vs uninfected and active TB vs LTBI individuals, as determined by cytokine release assays following peptide stimulation. This was complemented by analysing the distribution of functional and activation markers following PPE_MPTR stimulation. The remaining red blood cells were lysed and the distribution of functional states of $CD4^+$ and $CD8^+$ T-cells and B-cells in peripheral blood were analysed using specific antibody staining in conjunction with flow cytometry.

PPE_MPTR peptides induced a pro-inflammatory cell-mediated response characterized by detectable concentrations of IL-6, TNF-α and IL-17A. In response to PPE_MPTR peptides, significant differences in cytokine production were observed between individuals of different disease states. The PPE_MPTR peptides were shown to induce the expansion and activation of

memory $CD4^+$ and $CD8^+$ T-cells, with $CD4^+$ T-cell populations being the predominant responding population.

The results of this study highlight the heterogeneity of the host immune response against *M. tuberculosis*. The pro-inflammatory cell-mediated immune response and the emergence of circulating memory populations in response to stimulation with selected PPE_MPTR peptides, make these promising vaccine candidates. Future work in which further immunological characterization of these peptides is performed, either alone or in combination, would greatly advance our understanding of the role PPE_MPTR proteins play in the cell-mediated immune response.

Opsomming

Tuberkulose (TB) word veroorsaak deur *Mycobacterium tuberculosis* en is een van die top tien wêreldwye oorsake van sterftes, met meer as 95% van dié sterftes in lande met ‘n lae tot middelinkomste. Die uitwissing van TB binne dié lande vereis die ontwikkeling van meer effektiewe diagnostiese hulpmiddels, anti-TB behandeling en entstowwe. Die immunrespons teen *M. tuberculosis* word grotendeels beheer deur $CD4^+$ T-sel reaksies. *M. tuberculosis*-specific antigens that induce strong $CD4^+$ T-cell responses of interest for vaccine studies. Dus is *M. tuberculosis*-spesifieke antigene wat ‘n sterk $CD4^+$ T-sel reaksie kan induseer van belang vir entstof verwante studies. ‘n Effektiewe sel-bemiddelde immuunrespons vereis die aktivering van $CD4^+$ T-selle na die oordra van antigene deur middel van MHC-II molekules. MHC-II molekules word geënkodeer deur die polimorfiese menslike leukosiet antigeen (HLA) allele en duisende van hierdie allele kom voor binne ‘n bevolking. Die HLA allele tussen bevolkings verskil, daarom moet ‘n effektiewe entstof ‘n verskeidenheid epitope insluit wat verskeie HLA allele kan bind. Die PPE_MPTR proteïne is ‘n sub-familie van die PE/PPE proteïne en word gëenkodeer deur *pe/ppe* gene. Die *pe/ppe* gene beslaan ongeveer 10% van die *M. tuberculosis* H37Rv genoom, maar die funksie van die proteïne in *M. tuberculosis* patogenisiteit is nie bekend nie. Daar is bewys dat verskeie van die PE/PPE proteïne immuun stimulerende eienskappe het, maar min is bekend oor die immunogenesiteit van PPE_MPTR proteïne. Vorige werk in ons laboratorium het 35 PPE_MPTR epitope deur ‘n omgekeerde inenting werkstroom geïdentifiseer wat voorspel wat HLA allele met hoë affiniteit bind in Afrika bevolkings. Negentien epitope van ses PPE_MPTR proteïne (PPE_MPTR12, -13, -28, -40, -42 and -62) het hoë bevolkingsdekking getoon in vier Afrika bevolkings.

In die studie het ons funksionele toetse gedoen wat die immunogenesiteit van die negentien epitope geëvalueer het in Afrika bevolkings. Ons het ook ondersoek ingestel na die potensiaal van hierdie epitope om tussen geïnfekteerde en nie- geïnfekteerde pasïente en mense met aktiewe TB of LTBI te onderskei. Dit was gedoen deur ontleding van sitokien produksie en die funksionele en aktiveringsmerkers na pepteidstimulasie te ondersoek. Die oorblywende rooi bloed selle was gelys en die verspreiding van funksionele toestande van $CD4^+$ end $CD8^+$ T-selle en B-selle in die perifêre bloed is ondersoek deur vloei sitometrie.

PPE_MPTR proteïne het ‘n pro-inflammatoriese respons veroorsaak wat gekenmerk word deur ‘n waarneembaar konsentrasies van IL-6, TNF-α en IL-17A. Na peptiedstimulasie is buduidende verskille in sitokien produksie waargeneem in mense met verkillende siektetoestande. PPE_MPTR peptiede het tot die aktivering van geheue $CD4^+$ en $CD8^+$ T-selle

gelei. Daar is gevind dat die $CD4^+$ T-selle die oorheersende T-sel bevolking was wat met PPE_MPTR peptiede reageer het.

Die uitkoms van hierdie studie bekleemtoon die heterogenesiteit van die immunrespons teen *M. tuberculosis*. Die gevolglike pro-inflammatoriese response en die produksie van geheue T-sel bevolkings na PPE_MPTR stimulasie verwys na die potensiaal van die geselekteerde peptiede as entstof kandidate. Verdere immunologiese karakterisering van peptiede, alleen of in kombinasies, sal ons begrip oor die funksie van PPE_MPTR proteïne in die sel-bemiddelde immunrespons teen *M. tuberculosis* bevorder.

Table of Contents

Acknowledgments

I would like to extend my appreciation to the following people who gave me endless guidance, love and support. I could not have completed my Master of Science degree without you.

To my supervisor, Prof. Samantha Sampson. It's such a privilege to learn from and be guided by you. One of the best decisions I have made as a young scientist was joining your research group in my honour's year. You are such an inspiration to me, not only because of your love, passion and dedication for science, but also because of the way you care for your students. Thank you for helping me develop my critical thinking skills and for all the help, support and encouragement when all seemed to be lost, it provided the much-needed motivation to persevere.

To my co-supervisor, Dr. Nastassja Kriel. I cannot thank you enough for the way in which you helped me through my MSc degree. You are truly amazing, and I am so grateful to get the opportunity to learn from you. You have taught me so many valuable techniques and have guided me to become a strong and critical young scientist. Thank you for dropping everything to help when all seemed lost and letting me walk your cat to cheer me up.

To my co-supervisor, Dr. Andre Loxton. Thank you for providing me with the immunological expertise and protocols. Thank you for welcoming me so warmly into the Stellenbosch University Immunology Research Group, and for all the words of encouragement along the way.

To Andrea Gutschmidt. It has been a privilege to get to know you, learn from you and work alongside you. Thank you for providing monoclonal antibodies, expert flow cytometric training and advice. I really appreciate the time and effort you dedicated to me during my MSc and cannot thank you enough for the encouraging messages and invaluable guidance and support.

To Candice Snyders and Ilana van Rensberg (a.k.a. Luminex Queens). Thank you for making yourselves available to give me advice regarding anything Luminex related and for running my assays in such a timely manner.

To Elizna Maasdorp and Ncitè Da Camara. Thank you for your statistical knowledge and expertise and for dedicating many hours to analysing my data.

To Mr. Ryan Singh. Thank you for helping me understand statistics! Your intelligence is something else and provided me with so much wisdom! Thank you, to you and Jazz-hands, for keeping the mood light and the vibes high.

To my work wife, Su-Mari du Plessis. I don't know how I would have made it through this without you! Thank you for all the advice, bedarfie staps and encouraging post-its! You brightened up the most stressful of days.

To my family. Thank you to my parents, Grant and Shirley Young, my sister, her husband and two sons, Bronwyn, Eugene, Caleb and Elijah Englebrecht. Thank you for the endless words of wisdom, encouragement and advice. Without the continuous love and support from all of you I would not be where I am today. Thank you for raising me to be the best version of myself I can be, and for always believing in me and my capabilities.

To Andrew Lennox McMurchie. Thank you for your infinite love, support and encouragement. You were my constant ray of sunshine! Thank you for always believing in me and encouraging me to believe in myself and my capabilities. Thank you for never allowing me to give-up and for always helping me find the positives when everything seemed lost. I love you to the moon and back, and could not have done this without you by my side.

I would like to thank the Centre of Excellence for Biomedical Tuberculosis Research (CBTBR) and the National Research Foundation (NRF) for the financial support, without which, I would not have been able to complete my MSc.

I would like to thank the Harry Crossley Foundation and the NRF for providing me with project funding.

List of Abbreviations

°C	Degrees Celcius
µg	Microgram
µl	Microliter
AM	Alveolar macrophage
APC	Antigen presenting cell
APC	Allophycocyanin
AraLAM	Non–mannose-capped lipoarabinomannan
BAL	Bronchoalveolar lavage
BB700	Brilliant™ Blue 700
BCG	Bacillus Calmette-Guérin
BD	Becton-Dickinson
BMDM	Bone marrow derived macrophages
BV421	Brillian Violet™ 421
CD	Cluster of differentiation
CFP-10	Culture Filtrate Protein 10
CFU	Colony forming units
CO_2	Carbon dioxide
COX2	Cyclooxygenase 2
CR	Complememt receptor
CXCL11	C-X-C motif chemokine 11
CXCR3	C-X-C chemokine receptor 3
DC	Dendritic cell
DC-SIGN	Dendritic cell-specific intercellular adhesion molecule-3 grabbing nonintegrin
DMSO	Dimethyl sulfoxide
DNA	Deoxyribonucleic acid
DTH	Delayed-type hypersensitivity
EDTA	Ethylenediaminetetraacetic acid
EEA1	Early endosomal autoantigen-1
ELISA	Enzyme Linked immunosorbent assay
Erk	Extracellular signal-regulated kinase
ESAT-6	Early Secreted Antigen 6
ESX	ESAT-6 secretion system
FACS	Fluorescence-activated cell sorting
FBS	Fetal Bovine Serum
FDR	False Discovery Rate
FITC	Fluorescein isothiocyanate
FMO	Fluorescent Minus One
FSC	Forward Scatter
γδ T-cells	Gamma epsilon T-cells
GC	Guanine-Cytosine
GLA-SE	Glucopyranosyl lipid adjuvant-stable emulsion
GPI	Glycosylphosphatidylinositol

HC	Healthy control
HIV	Human Immunodeficiency Virus
HLA	Human Leukocyte Antigen
HMDM	Human Monocyte Derived Macrophage
HPLC/MS	High-performance liquid chromatography/Mass Spectrometry
IFN-γ	Interferon Gamma
IGRA	Interferon gamma release assay
IL	Interleukin
IL-12Rβ2	IL-12 recepter beta 2
IRAK	Interleukin-1 receptor-associated kinase 1
IRF	Interferon regultory factor?
Jnk	c-Jun N-terminal kinase
kDa	Kilodalton
LAM	Lipoarabinomannan
LAMP	Lysosomal associated membrane protein
LBPA	Lysobisphosphatidic acid
LPS	Lipopolysaccharide
LRR	Leucine rich repeats
LTBI	Latent tuberculosis infection
M. bovis	*Mycobacterium bovis*
mAb	Monoclonal antibody
ManLAM	Mannosylated Lipoarabinomannan
MAPK	Mitogen-activated protein kinase
MFI	Median Fluorescent Intensity
MHC	Major Histocompatibility Complex
ml	Mililitre
mM	Milimolar
MPTR	Major polymorphic tandem repeat
MR	Mannose receptor
mRNA	Messenger ribonucleic acid
n	Number
NF-κβ	Nuclear Factor kappa-light-chain-enhancer of activated B cells
NK cell	Natural Killer cell
OADC	Oleic Albumin Dextrose Catalase
OOR	Out-Of-Range
p.i	Post-infection
p19	19kDa lipoprotein
PAMP	Pathogen Associated Molecular Pattern
PBS	Phosphate buffered saline
PE	Phycoerythrin
PE-Cy7	Phycoerythrin-Cyanine 7
PE-PGRS	Proline-glutamic acid polymorphic guanine-cytosine-rich sequence
pg	Picagram
PHA	Phaseolus vulgaris phytohaemagglutinin

PI3K	Phosphatidylinositol-3-kinase
PI3P	Phosphatidylinositol-3-phosphate
PILAM	Phosphoinositol-capped LAM
PIM	Phosphatidylinositol mannoside
PknG	Protein Kinase G
PLA2R	M-type phospholipase A2 receptor
PPARγ	Peroxisome proliferator activated receptor gamma
PPD	Purified Protein Derivative
PPE	Proline-Proline-Glutamate
PRR	Pathogen recognition receptor
QFN	QuantiFERON®
QQ	Quantile-Quantile
rBCG	Recombinant BCG vaccine with Ag85A and ESAT-6
rcf	Reletive centrifugal force
RD1	Region of Difference 1
ROI	Reactive Oxygen Species
RORγt	Retinoic acid-related orphan receptor gamma t
RT	Room temperature
SOCS	Suppressor of cytokine signalling
SSC	Side Scatter
STAT	Signal transducer and activator of transcription
TB	Tuberculosis
Th	T-helper
TIR	Toll-IL-1 receptor
TLR	Toll like receptor
TNF-α	Tumour necrosis factor alpha
TRIF	TIR domain-containing adaptor inducing IFN-β
WBA	Whole Blood Assay
WHO	World Health Organisation

List of Tables

List of Figures

Chapter 1

Introduction

1.1 Background

1.1.1 The immune response to tuberculosis

Tuberculosis (TB), caused by *Mycobacterium tuberculosis* remains one of the world's greatest health problems to date, especially in low- and middle-income countries such as South Africa (WHO, 2018). The host immune response to TB infection is extremely complex and is not yet fully understood. The innate immune response to *M. tuberculosis* is largely governed by alveolar macrophages that trigger numerous signalling cascades after phagocytosing *M. tuberculosis*. These signalling cascades initiate an inflammatory response from the host and the adaptive immune response is initiated.

A critical link between the innate and adaptive immune response to *M. tuberculosis* is antigen presentation to $CD4^+$ T-cells via major histocompatibility complex (MHC) class II molecules on antigen presenting cells (APCs) such as macrophages. Following phagocytosis of *M. tuberculosis*, *M. tuberculosis* proteins get degraded into peptides which are then presented to $CD4^+$ T-cells by MHC-II molecules. MHC molecules, encoded by human leukocyte antigen (HLA) genes, and $CD4^+$ T-cells have indispensable roles during TB infection. As such, mice deficient for $CD4^+$ T-cells and MHC-II molecules were shown to be more susceptible to *M. tuberculosis* infection compared to wild type mice (Ladel *et al.*, 1995; Caruso *et al.*, 1999). The crucial role of $CD4^+$ T-cells was exemplified by the increased susceptibility of *M. tuberculosis* infection in HIV-positive individuals who are known to have an extremely reduced $CD4^+$ T-cell count (Hazenberg *et al.*, 2000; Geldmacher *et al.*, 2012). Adaptive immunity to TB infection is primarily mediated by $CD4^+$ T-lymphocytes ($CD4^+$ T-cells), although important roles for B-cells (Maglione and Chan, 2009; Kozakiewics *et al.*, 2013) and $CD8^+$ T-cells (Joosten *et al.*, 2010; Rozot *et al.*, 2013) have also been indicated. MHC-I molecules recognise peptides derived from intracellular proteins and present these to $CD8^+$ T-cells. MHC distribution within a population is heterogenous as there are thousands of HLA alleles present in a population, however an individual only carries a limited number in their genome (Tshabalala *et al.*, 2015). Therefore, an effective vaccine candidate will thus include

promiscuous epitopes that can bind to a wide range of HLA alleles (Longmate *et al*., 2001; Tshabalala *et al*., 2015).

In healthy individuals, *M. tuberculosis* infection may be eradicated by the co-ordinated action of innate and adaptive immunity. However in many cases the infection is merely contained within a granulomatous structure within the lungs (Pagan *et al.*, 2015)**.** Containment of *M. tuberculosis* within the granuloma requires constant immune regulation and therefore can fail in some individuals such as HIV-positive patients or those with diabetes or malnutrition (Diedrich *et al.*, 2016). When the immune system fails to contain the infection, *M. tuberculosis* may escape the restricted environment of the granuloma resulting in active TB disease (Pagán *et al.*, 2015).

1.1.2 Tuberculosis and the desperate need for new vaccines and diagnostic tools

In 2017, The World Health Organisation estimated ten million people worldwide to have developed active TB disease, with an estimated 1.6 million people dying as a result of the illness (WHO, 2018). The severity of the disease differs widely among countries, with fewer than 10 new cases per 100 000 people in most high-income countries to 150-500 new cases per 100 000 people in high TB burden countries. Worldwide, South Africa is ranked among the 30 high TB burden countries, along with other African countries including, Ethiopia, Congo and Zimbabwe, to name a few (WHO, 2018).

The only available vaccine for protection against TB is the Bacillus Calmette-Guérin (BCG) vaccine. The BCG vaccine was developed in 1931 and is a live attenuated vaccine derived from a closely related mycobacterial species, *Mycobacterium bovis.* BCG is administered to infants and has been shown to be effective in preventing TB disease in children, which presents as pulmonary TB or TB meningitis (Abubakar *et al.*, 2013; WHO, 2018). BCG has been shown to have varying levels of efficacy in the adult population, ranging from 0% to 80% (Rodrigues *et al.*, 1993; Colditz *et al.*, 1994; Fine, 1995; Trunz *et al.*, 2006; Abubakar *et al.*, 2013). The protective capability of BCG been shown to last no longer than 10 years, thus rendering the adolescent and adult population unprotected against TB infection (Sterne *et al.*, 1998; Ozeki *et al.*, 2011). The failure of BCG to prevent TB disease and the use of sub-optimal antibiotic treatment regimens to treat TB disease has increased the emergence of drug-resistant TB strains, thus further emphasizing the need for the development of more effective TB vaccines and improved treatment regimens.

Currently there are eleven new TB vaccine candidates in clinical trials; five in Phase I and six in Phase II (**Table 1.1**) (WHO, 2018). These vaccines include prophylactic vaccines, such as BCG, which aim to prevent the development of TB infection and disease. Other approaches to vaccine development include, post-exposure vaccines that help prevent reactivation or relapse of TB disease and therapeutic vaccines that can be used as an adjunct to existing TB drug regimens to improve the outcome of TB treatment (Loxton *et al.*, 2015). Vaccines can be broadly characterised into two different groups, live attenuated vaccines and subunit vaccines. Live attenuated vaccines are usually developed from an organism closely related to the disease-causing agent, which is less virulent and unable to cause disease but still capable of providing protective immunity. Subunit vaccines consist of selected antigens delivered by an adjuvant or a viral vector while other vaccines can be comprised entirely of mycobacterial lysate (Loxton *et al.*, 2015).

Two of the vaccine candidates in Table 1.1 contain antigens from the PE/PPE protein family. PPE_MPTR42 has been included in the ID93 vaccine candidate (Bertholet *et al.*, 2010) and PPE18 in the M72A vaccine candidate (Day *et al.*, 2013). These proteins are not the only members of the PE/PPE protein family shown to have immunomodulatory effects, as several PE/PPE proteins have been shown to elicit an immune response and could be potential candidates for *M. tuberculosis* vaccine development (Vordermeier *et al.*, 2012). These include PPE37 (Daim *et al.*, 2011), PPE57 (Xu *et al.*, 2015), PPE26 (Su *et al.*, 2015), PE13 (Li *et al.*, 2016) and heterodimers PE32/PPE65 (Khubaib *et al.*, 2016) and PE35/PPE68 (Tiwari *et al.*, 2014) . The effect of these, and other *M. tuberculosis* proteins, on the innate and adaptive immune systems will be discussed in Chapter 2.

Table 1.1: TB Vaccine candidates currently in clinical trails

Vaccine type	**Vaccine name**	**Phase**	**Description**	**Reference**
Live attenuated	MTBVAC	I	Two independent mutations for *phoP* (transcription factor coding for regulation of *M. tb* virulence) and *fadD26* (essential for synthesis of virulence factor phthiocerol dimycocerosates (DIM; surface lipid))	(Arbues *et al.*, 2013) (Spertini *et al.*, 2015)
	Recombinant BCG30 (rBCG30)	I	*M. bovis* BCG overexpressing *fnpB* (Ag85B), *esxA* (ESAT-6 virulence factor) and *ppe42*	(Lu *et al.*, 2012)
	VPM1002 (Δ*ureC hly*$^{+}$ BCG*)*	IIa	*M. bovis* BCG overexpressing the gene for listeriolysin (*hly) Listeria monocytogenes* *M. bovis* urease-C (*ureC)* gene deleted	(Grode *et al.*, 2005)
Adjuvanted subunit	ID93/GLA-SE	I	Recombinant fusion protein of Rv2608 (PPE42), Rv3619 (EsxV), Rv3620 (EsxW), Rv1813 (latency associated protein) adjuvanted to GLA-SE	(Bertholet *et al.*, 2010)
	Hybrid 1 (H1)-IC31 H1-CAF01	I I	Recombinant fusion protein of Ag85B & ESAT-6 adjuvanted with IC31 or CAF01	(van Dissel *et al.*, 2010, 2014)
	M72A/AS01	II	Fusion protein MTB32A (serine protease PepA) & MTB39A (PPE18) adjuvanted to AS01	(Day *et al.*, 2013)
Viral vector subunit	MVA85A	II	Modified vaccinia virus expressing *M. tb* Ag85A	(Beveridge *et al.*, 2007)
	Aeras402/ Crucell Ad35	II	Recombinant replication-deficient adenovirus expressing *M. tb* antigens TB10.4, Ag85A and Ag85B	(Abel *et al.*, 2010)
Therapeutic	RUTI	II	Detoxified fragments *M.tb* cells delivered in liposomes	(Cardona, 2006)
	M. vaccae	II	Triple-killed *Mycobacterium vaccae*	(Mayo *et al.,* 2000)

1.1.3 The PE/PPE protein family

An important knowledge gap in mycobacterial research is our incomplete understanding of the PE/PPE proteins. These PE/PPE proteins are encoded by a large multi-gene family known as the *pe/ppe* genes, which make-up approximately 10% of the coding capacity of the *M. tuberculosis* H37Rv genome (Cole *et al.*, 1998). The 99 *pe* and 69 *ppe* genes are characterised by encoded conserved N-terminal proline-glutamate (PE) and proline-proline-glutamate (PPE) motifs, respectively (**Figure 1.1**). The N-terminal sequence is relatively conserved between the two groups and consists of approximately 110 and 180 amino acids in the PE and PPE families, respectively (Cole *et al*., 1998). The corresponding PE/PPE proteins are further classified into subfamilies according to the amino acid characteristics of their C-terminal domain, which are highly polymorphic and vary in size and composition. A subset of the proteins belonging to the PE family contain multiple copies of polymorphic GC-rich repetitive sequences and are thus referred to as PE_PGRS proteins. Similarly, a subset of PPE family proteins are rich in repeats that contain an Asn-X-Gly-X-Gly-Asn-X-Gly $(NXGXGNXG)_n$ signature and are referred to as major polymorphic tandem repeat proteins (PPE_MPTR) (Cole *et al*., 1998).

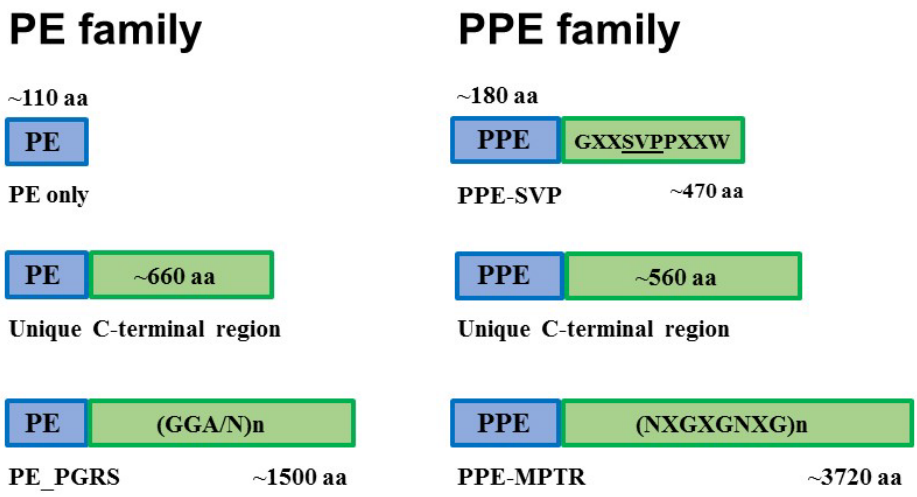

Figure 1.1: The PE/PPE Protein family. The N-terminal, or PE/PPE region is highly conserved between families with approximately 110 and 180 amino acids, respectively. The C-terminal is highly polymorphic, varying in size and composition and based on these characteristics the PE/PPE proteins can be divided into subfamilies. The subfamilies known as the polymorphic GC-rich sequence (PGRS) and major polymorphic tandem repeat (MPTR) represent some of the most variable regions in the *M. tuberculosis* genome. (*Image adapted from* Sampson, 2011).

PE_PGRS and PPE_MPTR proteins are restricted to pathogenic mycobacteria (Gey van Pittius *et al*., 2006) and due to their abundance in the genome of *M. tuberculosis*, it is speculated that they contribute to pathogenesis during TB infection. Large knowledge gaps exist regarding the function of PE and PPE proteins; however, they have been shown to be highly immunogenic (Sampson, 2011; Sayes *et al.*, 2012; Vordermeier *et al.*, 2012; Brennan, 2017). Microarray data demonstrated that 128/169 tested *pe/ppe* genes are differentially expressed during TB disease (Voskuil *et al*., 2004). These results were supported by the transcriptional profiles of *M. tuberculosis* isolated from pulmonary tissue, which demonstrated the upregulation of selected *pe/ppe* genes at the site of infection (Rachman *et al.*, 2006). The presence of these proteins at the site of infection, along with evidence showing the secretion of some PE/PPE proteins (Ates *et al.*, 2016), suggests that they could be involved in host-pathogen interactions that modulate the immune system. If this is so, they could show promise in vaccine development.

The PE_PGRS proteins have been more widely studied than the analogous PPE_MPTRs. PE_PGRS62 and PE_PGRS30 have been shown to be required for replication inside the macrophage and persistence in granulomas in *Mycobacterium marinum* (Ramakrishnan *et al.*, 2000). Localisation studies have suggested that PE_PGRS33 is located on the cell wall of *M. bovis* BCG and the non-virulent, *M. tuberculosis* H37Ra (Brennan *et al*., 2001), allowing PE_PGRS33 to easily interact with the host. Research supports host-pathogen interactions facilitated by PE_PGRS33. Expression of PE_PGRS33 in *Mycobacterium smegmatis* suggested PE_PGRS33 to play a role in macrophage necrosis and stimulate the secretion of tumour necrosis factor (TNF)-alpha (α) (Dheenadhayalan, *et al*, 2006) through interactions with toll-like receptor (TLR)-2 (Basu *et al*., 2007). In another study investigating the expression of a recombinant *M. bovis* PE_PGRS62 protein in *M. smegmatis*, it was suggested that PE_PGRS62 reduces phagolysosome formation and stimulates the production of IL-1β (Huang *et al*., 2012). Furthermore, certain PE_PGRS proteins have been deemed essential for the full virulence of *M. tuberculosis* during TB infection (Iantomasi *et al*., 2012).

1.1.4 PPE_MPTR proteins

Akin to PE_PGRS proteins, PPE_MPTR proteins are highly variable and are prone to recombination events and mutations (Cole *et al*., 1998). PPE_MPTR proteins are also speculated to be a source of antigenic variation, however there is no experimental evidence for this hypothesis. Like PE_PGRS proteins, some members of the PPE_MPTR family have been

shown to localise at the cell wall (Sampson *et al*., 2001), which suggests that they may also interact with the host, however, little is known about PPE_MPTR-host interactions.

There is evidence to suggest PPE_MPTR proteins can elicit immune responses (Choudhary *et al.*, 2003; Chakhaiyar *et al.*, 2004; Bertholet *et al.*, 2008). Consequently, certain members of the PPE_MPTR family have been suggested to be viable candidates for TB vaccine development. For example, PPE_MPTR42 has been implicated in eliciting T-cell responses in TB positive patients (Chakhaiyar *et al*., 2004; Bertholet *et al*., 2008) and inducing high humoral responses in patients re-infected with TB (Chakhaiyar *et al*., 2004). PPE_MPTR42 has also been included in the ID93 vaccine candidate along with Rv1813 and Rv3620 (**Table 1.1**) (Baldwin *et al.*, 2009; Bertholet *et al.*, 2010). Of the three antigens included in the ID93 vaccine candidate, only PPE_MPTR42 demonstrated protective efficacy by reducing lung CFU in mice challenged with *M. tuberculosis* and immunized with PPE_MPTR42-CpG. PPE_MPTR42 was also shown to be the most immunogenic, by being the only antigen to induce IFN-γ and TNF-α production (Bertholet *et al.*, 2008). Furthermore, when PPE_MPTR42 was included in a recombinant BCG vaccine (rBCG) as a fusion protein with antigen 85B (Ag85B) and ESAT-6 (**Table 1.1**), the cell-mediated immune response elicited to rBCG was much stronger than that to BCG alone (Lu *et al*., 2012).

Members of the PPE_MPTR protein family are clearly involved in the host-immune response to *M. tuberculosis* and show potential in the vaccine development pipeline. There are many unanswered questions regarding the PPE_MPTR-mediated immune response and the cellular populations responsible for governing this response. This includes the cytokine and chemokine profiles elicited by stimulation with these proteins and identifying which immune cell populations are responsible for producing these molecules. More research needs to be conducted to understand the role and pathophysiological effects of the PPE_MPTR protein family during *M. tuberculosis* disease, and to realise their full potential, in immunodiagnostic and vaccine development.

1.2 Problem Statement

As outlined above, TB remains a serious health problem. Eradication of TB disease desperately requires the development of more effective anti-tuberculosis (anti-TB) drugs, diagnostic tools and vaccines. The *M. tuberculosis*-specific T-cell response is dominated by $CD4^+$ T-cells (Orme *et al.,* 1993) and thus many of the current approaches to developing new vaccines and immune-based diagnostic tools focus on *M. tuberculosis* antigens that elicit T-cell responses.

Antigen-specific T-cells stimulate an immune response by recognising bacterial peptides (antigens) presented on human leukocyte antigen (HLA) molecules. The genes encoding HLA molecules are highly polymorphic and therefore thousands of HLA, and related alleles, can be found in a population. Each individual only encodes a certain number of these alleles, therefore a good vaccine candidate should include a range of epitopes that are able to bind to a wide range of HLA alleles, providing sufficient population coverage (Robinson *et al.*, 2015). Furthermore, there are certain HLA alleles that are differentially prevalent in groups of different ancestry, suggesting that different populations will respond differently to the same peptide due to variability in their HLA alleles (Longmate *et al.*, 2001).

Currently, the live attenuated *Mycobacterium bovis* Bacillus Calmette-Guerin (BCG) vaccine is used for immunisation against *M. tuberculosis.* The protective immunity elicited by *M. bovis* BCG has varying levels of efficacy, which have been attributed to strain variation between *M. bovis* BCG preparations, the genetic and nutritional differences between populations and various environmental influences such as the exposure to non-tuberculosis mycobacteria (Fine, 1995; Valadas, 2004). In addition to vaccination, the prompt and accurate diagnosis of TB disease could potentially aid in reducing *M. tuberculosis* transmission by enabling those who are infected to get effectively treated in the shortest time period.

Previous work in our laboratory has made use of a reverse vaccinology workflow which identified thirty-five PPE_MPTR epitopes that are tailored to HLA alleles common in African populations (Colic, Manuscript in Progress). Nineteen epitopes from six PPE_MPTR proteins (PPE_MPTR12, -13, -28, -40, -42 and -62) showed high population coverage across four different African populations, however functional studies need to be performed to confirm the potential of these peptides as possible vaccine candidates. In this study, we investigate the immune response to these computationally identified PPE_MPTR epitopes predicted to provide high population coverage in black South African, Zimbabwean, Ethiopian and Congolese populations.

1.3 Hypothesis

The PPE_MPTR epitopes in this study will elicit an immune response in an African cohort, as predicted by the reverse vaccinology approach (Colic, Manuscript in Progress).

1.4 Aim and Objectives

Aim:

To characterise the immune responses elicited by population-tailored PPE_MPTR epitopes in an African cohort.

Objectives:

I. Assess the immunogenicity of selected population-tailored PPE_MPTR peptides by measuring the resultant cytokine response in stimulated whole blood using cytokine release assays.
II. Determine the diagnostic potential of population-tailored PPE_MPTR epitopes by comparing T-cell responses elicited in individuals with active and latent *Mycobacterium tuberculosis* infection.
III. Investigate the PPE_MPTR-specific functional marker frequencies of lymphocyte populations in the whole blood of TB, LTBI and healthy individuals.

1.5 Thesis Overview

Chapter 2 **Literature review: "*Mycobacterium tuberculosis* interacts with and manipulates the host immune response."**

This review chapter provides an overview of current knowledge of the mechanisms *M. tuberculosis* uses to disrupt the host's immunoregulatory pathways.

Contribution: Developed outline, surveyed and synthesised literature, wrote and edited all drafts with input from supervisors.

Chapter 3 **Methods and Materials**

This chapter outlines the methodologies used to fulfil the above-mentioned objectives.

Contribution: Wrote and edited all drafts with input from supervisors.

Chapter 4 **Results**

This chapter presents the results of evaluation of the immunogenic potential of computationally identified population-tailored PPE_MPTR epitopes in an African cohort. The diagnostic potential of these epitopes is also evaluated. The immunophenotype/s of immune cells governing the PPE_MPTR-mediated cellular response is explored.

Contribution: Contributed to experimental design, participant recruitment, whole blood stimulation assays, antibody panel design and staining, flow cytometry, data analysis, interpretation and presentation. Wrote and edited all drafts with input from supervisors.

Chapter 5 Discussion

This chapter uses the results from Chapter 4 to gain a better understanding about the immunogenicity of PPE_MPTR proteins during TB disease. The potential of the computationally identified PPE_MPTR epitopes to elicit a population-tailored immune response is discussed, and their potential in TB diagnostics is evaluated.

Contribution: Interpretation and contextualisation of results. Wrote and edited all drafts with input from supervisors.

Chapter 6 Reference List

Chapter 7 Appendices

This chapter contains the Ethics Approval Letter and an example of the Signed Informed Consent Form used during recruitment. The activation states of $CD4^+$ and $CD8^+$ T-cells identified using flow cytometry are also represented here.

Chapter 2

Mycobacterium tuberculosis interacts with and manipulates the host immune response

2.1 Introduction

Each year, infection with *Mycobacterium tuberculosis* claims the lives of millions of people worldwide (WHO, 2018).The *M. tuberculosis* infection burden is further increased by the high prevalence of drug-resistant *M. tuberculosis*, where approximately 558 000 new multidrug resistant tuberculosis (TB) cases were reported in 2018 (WHO, 2018). Approximately one quarter of the global population is infected with TB, but show no signs or symptoms of the disease, a state of infection referred to as latent TB infection (LTBI) (WHO, 2018). People living with LTBI have a 5-15% chance of developing active disease within their lifetime (WHO, 2018). However, people who are immunocompromised, such as those co-infected with HIV, who have diabetes or are malnourished, have a higher risk of progressing from LTBI to active TB disease (WHO, 2018).

During TB infection, *M. tuberculosis* interacts with the hosts innate immune cells, such as alveolar macrophages (AMs), which express pathogen recognition receptors (PRRs). These proteins interact with pathogen-associated molecular patterns (PAMPs) and initiate a signalling cascade that determines the type of immune response elicited (Rajaram *et al.*, 2014). PAMPs are molecules shared by various pathogens and may include bacterial endotoxin lipopolysaccharide (LPS), terminal mannose residues, unmethylated GC-rich oligonucleotides and proteins such as the PE/PPE proteins, among others (Abbas *et al.,* 2001). Recognition of PAMPs by a specific repertoire of PRRs will stimulate the host innate immune response to release pro-inflammatory cytokines, such as tumour necrosis factor-alpha (TNF-α), interferon-gamma (IFN-γ) and interleukin-6 (IL-6) (Domingo-Gonzalez *et al.*, 2016). These cytokines recruit other immune cells to the site of infection and facilitate the presentation of pathogen-specific antigens to T- and B-lymphocytes (T- and B-cells), triggering the adaptive immune response.

The innate immune system clears most infections but can fail to do so when bacterial numbers are high, or if the pathogen is extremely virulent. In such cases, the adaptive immune response activates lymphocytes that target pathogen-specific moieties that amplify the innate immune

responses in the form of phagocytosis and killing of pathogens by innate immune cells. The adaptive immune response is dependent on antigen presentation to appropriate Major Histocompatibility Complex (MHC) molecules, dendritic cell migration to the draining lymph node and the activation of resting (naïve) T-cells (Wolf *et al*., 2008). The MHC class II molecules are encoded by the human leukocyte antigen (HLA) gene complex, consisting of ten variants which are uniquely expressed in different populations around the world.

TB disease encompasses complex interactions between *M. tuberculosis* and the host, many of which we do not fully understand. This is further complicated by the heterogenous nature of *M. tuberculosis* infections. There is an immense number of *M. tuberculosis* proteins that influence the progression and outcome of TB disease, and more insight into the function of understudied protein families, such as the PE/PPEs, can aid in gaining a more complete understanding of TB disease. The PE/PPE proteins are speculated to interact with both the innate and adaptive immune systems, however their precise role/s have not yet been defined. These knowledge gaps make it difficult to develop more effective anti-tuberculosis drugs, diagnostic tools and vaccines.

2.2 The Innate Immune response to *Mycobacterium tuberculosis* infection

The innate immune cells are typically the first cell types encountered by *M. tuberculosis* following inhalation and include AMs, neutrophils, natural killer (NK) and dendritic cells (DCs) (Basset *et al.*, 2003; Gantner *et al.*, 2003; Sia *et al.*, 2015). Once inhaled, *M. tuberculosis* bacilli are phagocytosed by AMs and can exploit mechanisms to prevent phagosome maturation by inhibiting the fusion between the phagosome and an active lysosome (Armstrong *et al.*, 1971; Indrigo *et al.*, 2003; Vergne *et al.*, 2003; MacGurn *et al.,* 2007; Sun *et al.*, 2010; Sullivan *et al.*, 2012; Schnettger *et al.*, 2017). Mycobacterial phagosomes typically lack lysosomal associated membrane proteins (LAMPs) and mature lysosomal hydrolases, creating a favourable niche for the bacilli to reside in.

M. tuberculosis-presented PAMPs interacting with PRRs present of the surface of AMs initiate specific signalling cascades, which activate the innate immune response. Some phagocytic cells have the same PRRs, however many of these cells express unique receptors which are dependent on the antigens which bind these receptors (Murphy, 2012). In parallel, a pro-inflammatory response is triggered, which involves the recruitment of mononuclear cells from the blood to infected macrophages, initiating the establishment of the granuloma. The infected

macrophages become surrounded by an assortment of immune cells resulting in the formation of a fibrous cuff which consists of fibroblasts and a surrounding layer of T-lymphocytes and foamy macrophages. The constant recruitment of new immune cells to the granuloma, results in the activation of the adaptive immune response. When the immune status changes or in the case of immunocompromised individuals, more foamy macrophages are recruited to the granulomatous structure, the centre undergoes necrosis and becomes hypoxic. Once the hypoxic centre bursts *M. tuberculosis* bacilli are released into the lungs, activating the immune response and recruiting antigen-presenting cells (APCs) to the lung in an attempt to control dissemination (Amaral *et al.,* 2016; Scriba *et al.*, 2016).

2.2.1 *Mycobacterium tuberculosis* interacts with the alveolar macrophage

Surfactant coated AMs are located beneath a monolayer of pulmonary surfactant along with surfactant-associated proteins-A to -D (SP-A to -D). SP-A and SP-D interact with different *M. tuberculosis*-specific PAMPs, with each PRR-PAMP interaction resulting in a different immune response (Gaynor *et al.*, 1995; Pasula *et al.*, 1997; Ferguson *et al.*, 1999, 2006). For example, when SP-A interacts with a 60 kDa cell-surface associated glycoprotein of *M. tuberculosis*, AM-mediated phagocytosis of *M. tuberculosis* is enhanced (Gaynor *et al.,* 1995; Pasula *et al*., 1997). Simultaneously, SP-D diminishes these interactions when bound to *M. tuberculosis* mannosylated lipoarabinomannan (ManLAM) (Ferguson *et al.*, 1999)

Even though AMs function to defend the host against *M. tuberculosis* dissemination, *M. tuberculosis* manipulates the intracellular environment of AMs to provide a favourable niche for replication (Malik *et al.*, 2000; Rohde *et al.,* 2007; Via *et al*., 1997). The exact mechanism employed by *M. tuberculosis* to interfere with phagolysosome maturation remains unclear, however, *M. tuberculosis* is thought to secrete several proteins which prevent phagosome-lysosome fusion. One such protein is PknG, one of the 11 protein kinases encoded by *M. tuberculosis*. *PknG* is dispensable for *M. bovis* BCG growth in 7H9-OADC media, however is required for intracellular growth (Walburger *et al.*, 2004). Further, only *M. bovis-pknG* deletion mutants were seen to localise to lysosomal organelles within macrophages (Walburger *et al.*, 2004).

There are many classes of PRRs that *M. tuberculosis* interacts with on the surface of the AM, with each receptor playing a different role in the recognition and uptake of *M. tuberculosis*-specific glycolipids, carbohydrates, glycoproteins and DNA motifs. The mannose receptor

(MR), dectin-1, toll-like receptors (TLRs) and complement receptor 3 (CR3) are the three main macrophage receptors that mediate *M. tuberculosis* entry into the AM and facilitate the downstream signalling events in response to infection (Rajaram *et al.*, 2014). The following section will focus on the effect *M. tuberculosis*-specific ligands have on the host immune response following interactions with the MR and members of the TLR family. The MR is one of the main classes of PRRs on the AM. Some members of the PE/PPE protein family have been shown to interact with some members of the TLR family on the AM, however their interaction with dectin-1, MR and CR3 require more investigation.

2.2.1.1 The Mannose Receptor (CD206)

The mannose receptor (MR) is a 175 kDa transmembrane glycoprotein (Wileman *et al.*, 1986) with eight carbohydrate recognition domains located on the surface of macrophages. The MR is one of the main PRRs facilitating entry of *M. tuberculosis* into the AM (Tailleux *et al.*, 2003) and can also be referred to as 'cluster of differentiation 206' (CD206) (East *et al.*, 2002). The MR is not only cell-surface localised, but can also be found within the MHC-II loading compartment of the macrophage, where it enhances MHC-II antigen presentation and the recruitment of $CD4^+$ T-cells (Koning, 1997; Prigozy *et al.*, 1997). Similar to mannose binding lectin, the MR also engages mannose containing *M. tuberculosis*-specific ligands such as lipoarabinomannan (LAM) and its derivatives ManLAM (Reiling *et al*., 2001). Lipomannans and LAMs are multi-glycosylated forms of biosynthetic precursor phosphatidylinositol mannoside (PIM), located on the cell wall of *M. tuberculosis* (Khoo *et al.,* 1995).

Human monocyte-derived macrophages (HMDMs) stimulated with *M. tuberculosis* H37Rv and ManLAM derived from *M. tuberculosis* H37Rv displayed enhanced expression of macrophage peroxisome proliferator activated receptor gamma (PPARγ) (Rajaram *et al.*, 2010). This was dependent on the activation of MAPK-p38 mediated by *M. tuberculosis* or ManLAM binding to MR. In contrast, stimulation with *M. bovis* BCG also resulted in the production of IL-8, however lower expression levels of PPARγ were observed. This was explained by NFκB-induced production of IL-8 due to *M. bovis* BCG, rather than via MAPK-p38 as seen with *M. tuberculosis* H37Rv or ManLAM (Rajaram *et al.*, 2010). PPARγ is required for intracellular growth and to induce the production of IL-8 and cyclooxygenase 2 (COX2) (Rajaram *et al.*, 2010), which are involved in downregulating inflammatory responses by the recruitment of neutrophils and lymphocytes that mediate granuloma formation (Ameixa and Friedland, 2001; Meyer *et al.*, 2003).

M. tuberculosis ManLAM-MR-mediated entry into the AM also prevents phagosome maturation and interferes with phagosome-lysosome fusion (Kang *et al*., 2005). During phagosomal maturation, there is progressive loss-and-gain of cellular markers that identify the endosome as 'early' or 'late'. Proteins involved in this process include those from the rab-family of GTPases and LAMP proteins (Desjardins *et al.,* 1994), as well as lipids such as, lysobisphosphatidic acid (LBPA) (Kobayashi *et al.*, 1998). Following phagocytosis of *M. tuberculosis* via MR, the phagosome interacts with early endosomes and acquires the expression of Rab-5 on its surface. The presence of *M. tuberculosis* ManLAM interferes with Ca^{2+} levels, which prevents the recruitment of the Rab-5 effector proteins, early endosomal autoantigen-1 (EEA1) and phosphatidylinositol-3-kinase (PI3K), hVPS34 (Malik, *et al.,* 2000; Malik *et al.*, 2003).

The activation product of hVPS34, phosphatidylinositol-3-phosphate (PI3P), is required to retain EEA1 to the early endosomal membrane. Without EEA1, the switch between Rab-5 and Rab-7, a late endosomal marker, is prevented, thus preventing the delivery of vacuolar ATPase (V-ATPase), lysosomal hydrolases and cathepsins from the trans-golgi network to the endosome (Via *et al.*, 1997). As a result, the intraluminal pH of the endosome does not decrease, and *M. tuberculosis* is able to create a favourable niche within the phagosome. Although ManLAM interferes in host recognition of *M. tuberculosis*, its precursor PIM enhances the fusion of *M. tuberculosis* phagosomes with early endosomes, and contributes to phagosome-lysosome fusion (Fratti *et al.*, 2003). This could be a way in which *M. tuberculosis* is able to manipulate the host through interactions with the MR, while still obtaining nutrients from the phagosome and aiding survival.

2.2.1.2 The Toll Like Receptor (TLR) Family

The interaction between *M. tuberculosis* and members of the TLR family occurs early during *M. tuberculosis* infection. TLRs are expressed on various immune cells, including AMs, DCs and certain types of T-cells and B-cells (Akira *et al.*, 2006). TLRs are type I integral membrane glycoproteins, classified as part of the IL-1 receptor (IL-1R) superfamily due to the similarities of the cytoplasmic regions, which are homologous to that of IL-1Rs and contain a Toll-IL-1 receptor (TIR) domain (Slack *et al.*, 2000) with an extracellular domain comprised of leucine-rich repeats (Akira and Takeda, 2004). There is a large repertoire of ligands that interact with TLRs, with some ligands interacting with more than one TLR to bring about an immune response. The complexity of these interactions is highlighted by the antagonist-agonist nature of TLR ligands, which is influenced by the TLR/s with which it interacts (**Table 2.1**).

Table 2.1: The effect of the immune response during TB infection following interactions between TLRs and M. tuberculosis-specific TLR ligands

			Effect of agonist/antagonist	Cell line / infection model	Reference
TLR2 **TLR1/2***	**Agonist**	p19 PE_PGRS33	Induce macrophage apoptosis	THP-1 / MDMs	(Lopez *et al.*, 2003) (Basu *et al.*, 2007)
		LprA LprG PPE17* PPE65	Promotes TNF-α production	THP-1	(Pecora *et al.*, 2004) (Bhat *et al.*, 2012) (Qureshi *et al.*, 2019)
	Antagonist	p19	MHC-II expression repressed	THP-1 / BMDMs	(Noss *et al.*, 2001; Drennan *et al.*, 2004; Fulton *et al.*, 2004)
		LprG, LprA PE_PGRS17 PE_PGRS33 PE_PGRS47	Inhibit MHC-II antigen processing	THP-1 / BMDMs HeLa cells C57BL/6 mice BMDCs; RAW264.7; C57BL/6 mice; SCID-C57BL/6 background mice	(Gehring *et al.*, 2004) (Koh *et al.*, 2009) (Brennan *et al.*, 2002) (Saini *et al.*, 2016)
		PPE18	Induces anti-inflammatory Th2-skewed immune response	Monocyte-derived macrophages	(Nair *et al.*, 2009)
		ESAT-6	Selectively inhibits LPS-driven activation of p38-MAPK, preventing the production of IFN-β and IFN-inducible genes	RAW264.7 Murine BMDMs	(Pathak *et al.*, 2007)
TLR9	**Antagonist**	CpG motifs	Large granuloma formation with increased eosinophils and decrease myeloid DCs	TLR9$^{-/-}$ mice	(Ito *et al.*, 2007)
TLR4	**Agonist**	LPS	Induces the production of pro-inflammatory cytokines Induces autophagy	RAW264.7	(Xu *et al.*, 2007).
		M. tb PIM_{4-6}	Promotes TLR4-CD14 or TLR4-MD2-dependent production of pro-inflammatory cytokines	C3H/HeJ mice	(Abel *et al.*, 2002)
	Antagonist	*M. tb*	Exacerbated pulmonary pathology, increased bacterial load, decreased IL-17A production	C3H/HeJ mice	(Abel *et al.*, 2002)
		M. bovis BCG PIM_6	Prevents MyD88-dependent, TRIF-independent secretion of pro-inflammatory cytokines	TLR2$^{-/-}$ mice Murine BMDMs	(Doz *et al.*, 2009)

The importance of TLRs in *M. tuberculosis* infection has been emphasized with *in vivo* and genetic association studies which demonstrated single nucleotide polymorphisms in TLR2 and TLR9 are associated with an increased susceptibility to TB infection (Velez *et al.*, 2010).

i Toll-Like Receptor-2

Surface expression of TLR2 has been shown to be required for resistance against *M. tuberculosis* infection, with TLR2-bound ligands stimulating the production of pro-inflammatory cytokines such as TNF-α and IL-12 (Underhill *et al.*, 1999; Pompei *et al.*, 2007). TLR2 is believed to be a regulator of inflammation during infection and studies have suggested that this regulatory role is indispensable under chronic or high bacterial load infections (Reiling *et al.*, 2002; Drennan *et al.*, 2004). As such, challenge of BMDMs derived from TLR2-deficient mice ($TLR2^{-/-}$) with *M. tuberculosis* demonstrated that *M. tuberculosis*-induced apoptosis requires TLR2 and the adaptor molecule, MyD88 (Sánchez *et al.*, 2009).

There are some TLR2 ligands that can act as an agonist or an antagonist when bound to TLR2, by 'activating' or 'inhibiting' the host immune response, respectively (**Table 2.1**). The purified 19kDa *M. tuberculosis* lipoprotein (p19) has also been shown to induce apoptosis (Lopez *et al.*, 2003), however, it can also function as an antagonist by transcriptionally repressing the expression of MHC-II molecules, thus preventing *M. tuberculosis* antigen processing (Noss *et al.*, 2001; Drennan *et al.*, 2004; Fulton *et al.*, 2004). Even in the presence of IFN-γ (which is known to increase the expression of MHC-II molecules), there were few MHC-II-peptide complexes formed (Fulton *et al.*, 2004) and ultimately the recruitment of fewer activated $CD4^+$ T-cells. However, there is evidence for elevated numbers of $CD4^+$ and $CD8^+$ T-cells in lung homogenates of $TLR2^{-/-}$ mice upon *M. tuberculosis* challenge (Drennan *et al.*, 2004), which was thought to be a result of the observed increase in pulmonary IFN-γ levels (Drennan *et al*., 2004; Reiling *et al*., 2002). These results suggest that the recruitment of $CD4^+$ and $CD8^+$ T-cells is not solely dependent on stimulation of TLR2, and that the simultaneous engagement of *M. tuberculosis*-specific PAMPs to other PRRs could have initiated signalling cascades that resulted in the recruitment of $CD4^+$ and $CD8^+$ T-cells to the lung. Other *M. tuberculosis* lipoproteins, LprG and LprA, have also been shown to inhibit MHC-II antigen processing through TLR2 (Gehring *et al.*, 2004). Even as monomers, these lipoproteins display their agonist-antagonistic nature by inducing the secretion of pro-inflammatory cytokines such as TNF-α, while preventing MHC-II antigen processing by THP-1 and primary macrophages (Gehring *et al.*, 2004; Pecora *et al.*, 2004).

ii Toll-Like Receptor-9

Unmethylated CpG dinucleotide motifs found in bacterial DNA have been shown to induce a strong T-helper-1 (Th1) inflammatory response (Jakob *et al.*, 1998; Sparwasser *et al.*, 1998), and act as ligands for TLR9 (Hemmi *et al.*, 2000). *In situ* hybridization and immunohistochemistry of mouse and human lung tissues demonstrated that TLR9 expression was increased in patients with chronic obstructive pulmonary disease (Schneberger *et al.*, 2013), suggesting that TLR9 plays a role in mediating inflammation. It has been demonstrated that TLR9 plays an important role in regulating Th1 immune responses that are induced during *M. tuberculosis* infection. TLR9-deficient ($TLR9^{-/-}$) mice tolerate low-dose *M. tuberculosis* (50-100 CFU) aerosol infections but succumb to high dose (500 CFU) aerosol infections, as a result of reduced pulmonary concentrations of IFN-γ and IL-12p40 and a decrease in pulmonary IFN-γ^{+} $CD4^{+}$ T-cells (Bafica *et al.*, 2005).

The role TLR9 plays in maintaining a protective Th1 granulomatous response during TB infection was demonstrated using a model of granulomatous lung inflammation using PPD-coupled beads. Mice were immunized with inactivated *M. tuberculosis* (complete Freund's adjuvant; CFA) and challenged 14 days later by tail-vein with PPD-coupled beads (Ito *et al.*, 2007). Larger granulomas formed in the lungs of $TLR9^{-/-}$mice compared to wild-type control mice (Ito *et al.*, 2007; Ito *et al.*, 2009). The increased granulomatous size was accompanied with more eosinophils and pulmonary $F4/80^{+}$ macrophages (Ito *et al.*, 2007), and with fewer granuloma-associated myeloid DCs (Ito *et al.*, 2009) and $CD3^{+}CD4^{+}$ T-cells (Ito *et al.*, 2007). Furthermore, the granulomas in $TLR9^{-/-}$ mice produced IL-4, IL-5 and IL-13, typically associated with an anti-inflammatory Th2 immune response.

$F4/80^{+}$ is a murine macrophage marker highly expressed on macrophages found in T-cell independent areas of secondary lymph tissue such as the spleen or peritoneum (Gordon *et al.*, 1992). The $F4/80^{+}$ macrophages found in TLR9-deficient mice were phenotypically identified as M2 (anti-inflammatory) macrophages due to the significantly low mRNA expression level of iNOS (typically abundant in M1 (pro-inflammatory) macrophages), and the increased expression levels of Arginase-1 and FIZZ-1, both typical of M2 macrophages (Ito, Schaller, Cory M. Hogaboam, *et al.*, 2007). It is important to note that M1/M2 macrophage phenotypes change according to the homeostatic needs of the host, allowing M1 macrophages to develop into M2 macrophages, and vice versa (Mills, 2015) (**Figure 2.1**). Interestingly, $MyD88^{-/-}$ mice and those doubly deficient for TLR9 and TLR2 ($TLR9^{-/-}TLR2^{-/-}$) were highly susceptible to low dose challenge, with $TLR9^{-/-}TLR2^{-/-}$ mice succumbing to infection 3 weeks earlier than

single knockout mice (Bafica *et al.*, 2005). This suggests that TLR9 interacts with TLR2 to mediate the production of pro-inflammatory cytokines, and that this dimerization is necessary to produce IFN-γ^+ $CD4^+$ and IFN-γ^+ $CD8^+$ T-cells during low- and high dose *M. tuberculosis* challenge (Bafica *et al.*, 2005).

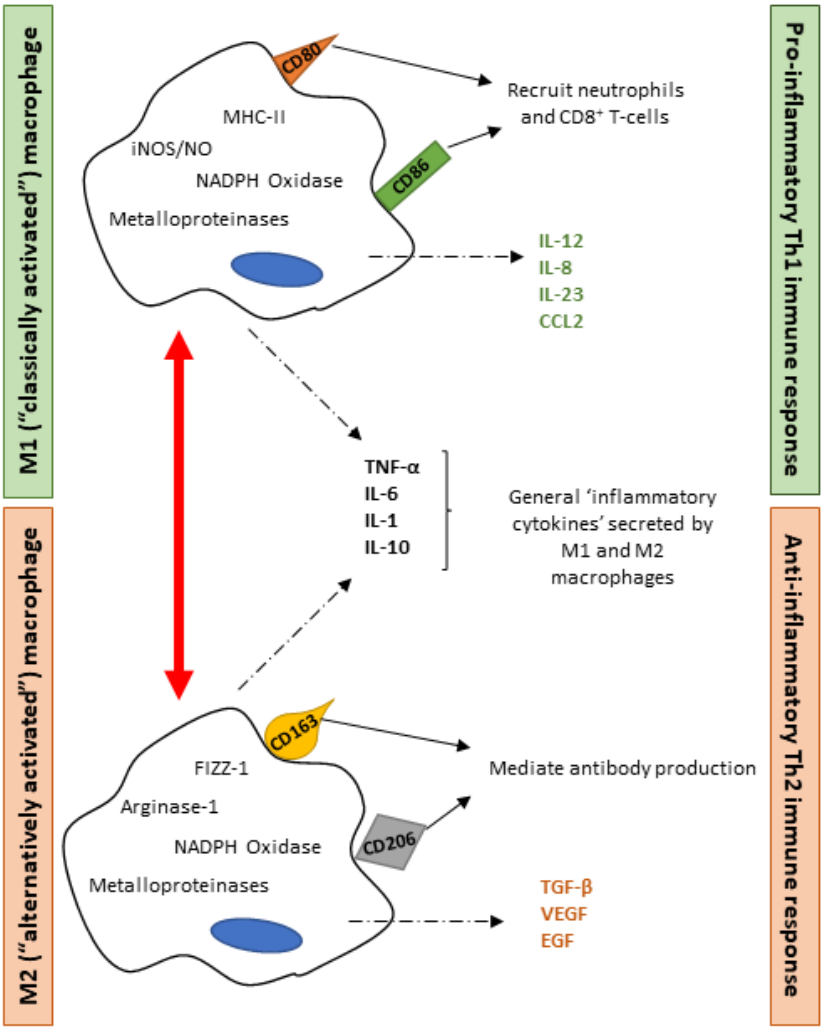

Figure 2.1: Macrophage activation states. M1 (or "classically activated") macrophages are known to produce a pro-inflammatory Th1 immune response through the secretion of IL-12 and IL-8. M1 macrophages express CD80 and CD86 on their surface that recruit neutrophils and cytotoxic T-cells. M2 (or "alternatively activated") macrophages are associated with inducing an anti-inflammatory Th2 immune response through the production of TGF-β and growth factors, VEGF and EGF. M2 macrophages express CD163 and CD206 and mediate the production of antibodies to further mediate the Th2 immune response. The red arrow indicates the ability of M1/M2 macrophages to modulate immune responses by alterng their phenotype. *Figure adapted from* (Mills, 2015).

Collectively, these studies suggest TLR9 to play an important role maintaining a Th1 immune response during chronic *M. tuberculosis* infection and works synergistically with TLR2 to promote protection during early infection (Bafica *et al.*, 2005; Ito *et al.*, 2007; Ito *et al.*, 2009). In its absence, granulomas are enlarged and pro-inflammatory responses from granulomas are

down-regulated (Ito *et al.*, 2007). The *M. tuberculosis* ligands containing CpG dinucleotide motifs that specifically interact with TLR9, or with dimerized TLR9/TLR2 have not yet been identified. It is possible that *M. tuberculosis* ligands for TLR2 also interact with TLR9, just via a different recognition pathway, however more evidence is needed to clarify this.

iii Toll-Like Receptor-4

The immunomodulatory effects mediated upon activation through TLR4 need to be further examined, however available literature suggests TLR4 plays a bigger role in secondary immune responses to *M. tuberculosis*, rather than primary host defence. Bacterial endotoxin, lipopolysaccharide (LPS), has been experimentally demonstrated to signal through TLR4 (Poltorak *et al.*, 1998; Hoshino *et al.*, 1999) and LPS-induced autophagy through TLR4 is achieved in a TIR domain-containing adaptor inducing IFN-β (TRIF)-dependent MyD88-independent manner (Xu *et al.*, 2007) (**Figure 2.2**). Furthermore, along with TLR2 and MyD88, TLR4 has demonstrated a major role in *M. tuberculosis*-induced apoptosis (Sánchez *et al.*, 2009).

The LPS-TLR4 interaction activates MAP kinases (MAPK). The *M. tuberculosis* ESAT-6 antigen has been shown to interfere with this signal transduction pathway by selectively inhibiting the LPS-driven activation of p38-MAPK (Pathak *et al.*, 2007). The inhibition was thought to be 'selective' due to the unaffected activation states of extracellular signal-regulated kinase (Erk) and c-Jun N-terminal kinase (Jnk). The activity of apoptosis signal-regulating kinase 1 (ASK1), which is involved in signalling upstream of p38, was also shown to be inhibited in the presence of ESAT-6. The ASK1-p38 signalling axis is important for the LPS-induced activation of IRF3 (Sakaguchi *et al.*, 2003), which following translocation to the nucleus, induces transcription of IFN-β and IFN-inducible genes. In the presence of ESAT-6, IRF3 failed to translocate to the nucleus, thus inhibiting the production of IFN-β and IFN-inducible genes (Pathak *et al.*, 2007) (**Figure 2.2**).

.

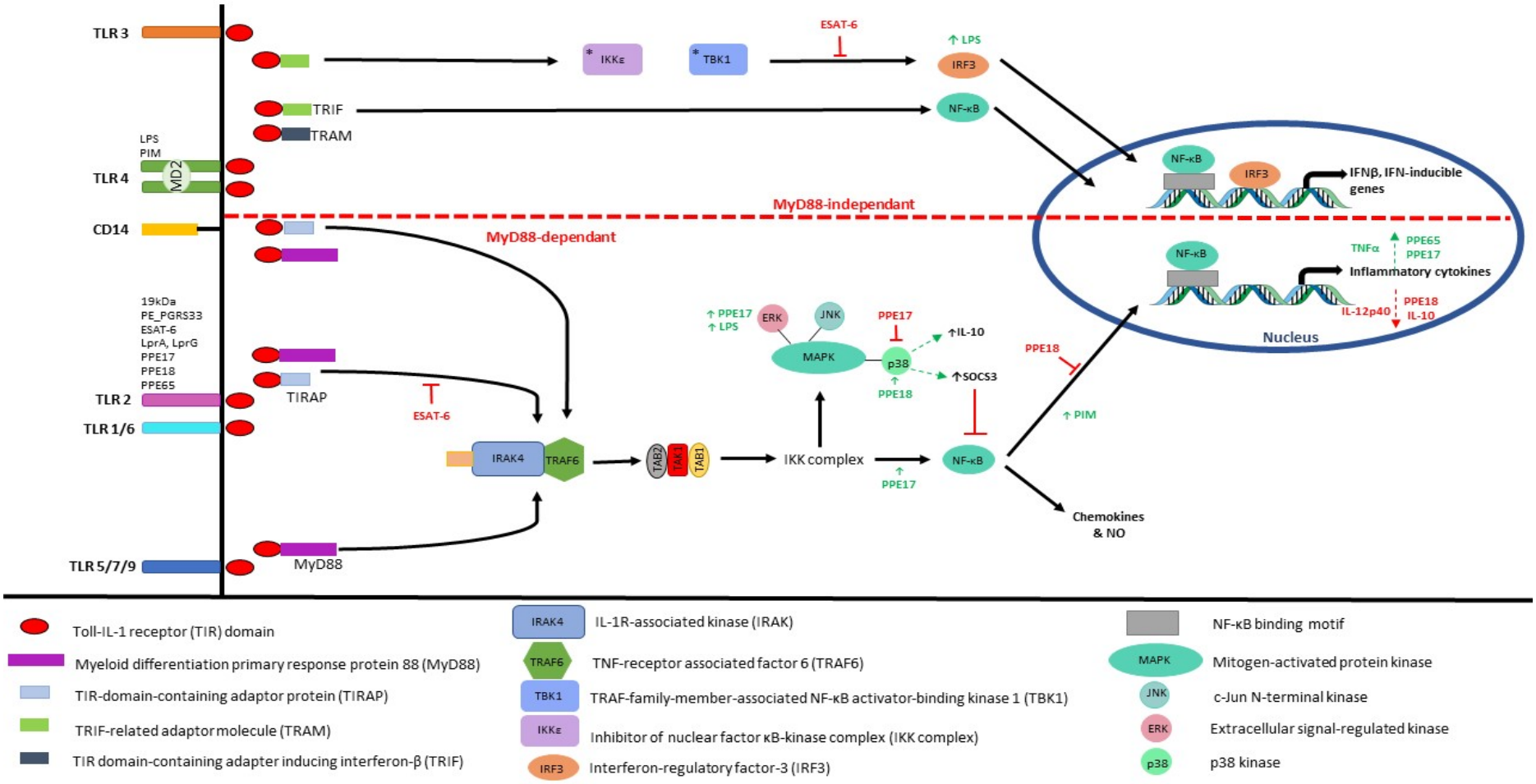

Figure 2.2: Signal transduction through TLRs. Signal transduction through the TLRs is initiated upon binding of specific ligands to their respective TLRs. Once bound to the ligand, various signal transduction pathways are activated through binding of adaptor molecules to the TIR domain; these can be classified as MyD88-dependent or MyD88-independent. MyD88-dependent signalling involves the binding of MyD88 to the TIR domain of the TLR and results in the phosphorylation and activation of the early phase NF-κB complex that leads to the production of pro-inflammatory cytokines (TNF-α/IL-12p40). The initiation of MyD88-independent signalling requires two additional adapter molecules, TRIF and TRAM, and involves the phosphorylation and activation of late-phase NF-κB and IRF3, leading to the production of IFN-β and other IFN-inducible genes. (*Image adapted from "Toll-like receptor signalling" (Akira et al., 2004)).*

Supporting the role TLR4 plays in the secondary host response, TLR4 has been implicated in the production of IL-17A from IL-17A/IFN-γ-positive $CD4^+$ memory T-cells and γδ T-cells (Veerdonk *et al.*, 2010). IL-17A has a role in maintaining the inflammatory response, as it has been implicated in the maintenance of granuloma formation and the recruitment of Th1 T-cells to the site of infection (Umemura *et al.*, 2007). *In vivo* experiments have also demonstrated the importance of TLR4 in mediating a pro-inflammatory response (Poltorak *et al.*, 1998; Abel *et al.*, 2002). Compared to wild type mice (C3H/HeN), TLR4 mutant mice (C3H/HeJ) were unable to control bacterial burden and all succumbed to infection within 5 months, whereas C3H/HeN mice survived the duration of the experiment (6 months) (Abel *et al.*, 2002). This could be attributed to the lack of IL-17A that dampens the Th1 immune responses and impairs mycobacterial containment within the granuloma. As such, without a functional TLR4, a state of chronic inflammation was observed with dissemination into the liver and spleen (Abel *et al.*, 2002).

Evidently, without a functional TLR4, necrosis rather than apoptosis is significantly upregulated (Sánchez *et al.*, 2009), which could explain the exacerbated inflammation observed. Increased inflammation was accompanied by a significantly reduced pro-inflammatory bronchoalveolar lavage (BAL) cytokine profile, showing the reduction of IL-12p40 (Abel *et al.*, 2002). In addition to IL-12p40, TLR4-mutant and wild-type mice lungs also showed significantly lower TNF-α levels, and only slightly reduced IFN-γ (Abel *et al.*, 2002). Interestingly, in another study no difference in pulmonary bacterial load between C3H/HeJ-, $TLR2^{-/-}$- and $CD14^{-/-}$ mice compared to the appropriate wild-type controls was observed for low dose *M. tuberculosis* infection (Reiling *et al.*, 2002). Furthermore, no significant differences in pro-inflammatory cytokine production was observed between C3H/HeJ mice and wild-type mice (Reiling *et al.*, 2002). A defect in the immune response similar to that seen by Abel *et al* was only identified during high-dose *M. tuberculosis* challenge (2000 CFU). The discrepancy between these studies is unclear as the reported experimental conditions in which both studies were conducted were identical.

M. tuberculosis PIM is a ligand for TLR4 and interacts with this receptor as a GPI anchor of LAM and lipomannan. *M. tuberculosis* PIM_{4-6} have been shown to induce a pro-inflammatory immune response in a TLR4/CD14- or TLR4/MD2-dependant manner, by inducing NFκB transctivation (Abel *et al.*, 2002). However, *M. bovis* BCG PIM_6, negatively regulates the production of MyD88-dependant, TRIF-independent secretion of pro-inflammatory cytokines from LPS/TLR4 activated macrophages (Doz *et al.*, 2009). This suggests that there are

structural differences between PIM from *M. tuberculosis* and *M. bovis* BCG that allow *M. tuberculosis* PIM to enhance a pro-inflammatory response.

2.2.1.3 Interactions between the PE/PPE proteins and receptors on the alveolar macrophage

Some members of the PE/PPE protein family have been shown to interact with TLR2 and modulate host immune responses (Basu *et al.*, 2007; Nair *et al.*, 2009; Udgata *et al.*, 2015). Due to the similarity of PE_PGRS proteins to the Epstein-Barr virus nuclear antigen, it was speculated that these proteins may also interfere with antigen processing and presentation (Cole *et al.*, 1998). In support of this, the inhibition of antigen processing was demonstrated for PE_PGRS33 (Brennan and Delogu, 2002), PE_PGRS17 (Koh *et al.*, 2009) and PE_PGRS47 (Saini *et al.*, 2016). PE_PGRS33 has also been implicated with inducing macrophage apoptosis in a TLR2-TNF-α-dependant mechanism (Basu *et al.*, 2007) (**Table 2.1**), and has also been shown to trigger macrophage necrosis and enhance the intracellular survival of mycobacteria (Dheenadhayalan *et* al., 2006), however the involvement of TLR2 in the latter remain unclear.

Localised in the cell wall of *M. tuberculosis*, PPE18 has been shown to specifically interact with TLR2 through its leucine-rich repeat 11 ~ 15 domain and induce a Th2-skewed immune response (Nair *et al.*, 2009; Udgata *et al.*, 2015). Recombinant *M. tuberculosis* PPE18 was shown to induce the production of IL-10 by triggering the phosphorylation of p38 MAPK and supressing the production of IL-12p40 (**Table 2.1**) (Nair *et al.*, 2009). It was later demonstrated that for PPE18 to inhibit the production of IL-12p40, it upregulates the expression of suppressor of cytokine signalling 3 (SOCS3) which physically interacts with IκBα- NFκB complex, preventing the translocation to the nucleus and induction of pro-inflammatory cytokines (**Figure 2.2**) (Nair *et al.,* 2011). Furthermore, PPE18 was also shown to interfere with IRAK-PKCα signalling cascade (Udgata *et al.*, 2015), resulting in the proliferation of Th2 T-cells that produce high levels of IL-5 rather than IFN-γ (Nair *et al.*, 2009) (**Table 2.2**). By skewing the immune response towards an anti-inflammatory Th2 response, *M. tuberculosis* PPE18 down-regulates the inflammatory Th1 response and establishes a favourable environment to persist.

Table 2.2: Major effector CD4⁺ T-cell populations governing the host immune response during TB disease

CD4⁺ T-cell effector population	Role in the immune response in TB infection	Cytokine profile	References
T-helper 1 CD4⁺ T-cells (Th1)	Activate inflammatory effector functions in alveolar macrophages, resulting in effective control of TB disease.	IFNγ IL-12	(Prezzemolo *et al.*, 2014) (Lyadova *et al.*, 2015)
T-helper 2 CD4⁺ T-cells (Th2)	Associated with dampening of the immune response during TB infection by counter-regulating Th1 CD4⁺ T-cells.	IL-4 IL-5 IL-13	(Prezzemolo *et al.*, 2014)
T-helper 17 CD4⁺ T-cells (Th17)	Recruitment of monocytes and Th1 CD4⁺ T-cells to the site of granuloma formation during early TB disease. Main cell type producing IL-17	IL-17 IL-22 IL-26 GM-CSF	(Prezzemolo *et al.*, 2014) (Lyadova *et al.*, 2015)

PPE17 and PPE65 have also been shown to interact with TLR2, but unlike PPE18, they interact with the 16 ~ 20 leucine-rich repeat domain of TLR2 (Bhat *et al.*, 2012; Qureshi *et al.*, 2019) and induce a pro-inflammatory immune response (Bhat *et al.*, 2012; Udgata *et al.*, 2015; Qureshi *et al.*, 2019). When bound to TLR2, PPE17 was shown to increase the intracellular levels of NFκB, resulting in production of high TNF-α concentrations (Bhat *et al.*, 2012) (**Table 2.1**). Similarly, THP-1 macrophages infected with recombinant *M. smegmatis* expressing PPE65, produced higher levels of TNF-α compared to uninfected cells, however the mechanism through which this is achieved remains unclear (Qureshi *et al.*, 2019).

PPE17 has also been shown to promote dimerization between TLR2 and TLR1 (Udgata *et al.*, 2015), which may explain the contrasting immune responses observed for PPE18, PPE17 and PPE65. There is also evidence to suggest that PPE17 requires the hetero-dimerization of TLR1/2 to induce TNF-α, as silencing of TLR1 resulted in the downregulation of TNF-α (Udgata *et al.*, 2015). In this study, the production of TNF-α was shown to require phosphorylation of ERK1/2, a process dependent on the translocation of nuclear IRAK3 into the cytosol (Udgata *et al.*, 2015). Although IRAK3 activated ERK1/2, it was shown to have inhibitory effects on p38 MAPK (Udgata *et al.*, 2015). This suggests that PPE17 is able to

interact with various components within the cell and that where TLR2 ligands bind determines which downstream signalling cascade is triggered, either favouring a Th1- or Th2-type immune response.

PE/PPEs interaction with TLR2 can activate either pro- or anti-inflammatory immune responses, which may be dependent on which downstream signalling cascade is triggered. The exact mechanisms governing this outcome are not fully understood, however one can speculate that interactions of TLR2 ligands with different ligand-specific sites in the LRR domain can induce conformational changes of downstream complexes, altering the type of signals induced. The section of the LRR engaged could also influence TLR2 dimerization with itself, or other TLRs, thus also influencing the type of response initiated. The majority of the interactions described between PE/PPEs and TLR2 lead to an anti-inflammatory response. The differential expression of the *pe/ppe* genes during TB infection (Voskuil *et al*., 2004) could also influence which protein-TLR interaction may take place at different stages of infection, regulating the internal environment to favour *M. tuberculosis*.

The interaction between members of the PE/PPE protein family and the MR have not yet been described in literature. We know that PE_PGRS17, -33 and -47 inhibits antigen processing from MHC-II molecules when bound to TLR2, and the MR can be found within the MHC-II loading compartment of the macrophage. The close proximity within the MHC-II loading compartment may allow PE/PPEs to interact with the MR, however this is unlikely as the MR generally recognises mannosylated carbohydrates (Reiling *et al.*, 2001). Interactions between PE/PPEs and another member of the MR family, M-type phospholipase A_2 receptor (PLA_2R), may be worth investigating as PLA_2R has been shown to facilitate protein-protein interactions through its C-type lectin-like domain 5 (East *et al.*, 2002), however functional studies will need to be performed to confirm this.

2.2.2 *Mycobacterium tuberculosis* interacts with dendritic cells

DCs are critical in linking the innate and adaptive immune systems and have a wide variety of functions including antigen processing and presentation, T-cell recruitment and clonal expansion and co-stimulatory effects. Transportation to the mediastinal lymph node allows *M. tuberculosis*-infected DCs to interact with naïve T-cells, present them with antigen, resulting in the naïve T-cell acquiring an effector T-cell function by differentiating into a Th1, Th2 or Th17 T-cell (depending on the stimulus), thus triggering the adaptive immune response (Wolf *et al.*, 2007). During DC migration, the surface expression of mannose and Fc-receptors

becomes downregulated (Geijtenbeek *et al.*, 2003), and expression for adhesin, antigen-presenting and co-stimulatory molecules are upregulated, constituting a mature DC phenotype (Banchereau *et al.*, 1998). Additionally, chemokine receptors are upregulated on mature DCs, which improve the ability of mature DCs to migrate to the lymphoid tissue for antigen presentation (Al-Ashmawy, 2018).

Studies done using DCs generated from human peripheral blood and murine-derived DCs have supported early literature by showing the ability of DCs to internalize *M. tuberculosis*, which results in the production of pro-inflammatory cytokines TNF-α, IL-12 and IL-1 (Henderson *et al.*, 1997; Bodnar *et al.*, 2001). *M. tuberculosis*-containing DCs had increased surface expression of MHC-I and co-stimulatory CD54, CD40 and CD80 molecules (Henderson *et al.*, 1997; Bodnar *et al.*, 2001). Culture filtrate protein 10 (CFP-10) has been shown to differentiate freshly isolated bone marrow cells to DC-like cells with the upregulation of CD11b and CD11c; MHC class I and II molecules and T-cell costimulatory molecules CD80, CD86, CD40 and CD54 (Latchumanan *et al.*, 2002). *M. tuberculosis* lipoprotein LprA has also been shown to induce a mature DC phenotype associated with the upregulation of cell-surface CD40, CD80 and MHC-II molecules and the production of TNF-α, IL-12 and IL-10 (Pecora *et al.*, 2004). These studies demonstrate the highly responsive nature DCs have to *M. tuberculosis* and its products and emphasizes the highly heterogenous repertoire of ligands able to interact with DCs.

Although DCs have been shown to internalize a higher percentage of *M. tuberculosis* compared to other immune cells (Wolf *et al.*, 2007), they do not support the intracellular growth of *M. tuberculosis* (Bodnar *et al.*, 2001; Tailleux *et al.*, 2003). This is expected as the DCs need to present antigen via MHC molecules to T-cells, which requires the generation of peptides from the engulfed *M. tuberculosis* bacilli. Another possible reason that *M. tuberculosis* is unable to proliferate within DCs could be due to DC-lysosome co-localisation (Geijtenbeek *et al.*, 2003) during which, DCs may possibly acquire lysosomal hydrolases which will prevent the intracellular growth of *M. tuberculosis*. DCs have different functions, in terms of antigen capture and presentation, depending on which stage of activation and maturation they exist. Natarajan *et al* investigated the ability of CFP-10 to induce the maturation of $CD8a^+/CD11c^+$ and $CD8a^-/CD11c^+$ mouse splenic DCs (Natarajan *et al.*, 2003). $CD8a^+/CD11c^+$ induce a pro-inflammatory Th1 response while $CD8a^-/CD11c^+$ typically induce an anti-inflammatory Th2 response (Reid *et al.*, 2000). CFP-10 stimulation of DC subsets was shown to induce the full maturation of both subsets compared to unstimulated DCs. Both CFP-10-stimulated DC

subsets released high concentrations of IFN-γ, however only the $CD8a^+/CD11c^+$ DC subset released high concentrations of IL-12p40 (Natarajan *et al.*, 2003). The cytokine profiles of $CD8a^-$ and $CD8a^+$ DCs suggest that these subsets induce opposing immune responses, but both subsets demonstrated the ability to activate $CD4^+$ T-cells in response to CFP-10. This emphasizes the complexity of this immune response and highlights that other factors are involved that influence the outcome of the T-cell response.

Although CFP-10-matured DC subsets appear to be fully-capable of processing and presenting antigen via MHC-II molecules, they do not respond to secondary antigenic challenge with *M. tuberculosis* whole cell extract T-cells *in vivo* (Natarajan *et al.*, 2003; Balkhi *et al.*, 2004). The significantly reduced levels of IL-2 and, especially IFN-γ, from these DCs is interesting as whole cell extract contains various components (proteins, lipids and carbohydrates) of *M. tuberculosis* that may be released from the macrophage during infection. These results suggest that DCs that have engulfed CFP-10 secretory antigen become less capable of inducing a proliferative and proinflammatory T-cell response. Furthermore, CFP-10-matured DCs maintain their phagocytic ability (Natarajan *et al.*, 2003), while modulating the levels of reactive oxygen species to promote mycobacterial survival within DCs (Sinha *et al.*, 2006). It is possible that *M. tuberculosis* uses CFP-10 to dampen the proinflammatory response upon secondary challenge and manipulate DCs to migrate to secondary lymphoid organs and disseminate, thus contributing to the spread of infection. Alternatively, CFP-10 can be used by *M. tuberculosis* to create a favourable niche in which to proliferate.

2.2.2.1 CD209 – DC-SIGN

Dendritic cell-specific intercellular adhesion molecule-3 grabbing nonintegrin (DC-SIGN) is a calcium-dependant C-type transmembrane lectin with a C-terminal carbohydrate recognition domain (Geijtenbeek *et al.*, 2003). Monoclonal antibodies (mAb) specific for DC-SIGN, prevented ~90% of *M. tuberculosis* attachment to monocyte-derived DCs (Tailleux *et al.*, 2003). This suggests that DC-SIGN is the major receptor on immature DCs that facilitates interactions with *M. tuberculosis* (Geijtenbeek *et al.*, 2003; Tailleux *et al.*, 2003) through the recognition of cell wall associated mannose-capped lipoglycans (Maeda *et al.*, 2003) such as LAM, ManLAM (Geijtenbeek *et al.*, 2003; Tailleux *et al.*, 2003) and lipomannan.

Although present in the cell wall of *M. tuberculosis* and *M. bovis* BCG, ManLAM can also be secreted by *M. tuberculosis*-infected macrophages, and circulate as a virulence factor, thus influencing the activity of other APCs. It is interesting that the total ManLAM fractions from

M. tuberculosis and *M. bovis* BCG were shown to inhibit the production of IL-12p70 from LPS-stimulated human monocyte derived-DCs (Nigou *et al.*, 2001; Geijtenbeek *et al.*, 2003), whereas internalization with whole bacilli resulted in the production of IL-12, TNF-α and IL-1 (Henderson *et al.*, 1997; Bodnar *et al.*, 2001). This suggests that ManLAM dampens the pro-inflammatory response induced by activated DCs. As such, there is evidence to suggest this to be true as ManLAM isolated from *M. tuberculosis* H37Rv was shown to increase the expression of SOCS1 following interaction with DC-SIGNR1 on mouse bone marrow derived dendritic cells (Srivastava *et al.*, 2009).

The interaction between DC-SIGN and ManLAM seems to depend on the presence of the mannooligosaccharide caps and lipidic part of the GPI anchor. ManLAMs devoid of these mannose caps showed reduced binding to DC-SIGN and the impaired inhibitory ability on the production of IL-12p70 from DCs (Nigou *et al.*, 2001). These results suggest that lipoglycans lacking mannose caps are not recognised as effectively by DC-SIGN compared to mannosylated lipoglycans. Furthermore, these results highlight the varying immune response that can be elicited by different mycobacterial strains harbouring structural differences in the mannosylated lipoglycans. Evidently, *M. smegmatis* phosphoinositol-capped LAM (PILAM) (Nigou *et al.*, 2001), nor AraLAM (Geijtenbeek *et al.*, 2003) showed inhibitory ability on the secretion of IL-12 from DC-SIGN.

M. tuberculosis and *M. bovis* BCG have been shown to induce DC maturation, however ManLAM-bound DC-SIGN has been implicated in interfering with DC maturation (Geijtenbeek *et al.*, 2003). In the presence of ManLAM alone, DC maturation markers CD80, CD83, CD86 or MHC-II showed no-upregulation. LPS-bound TLR4 stimulates intracellular signalling that induces DC maturation, however in the presence of ManLAM, LPS-activated DCs also failed to acquire a mature phenotype. *M. bovis* BCG-induced DC maturation was inhibited in the presence of ManLAM but was seen to be restored following preincubation with antibodies specific for DC-SIGN (Geijtenbeek *et al.*, 2003). These results suggest that when secreted as a virulence factor from *M. tuberculosis*-infected macrophages, ManLAM is able to interfere with DC maturation through DC-SIGN-dependant pathways and the LPS-TLR4 induced DC maturation pathway.

IL-10, an immunosuppressive cytokine involved in dampening immune responses, was seen to be induced in the presence of ManLAM (Geijtenbeek *et al.*, 2003). IL-10 has many immunosuppressive abilities, including, inhibiting expression of MHC-II and co-stimulatory molecules and preventing the production of pro-inflammatory cytokines, such IL-12 and TNF-

α (Couper *et al.*, 2008). The release of IL-10 could have contributed to the low level of activation markers observed in the above studies, thus could also play a role in interfering with DC maturation. IL-10 prevents the activity of effector T-cells, therefore preventing an effective immune response and control of *M. tuberculosis.*

The host cell could have a mechanism of counteracting this clever immune-evasion strategy of *M. tuberculosis.* Following uptake into the DC via DC-SIGN, both whole bacilli and purified ManLAM-infected DCs were seen to colocalize with lysosomes, and lose the expression of DC-SIGN on their surface (Geijtenbeek *et al.*, 2003). This could explain why DCs do not support intracellular growth of *M. tuberculosis*; once co-localised with lysosomes, there could be exchange of lysosomal hydrolases between the lysosome and DCs, which prevents intracellular growth. The discrepancies observed in DC maturation following incubation with whole bacilli or purified virulence factors suggest that internalization of *M. tuberculosis* by DCs activates the immune system. Interaction between DCs and virulence factors mediated by DC-SIGN seem to have an opposing effect on each other and dampen the host immune response, giving *M. tuberculosis* time to establish infection.

2.2.2.2 Toll-like receptors and dectin-1

The important role of TLRs in activating cellular immune responses has been well defined. We have already mentioned the importance of macrophage TLRs during TB pathogenesis and the ability of *M. tuberculosis* and its derived antigens to dampen or activate immune responses using these receptors. *M. tuberculosis* secreted antigens have also been shown to modulate the host immune response by interacting with TLRs expressed on DCs. Although there is no evidence for PE/PPE interaction with TLRs on DCs, *M. tuberculosis* p19 has been shown to promote DC maturation and induce the production of pro-inflammatory cytokine, IL-12 from DCs in a TLR2-dependent manner (Thoma-Uszynski *et al.*, 2000; Hertz *et al.*, 2001).

The mycobacterial cell wall constitutes ligands for phagocytic, and proinflammatory receptors, both of which share intracellular signalling molecules, thus suggesting that various classes of receptors interact with each other to induce an effective immune response (Underhill and Ozinsky, 2002). This is also the case for dectin-1 found on DCs. In response to zymosan, LPS and Pam_3Csk_4 (synthetic lipopeptide), the simultaneous engagement of dectin-1 and TLR2 was shown to enhance pro-inflammatory cytokine production in murine BMDMs and bone marrow-derived DCs, compared to engagement of one receptor alone (Gantner *et al.*, 2003). In a similar study using murine splenic DCs stimulated with live mycobacteria (*M. tuberculosis*

H37Rv, *M. bovis* BCG and *M. avium*), the production of pro-inflammatory cytokine, IL-12p40 was abrogated in the absence of dectin-1 and TLR2 (Rothfuchs *et al.*, 2007). This suggests that dectin-1 is able to function independently of TLR2, however the presence of both receptors enhances the pro-inflammatory immune response.

The synergistic action of dectin-1 and other TLRs has also been demonstrated. Pompei *et al.* demonstrated the ability of TLR9 and TLR2 to remodel the IL-12p40 promoter thus influencing the inflammatory response mediated following engagement of dectin-1 with pathogenic mycobacterial strains (Pompei *et al.*, 2007). It is interesting to note that TLR9-deficient mice produced no IL-12p40 from DCs and those lacking TLR2 were unable to produce IL-12p40 from macrophages. However, when both TLR9 and TLR2 are absent, DCs and macrophages are both unable to produce IL-12p40 (Pompei *et al.*, 2007), suggesting that both receptors provide unique functional elements that are needed for initiating a pro-inflammatory response.

The interaction between dectin-1 and other receptors does not always lead to an inflammatory response. A study by Zenaro *et al.* showed that *M. tuberculosis* induced the release of TNF-α, IL-1β, IL-6 and IL-23 from monocyte derived DCs in a dectin-1 dependent manner (Zenaro *et al.*, 2009). In agreement with other studies, these cytokines stimulated the formation of $CD4^+$ T-cells with characteristics of Th1 or Th17 and Th1 and Th17 cells (LeibundGut-Landmann *et al.*, 2007; Manicassamy *et al.*, 2009; Zenaro *et al.*, 2009). Both these processes were inhibited by stimulation of DC-SIGN and MR and was reactivated in the presence of monoclonal antibodies blocking DC-SIGN and MR (Zenaro *et al.*, 2009). This suggests that signals initiated by the MR and DC-SIGN interfere with pro-inflammatory signals initiated by dectin-1. In TB infection, Th1-cells play a protective role by producing IFN-γ, while Th17-cells have been implicated in tissue damage and neutrophilic inflammation thus playing a role in the lung pathology associated with TB disease. In the studies above, it appears as though *M. tuberculosis* has used dectin-1 to induce a Th17 response to increase the pathological effects of TB disease and promote its own survival.

Murine studies with mice deficient for the *Clec4n* gene, encoding the dectin-2 receptor, demonstrated the critical role for dectin-2 in the host response during mycobacterial infection (Yonekawa *et al.*, 2014). Dectin-2-deficient mice had higher bacterial burden and displayed increased lung histopathology compared to wild-type mice. It was also demonstrated that *M. tuberculosis* ManLAM is a direct ligand for the dectin-2 receptor, resulting in the release of pro- and anti-inflammatory cytokines from bone marrow-derived DCs. Furthermore, dectin-2 bound ManLAM promoted DC maturation and antigen specific T-cell responses in TB patients

(Yonekawa *et al.*, 2014). The recognition of ManLAM by dectin-2 was shown to be dependent on the mannose caps of ManLAM and the mannose-recognition property of dectin-2. The production of anti- and pro-inflammatory cytokines following interactions between dectin-2 and ManLAM on DCs may be beneficial to the host in balancing the immune response to *M. tuberculosis.* ManLAM did not induce an inflammatory response *in vivo* (Yonekawa *et al.*, 2014) and could thus be used, in conjunction with dectin-2 as hydrophilic 'regulatory adjuvant' that promotes the development of the adaptive immune response.

AMs and DCs are in a constant battle for immune control during TB infection due to the differential expression of *M. tuberculosis* virulence factors during infection (Gupta *et al.*, 2010). Antigens produced by *M. tuberculosis* on day 1 (D1) of infection are essential for intracellular survival within the AM and enhance the maturation and activation of DCs, however, these, and antigens produced after D5 of infection prevented AM activation and downregulated the expression of MHC-I and II. Consequently, even if activated T-cells were present, no antigen presentation could have occured between the AM and the T-cell. Most antigens expressed on D5 also played a major role in promoting latency and dampened DC function by downmodulating the surface expression of CD54 and MHC-I and II molecules (Gupta *et al.*, 2010).

These inhibitory effects could be attributed to the increased SOCS1 (suppressor of cytokine signalling 1) expression in both DCs and macrophages. SOCS1 is the most characterized member of the SOCS protein family primarily involved in regulating cytokine expression and cytokine receptor-mediated gene expression of immune cells (Alexander, 2002). In DCs, the increase in SOCS1 expression occurred early during infection in a TLR2-dependent manner by D1 antigen Rv2463. Furthermore, both antigens repressed the oxidative burst from the DC (Gupta *et al.*, 2010). Prevention of ROI in the DC allowed the intracellular survival of *M. tuberculosis*, while interfering with cytokine signalling during early infection, with possible negative implications for T-cell priming and Th1 responses from DCs. This study highlights how elegantly *M. tuberculosis* interacts with two of the most important innate immune cells to induce the dysregulation of the host immune response and ensure its own survival.

These studies truly emphasize the heterogenous innate immune response induced, depending on what type of immune cell is interacting with *M. tuberculosis* during infection. Receptors behave differently on different innate cells, thus allowing many avenues of immune activation, leading to a pro-inflammatory response. However, this heterogeneity also provides *M. tuberculosis* with an advantage as there are many mechanisms at its disposal that it can

manipulate for immune evasion. The interactions between *M. tuberculosis* and the innate immune cells have implications for the resulting adaptive immune response, within which there are new targets for *M. tuberculosis* manipulation.

2.3 The Adaptive Immune response to *Mycobacterium tuberculosis* infection

One extremely important characteristic of the adaptive immune system is its ability to recognise known *M. tuberculosis* antigens and rapidly produce effector $CD4^+$ T-cells and antibodies specifically for that antigen, allowing for a quicker and more specialized host defence response (Alberts *et al.*, 2002). The adaptive immune response can be classified as a cell-mediated- or humoral immune response, both working together to defend the host against *M. tuberculosis*. The cell-mediated response is mainly governed by $CD4^+$ T-cells that attempt to destroy the intracellular pathogen and stimulate the release of cytokines that sequester other immune cells to the site of infection. The humoral immune response is governed by B-cells that produce antibodies which help prevent intracellular pathogens from disseminating (Janeway *et al.*, 2001). B-cell antigen binding and internalisation results in the activation of helper T-cells through peptide presentation. The bound antigen, along with the signals produced by the activated helper T-cells, induces the proliferation and differentiation of the B-cell into plasma cells, which secrete antibodies specific for the bound antigen. These antibodies function to eliminate the pathogen by neutralization, opsonisation or through activating the complement pathway (Janeway *et al.*, 2001).

2.3.1 Initiating the adaptive immune response during TB infection

The adaptive immune response to TB infection is initiated once *M. tuberculosis* disseminates to the pulmonary lymph node (Chackerian *et al.*, 2002; Wolf *et al.*, 2008), which becomes rich in *M. tuberculosis*-specific T-cells 2-3 days post dissemination (Chackerian *et al.*, 2002). The faster dissemination occurs, the more efficient the adaptive immune response to *M. tuberculosis* will be. DCs are instrumental in this process and differ in functionality depending on which part of the lung they originate. DCs found in lung mucosa present antigen more efficiently than those in lung parenchyma (von Garnier *et al.*, 2005), which may be due to the highly regulated environment of AMs within the mucosa that may prevent these DCs from migrating to the lymph node. Alternatively, the slow-growing nature of *M. tuberculosis* might

suggest that time is required for the bacterial burden to increase to a level that may activate the adaptive immune response.

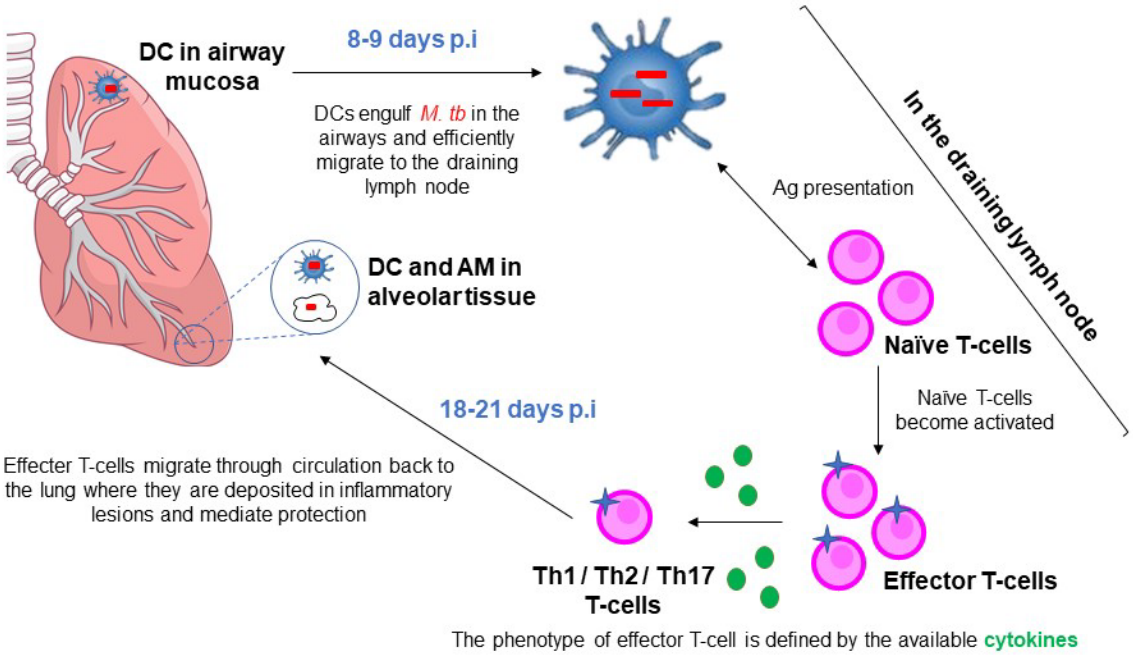

Figure 2.3: The initiation of the adaptive immune response during *M tuberculosis* infection. Aerosol infection mimics the natural route of infection during TB disease. Low numbers of *M. tuberculosis* are deposited in the lungs where they are phagocytosed by antigen presenting cells such as alveolar macrophages and dendritic cells. DCs are instrumental in transporting *M. tuberculosis* to the draining lymph node where they present *M. tuberculosis* antigens to naïve T-cells via MHC-I and MHC-II. Once primed, these effector T-cells will differentiate into different effector subsets and will migrate back to the lung through circulation. The effector T-cells are attracted to the site of infection through inflammatory signals. Once in the inflammatory lesion, the T-cells respond to the inflammatory response by activating resident APCs. When an appropriate immune response has been initiated by T-cells and activated macrophages, intracellular growth *M. tuberculosis* will be inhibited. (Image adapted from Cooper, 2009).

Activated T-cells can circulate back to the lung and activate resident APCs, a process that takes roughly seven days. IFN-γ-producing T-cells can detected in the lung at 14 days post infection (p.i), however, inhibition of *M. tuberculosis* proliferation is only detected at 20 days p.i (Cooper, 2009), suggesting that IFN-γ needs to accumulate at the site of infection before growth can be restricted. Following antigen presentation, activated T-cells differentiate into various effector subsets in response to the pathogenic stimulus. The effector phenotype is also influenced by the availability of cytokines and co-stimulatory molecules, and type of APC (Luckheeram *et al.*, 2011). Cytokine-derived signals are the major determinants of the resultant T-cell lineage of the naïve T-cell. They activate signal transducer and activator of transcription (STAT) factors that bind lineage-specifying transcription factors and induce the transcription

of pro-inflammatory cytokines in the nucleus. This process results in the generation of a specific $CD4^+$ T-cell lineage (Lyadova and Panteleev, 2015). Two of the most important effector $CD4^+$ T-cell subsets involved in the maintenance and regulation of the adaptive immune responses during TB infection are T-helper 1 (Th1) and Th17 $CD4^+$ T-cells (**Table 2.2**) (Khader *et al.*, 2009; Zenaro *et al.*, 2009; Ottenhoff, 2012; Lyadova *et al.*, 2015). Attempting to better understand the *M. tuberculosis*-specific adaptive immune response and the factors that tip the balance between protection and immunopathology will allow us to identify correlates of protection which could possibly lead to advances in the TB vaccine development pipeline.

2.3.2 The Th1-mediated cellular response during TB infection

M. tuberculosis has been shown to impair Th1 mediated cellular responses (Almeida *et al.*, 2009). IL-12 and IFN-γ are the major cytokines involved during Th1 cell development. Naïve $CD4^+$ T-cells express functional IFN-γ receptors on their surface, however the signalling subunit of the IL-12 receptor, IL-12Rβ2 is only induced upon antigen activation of the T-cell (Szabo *et al.*, 1997; Afkarian *et al.*, 2002). Following cytokine-receptor interactions on naïve T-cells, STAT4 and STAT1 are induced (Kaplan *et al.*, 1996; Lighvani *et al.*, 2002).

These transcription factors induce the Th1 lineage specific 'master regulator' T-bet (Afkarian *et al.*, 2002; O'Shea *et al.*, 2011) that is responsible for the activation of Th1 genes, such as IFN-γ, and the negative regulation of Th2 and Th17 cells (Hwang *et al.*, 2005; Djuretic *et al.*, 2007; Lazarevic *et al.*, 2011; Zhu *et al.*, 2012) (Figure 2.4). T-bet induction was significantly reduced in IFN-γ-deficient mice, while stimulation of human myeloid antigen-presenting cells with IFN-γ alone resulted in T-bet induction (Lighvani *et al.*, 2002). For maximum IFN-γ production, it was shown that a second transcription factor, Runx3, was required (Djuretic *et al.*, 2007), suggesting that STAT4 and IL-12 play a redundant role to STAT1 and IFN-γ, and mainly function to enhance the development of Th1 cells and Th1 mediated immune response against *M. tuberculosis.*

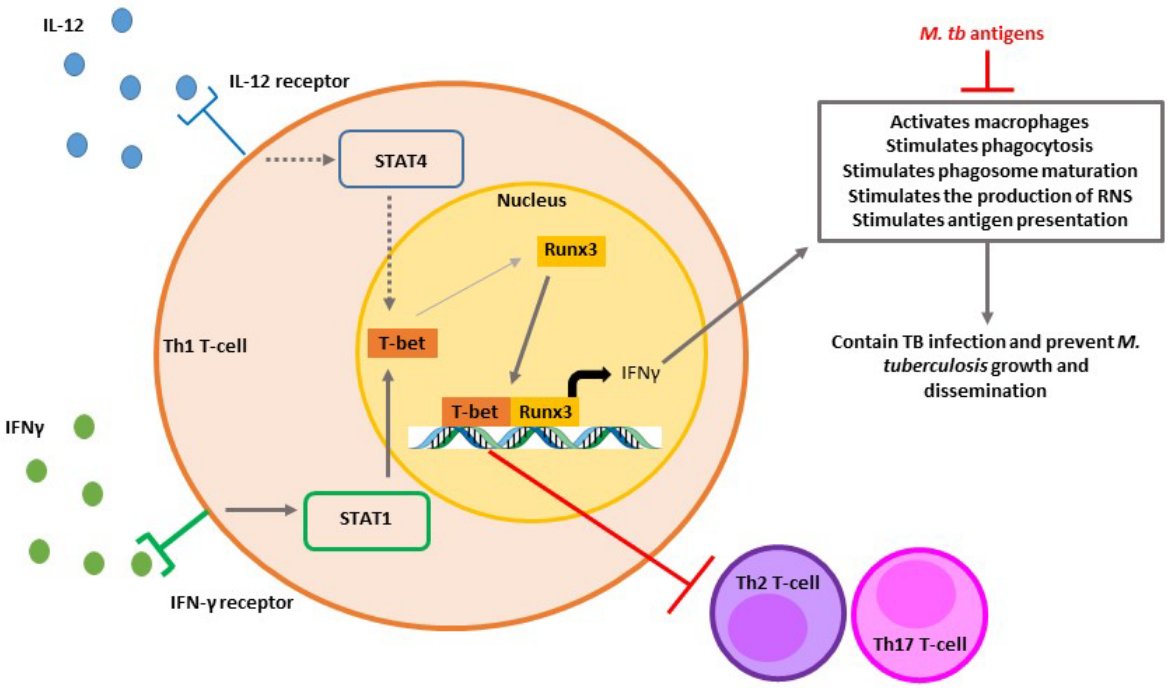

Figure 2.4: Induction of Th1 immune responses during *M tuberculosis*. The Th1 immune response to *M. tuberculosis* infection is mainly mediated through IFN-γ-induced STAT-1-dependent production of proinflammatory cytokines. This process is also mediated through IL-12-induced STAT4-dependent production of proinflammatory cytokines. T-cells in which this occurs are classified as Th1 $CD4^+$ T-cells and have a number of mechanisms that aid in eliminating or containing *M. tuberculosis* in antigen-presenting cells in the lung. As discussed in Chapter 2.2, *M tuberculosis* has developed various ways in which to disrupt this pro-inflammatory response. *(Original image created by C. Young)*.

The importance of IFN-γ and IL-12 during *M. tuberculosis* infection has been well documented using murine knock-out models. IFN-γ-knockout mice were unable to control intracellular *M tuberculosis* growth and showed increased levels of necrosis (Cooper *et al.*, 1993; Flynn *et al.*, 1993). Macrophages isolated from IFN-γ-knockout mice showed reduced surface expression of MHC-II molecules and impaired ability to produce antimicrobial peptides. These IFN-γ-knockout mice were even susceptible to intravenous *M. bovis* BCG infection (Dalton *et al.*, 1993). Mice lacking IL-12 have also shown impaired ability to control the intracellular growth of *M. tuberculosis*, with decreased T-cell activation and accumulation at the site of infection (Orme *et al.*, 1997). Genetic studies done on patients with disseminated mycobacterial infection identified an important role for the IL-12 receptor subunit, IL-12Rβ1. T-lymphocytes isolated from these patients were unable to produce IFN-γ in response to tuberculin. This suggests that the ability of $CD4^+$ Th1 cells to produce effective levels IFN-γ depend on the co-stimulation of IL-12 and IFN-γ with functional receptors (Altare *et al.*, 1998). Based on the literature covered in **Section 2.2**, it is safe to assume that during chronic infection, circulating *M. tuberculosis*

antigens may interfere with Th1 $CD4^+$ T-cell priming and differentiation and could therefore contribute to the impaired IFN-γ production by Th1 cells observed in TB positive patients. When exposed to *M. tuberculosis* antigens, T-cells from TB positive patients showed delayed phosphorylation, thus activation, of ERK and MAPK-p38 with the lowest levels of IFN-γ producing T-cells correlating with greatest reduction in phosphorylation (Pasquinelli *et al.*, 2013).

Although members of the PE/PPE family are being considered for vaccine development due to suggested immunostimulatory effects, there is evidence implicating certain PE/PPE proteins in dampening Th1 mediated cellular responses (Gong *et al.*, 1996; Nair *et al.*, 2009; O' Leary *et al.,* 2011; Khubaib *et al.*, 2016). A study to investigate the effects of co-operonic PE32/PPE65 proteins on the immune response in RAW 264.7 macrophages showed a dose-dependent increase of anti-inflammatory IL-10 and decrease of pro-inflammatory TNF-α (Khubaib *et al.*, 2016). Additionally, the levels of IFN-γ found in the supernatant of PE32/PPE65 stimulated splenocytes were significantly decreased, which correlated with the reduced $CD4^+$ and $CD8^+$ T-cells producing IL-2 and IFN-γ (Khubaib *et al.*, 2016). *M. tuberculosis* infection of macrophages has been shown to induce IL-10 production, which has been implicated in inhibiting phagosome maturation and IFN-γ production (Gong *et al.*, 1996; O' Leary *et al.*, 2011). *M. tuberculosis* PPE18 may contribute to this effect as it has also been shown to induce the production of IL-10 from macrophages (Nair *et al.*, 2009).

2.3.3 The Th17-mediated cellular response during TB infection

Th17 T-cells are most commonly known for the role they play in autoimmune diseases (Steinman, 2007; Zambrano-Zaragoza *et al.*, 2014), suggesting that these cells induce a potentially unfavourable immune response during mycobacterial infection. The development of Th17 cells is mediated by the combined stimulatory signal of IL-6, IL-21, IL-23 and IL-1β (Torrado and Cooper, 2011) (Figure 2.5). Once engaged on the T-cell, these cytokines induce the expression of the transcription factor RORγt in a STAT-3 dependent way (Ivanov *et al.*, 2006).

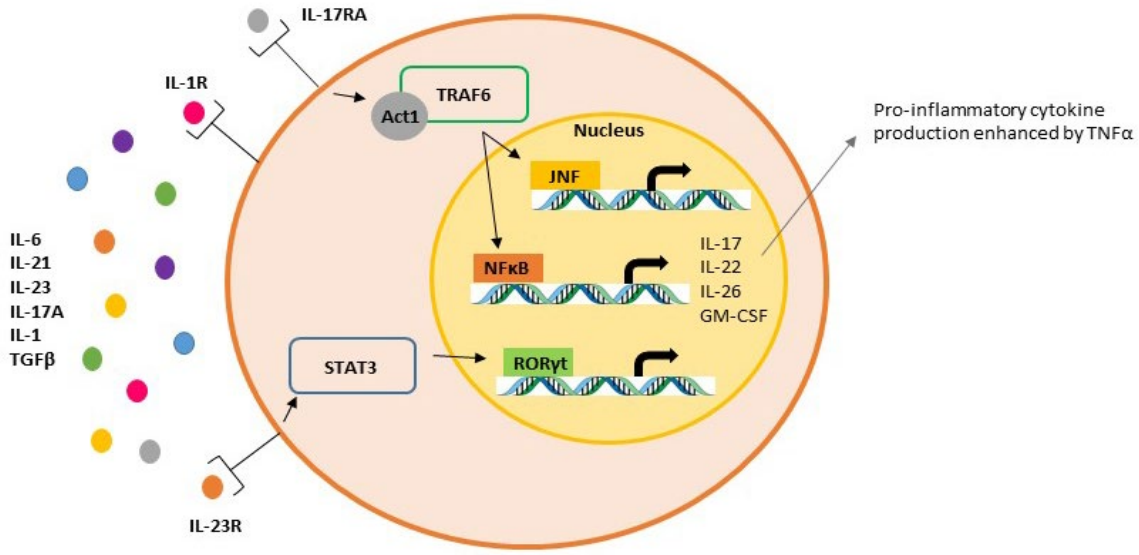

Figure 2.5: Th17 T-cell development and their role in TB disease. *M. tuberculosis* induced Th17 immune responses are initiated following the differentiation of naïve $CD4^+$ T-cells into Th17 $CD4^+$ T-cells. This process is mediated by the presence of various cytokines and their respective interactions with their receptors. Th17 immune responses are mainly mediated through the STAT3-mediated activation of RORγt that induces that transcription of pro-inflammatory cytokines. Alternatively, Th17 differentiation can be mediated by TRAF6-Act1-mediated activation of NFκB and JNF which induces the transcription of pro-inflammatory cytokines. Both processes can be enhanced by TNF-α. *(Original image created by C. Young).*

IL-17 is classified as the major Th17 effector cytokine, however IL-22, IL-26 and GM-CSF also have important roles in the inflammatory process (Codarri *et al.*, 2011; Torrado and Cooper, 2011). IL-17 has been implicated in neutrophil recruitment, granuloma formation and delayed-type hypersensitivity (DTH) responses to PPD (Umemura *et al.*, 2007). The reduced DTH response in the absence of IL-17 suggests that IL-17 is indispensable for an efficient cell-mediated immune response. However, impaired granuloma formation is not necessarily a negative outcome for the progression of TB disease as the granuloma provides a protected niche for *M. tuberculosis* to reside in and may promote dissemination once it bursts.

A population of T-cells known as the γδ T-cells are thought to be responsible for IL-17 production (Umemura *et al.*, 2007). However, this was shown to not be the case in healthy, *M. tuberculosis*-exposed individuals in response to PPD and viable *M. bovis* BCG (Scriba *et al.*, 2008). In these individuals, $CD4^+$ T-cells were shown to be the major contributor to IL-17 production (Scriba *et al.*, 2008). It was suggested that the differences between these two studies could be attributed to the presence of non-protein components in PPD and *M. bovis* BCG that induced cytokines from γδ T-cells. Furthermore, γδ T-cells have mainly been implicated during early immunity whereas $CD4^+$ T-cells are mainly involved during memory responses.

It has been suggested that IL-17 producing $CD4^+$ T-cells are absent during active TB disease (Perreau *et al.*, 2013). However, whole blood from baseline active TB patients (no TB treatment) was shown to have reduced quantities of PPD-specific and BCG-specific IL-17^+ IL-22^+ $CD4^+$ T-cells compared to exposed healthy controls. Consequently, the levels of IL-17 and IL-22 in whole blood of baseline active TB patients was also reduced. Interestingly, the bronchoalveolar lavage (BAL) fluid from baseline active TB patients showed reduced IL-17 and elevated IL-22 levels, which was attributed to Th1-mediated downregulation of Th17 development and IL-17 production during TB (Scriba *et al.*, 2008). Associated with elevated IL-22 in the BAL fluid was the increase of BAL neutrophils and alveolar lymphocytes and a reduction in AMs.

Investigation into Th17-mediated responses following vaccination to an ESAT-6-adjuvanted vaccine demonstrated that IL-17^+ $CD4^+$ T-cells accumulated more rapidly in vaccinated mouse lungs compared to IFN-γ^+ $CD4^+$ T-cells (Khader *et al.*, 2007). The accumulation of Th17 cells in the lung correlated with the induction of CXCR3 (CD183) chemokines, CXCL9, CXCL10 and CXCL11, which was prevented in the absence of IL-17 and IL-23. IFN-γ recall responses were also inhibited in the absence of IL-17 and IL-23, while the absence of IL-23 alone prevented the production of IL-17 from vaccinated mice (Khader *et al.*, 2007). Similarly, IL-17 production in *M. bovis* BCG vaccinated mice challenged with *M. tuberculosis* was also shown to be dependent on IL-23 (Umemura *et al.*, 2007), however human PBMCs stimulated with *M. tuberculosis* H37Rv demonstrated IL-17 production to be dependent on signalling through the IL-1 receptor (Veerdonk *et al.*, 2010).

From the results above, it is speculated that Th17 cells play a role in monitoring the peripheral environment, responding rapidly to antigen stimulation and recruiting other effector cells to control *M tuberculosis* growth. The production of IL-23 seems to play an indispensable role during Th17-mediated protection in vaccinated mice challenged with *M. tuberculosis*, due to its role in the formation of a large mononuclear granulomatous structure and establishing a Th17 memory population following vaccination (Khader *et al.*, 2007).

2.3.4 The PE/PPE-induced cellular response during TB infection

PE/PPE protein interactions with cells of the innate immune system have been shown to have an influence on the pathophysiological outcomes of TB disease (Sampson, 2011). In addition, there are numerous reports of cell-mediated and humoral immune responses to various PE/PPE family members (Sampson, 2011; Brennan, 2017). A comprehensive analysis of the

immunogenicity of 36 PE/PPE proteins, from 4 phylogenetic sub-groups, in *M. bovis*-infected cattle and *M. tuberculosis*-infected humans elegantly demonstrated the immunogenic potential of numerous (1043) PE/PPE-derived peptides. Interestingly, there were very similar immunodominant peptides in bovine and human hosts, and between patients with active and latent TB disease. Numerous PE/PPE peptides induced an immune response that was sustained throughout disease progression, which suggests that these peptides may have an important functional role during pathogenesis (Vordermeier *et al.*, 2012).

The study by Vordermeier *et al.* is the most comprehensive analysis of PE/PPE immunogenicity to date, however, insight into the effect these proteins have on cytokines (other than IFN-γ) and the immunophenotype of responding cell populations was not in the scope of the study. Immunization with PPE39 (Rv2353c) from the hypervirulent *M. tuberculosis* strain Beijing/K was shown to induce a combined Th1/Th17 immune response as measured by the increased levels of IFN-γ, IL-2, IL-6 and IL-17 in the lungs and spleen, 4 and 9 weeks post challenge (Kim *et al.*, 2017). PPE39-immunized mice also had fewer inflammatory lesions and reduced bacterial burden in the lung compared to unimmunized mice (Kim *et al.*, 2017). Interestingly, IFN-γ levels continued to increase between 4 and 9 weeks, whereas the levels of the other cytokines did not. This gives us some insight into the cell populations governing the PPE39-mediated immune response and suggests that Th17 T-cells enhance early protection against challenge, and as the infection becomes more chronic, Th1 T-cells become the major role players in protection (Kim *et al.*, 2017).

The expression of PPE34 (Rv1917c) has been shown to be selectively enhanced in *M. tuberculosis* infected murine macrophages (Schnappinger *et al.*, 2003). PPE34-matured human DCs demonstrated the ability to activate naïve $CD4^+$ T-cells, however their polarization was skewed to an anti-inflammatory Th2-mediated cellular response, as characterised by the production of IL-4, IL-5 and IL-10 (Bansal *et al.*, 2010). $CD4^+$ T-cells isolated from pulmonary TB patients secreted no IFN-γ and significantly higher levels of IL-5 compared to healthy controls following PPE34 stimulation. Furthermore, the Th2-mediated immune response elicited by PPE34 was seen to be critically dependant on the expression of PGE_2 and COX-2 (Bansal *et al.*, 2010). PGE_2 is a biosynthetic product of COX-2 mediated inflammatory enzymatic reactions and has been shown to be a potent inflammatory mediator that favours a Th2 response (Meyer *et al.*, 2003). Th2-mediated responses inhibited Th1 responses as demonstrated by the lack of IFN-γ released by $CD4^+$ T-cells. It would be interesting to investigate the effect of PPE34 on granuloma formation as Th2 cytokines have been implicated

in producing granulocytic granulomas during TB infection as opposed to mononuclear ones (Domingo-Gonzalez *et al.*, 2016)

The effect PE/PPE proteins have on the immune response was further exemplified in a study in which the all ESX-5 *pe/ppe*-associated genes (*ppe25-pe19*) from *M. tuberculosis* H37Rv were deleted (Sayes *et al.*, 2012). Mice infected with the deletion mutant (Δ*ppe25-pe19*) produced significantly higher levels of IFN-γ in response to ESAT-6 and CFP-10 when compared to IFN-γ produced by mice infected with *M. tuberculosis* H37Rv (Sayes *et al.*, 2012). The protective responses elicited by the mutant strain Δ*ppe25-pe19* were also shown to be higher than those produced in response to the recombinant RD1 BCG vaccine (Pym *et al.*, 2003; Sayes *et al.*, 2012). When challenged with *M. tuberculosis*, Δ*ppe25-pe19*-vaccinated mice demonstrated a reduced bacterial burden in the lungs and spleen with an evident decrease in lung lesions, when compared to BCG-vaccinated mice (Sayes *et al.*, 2012). Furthermore, the Δ*ppe25-pe19* strain proved safe to use in severely immunocompromised mice while inducing IFN-γ in response to CFP-10 and ESAT-6. These results provide compelling evidence that warrants the further investigation of *M. tuberculosis*::Δ*ppe25-pe19* as a vaccine candidate.

As such, several epitopes from PPE25 and PE19 have demonstrated substantial cross-reactivity with $CD4^+$ T-cells (Sayes *et al.*, 2012). It has been speculated that multiple PE/PPE proteins could be recognised by the same T-cell population due the significant T-cell response elicited by PE/PPE peptides from the conserved N-terminal (Vordermeier *et al.*, 2012). This was confirmed when short-term bovine T cell lines, raised by primary stimulation with a particular PE or PPE peptide were shown to release IFN-γ in response to stimulation with a different PE or PPE peptide (Vordermeier *et al.*, 2012). These results suggest that the differentially expressed *pe/ppe* genes (with variations in their amino acid sequences) may still be recognised by cross-reactive T-cells, making these proteins promising candidates for the development of new TB vaccines.

The studies highlighted above have provided some insight into the immune response elicited to selected members of the PE/PPE protein family. However, information regarding the immune response elicited by the PE_PGRS and PPE_MPTR subgroups is desperately required to gain a better understanding of the functional and immunological consequences of their highly variable C-terminal region. A member of the PPE_MPTR subfamily, PPE_MPTR42 (Rv2608), has been identified as a promising T-cell antigen for the development of new TB vaccines (Bertholet *et al.*, 2008; Baldwin *et al.*, 2009) and has been evaluated among 68 other *M. tuberculosis* antigens as a vaccine candidate in a murine model of TB (Bertholet *et al.*,

2008). Following challenge with *M. tuberculosis* H37Rv and Erdman, PPE_MPTR42 adjuvanted with low dose CpG (PPE_MPTR42/CpG) displayed the highest protective efficacy as demonstrated by the greatest decrease in mean pulmonary CFU counts, which were comparable to CFUs in the lungs of recombinant-BCG-vaccinated mice. Furthermore, PPE_MPTR42 elicited strong $CD4^+$ and $CD8^+$ T-cell responses to a variety of HLA types and immune responses were predominately Th1-skewed (Bertholet *et al.*, 2008).

Due to the protective efficacy and strong immunogenicity elicited by PPE_MPTR42, it was included with Rv1813c (conserved hypothetical protein), Rv3620 (esxW) and Rv3619 (esxV) in the ID93 vaccine candidate, adjuvanted with GLA-SE (Bertholet *et al.*, 2010). ID93/GLA-SE was shown to be highly immunogenic in mice, guinea pigs and cynomolgus monkeys and induced the formation of polyfunctional $CD4^+$ Th1 T-cells that produced antigen specific IFN-γ, TNF-α and IL-2. Following immunization with ID93 and challenge with virulent or multi-drug resistant *M. tuberculosis,* there was a significant reduction in pulmonary bacterial burden in ID93-immunized mice versus the control mice. Furthermore, boosting BCG-vaccinated guinea pigs with ID93/GLA-SE prevented death following challenge with *M. tuberculosis* H37Rv and resulted in reduced pulmonary pathology and bacterial burden (Bertholet *et al.*, 2010).

PPE_MPTR42 has also been included in a recombinant BCG (rBCG) vaccine with Ag85A and ESAT-6 (Lu *et al.*, 2012). Mice immunized with rBCG elicited a more effective humoral response and an improved Th1 immune response compared to mice immunized with *M. bovis* BCG. The immune response to rBCG was primarily governed by cytotoxic $CD8^+$ T-cells as seen by the significantly higher proliferation of $CD8^+$ T-cells in rBCG-vaccinated compared to *M. bovis* BCG-vaccinated mice. The improved cell-mediated immune response was characterized by the production of Th1 cytokines, higher antibody titres, and more $CD8^+$ T-cells. Th1 cytokines induced Th1 mediated immune responses which were necessary for protection against mycobacteria, furthermore $CD8^+$ T-cells eliminated mycobacterial infection by lysing infected cells.

2.4 Conclusion

In this review we have highlighted the heterogenous immune response to TB infection, a complex reaction that is not fully understood. The large number of innate immune receptors and innate mechanisms *M. tuberculosis* can interact with and modulate, make characterising cell-mediated immune responses very challenging. This becomes even more complicated when

investigating the effect of understudied *M. tuberculosis* protein families, such as the PE/PPE proteins. Although tremendous advances have been made in our knowledge about *M. tuberculosis* and its modulatory abilities on the host immune system, it is clear that there are still many areas of uncertainty and speculation. Continued investigation into the cellular responses to *M. tuberculosis* will aid in identifying potential mechanisms and antigens that can be targeted for immunodiagnostics and vaccine development. As highlighted in this review, members of the PE/PPE protein family have shown potential as possible vaccine candidates, however more investigation needs to be done concerning their role in the immune response (**See Chapter 4)**.

An effective immune response is achieved when both the innate and adaptive immune systems work synergistically to overcome an infection, therefore, in this review chapter, we attempted to unravel the effect PE/PPE, and other *M. tuberculosis* proteins have on the innate and adaptive immune response during TB disease. In the remaining chapters of this thesis, we will explore how the adaptive immune response is activated in response to PPE_MPTR proteins and characterise the type of cell-mediated immune response induced by these peptides in an African context. Furthermore, their potential as a correlate of active TB disease will also be evaluated.

Properly understanding how *M. tuberculosis* exploits and manipulates both arms of the host immune system may help to decipher the highly heterogeneous immune response observed during infection with *M. tuberculosis.* With this knowledge, new approaches can be developed that prevent *M. tuberculosis* from manipulating the host immune response and may succeed in eradicating *M. tuberculosis* shortly after entry into host cells.

Chapter 3

Methods and Materials

3.1 Ethics Statement

Ethical approval for this study was obtained from the Committee for Human Research of the University of Stellenbosch with ethics number N16/05/070 (**Section 7.1**). All the study participants gave written informed consent for participation in the study (**Section 7.2**).

3.2 Peptide reconstitution

PPE_MPTR, ESAT-6 (EsxA) and CFP-10 (EsxB) peptides (**Table 3.1**) used in this study were synthesised by GL Biochem Ltd (Shanghai) and subjected to HPLC/MS to confirm purity. Lyophilized peptides were centrifuged at 18 928 rcf for 2 minutes prior to reconstitution to 4 mg/ml in 800 µl Phosphate Buffered Saline (PBS; Thermo Fisher). Peptides were stored as 200 µl and 10 µl aliquoted volumes at -80°C until use. Two positive controls were selected for whole blood assays (WBAs); *Phaseolus vulgaris* phytohaemagglutinin (PHA) (10 µg/ml) (Sigma-Aldrich) as a non-specific positive control to confirm that the stimulation assay is working, and *M. tuberculosis* purified protein derivative (PPD) (10 µg/ml) (Sigma-Aldrich) as a *M. tuberculosis*-specific control. Phosphate-buffered saline (PBS) was used as a negative, unstimulated control.

Table 3.1: ESAT-6 and CFP-10 peptides used in this study (Vordermeier *et al.*, 2001)

Epitope	*M. tb* H37Rv annotation	Sequence
CFP-10.1	Rv3874	MAEMKTDAATLAQEAGNF
CFP-10.2		QEAGNFERISGDLKTQ
CFP-10.3		ERISGDLKTQIDQVESTA
CFP-10.4		IDQVESTAGSLQGQWRG
CFP-10.5		GSLQGQWRGAAGTAAQAA
CFP-10.6		AGTAAQAAVVRFQEAANK
CFP-10.7		VVRFQEAANKQKQELDEI
CFP-10.8		QKQELDEISTNIRQAGVQYS
CFP-10.9		NIRQAGVQYSRADEEQQQ
CFP-10.10		RADEEQQQALSSQMGF
ESAT-6 p45	Rv3875	MTEQQWNFAGIEAAAS
ESAT-6 p46		AGIEAAASAIQGNVTS
ESAT-6 p47		AIQGNVTSIHSLLDEG
ESAT-6 p48		IHSLLDEGKQSLTKLA
ESAT-6 p49		KQSLTKLAAAWGGSGS
ESAT-6 p50		AAWGGSGSEAYQGVQQ
ESAT-6 p51		EAYQGVQQKWDATATE
ESAT-6 p52		KWDATATELNNALQNL
ESAT-6 p53		LNNALQNLARTISEAG
ESAT-6 p54		ARTISEAGQAMASTEG
ESAT-6 p55		QAMASTEGNVTGMFA

3.3 Peptide concentration optimization experiments

For optimization of PPE_MPTR peptide concentrations, two participants were recruited from The Division of Molecular Biology and Human Genetics, Faculty of Medicine and Health Science, Stellenbosch University. One participant had previously tested positive for the interferon-gamma (IFN-γ) release assay (IGRA) and one participant tested negative. Nine millilitres (9 mL) of undiluted, heparinized whole blood was obtained from both study participants with informed signed consent.

To determine the optimal concentration for peptide reactivity, a range of peptide concentrations was used to stimulate whole blood in a whole blood assay (WBA) experiment. Peptides were diluted into a final volume of 20 µl in a 96-well U bottom plate prior to the addition of 180 µl undiluted, heparinized whole blood. Peptide concentrations ranged from 20, 10, 5 or 1 µg/ml for the peptides P1-P19 and controls peptides ESAT-6 and CFP-10, in a final volume of 200 µl. The 96-well U bottom plates were incubated for 24 hours in a humidified, 5% CO_2, 37°C

incubator, after which plates were centrifuged at 500 rcf for 10 minutes. Approximately 100 µl of supernatant was harvested from each well and stored at -80°C until Luminex analysis.

The concentration (pg/ml) of six host markers [interferon-gamma (IFN-γ); interleukin-6 (IL-6); IL-10; IL-17A; IL-13 and tumour necrosis factor-alpha (TNF-α)] were measured from supernatants using a customized Human Magnetic Luminex Screening Assay (R&D Systems, Whitehead Scientific) on the Bio Plex platform (Bio Plex™, Bio Rad Laboratories), according to the manufacturer's instructions. Culture supernatants were thawed at room temperature (RT) prior to a 2-fold dilution with calibrator diluent RD6-52. One Luminex kit was used to determine the analyte concentrations from 100 µl of sample in two 96-well flat bottom plates. The standard curve range between analytes varied and can be seen in **Table 3.2**. Bio-Plex Manager Software, version 4.1.1 was used to analyse the bead median fluorescence intensity and to plot fluorescent intensity values to corresponding analyte concentrations on a standard curve. The upper and lower limit of detection for each analyte on the standard curve was generated using a set of standards as per the manufacturer's instruction.

Table 3.2: Standard curve range of analytes during peptide concentration optimization experiments

	Standard Curve Concentration Range (pg/ml)
IFN-γ	50 – 15 000
IL-13	300 – 91 000
IL-6	0 – 1 200
IL-10	0 – 1 200
IL-17A	10 – 4 000
TNF-α	0 – 3 000

Before data analyses was performed on the raw data generated from the Bio-Plex Manager Software, the controls were scrutinized to ensure they were within their specified ranges of the kit. Following this, the out-of-range (OOR) values for each analyte per plate were removed from the raw data (Microsoft Excel, Windows 10 Pro, version 1803). If the observed analyte concentration for a sample was below the limit of detection (<OOR), one was subtracted from the lowest observed concentration of that specific analyte on that plate (<OOR-1). If the observed analyte concentration for a sample was above the limit of detection (>OOR), one was added to the highest observed analyte concentration for the specific plate (>OOR+1). Microsoft Excel was used to analyse cytokine concentration data. The data generated in this experiment was used to select peptide concentrations for the experiments performed in **Section 3.4** and **3.5**.

3.4 Validating the immunogenicity of population-tailored PPE_MPTR peptides

To determine if computationally-identified PPE_MPTR epitopes elicit an immune response in a subset of the African population, eleven study participants from South Africa, Zimbabwe, Congo and Ethiopia (**Table 3.3**) were recruited from the Faculty of Medicine and Health Science, Stellenbosch University.

Table 3.3: Study participants used to assess the immunogenicity of the chosen PPE_MPTR peptides.

Population Heritage	No. of participants (n)	No. of QFN+ participants (n)
South Africans	6	2
Zimbabwean	2	0
Congolese	1	1
Ethiopian	2	2
Total	**11**	**5**

Table 3.4: The chosen concentration for whole blood stimulation with PPE_MPTR peptides and control peptides, ESAT-6 and CFP-10. The concentrations of PPE_MPTR peptides were determined by comparing the cytokine responses to a gradiant of PPE_MPTR peptide concentrations. The concentration at which the most cytokines were produced at the highest concentrations were chosen.

Peptide	Final [peptide] in 200 µl
P1 and P19	5 µg/ml
P2 to P17	10 µg/ml
P18	1 µg/ml
ESAT-6 peptide pool*	10 µg/ml
CFP-10 peptide pool*	10 µg/ml
* Optimal concentration of 10 µg/ml determined from literature	

Nine millilitres (9 mL) of undiluted, heparinized whole blood was obtained from all study participants with informed signed consent. Previous exposure to *Mycobacterium tuberculosis* was assessed using the QuantiFERON®-TB Gold Test. Participants with previous exposure to *M. tuberculosis* tested positive for the IFN-γ-ELISA (QuantiFeron® +; QFN+), and those without previous exposure to *M. tuberculosis* tested negative for the IFN-γ ELISA (QFN-). All participants were HIV-negative, Hepatitis-B-negative and without signs or symptoms of any illness at the time of sample collection. On the day of the WBA experiment, 20 µl of the peptides were aliquoted into 96-well U-bottom plates and 180 µl of undiluted, heparinized whole blood was added to the peptide and control wells, to achieve the optimized final peptide

concentration (**Table 3.4)**. The plates were incubated for 24 hours in a humidified, 5% CO_2, 37°C incubator, after which, plates were centrifuged at 500 rcf for 10 minutes. Approximately 100 µl of supernatant was harvested from each of the peptide and control wells and stored at -80°C until Luminex analysis.

A customized Human Magnetic Luminex Screening Assay (R&D Systems, WhiteSci) was used to measure the concentration of seven host markers [IFN-γ; IL-1β; IL-4; IL-6; IL-10; IL-17A; TNF-α] on the Bio Plex platform (Bio Plex™, Bio Rad Laboratories), according to the manufacturer's instructions. The customized Human Magnetic Luminex Screening Assay was performed as previously described in **Section 3.3**. The standard curve range for the different analytes is provided in **Table 3.5**.

Table 3.5: Standard curve concentration range of analytes

	Standard curve concentration range (pg/ml)
IL-1β	10 - 5 000
IL-10	4 000 - 12 000
IL-4	10 - 4 000
TNF-α	10 - 3 000
IFN-γ	50 – 15 000
IL-6	1 – 1 500
IL-17A	10 – 4 000

The raw data generated from the Bio-Plex Manager Software was manually filtered as previously described in **Section 3.3**. In addition to this, the percentage of <OOR values was calculated, and analytes containing more than 70% <OOR values were omitted from further analysis. This data was imported into GraphPad Prism version 8.3.0 where the PPE_MPTR-specific cytokine responses to the 19 PPE_MPTR peptides were evaluated. Box-and-whisker plots depicting the median cytokine response between QFN+ and QFN- participants of this cohort were plotted using the Log cytokine concentration values (pg/ml) in response to peptides. The peptides which induced the production of the four or more cytokines (above unstimulated levels) were selected for flow cytometric analysis. R-Studio version 3.5.3 was used to do statistical analyses on these data and can be seen in **Section 3.6**.

3.5 Assessing the diagnostic potential of population-tailored PPE_MPTR peptide

To assess the diagnostic potential of the computationally predicted PPE_MPTR epitopes, twenty-one study participants (n=21) were recruited from high incident TB communities surrounding Tygerberg Hospital, namely Ravensmead and Uitsig, Cape Town, South Africa (**Table 3.6**). Participants with baseline active TB were newly diagnosed cases, showing TB symptoms, with a positive *M. tuberculosis* culture and a positive GeneXpert result. Participants with latent TB infection (LTBI) were all asymptomatic with a positive IFN-γ-ELISA result and a negative *M. tuberculosis* culture and GeneXpert result. Healthy controls were negative for the IFN-γ-ELISA, GeneXpert and *M. tuberculosis* culture. All participants were HIV- and Hepatitis-B-negative. To increase the sample size of this cohort for post-hoc statistical analyses, the South African study participants from **Section 3.4** (**Table 3.3**) were also included.

Only South African study participants from **Section 3.4** were included in the statistical analyses as the individuals recruited from high incident TB communities included only South African participants. Study participants were split into 2 groups; '*cases*' and '*controls*' and can be seen in **Table 3.6**.

Table 3.6: Study participants used to investigate the diagnostic potential of PPE_MPTR peptides. Twenty-one study participants were recruited from high incident TB communities surrounding Tygerberg Hospital. To increase the sample size of the cohort for pos-hoc statistical analysis, six South African individuals from **Section 3.4** were also included.

Groups	Study participants	Sample size (n)	Total sample size in analysis (N)
Cases	TB*	5	**5**
Controls			
LTBI	LTBI* QFN+ (SA)	5 2	**7**
HC	HC* QFN- (SA)	11 4	**15**
Total number of samples in statistical analysis			**27**

* Study participants recruited from high incident TB communities surrounding Tygerberg Hospital
TB = active TB individuals; LTBI = latently infected individuals; HC = healthy controls

Nine millilitres (9 mL) of undiluted, heparinized whole blood was obtained from all study participants as mentioned in **Section 3.4**, to measure the cytokine response to the candidate epitopes. WBA experiments were performed as described in **Section 3.4.** and approximately 100 µl supernatant from each well was stored at -80°C until Luminex analysis. A customized

Human Magnetic Luminex Screening Assay (R&D Systems, Whitehead Scientific, South Africa); was used to measure the concentration of seven host markers [IFN-γ; IL-1β; IL-4; IL-6; IL-10; IL-17A; TNF-α] in the supernatants of TB, LTBI and healthy control samples on the Bio Plex platform (Bio Plex™, Bio Rad Laboratories), according to the manufacturer's instructions (Whitehead Scientific, South Africa). The Luminex Multiplex Immunoassay was performed as stated in **Section 3.4**. The standard curve range between analytes varied and can be seen in **Table 3.5**. The raw data generated from the Bio-Plex Manager Software was manually filtered as stated in **Section 3.3** and analysed as described in **Section 3.4**. Statistical analyses were performed on these data using R-Studio version 3.5.3 as described in **Section 3.6**.

3.6 Luminex Multiplex Immunoassay Data Analysis

The data generated from Luminex Multiplex Immunoassay experiments in **Sections 3.4** and **3.5** underwent statistical analyses using R-Studio version 3.5.3. Briefly, the data for thirty-two individuals, seven analytes and 24 stimulations underwent quality assessment and missing concentration-values removed using the 'Base-R' (R Core Team, 3.5.3) and 'TidyVerse' (Wickam, 2017) packages on R-Studio. These data were transformed by winsorizing, to limit the effect of outlier data points on the statistical analyses. The winsorized mean of data was obtained by replacing the smallest and the largest values in the dataset by the data values closest to them. Using the winsorized data, the stimulation-specific cytokine concentrations were determined by subtracting the unstimulated conditions from the stimulated conditions. PBS-stimulated cytokine responses were classified as 'unstimulated/blank' and ESAT-6 and CFP-10 cytokine responses were used as positive controls.

The winsorized data generated from the Luminex experiments in **Section 3.5** were statistically analysed. This data, '*All-Groups Dataset*' included cytokine responses from 27 participants of South African origin, namely, the 21 individuals recruited from high-incident TB communities surrounding Tygerberg hospital, and the six South African individuals from **Table 3.3**. The Wilcoxon-signed-rank-test was used to compare cytokine responses to PPE_MPTR peptides. The comparisons included: *Controls* vs *Cases*, LTBI vs TB and LTBI vs HC. Bonferroni-Test-Correction, with a false discover rate (FDR) = 0.05, was used to adjust for multiple testing. Due to the small sample size of this study, the raw significant p-values were used to generate boxplots that demonstrated significant differences in cytokine production between groups.

3.7 Red Blood Cell Lysis and Peripheral Blood Cell Isolation

To determine the proportions of immune cell subsets and their levels of activation in response to PPE_MPTR peptides, the remaining whole blood pellet from the WBA was lysed and cryopreserved for subsequent flow cytometric analyses. The red cell pellet was incubated with 2 mM ethylenediaminetetraacetic acid (EDTA) for 15 minutes at RT. Following incubation, the red pellet was added to 1X FACS Lysing Solution (Becton-Dickinson Biosciences; BD Biosciences), in the dark. The cells were vortexed on maximum speed for 10 seconds and incubated in the dark for 10 minutes, followed by centrifugation at 500 rcf for 10 minutes. Cells were immediately placed on ice before discarding the supernatant. The remaining cell pellet was resuspended in 500 µl ice-cold fetal bovine serum (FBS), to which 500 µl cryosolution (2% DMSO; 8% FBS) was added (drop-wise). Cells (1 mL) were placed in a MrFrosty freezing container (Thermo Scientific) filled with 250 mL 100% isopropanol for 24-hours at -80°C, and subsequently stored at -80°C.

3.8 Flow cytometry

Flow cytometry was performed on selected peripheral blood cell samples from the 21 individuals recruited from high-incident TB communities surrounding Tygerberg hospital (**Section 3.5**). Samples were chosen based on the number of cytokines produced in response to individual PPE_MPTR peptides as measured in Luminex assays and only samples stimulated with peptides inducing the production of more than four cytokines were chosen for flow cytometric analysis. The distribution of immune cells, memory and activation states were identified using a panel of ten fluorophore-conjugated monoclonal antibodies (mAbs) (BD BioSciences and BioLegend) (**Table 3.7**).

Table 3.7: Flourophore-conjugated monoclonal antibodies chosen for this study

Lymphocyte population	Surface marker	mAb	Clone	Isotype control	mAb dilution	Source
$CD8^+$ T-cells	CD8	FITC	SK1	Mouse IgG_1, κ	1:10	BD BioSciences
$CD3^+$ T-cells	CD3	BV421	UCHT1	Mouse IgG_1, κ	1:40	BD BioSciences
$CD4^+$ T-cells	CD4	APC-H7	SK4	Mouse IgG_1, κ	1:40	BD BioSciences
B-cells	CD19	BB700	HIB19	Mouse IgG_1, κ	1:40	BD BioSciences
Th1 cells	CD183	PE	G025H7	Mouse IgG_1, κ	1:10	BioLegend
Th2 cells	CD193	BV605	5E8	Mouse IgG_{2b}, κ	1:10	BioLegend
Th17 cells	CD196	APC	G034E3	Mouse IgG_{2b}, κ	1:20	BioLegend
Memory cells	CD45RA	BV510	HI100	Mouse IgG_{2b}, κ	1:40	BioLegend
	CD28	PE-Cy7	CD28.2	Mouse IgG_1, κ	1:160	BioLegend
Activated cells	CD25	PE-Cy5	BC96	Mouse IgG_1, κ	1:80	BioLegend

3.8.1 Antibody Staining

Cryopreserved peripheral blood cell samples (1 mL) were thawed at RT before the cells were added to 10 mL staining buffer (2% FBS in PBS) and centrifuged at 400 rcf for 5 minutes to retain the cell pellet. The staining buffer was discarded, and the cell pellet was transferred to a 96-well U-bottom plate before centrifugation at 400 rcf for 5 minutes. The remaining staining buffer was discarded from the plate, and the cell pellet resuspended in 20 µl mAb master mix. The antibody master mix consisted of PBS with all ten mAbs at the optimal concentrations as decided from titration experiments (**Section 3.8.2**). The cells were incubated with the mAb mastermix in the dark for 60 minutes at 4°C, resuspending mid-way through the incubation. Cells were subsequently resuspended in 200 µl staining buffer and centrifuged at 400 rcf for 5 minutes. The staining buffer was discarded and the cells were washed again with 200 µl staining buffer (without resuspending). Following centrifugation at 400 rcf for 5 minutes, the cell pellet was resuspended in 200 µl staining buffer and placed in the dark at 4°C until acquisition on the BD LSR II™ using the BD FACSDiva 8.0.1 software.

3.8.2 Antibody titration and voltration experiments

Antibody titration and voltration optimization experiments were performed for each mAb in this study. Antibody titration experiments were performed to determine which mAb concentration was most optimal in identifying the cell population of interest. PHA-stimulated whole blood was used for CD45RA-BV510, CD28-PE-Cy7 and CD25-PE-Cy5 mAb titrations. These mAbs are specific for activation and memory receptors, therefore PHA-stimulated blood was used to activate the whole blood cells, allowing the identification of these activated populations (**Table 3.7**). Unstimulated whole blood was used for CD8-FITC, CD3-BV421, CD4-APC-H7, CD19-BB700, CD183-PE, CD193-BV605 and CD196-APC mAb titrations. These receptors are expressed on lymphocyte populations regardless of activation, and therefore unstimulated whole blood could be used. All whole blood samples were prepared using the same experimental conditions as study samples. All samples stained for antibody and voltration experiments were done using the protocol in **Section 3.8.1**.

The starting serial dilution for each mAb titration was twice that of the concentration recommended in the antibody datasheet. Six serial dilutions (1:10, 1:20, 1:40, 1:80, 1:160) were prepared for all mAbs except for CD8-FITC, which also included a 1:5 dilution. An unstained control was included for each mAb to identify the negative population. The serial dilutions were prepared in 0.5 mL Eppendorf tubes® in a final volume of 60 µl. For a starting serial dilution of 1:10, 6 µl of undiluted mAb was added to 54 µl staining buffer and mixed well, after which 30 µl was serially transferred until all appropriate dilutions were made. The peripheral blood cell samples used for antibody titration experiments were stained according to the protocol in **Section 3.8.1**, however samples were incubated in BD polystyrene flow tubes instead of a 96-well U bottom plate. Data was acquired on the BD LSR II™ using the BD FACSDiva 8.0.1 software. The data was analysed using the FlowJo™ 10.6.1 software to obtain the median fluorescent intensity (MFI) of the negative and positive populations for each mAb. This data was exported to Microsoft Excel and converted to a ratio (MFI_{pos}/MFI_{neg}) which was used to generate line graphs. The optimal mAb concentration was determined by the highest MFI_{pos}/MFI_{neg} ratio as seen on the line graph.

Following the identification of optimal mAb concentration, voltration optimisation experiments were performed to identify which voltage setting best separates the negative and positive cell populations. PHA-stimulated whole blood samples were stained according to the protocol in **Section 3.8.1**, however samples were incubated in BD polystyrene flow tubes instead of a 96-well U bottom plate. Samples were acquired at different voltages between 300V

and 800V in 50V increments and the acquired data was further analysed using FlowJo™ 10.6.1 software to identify which voltage provided the best separation of positive and negative populations per antibody.

3.8.3 Compensation and FMO controls

Compensation was performed to limit fluorescent spill-over of excited fluorophores into other detectors on the flow cytometer. Fluorescent Minus One (FMO) experiments were used to evaluate the effect of spill-over of fluorochromes into the channel of interest and to ensure that the compensation set-up had no errors. FMO are samples that include all mAbs except the one of interest, allowing the true positive population to be identified. FMO controls were acquired each time study sample acquisition occurred to aid in identifying the true positive populations during data analysis and to account for the variable detector settings between runs as mentioned in **Section 3.8.4**. PHA-stimulated peripheral blood cell samples were used for FMO experiments and stained according to the protocol in **Section 3.8.1**.

Compensation controls were prepared for each acquisition and mAb using the BD Anti-mouse Compensation Particle set (LOT: 552846; BD BioSciences). An unstained control was also included to identify the negative population. Briefly, one drop of each compensation particle (negative comp bead and comp bead anti-mouse) was added to 100 µl staining buffer containing the appropriate mAb concentration. This was vortexed and incubated in the dark for 1 hour at 4°C after which 2 mL staining buffer was added to the beads, which were centrifuged at 200 rcf for 10 minutes. The pellet was resuspended in 500 µl staining buffer and kept in the dark at 4°C until acquisition. Compensation was calculated using MFI values by the BD FACSDiva 8.0.1 software before sample acquisition on the BD LSR II™ (**Table 3.8**). Compensation was also performed during data analyses on FlowJo™ 10.6.1 and applied to all the samples acquired under the same acquisition settings.

Table 3.8: Flourescent Dectector Target MFI Values for each mAb

Detector	Target MFI ± 10%	Target MFI Range
FITC	2210± 221	1989 – 2431
PE	47328 ± 4732	42 596 – 52 060
PE-Cy5	60 490 ± 6049	54 441 – 66 539
BB700	25 763 ± 2576	23 183 – 28 339
PE-Cy7	10 271 ± 1027	9244 – 11 278
BV421	18 030 ± 1803	16 227 – 19 833
BV510	17 946 ± 1794	16 152 – 19 740
BV605	16 769 ± 1676	15 093 – 18 445
APC	52 138 ± 5313	46 825 – 57 451
APC-H7	1218 ± 121	1096 – 1339

3.8.4 Sample Acquisition

Samples were acquired on the BD LSR II™ flow cytometer at the Central Analytical Facility (CAF) at The Faculty of Medicine and Health Sciences, Tygerberg Campus and at the IDM Flow Core Facility, University of Cape Town. The FACSDiva 8.0.1 software was used to create data from the flow cytometers as FCS files.

Before acquiring samples on the BD LSR II™, BD FACSDiva CS&T Research Beads (LOT: 82158; BD BioSciences) were used to ensure the cytometer was properly calibrated before use. The detector settings (voltage) used for each parameter, except forward scatter (FSC), fluctuated between runs (**Table 3.9**). As a consequence, populations shift during acquisition and the appropriate controls (**Section 3.8.3**) needed to be included during each sample acquisition. Compensation controls were acquired until 5000 events were recorded and FMO controls were recorded until 10 000 events were recorded. FMO controls can be used to adjust the gates between positive and negative populations during data analysis on FlowJo™ 10.6.1. Fully stained samples were acquired until 1 000 000 events were recorded or once the available volume of sample was depleted.

Table 3.9: LSR II Configuration and detectors used to acquire samples during this study.

Laser	Wavelength	Detector array	Detector	Parameter	Voltage range (V)
Blue	488nm	Octagon	FSC	FSC	505
			A	PE-Cy7	502-504
			B	BB700	503-507
			C	PE-Cy5	604-613
			E	PE	545-554
			F	FITC	500-505
			G	SSC	352-355
Violet	405nm	Trigon	A	BV605	497-508
			B	BV510	501-517
			C	BV421	500-525
Red	633nm	Trigon	A	APC-H7	690-695
			C	APC	655-668

3.8.5 Data Analysis for Flow Cytometric Data

Sample acquisition on the BD LSR II™ generated FCS files that were exported from the FACSDiva software. The FCS files were imported and analysed using FlowJo™ 10.6.1. Compensation was calculated on FlowJo™ 10.6.1 and the compensation matrix analysed to determine if any parameters needed adjusting to get clear separation between populations. Compensation was applied to all sample and FMO controls run together on the same day. FMO samples were used to set up the gating strategy template (**Figure 3.1** and **Figure 3.2**) on the FlowJo™ workspace that was applied each time samples were analysed. When analysing the data files, a plot of the cytometer time run (SSC-A vs Time) was analysed to access the stability of the cytometer during each run. Stable time gates were further analysed using FSC-H vs FSC-A to identify the single cells detected by the lasers. The single cells were separated based on size (SSC-A vs FSC-A) to identify the lymphocyte fraction within which, the T- and B-cells were distinguished and immunophenotyped (**Figure 3.1** and **Figure 3.2**).

The relative frequencies of T-helper cell populations (Th1, 2 and 17) were calculated as a percentage of the $CD3^+CD4^+$ T-cell population ($CD4^+$ T-cells). The frequency of T-helper cell populations in different memory states (T_N, T_{EM}, T_{CM} and T_{TEMRA}) was calculated as a percentage of the grandparent T-helper cell population. The frequency of activated memory populations was calculated as a percentage of the T-helper population. All statistical analyses were done using FlowJo™ 10.6.1.

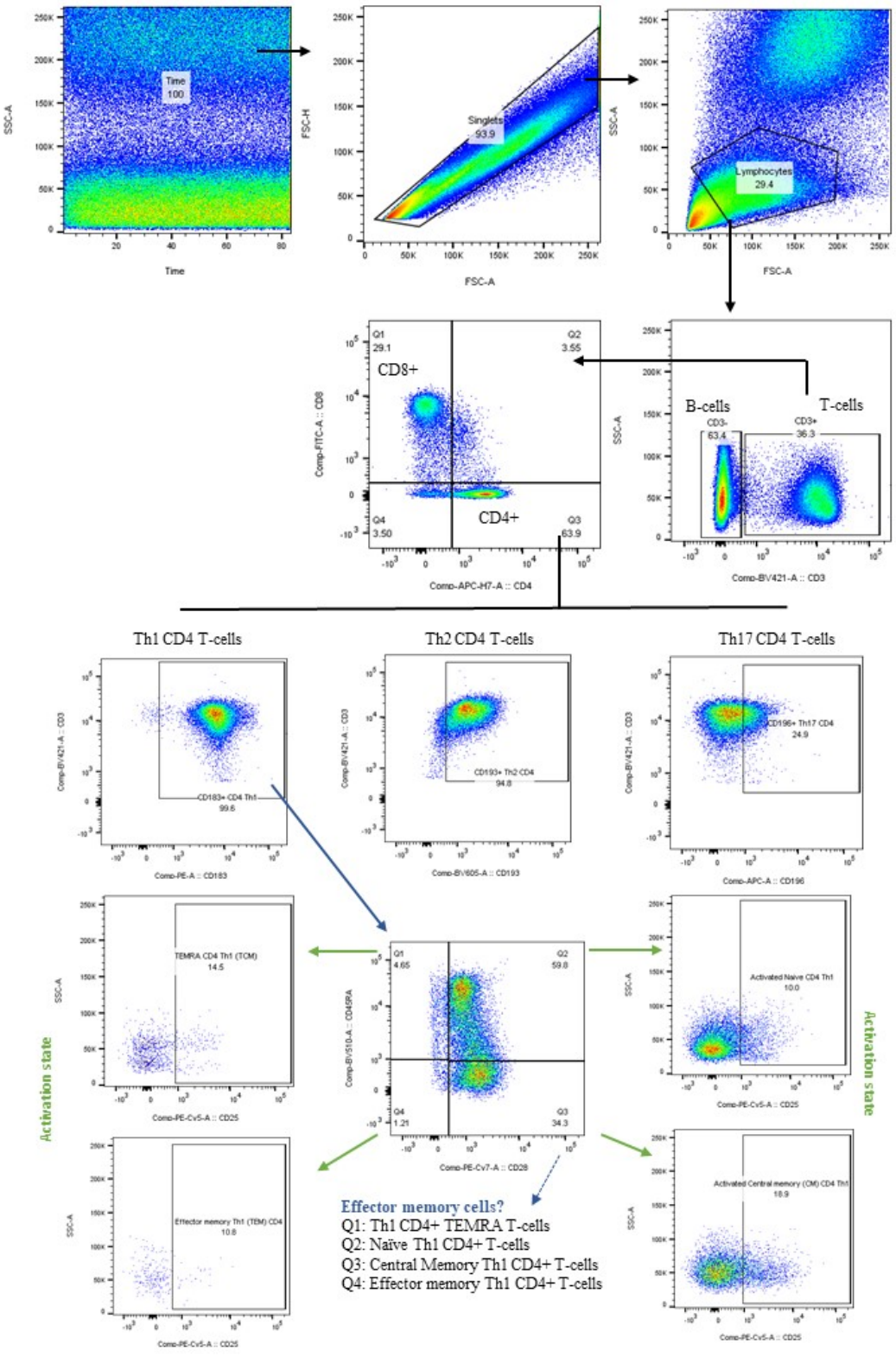

Figure 3.1: Flow cytometry gating strategy applied to identify the relative numbers and activation states of $CD3^+CD4^+$ and $CD3^+CD8^+$ T-lymphocytes. Firstly, the T-helper differentiation state was identified (Th1, Th2, Th17), followed by the relavant proportion of memory cells and their subsequent levels of activation.

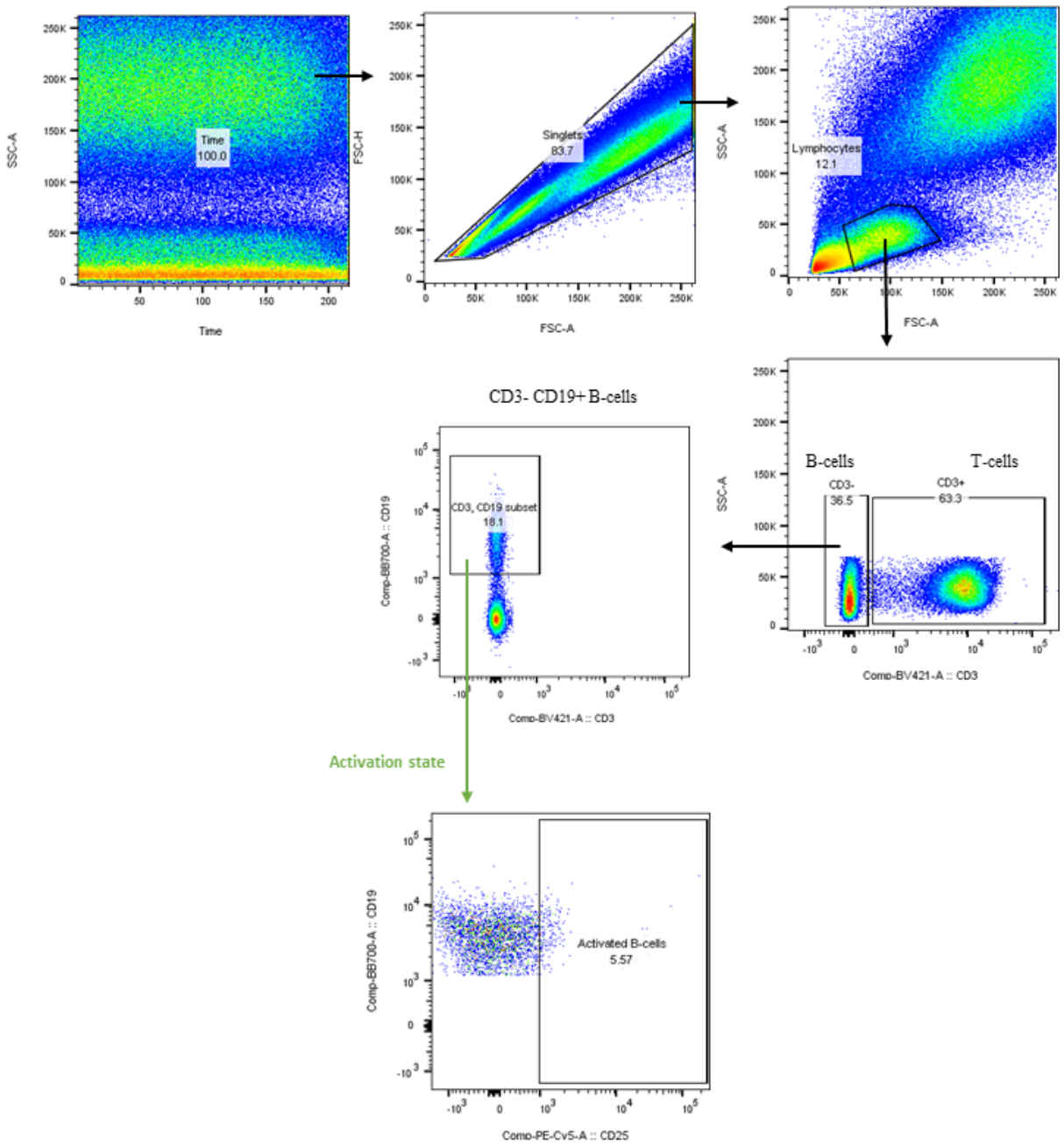

Figure 3.2: Flow cytometry gating strategy applied to the identify the percentage of B-cells in response to PPE_MPTR-stimulation, and their subsequent level of activation. B-cells were defined as $CD3^{-}CD19^{+}$ populations, with activated B-cell populations expressing CD25 ($CD3^{-}CD19^{+}CD25^{+}$).

Chapter 4

Results

4.1 Introduction

The PPE_MPTR proteins of *Mycobacterium tuberculosis* are hypothesized to contribute to *M. tuberculosis* pathogenesis and disease progression. The cell-membrane localisation of PPE_MPTR proteins is thought to facilitate interactions with host immune cells, however these interactions at the host-pathogen interface are not well characterised. Several PE/PPE proteins have demonstrated immunogenic potential (Vordermeier *et al.*, 2012), however the immunogenicity of PPE_MPTR proteins is under explored.

A previous study identified some promising PPE_MPTR epitopes as subunit vaccine candidates for *M. tuberculosis* (Colic *et al.*, Manuscript in progress) (**Table 4.1**). Thirty-five computationally identified epitopes were predicted to elicit a strong immune response in high burden TB African countries (Colic *et al.*, Manuscript in progress). Human populations from different geographical regions have different human leukocyte antigen (HLA) allele frequencies (Longmate *et al.*, 2001) and based on the differential distribution of HLA alleles across geographical regions, nineteen of the identified thirty-five epitopes were selected for this study (**Table 4.1**). These were also representatives of six different PPE_MPTR proteins. Nineteen peptides representing these epitopes were commercially synthesized by GL Biochem Ltd (Shanghai) for use in this study. These peptides were predicted to have a high likelihood of binding to HLA alleles frequently found in South African, Zimbabwean, Congolese and Ethiopian populations (González-Galarza *et al.*, 2015). Based on this, we predicted that these would be more likely to elicit an *M. tuberculosis*-specific immune response.

In this study we sought to provide functional evidence for the immunogenicity of the nineteen epitopes computationally identified and predicted to elicit an immune response in individuals from the four geographical regions, in Africa, stated above. The immune responses to these peptides were also investigated and compared in newly diagnosed TB patients with active disease, latently infected individuals and healthy controls. Lastly, to gain insight into the immune cell populations governing the immune response against the computationally identified PPE_MPTR epitopes, flow cytometric analysis was conducted on the isolated whole blood fraction of newly diagnosed active TB, latently infected and healthy control samples.

Specific fluorophore-conjugated monoclonal antibodies were selected to assess the relative percentages and activation states of the immune cells in response to stimulation with PPE_MPTR-derived peptides.

Table 4.1: Population coverage of computationally identified PPE_MPTR epitopes in four high burden TB African countries. Epitopes that provided a population coverage of more than 50% is highlighted in orange. Nineteen of these peptides were included in this study, and are represented by P1-P19.

Protein	Epitope	Zimbabwe	South Africa	Ethiopia	Congo	Peptides in this study
Rv0755c	TNSLRMYLGAGSRPL	48.73%	23.96%	62.88%	47.71%	**P1**
	NSLRMYLGAGSRPLL	48.73%	23.96%	62.88%	47.71%	
	SLRMYLGAGSRPLLA	53.90%	24.66%	66.19%	51.61%	
	LRMYLGAGSRPLLAA	53.90%	24.66%	66.19%	51.61%	**P2**
Rv0878c	TARECSIRVIISRVS	62.67%	23.96%	36.48%	53.31%	**P3**
	ARECSIRVIISRVSS	63.52%	23.96%	36.48%	53.31%	
	RECSIRVIISRVSST	72.44%	45.98%	53.90%	64.41%	**P4**
	ECSIRVIISRVSSTG	71.48%	45.98%	50.11%	60.84%	**P5**
	CSIRVIISRVSSTGA	72.44%	45.98%	53.90%	64.41%	**P6**
	SIRVIISRVSSTGAP	70.73%	45.98%	50.11%	60.84%	
	IRVIISRVSSTGAPP	70.73%	45.98%	50.11%	60.84%	**P7**
Rv1800	TMTQYYIIRTENLPL	29.10%	5.91%	77.58%	44.29%	**P8**
	MTQYYIIRTENLPLL	35.20%	6.68%	80.14%	48.32%	**P9**
	TQYYIIRTENLPLLE	35.20%	6.68%	80.14%	48.32%	**P10**
	QYYIIRTENLPLLEP	29.10%	5.91%	76.00%	42.63%	
	PEVSPVVIADALVAG	53.08%	45.98%	46.91%	49.76%	
	EVSPVVIADALVAGT	53.08%	45.98%	46.91%	49.76%	
	VSPVVIADALVAGTQ	53.08%	45.98%	46.91%	49.76%	
	SPVVIADALVAGTQQ	53.08%	45.98%	46.91%	49.76%	
	GGLQLLIIISAGRTI	53.62%	0.00%	36.50%	42.16%	
	GLQLLIIISAGRTIA	72.12%	0.00%	50.18%	42.16%	
	LQLLIIISAGRTIAN	72.12%	0.00%	50.18%	42.16%	
Rv2356c	RSAFVQLVLSNVFGQ	57.75%	23.96%	29.94%	50.04%	**P11**
	SAFVQLVLSNVFGQN	57.75%	23.96%	29.94%	50.04%	
Rv2608	GNEVVVFGTSQSATI	40.71%	23.96%	50.76%	45.89%	**P12**
	TIATFEMRYLQSLPA	62.67%	23.96%	42.85%	53.31%	**P13**
	IATFEMRYLQSLPAH	67.05%	24.66%	46.97%	56.99%	**P14**
	ATFEMRYLQSLPAHL	91.99%	26.21%	90.95%	77.47%	
	TFEMRYLQSLPAHLR	95.29%	40.86%	90.95%	80.62%	**P15**
	FEMRYLQSLPAHLRP	95.29%	40.86%	90.95%	80.62%	
	EMRYLQSLPAHLRPG	94.29%	40.86%	86.33%	78.64%	**P16**
	MRYLQSLPAHLRPGL	78.47%	40.86%	46.97%	67.48%	**P17**
Rv3533c	HPLLVAANRNAFAQL	40.71%	58.40%	26.01%	32.83%	**P18**
	PPELNSLRMFTGAGS	64.48%	25.52%	36.48%	56.40%	**P19**
	PELNSLRMFTGAGSA	64.48%	25.52%	36.48%	56.40%	

4.1.1 Peptide concentration optimization

To determine the optimal concentration for peptide reactivity, a range of peptide concentrations (20, 10, 5, 1 µg/ml) was used to stimulate whole blood from two participants from The Division of Molecular Biology and Human Genetics, Faculty of Medicine and Health Science, Stellenbosch University. Microsoft Excel (Windows 10 ProfessionalPlus, 2016) was used to ensure the controls included with the kit fell within their specified concentration ranges through the removal of the out-of-range values as described in **Section 3.3.**

Optimal peptide reactivity concentrations were determined by identifying the peptide concentration that induced the most cytokines and the concentration at which the highest cytokine responses were measured. PPE_MPTR peptides 2 to 18 (P2 to P18) met these criterion at a concentration of 10 µg/ml. Interestingly, P1 and P19 stimulated cytokine production at concentrations of 5 µg/ml and 1 µg/ml, respectively (**Figure 4.1**). The peptides that elicited the lowest cytokine concentrations overall were P1, P15 and P18. The controls included ESAT-6, CFP-10, PHA and PPD and were all used at 10 µg/ml as described in literature (Vordermeier *et al.*, 2001)

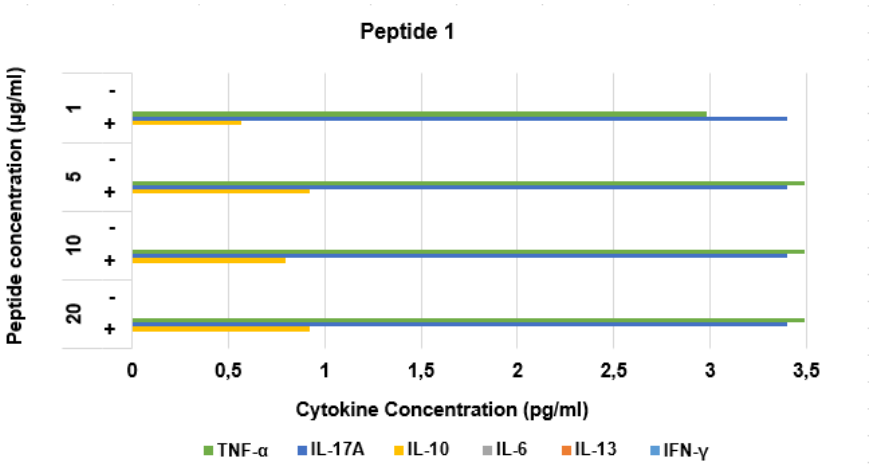

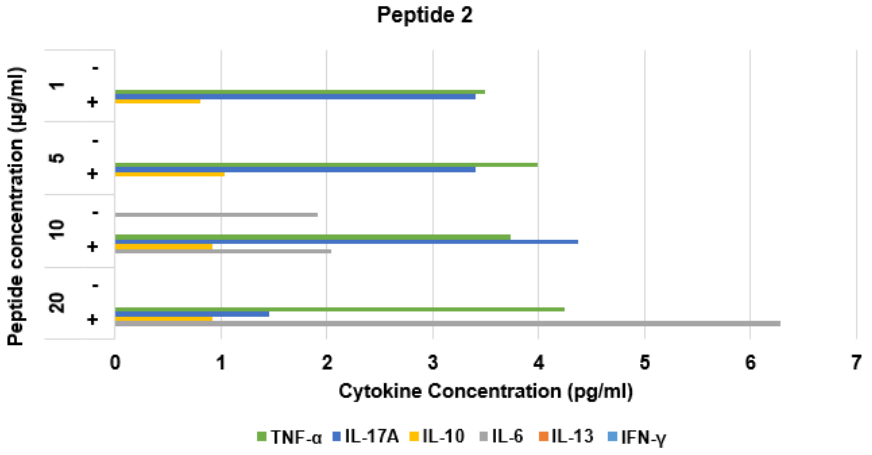

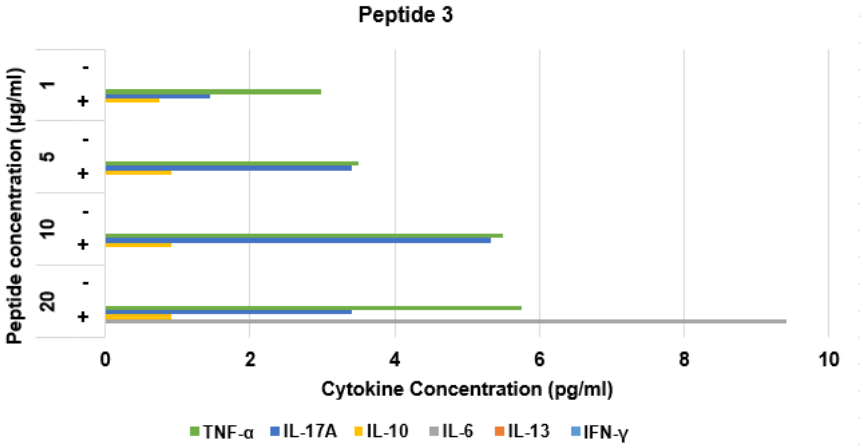

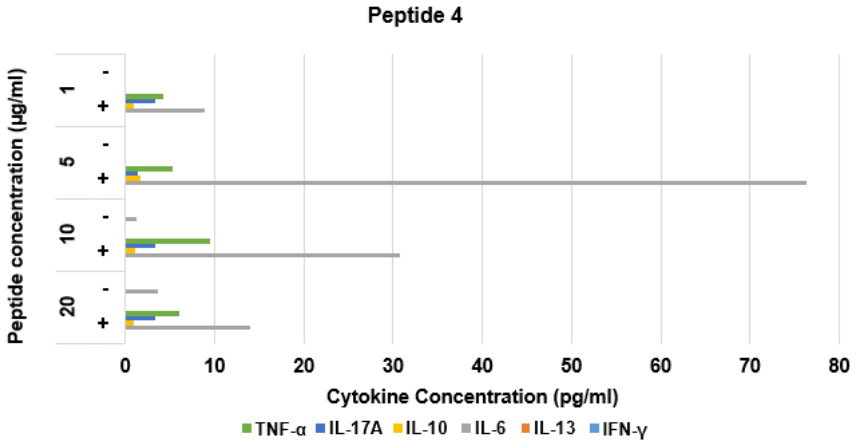

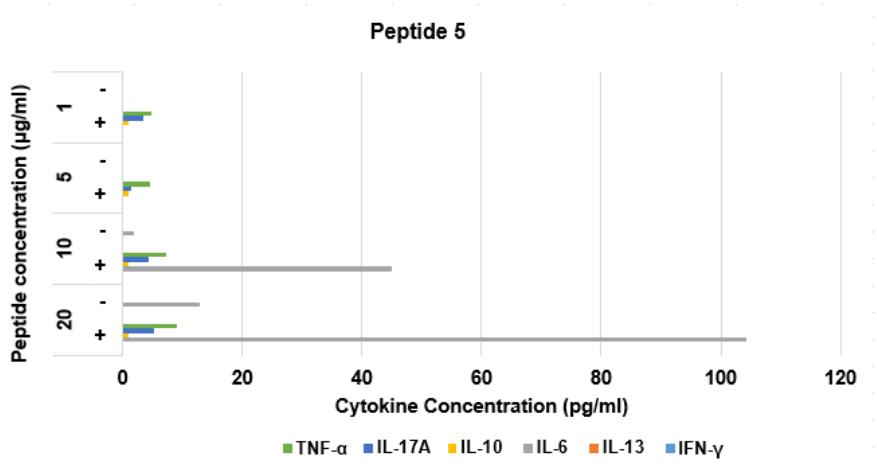

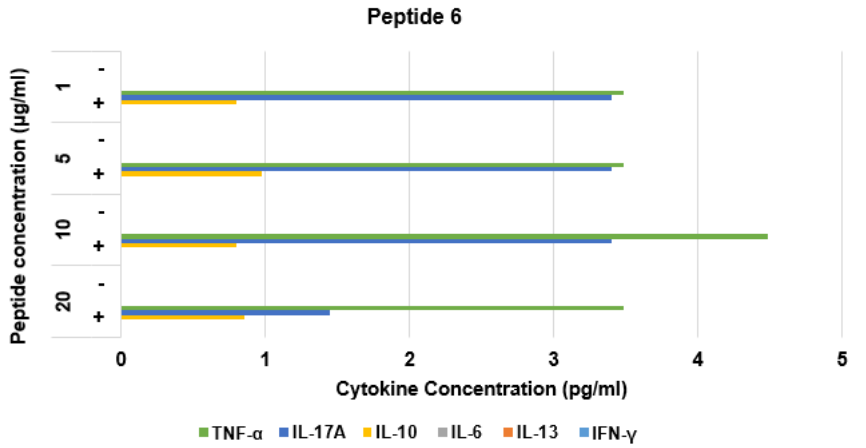

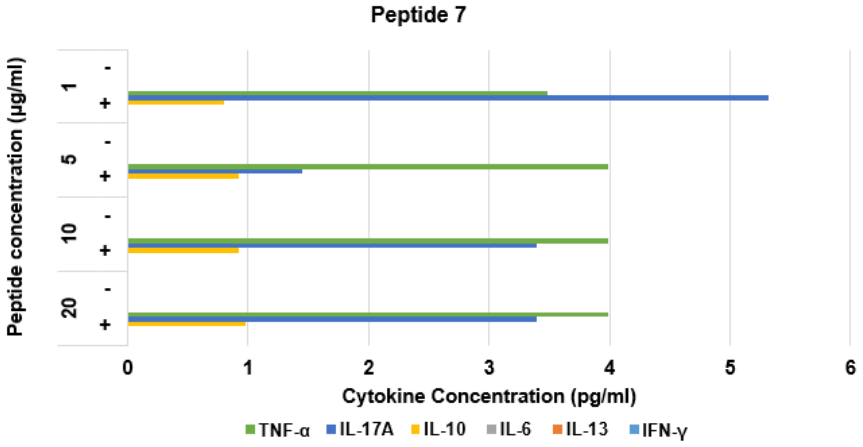

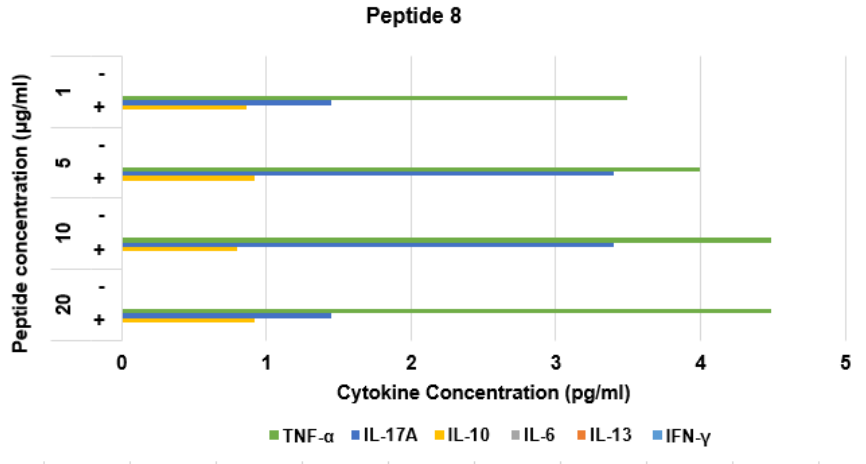

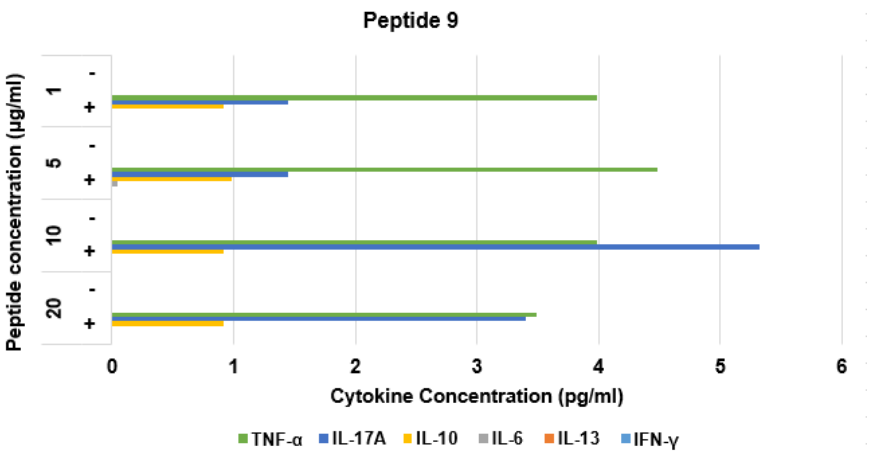

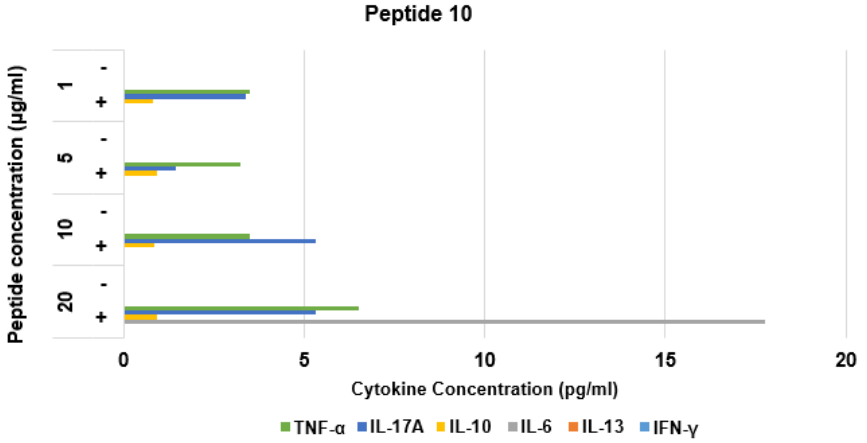

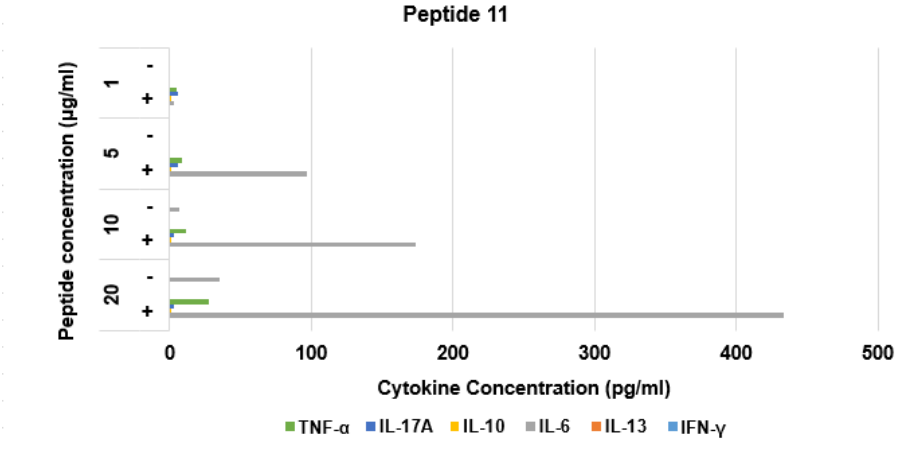

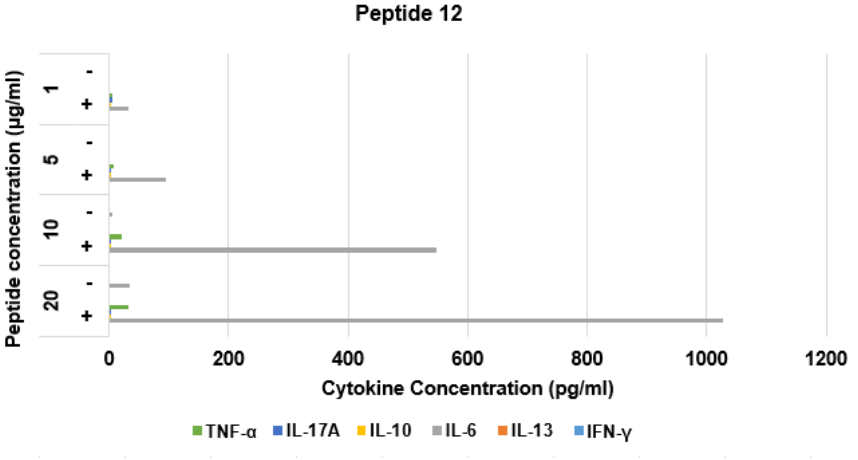

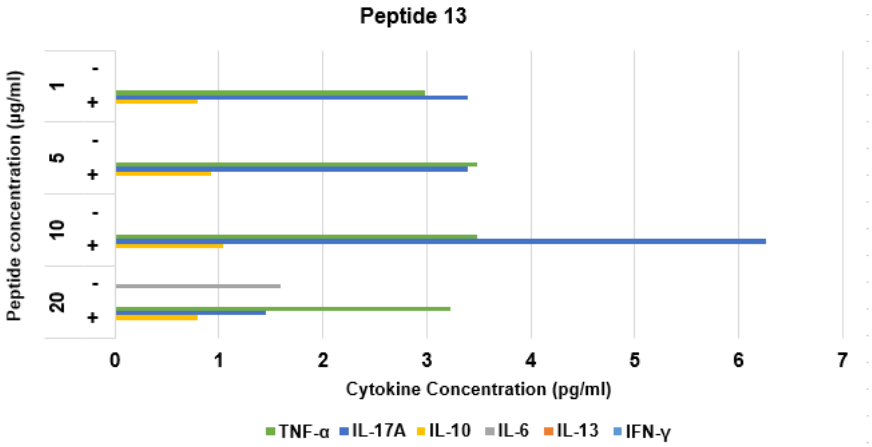

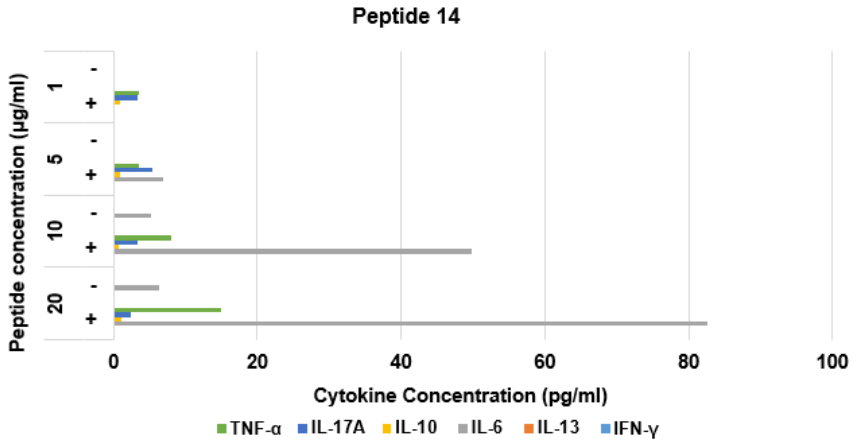

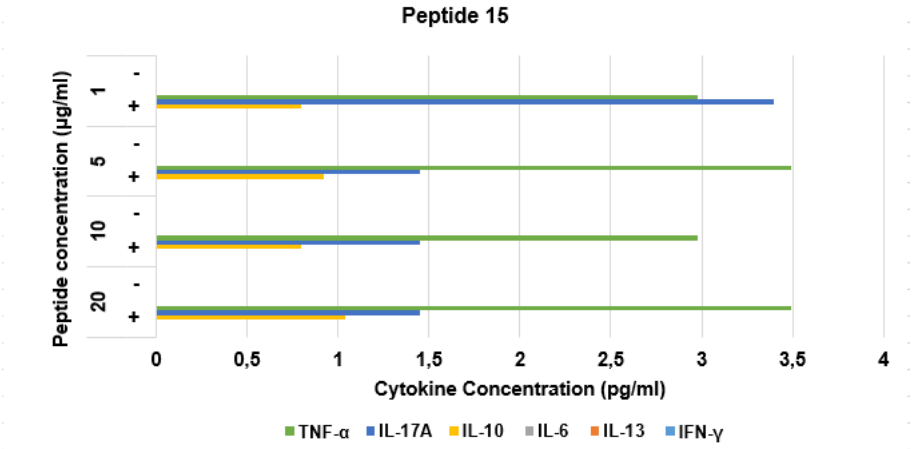

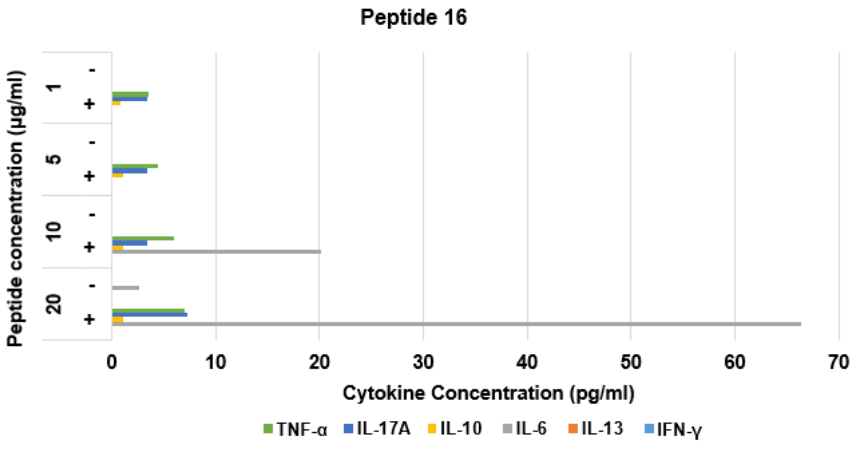

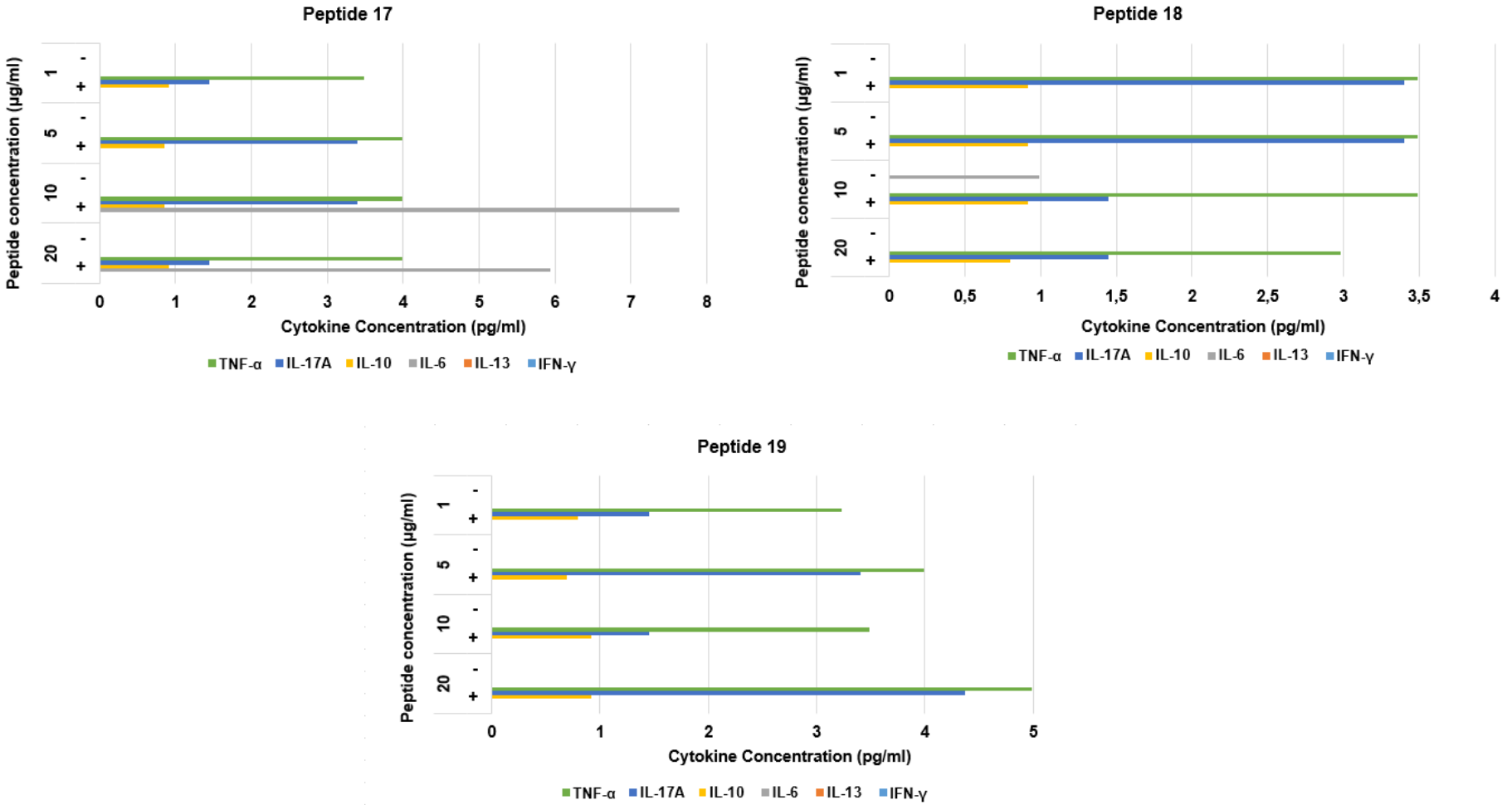

Figure 4.1: Clustered Bar Graphs used to assess the optimal peptide reactivity by comparing the cytokine responses to a gradiant of peptide concentrations. The x-axis represents the cytokine concentrations of TNF-α (green), IL-17A (dark blue), IL-10 (yellow), IL-6 (grey), IL-13 (orange) and IFN-γ (light blue) in pg/ml. The y-axis represents the peptide concentrations (20, 10, 5, 1 µg/ml) in QFN+ (indicated with +) and QFN- (indicated with -) individuals.

4.1.2 The Immunogenicity of population-tailored PPE_MPTR peptides

To functionally validate the immunogenicity of the computationally-identified PPE_MPTR peptides in an African cohort (**Table 3.3**), the concentration of seven cytokines in response to these peptides were measured using a customized Human Magnetic Luminex Screening Assay as a screening tool (Whitehead Scientific, South Africa). These peptides were predicted to elicit an immune response in *M. tuberculosis*-exposed individuals based on their predicted binding to the HLA alleles commonly encoded by individuals from this African cohort. We stimulated peripheral blood with peptide candidates and assessed the immunogenicity thereof in QFN+ individuals (Essone *et al.*, 2019).

Luminex Data Quality Assessment

Before Luminex data analyses was performed, the observed absolute concentrations of the kit standards were analysed to ensure they fell within their specified concentration ranges. To assess the quality of these data, the percentage of OOR values for each analyte was determined, and analytes with more than 70% below-OOR (<OOR) values were excluded from data analysis (IFN-γ, IL-1β and IL-4) (**Table 4.2**). The percentage <OOR values was calculated from a total number of 768 data points which included data from 32 study participants in response to 24 stimulations.

Table 4.2: Percentage of below Out-Of-Range (<OOR) values observed during Luminex Data Quality Assessment. The number of <OOR values for 32 study participants in response to 24 stimulations were caluclated as a percentage of the total number of data points (n=768). Analytes included in further analysis are highlighted in grey.

Analyte	Number <OOR values	% < OOR
IL-1β	558/768	72%
IL-4	560/768	73%
IL-6	130/768	17%
IL-10	381/768	50%
IL-17A	476/768	62%
IFN-γ	561/768	73%
TNF-α	307/768	40%

To perform statistical analyses on the concentration data for TNF-α, IL-6, IL-17A and IL-10, the OOR values were arbitrarily assigned values; if a data point was <OOR, one was subtracted from the lowest observed analyte concentration on that specific plate, and if the data point was >OOR, one was added to the highest observed analyte concentration for that specific plate.

Luminex Data are not normally distributed

To determine if the remaining data followed a normal distribution, GraphPad Prism 8.3.0 was used to run normality tests. Three tests were performed to evaluate the normal distribution of Luminex data, namely the D'Agostino & Pearson, Shapiro-Wilk and Kolmogorov-Smirnov test. Each normality test computed a significant p-value of <0.0001 for each analyte, which indicated that the data were significantly different from the normal distribution. The non-normal distribution of these data is represented in Quantile-quantile (QQ)-plots and can be seen in **Figure 4.2**. The QQ-plots compare the quantiles in which datapoints are predicted to be found (if they are from a normal distribution) and the actual quantiles observed for the data. If data originate from a normal distribution, there should be no deviations from the straight dotted line (red) seen on the QQ-plot in **Figure 4.2**. The quantiles in which our study data are found do not align with the predicted quantiles of a normal distribution, therefore they deviate from the straight line seen in the QQ-plots (**Figure 4.2**).

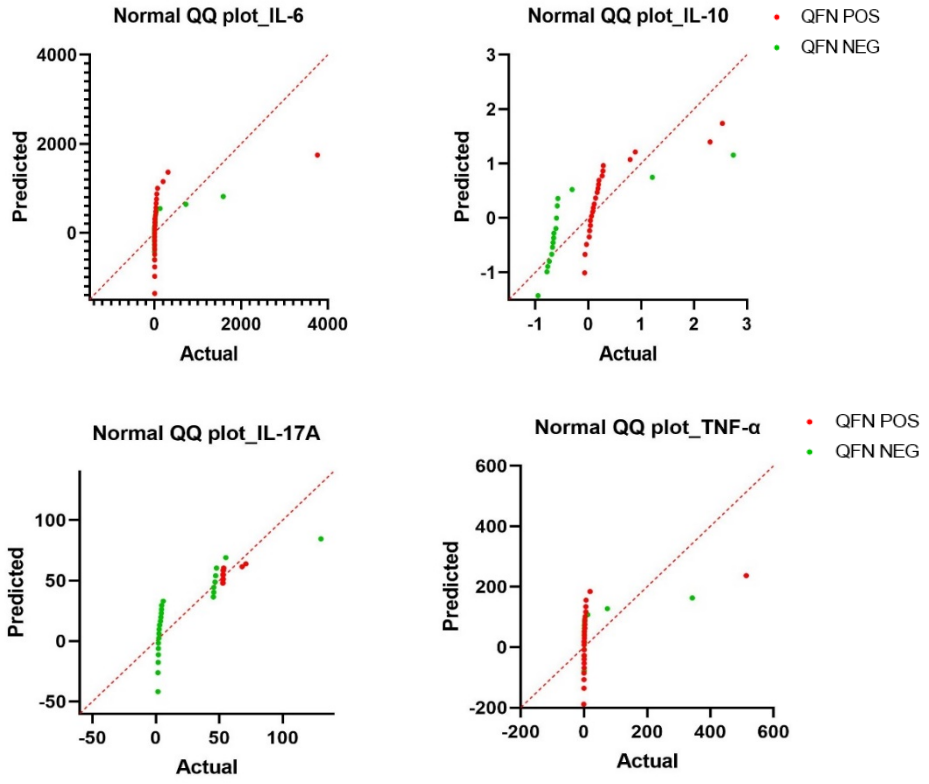

Figure 4.2: QQ-plots demonstrating the non-normal distribution of data generated from Human Multiplex Luminex Assay from individuals in an African cohort. The x-axis represents the quantiles into which the study data fall (actual) and the y-axis represents the quantiles of a normal distribution (predicted). QFN+ (n=5) individuals are represented in red and QFN- (n=6) individuals are represented in green. *Data points for QFN- individuals lie directly behind data points for QFN+ individuals for TNF-α and IL-6 cytokines. **Data points for QFN+ individuals lie behind data points for QFN- individuals for IL-17A.

Analyte concentrations in response to control stimulations

The analyte responses of QFN+ and QFN- individuals towards control stimulations were assessed prior to investigating the influence of PPE_MPTR peptides on cytokine concentration. The responses to control stimulations provide information regarding the (i) baseline immune response of an individual (unstimulated) and (ii) immune response to known *M. tuberculosis* antigens (ESAT-6 and CFP-10). These results provide the backdrop for analysis of the cytokine responses following PPE_MPTR peptide stimulation.

The median control-stimulated and unstimulated cytokine responses were compared between QFN+ and QFN- participants (**Figure 4.3** and **Figure 4.4**). Low background levels of all analytes were observed for the unstimulated controls (**Figure 4.3** and **Figure 4.4**). The measured concentration of TNF-α in the unstimulated control was comparable between QFN+ and QFN- individuals (**Figure 4.4a**). Unstimulated controls for IL-6 (**Figure 4.3b**) and IL-10 (**Figure 4.4b**) demonstrated a lower concentration of these cytokines in QFN- individuals. In the case of IL-17A, higher concentrations were produced by QFN- individuals in unstimulated conditions compared to QFN+ individuals (**Figure 4.3a**).

In response to PHA, all individuals produced higher concentrations of IL-17A, IL-6, TNF-a and IL-10 than measured in the unstimulated control, as expected (**Figure 4.3** and **Figure 4.4)**. QFN+ individuals produced higher concentrations of IL-6 in response to PHA compared to QFN- individuals (**Figure 4.3b**). However, the concentrations of IL-17A (**Figure 4.3a**), TNF-α and IL-10 (**Figure 4.4a, b**) in response to PHA were higher in QFN- individuals compared to QFN+ individuals. PPD-stimulation induced higher concentrations of IL-17A, IL-6, TNF-α and IL-10 in QFN+ and QFN- individuals than observed in unstimulated controls (**Figure 4.3** and **Figure 4.4**). As expected, in response to PPD, QFN+ individuals produced higher concentrations of IL-6 (**Figure 4.3b**), TNF-α and IL-10 (**Figure 4.4**) when compared to QFN- individuals, whereas comparable IL-17A concentrations were observed between QFN+ and QFN- individuals.

In response to ESAT-6, only IL-10 was produced in higher concentrations compared to unstimulated levels, and unexpectedly, this was observed for QFN- individuals (**Figure 4.4b**). In response to CFP-10, QFN- individuals produced higher concentrations of IL-6 (**Figure 4.3b**), TNF-α and IL-10 (**Figure 4.4**) above unstimulated levels. QFN+ individuals only produced higher concentrations of IL-6 and TNF-α above unstimulated levels (**Figure 4.3b** and **Figure 4.4a**), with the concentration of IL-10 comparable to that observed for the

unstimulated control in QFN+ individuals (**Figure 4.4b**). The concentrations of IL-6 and TNF-α measured in response to CFP-10 and ESAT-6 were higher in QFN+ individuals than QFN- individuals (**Figure 4.3b** and **Figure 4.4a**), however the concentrations of IL-17A and IL-10 were higher in QFN- individuals compared to QFN+ individuals (**Figure 4.3a** and **Figure 4.4b**).

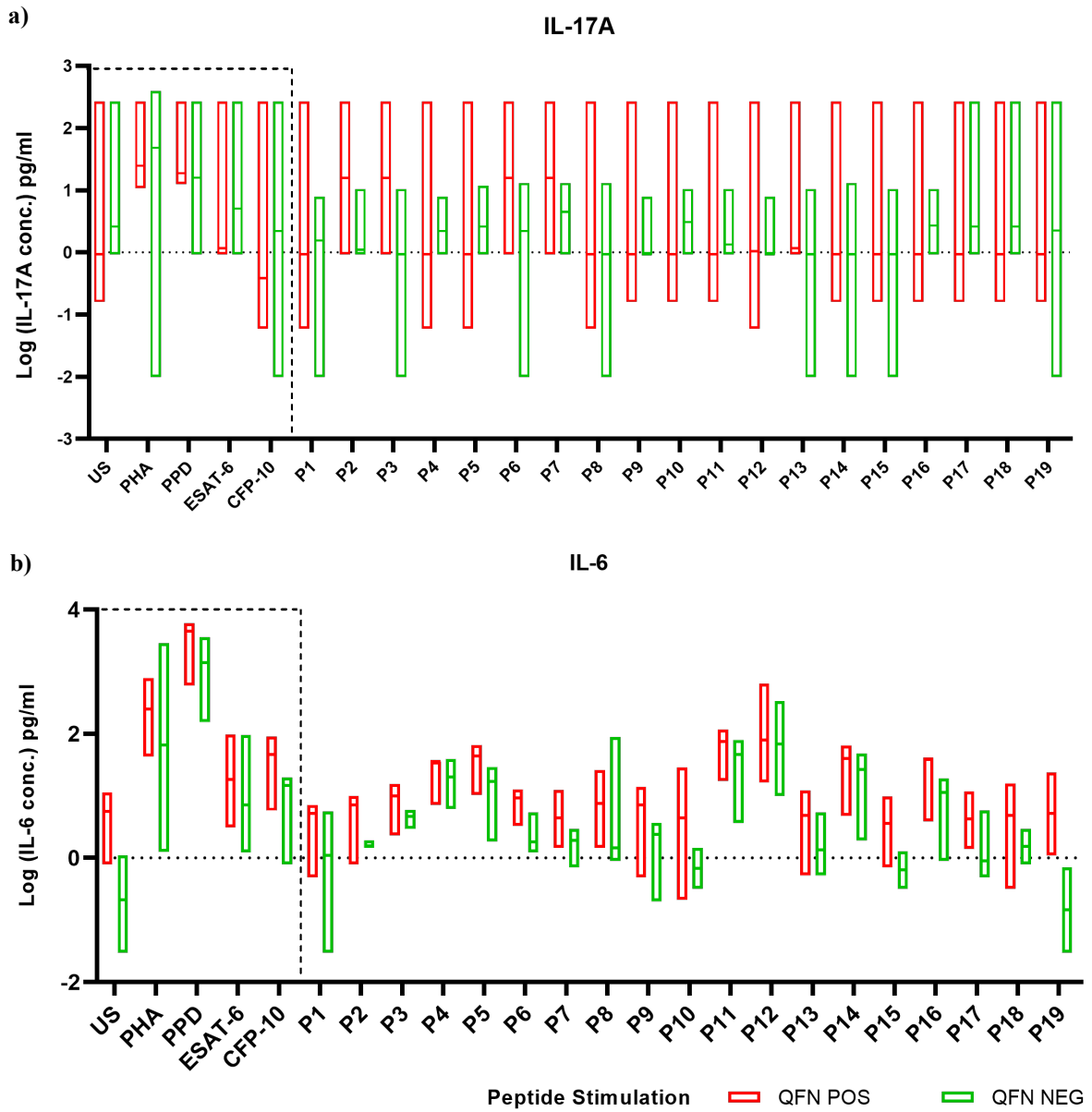

Figure 4.3: The concentration of a) IL-17A and b) IL-6 observed in QFN+ and QFN- individuals from an African cohort in response to PPE_MPTR peptides. The floating bars represent the minimum-to-maximum log transformed concentration values, with the median concentration represented by the horizontal line. Values below zero indicate low absolute concentration values were obtained in response to stimulation condition before data was log transformed. The controls used in this study can be seen within the dotted box and include US = Unstimulated; PHA= *Phaseolus vulgaris* phytohaemagglutinin; PPD= Purified protein derivative; ESAT-6 = Early Secreted Antigen -6 and CFP-10 = Culture Filtrate Protein-10. QNF+ individuals = red and QFN-ve individuals = green. P1-P19 = candidate PPE_MPTR peptides investigated in this study.

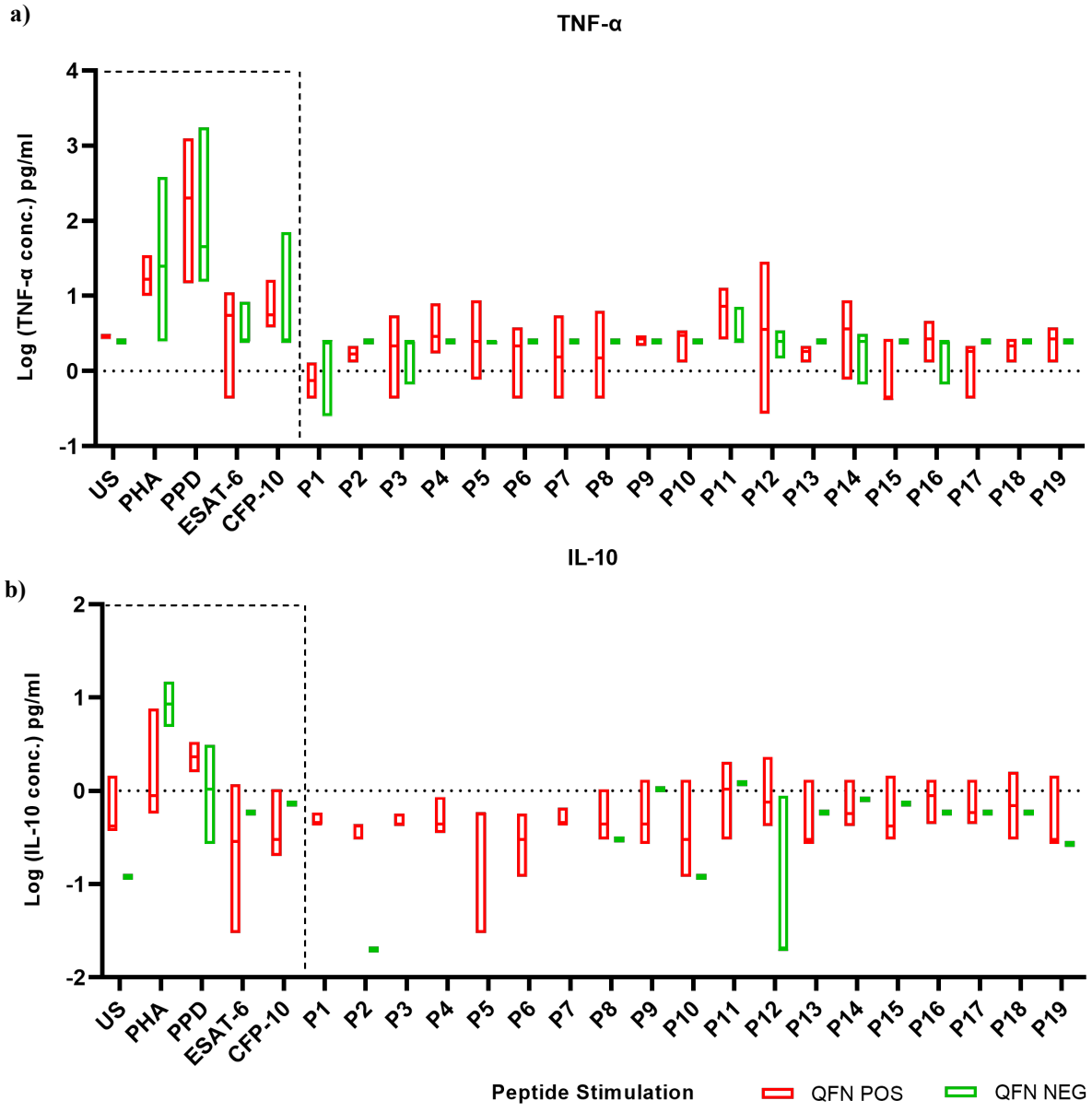

Figure 4.4: The concentration of a) TNF-α and b) IL-10 observed in QFN+ and QFN- individuals from an African cohort in response to PPE_MPTR peptides. The floating bars represent the minimum-to-maximum log transformed concentration values, with the median concentration represented by the horizontal line. Values below zero indicate low absolute concentration values were obtained in response to stimulation condition before data was log transformed. The controls used in this study can be seen within the dotted box and include US = Unstimulated; PHA= *Phaseolus vulgaris* phytohaemagglutinin; PPD= Purified protein derivative; ESAT-6 = Early Secreted Antigen -6 and CFP-10 = Culture Filtrate Protein-10. QNF+ individuals = red and QFN-ve individuals = green. P1-P19 = candidate PPE_MPTR peptides investigated in this study.

Analyte concentrations induced in response to candidate PPE_MPTR peptides

The median PPE_MPTR-specific cytokine concentration was used to evaluate which PPE_MPTR peptides induced the production of the most cytokines in African individuals. Overall, the PPE_MPTR peptides elicited higher cytokine responses in QFN+ individuals compared to QFN- individuals (**Figure 4.3** and **Figure 4.4**), however the measured absolute cytokine concentrations detected by the Luminex screening assay were low for all analytes investigated.

IL-17A

In QFN+ individuals, the concentration of IL-17A in response to P2, P3, P6 and P7 was higher than observed for QFN- individuals (**Figure 4.3a**). These PPE_MPTR-induced IL-17A concentrations in QFN+ individuals were greater than what was seen in response to ESAT-6 and CFP-10. In response to P4, P5, P10, P11, P16, P17, P18, P19, all QFN- individuals induced higher concentrations of IL-17A compared to QFN+ individuals, however these peptides were all at similar levels observed for the unstimulated control (**Figure 4.3a**), suggesting that these are background responses.

IL-6

In response to P2, P3, P4, P5, P6, P8, P9, P11, P12, P14 and P16, QFN+ individuals produced higher concentrations of IL-6 compared to QFN- individuals (**Figure 4.3b**). The remaining peptides also produced more IL-6 in QFN+ individuals, however these peptides induced lower IL-6 concentrations than observed for the unstimulated.

TNF-α

There were only three PPE_MPTR peptides that produced higher concentrations of TNF-α in QFN+ individuals compared to QFN- individuals. These included P11, P12 and P14 (**Figure 4.4a**).

IL-10

QFN+ and QFN- individuals produced very low median absolute concentrations of IL-10 in response to PPE_MPTR peptides (**Figure 4.4b**). All peptides induced lower IL-10 concentrations from QFN+ individuals than QFN- individuals.

In summary, selected PPE_MPTR peptides induced higher cytokine responses from QFN+ individuals than QFN- individuals in our study. This suggests that previous sensitization to *M. tuberculosis* results in the production of higher cytokine concentrations from these individuals,

thereby suggesting QFN+ individuals elicit a *M. tuberculosis*-specific response. In response to PPE_MPTR peptides, the Luminex platform detected very low concentrations of pro-inflammatory cytokines IL-6, IL-17A and TNF-α. On the basis of detected cytokine production, PPE_MPTR peptides P4, P5, P11, P12, P14 and P16 were considered the most immunogenic and further analysed using flow cytometry (**Section 4.1.4**).

4.1.3 Assessing the diagnostic potential of population-tailored PPE_MPTR peptides

The diagnostic potential of the computationally identified PPE_MPTR peptides was investigated by comparing PPE_MPTR-specific cytokine responses in individuals (i) *cases* vs *controls*; (ii) LTBI vs TB and (iii) LTBI vs healthy controls. This was done to assess if the candidate PPE_MPTR peptides elicited notably different immune responses between individuals (i) with or without active TB infection; (ii) latently infected or diagnosed with active TB and (iii) latently infected or healthy individuals. Study participants included in *cases* (n=5) included the five baseline active TB individuals recruited from high incident TB communities around Tygerberg Hospital. The study participants included as *controls* (n=22) included 'healthy controls'(n=11) and 'LTBI' individuals (n=5) recruited from high incident TB communities around Tygerberg Hospital. Four QFN- (n=4) and two QFN+ (n=2) South African participants (**Table 3.3**) were also included in these analyses and were added to the group of eleven 'healthy controls' and five 'LTBI' individuals, respectively (**Table 3.6**).

The PPE_MPTR peptide-specific cytokine concentration was calculated as the difference in cytokine concentration between unstimulated and PPE_MPTR peptide-stimulated responses (delta cytokine concentration). Non-parametric data analysis was done using the Wilcoxon-Signed Rank Test, which identified 11 significant differences (raw p-values < 0.05) between groups. Given that this is a pilot study that is aimed at identifying trends in PPE_MPTR cytokine responses, these 11 differences were further assessed. However, it should be noted that before data was corrected for multiple testing (621 tests) using Bonferroni Test Correction (FDR of 0.05), no significant p-value remained (corrected p-value) suggesting that the 11 significant raw p-values observed prior to Bonferroni Test Correction may have occurred by chance.

The computationally-identified PPE_MPTR peptides that induced significant differences in cytokine concentration between '*cases* and *controls*' or 'LTBI and TB' or 'LTBI and HCs' can be seen in **(Table 4.3)**.

Table 4.3: PPE_MPTR peptides inducing differences in cytokine production. The Wilcoxon-Signed Rank Test identified 11 differences in cytokine production between groups in response to PPE_MPTR peptides that had a p-value below 0.05. The smallest p-value was observed between *cases* and *controls* for the production of IL-6 in response to P17 (highlighted in grey). Following Bonferroni Test Correction (FDR = 0.05), no significant p-values remained. The raw p-values were used for further analyses.

Peptide	Cytokine	Groups	Raw p-value < 0.05	Corrected p-value < 0.05
P4	IL-6	LTBI vs TB	0,0303030	18,8181818
P8	IL-6	LTBI vs TB	0,0419966	26,0799328
P11	IL-17A	*Cases* vs *Controls*	0,0346458	21,5150462
P12	IL-6	LTBI vs TB	0,0479797	29,7954545
P17	IL-6	*Cases* vs *Controls*	0,0088417	5,4907561
		LTBI vs TB	0,0479797	29,7954545
P19	TNF-α	LTBI vs HC	0,0262806	16,3202816
CFP-10*	IL-6	*Cases* vs *Controls*	0,0051410	3,19261020
	TNF-α	*Cases* vs *Controls*	0,0295002	18,3196479
PPD*	TNF-α	LTBI vs HC	0,0200034	12,4221362
PHA*	IL-17A	LTBI vs HC	0,0250226	15,5390349
*CFP-10, PHA and PPD were included as controls.				

Cases vs *Controls*

The cytokine responses to candidate PPE_MPTR peptides was compared between individuals diagnosed with baseline active TB disease and those without active TB disease. These results may indicate whether candidate PPE_MPTR peptides are able to distinguish between individuals with and without active TB disease.

PPE_MPTR peptides that induced the most significant differences in cytokine production, as measured by the raw p-value, between *cases* (n=5) and *controls* (n=22) were P17 (IL-6) and P11 (IL-17A) (**Figure 4.5**). In response to P17, *cases* produced a median IL-6 concentration of 4 pg/ml (*controls* 0 pg/ml). Of the 22 *controls*, 40% (9/22) did not produce detectable IL-6 in response to P17, compared to 20% (1/5) observed for the *cases* (**Figure 4.5b**).

The median IL-17A concentration detected in response to P11 was also significantly higher in *cases* compared to *controls* (**Figure 4.5b**), with *cases* producing a median IL-17A concentration of 10 pg/ml (*Controls:* 0 pg/ml). There were 60% (3/5) of *cases* that produced no IL-17A in response to P11, with 40% (2/5) producing >100 pg/ml IL-17A in response to

P11. Of the *controls*, 90% (20/22) produced no IL-17A in response to P11, with 10% (2/22) participants producing IL-17A concentrations comparable with *cases* (**Figure 4.5b**).

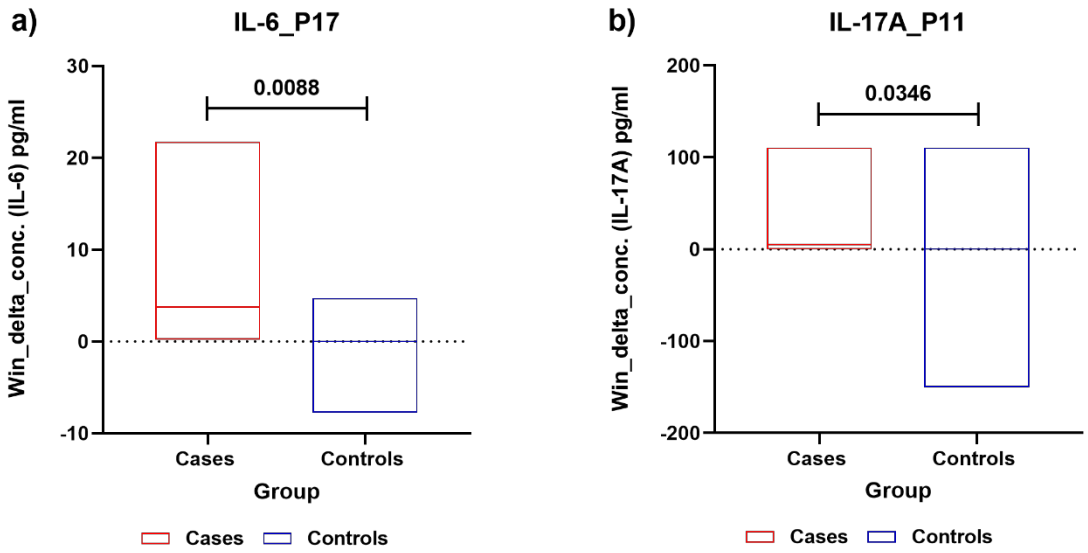

Figure 4.5: Box plot demonstrating significant differences in a) IL-6 and b) IL-17A concentration between *cases* and *controls* in response to P17 and P11, respectively. The winsorized delta cytokine concentration is plotted on the graph with the significance bar depicting the raw p-value. The box plots represent the minimum to maximum cytokine concentration, with the horizontal line showing the median cytokine concentration. Delta cytokine concentration = PPE_MPTR-specific conc. - Unstimulated cytokine conc. *Cases* (n=5) are represented in red and *controls* (n=22) in blue.

TB vs LTBI individuals

The cytokine responses to candidate PPE_MPTR peptides was compared between individuals living with latent TB infection and those diagnosed with baseline active TB disease. Individuals with active TB disease are expected to elicit higher cytokine responses to PPE_MPTR peptides compared to individuals with LTBI.

Significant differences in cytokine production were observed for IL-6 in response to P12 and P17 (**Figure 4.6**) as well as against P4 and P8 (**Figure 4.7**). Overall, TB individuals produced higher concentrations of IL-6 in response to P12 compared to LTBI individuals with a median of 175 pg/ml (LTBI: 30 pg/ml) (**Figure 4.6a**). In response to P17, the median IL-6 concentration produced by TB individuals was 4 pg/ml compared to 1 pg/ml observed in LTBI individuals (**Figure 4.6b**). Only one TB participant (20%) produced no IL-6 in response to P17, compared to 28% (2/7) observed for LTBI individuals (**Figure 4.6b**). Similarly to what was observed between *cases* and *controls* in **Figure 4.5a**, the IL-6 produced by the remaining 72% (5/7) LTBI individuals was less compared to the IL-6 produced by TB participants (**Figure 4.6b**). The median IL-6 concentration observed by LTBI individuals in response to

P17 is comparable to the median IL-6 concentration observed for *controls* in response to P17 (**Figure 4.5a**). Interestingly, the range of IL-6 produced by *controls* in response to P17 (**Figure 4.5a**) was greater than observed for LTBI individuals alone (**Figure 4.6b**), with some healthy controls releasing more IL-6 than LTBI individuals.

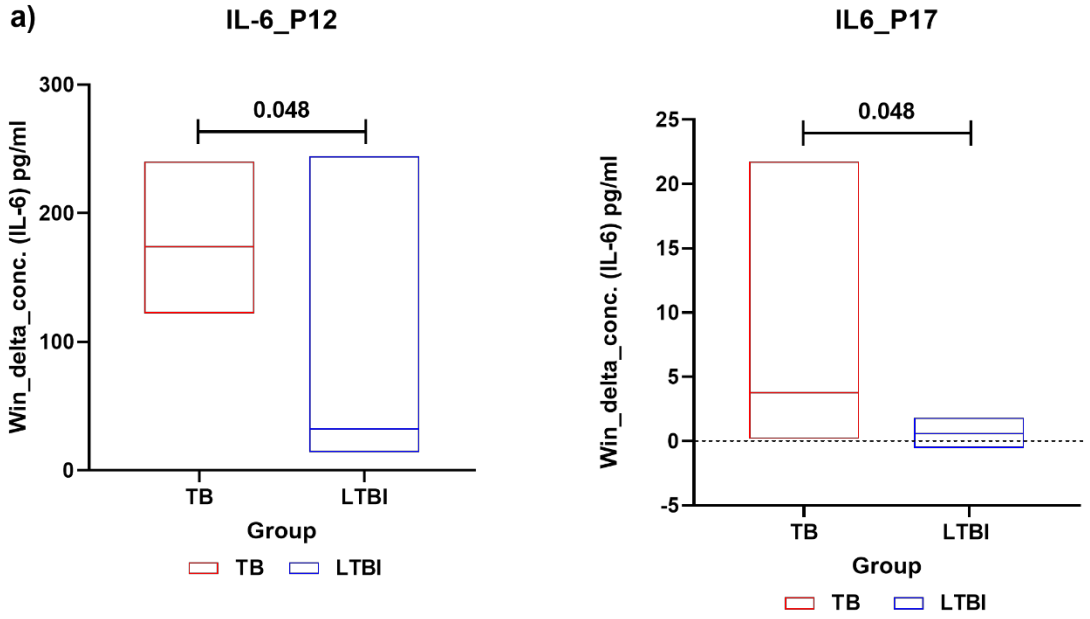

Figure 4.6: Box plot demonstrating significant differences in IL-6 concentration released from baseline active TB and LTBI individuals in response to a) P12 and b) P17. The winsorized delta cytokine concentration is plotted on the graph with the significance bar depicting the raw p-value. The box plots represent the minimum to maximum cytokine concentration, with the horizontal line showing the median cytokine concentration. Delta cytokine concentration = PPE_MPTR-specific conc. - Unstimulated cytokine conc. TB: baseline active TB participants (n=5) are represented in red. LTBI = latently infected individuals (n=7) in blue.

The median IL-6 concentration produced in response to P4 by TB and LTBI individuals was 18 pg/ml and 6 pg/ml, respectively (**Figure 4.7a, b**). There was one LTBI individual who produced concentrations of IL-6 in response to P4 comparable with TB individuals (**Figure 4.7a**), with the remaining LTBI individuals producing lower IL-6 concentrations than TB individuals. The median IL-6 concentration produced in response to P8 by TB and LTBI individuals was 4 pg/ml and 0 pg/ml, respectively (**Figure 4.7b**).

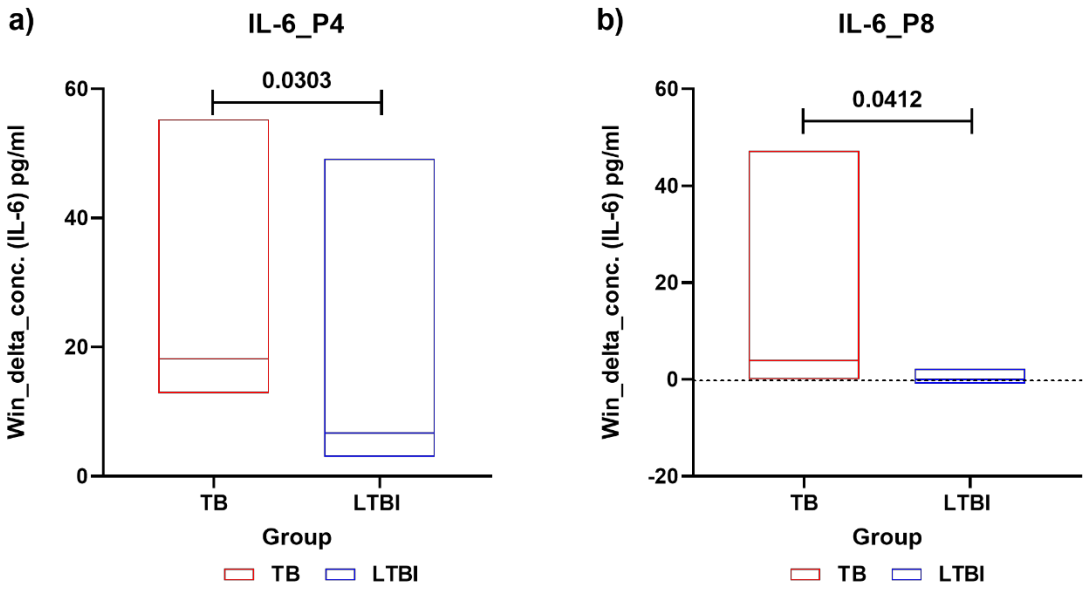

Figure 4.7: Box plot demonstrating significant differences in IL-6 concentration released from baseline active TB and LTBI individuals in response to a) P4 and b) P8. The winsorized delta cytokine concentration is plotted on the graph with the significance bar depicting the raw p-value. The box plots represent the minimum to maximum cytokine concentration, with the horizontal line showing the median cytokine concentration. Delta cytokine concentration = PPE_MPTR-specific conc. - Unstimulated cytokine conc. TB: baseline active TB participants (n=5) are represented in red. LTBI = latently infected individuals (n=7) in blue.

LTBI vs Healthy Controls

The PPE_MPTR-specific cytokine responses between latently infected and healthy individuals was compared to determine if the candidate peptides can identify individuals with LTBI. The PPE_MPTR-specific cytokine response is expected to be higher in LTBI individuals compared to healthy individuals.

PPE_MPTR peptide, P19, induced a significantly higher median concentration of TNF-α in LTBI individuals (0.75 pg/ml) compared to healthy individuals (0 pg/ml) (**Figure 4.8**). A single healthy control produced TNF-α in response to P19, and interestingly at a higher concentration (2.5 pg/ml) than observed for all LTBI individuals (**Figure 4.8**).

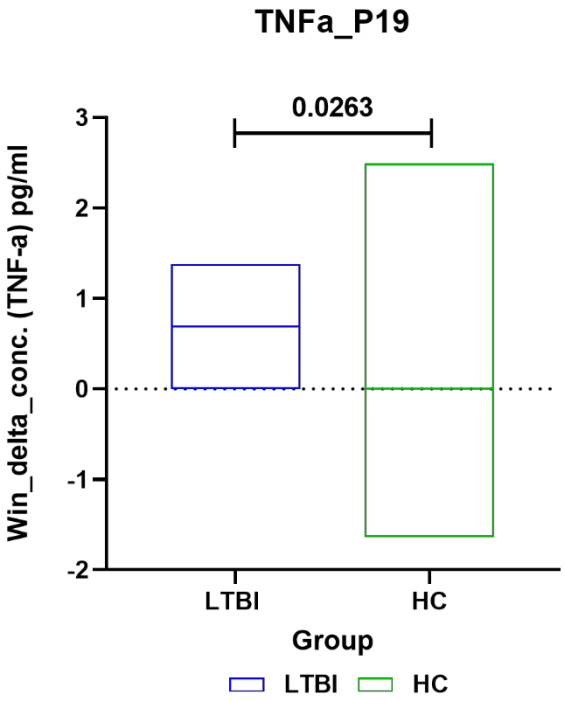

Figure 4.8: Box plot demonstrating significant differences in TNF-α concentrations in LTBI individuals and healthy controls in response to P19. The winsorized delta cytokine concentration is plotted on the graph with the significance bar depicting the raw p-value. The box plots represent the minimum to maximum cytokine concentration, with the horizontal line showing the median cytokine concentration. Delta cytokine concentration = PPE_MPTR-specific conc. - Unstimulated cytokine conc. LTBI = latently infected individuals (n=7) in blue. HC = healthy control (n=15) in green.

4.1.4 PPE_MPTR-specific functional marker frequencies of lymphocyte populations in the peripheral blood of TB, LTBI and healthy individuals

Little is currently known about the cellular populations that are responsible for the PPE_MPTR-specific immune response. Flow cytometry was therefore used to assess the distribution of functional markers and activation states of $CD4^+$ and $CD8^+$ T-lymphocytes and B-lymphocytes in the peripheral blood of TB, LTBI and healthy individuals. PPE_MPTR peptides were selected for flow cytometry experiments based on results of multiplex cytokine assays performed on individuals from South Africa, Zimbabwe, Congo and Ethiopia (See **Section 4.1.1**). Six peptides that induced the production of more than three cytokines were selected, namely P4, P5, P11, P12, P14 and P16. These were representative of four PPE_MPTR proteins. Although it was not a selection criterion, it is interesting to note that P4, P11 and P12 elicited significantly different cytokine responses between individuals of different health statuses (unexposed, uninfected healthy individuals / baseline (untreated) active TB individuals / latently infected individuals) (**Section 4.1.3**).

Positive controls included peripheral blood cells stimulated with ESAT-6 and CFP-10 peptide cocktails, and PBS-stimulated blood was included as the negative control. Stimulated peripheral blood cells from the 21 study participants recruited from high-incident TB communities surrounding Tygerberg Hospital (**Table 3.6**) were analysed as stated in **Section 3.8**. Ten-fluorophore-conjugated monoclonal antibodies were used to define the immunophenotypes of T- and B-cells in response to the selected PPE_MPTR peptides (**Table 4.4** and **Figure 3.1** and **Figure 3.2**). Before acquiring samples on the BD LSR II™, BD FACSDiva CS&T Research Beads were used to ensure the cytometer was properly calibrated before use.

Table 4.4: Markers used to assess the phenotype and activation status of different memory subsets of T- and B- cells.

T-helper $CD3^+CD4^+$ / $CD3^+CD8^+$ population	**Marker**
Th1	$CD183^+$
Th2	$CD193^+$
Th17	$CD196^+$
Memory State	
Effector memory (T_{EM})	$CD45RA^-CD28^-$
Central memory (T_{CM})	$CD45RA^-CD28^+$
Naïve (T_N)	$CD45RA^+CD28^+$
Effector memory cells re-expressing CD45RA (T_{TEMRA})	$CD45RA^+CD28^-$
Activated cells (a)	$CD25^+$
aT_{EM}	$CD45RA^-CD28^-CD25^+$
aT_{CM}	$CD45RA^-CD28^+CD25^+$
aT_{Naive}	$CD45RA^+CD28^+CD25^+$
aT_{TEMRA}	$CD45RA^+CD28^-CD25^+$
$CD3^-$ B-cell populations	$CD3^-$
B-cell population	$CD3^-CD19^+$
Activated B-cells (aB-cells)	$CD3^-CD19^+CD25^+$

4.1.4.1 Distribution of $CD4^+$ and $CD8^+$ T-cells in PPE_MPTR-stimulated peripheral blood

T-lymphocyte populations in the peripheral blood of TB, LTBI and healthy individuals were defined based on the expression of CD3 ($CD3^+$). Subsequently, $CD4^+$ and $CD8^+$ cells were identified by the expression of CD4 and CD8, respectively (**Table 4.4**). Immunity to *M. tuberculosis* is critically dependent on $CD4^+$ T-cells and the production of a pro-inflammatory response (Ancelet and Kirman, 2012). The role of $CD8^+$ T-cells in TB disease is less clear, however they have been shown to be required for an optimal immune response against *M. tuberculosis* (Prezzemolo *et al.*, 2014).

To better understand the adaptive immune response to the candidate PPE_MPTR peptides, two of the most important T-helper (Th) subsets involved in maintaining the adaptive immune response during TB infection were investigated, namely the Th1 ($CD183^+$) and Th17 ($CD196^+$) $CD4^+$ cells (Khader *et al.*, 2009; Ottenhoff, 2012). Due to the antagonizing effects Th2-derived cytokines have on Th1-mediated control of *M. tuberculosis* (Rook, 2007) and the important role of Th2 T-cells in promoting antibody-mediated (humoral) immunity (Walker and McKenzie, 2018), the PPE_MPTR-specific distribution of Th2 $CD4^+$ T-cells was also investigated. Because little is known regarding the frequency distribution of both $CD4^+$ and

$CD8^+$ T-cells in response to PPE_MPTR proteins, the corresponding $CD8^+$ T-cell populations were also investigated.

Lymphocytes found in peripheral whole blood of individuals are typically comprised of approximately 60% $CD4^+$ T-cells and 40% $CD8^+$ T-cells (McBride and Striker, 2017). As such, the proportion of observed $CD4^+$ and $CD8^+$ T-cells in response to ESAT-6, CFP-10 and PBS (unstimulated) was as expected, with 60% $CD4^+$ T-cells and 40% $CD8^+$ T-cells (**Figure 4.9**). Likewise, following stimulation with PPE_MPTR peptides, a similar distribution of $CD4^+$ T-cells and $CD8^+$ T-cells was observed in peripheral blood of TB, LTBI and healthy individuals with the expected proportions of $CD4^+$ T-cells (60%) and $CD8^+$ T-cells (40%) (**Figure 4.10**). These results indicate that the proportions of $CD4^+$ and $CD8^+$ T-cell subsets are not fundamentally different between TB, LTBI and healthy individuals, suggesting that any observed differences in memory and activation states of T-helper cell populations is specific to PPE_MPTR-stimulation.

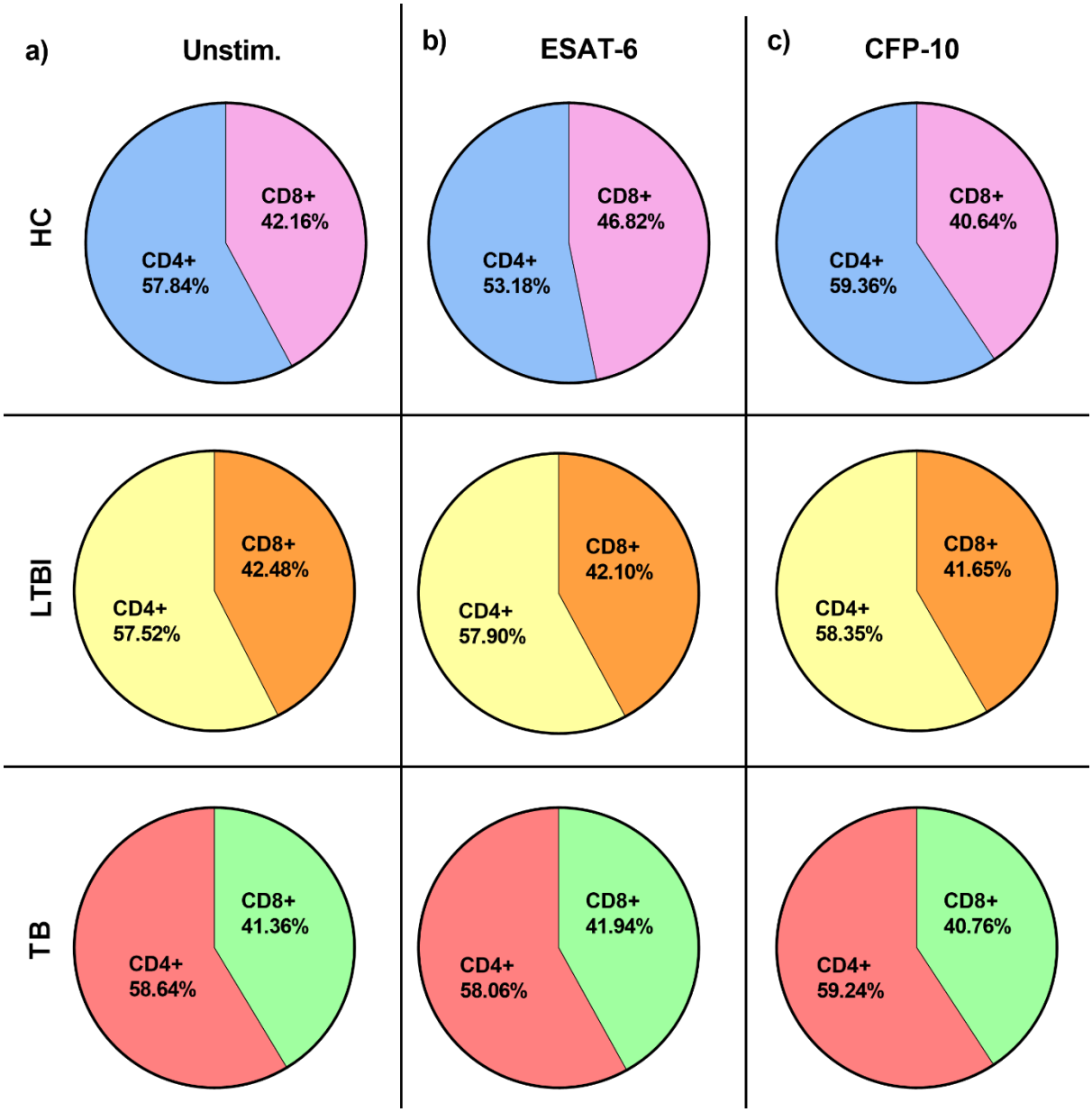

Figure 4.9: Circulating CD4⁺- and CD8⁺ T-cells in the peripheral blood of healthy, LTBI and active TB individuals in (a) unstimulated conditions or in response to (b) ESAT-6 (c) CFP-10. The proportion (%) of CD4⁺ and CD8⁺ T-cells are represented as a mean percentage of the total circulating CD3⁺ population in the peripheral blood of TB (n=5), LTBI (n=5) and healthy individuals (n=11) recruited from high incident TB areas surrounding Tygerberg Hostpital. LTBI = latent tuberculosis infection. HC = healthy control. ESAT-6 = Early Secreted Antigen-6. CFP-10 = Culture Filtrate Protein 10. Unstimulated = PBS.

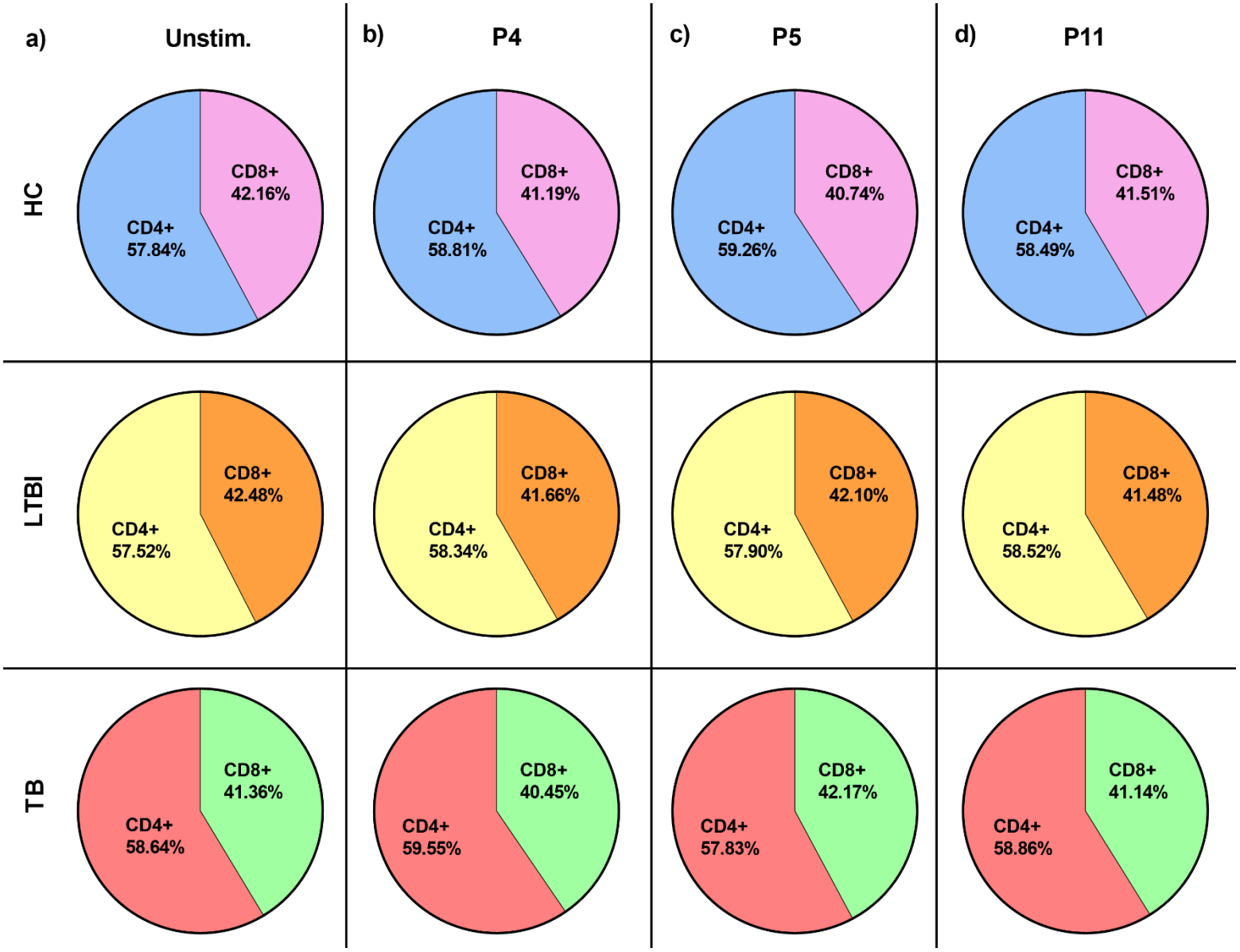

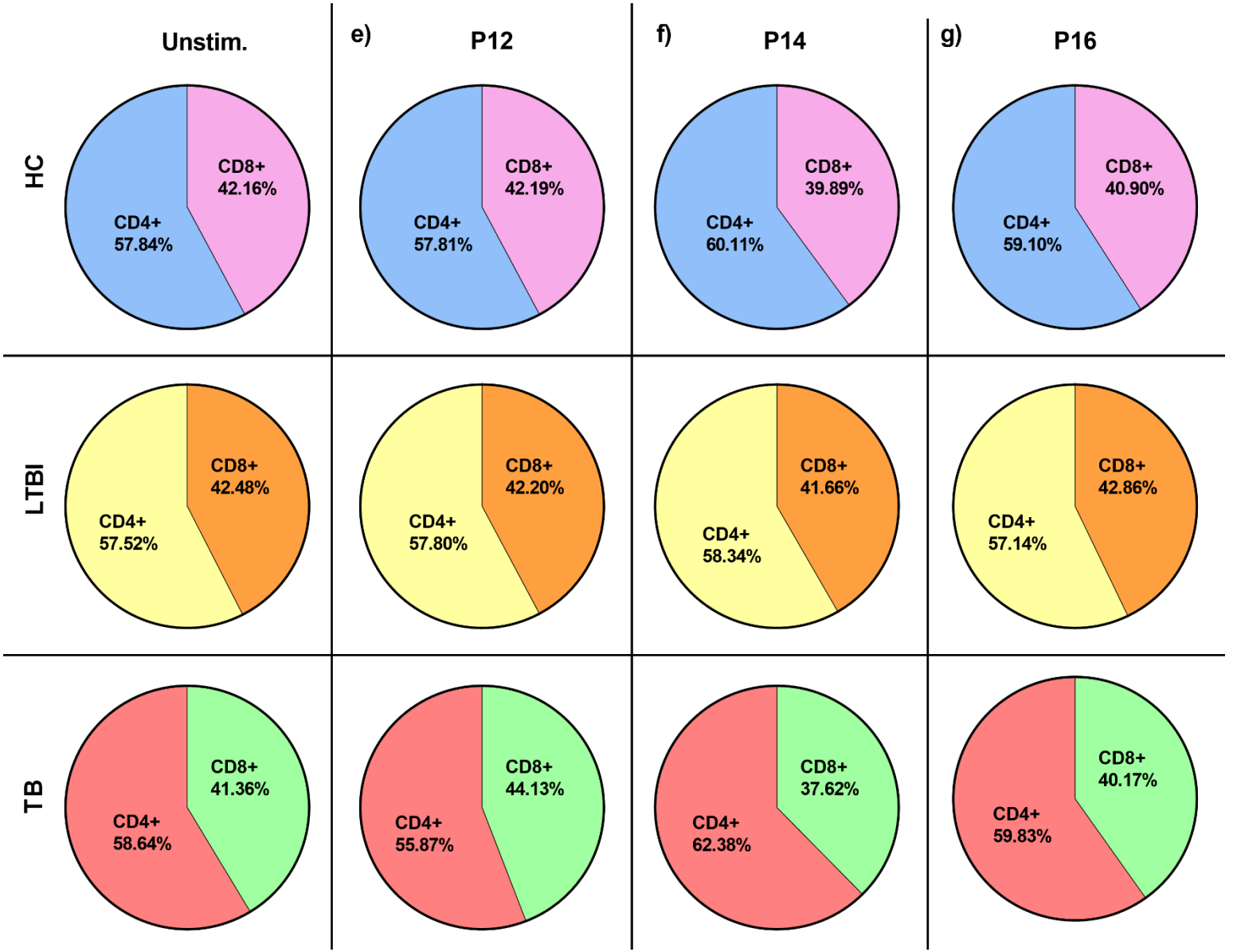

Figure 4.10 (previous page): Circulating CD4⁺- and CD8⁺ T-cells in the peripheral blood of healthy, LTBI and active TB individuals in unstimulated conditions or in response to PPE_MPTR peptides. (a) unstimulated **(b)** P4 **(c)** P5 **(d)** P11 **(e)** P12 **(f)** P14 and **(g)** P16. The proportion (%) of $CD4^+$ and $CD8^+$ T-cells are represented as a mean percentage of the total circulating $CD3^+$ population in the peripheral blood of TB (n=5), LTBI (n=5) and healthy individuals (n=11) recruited from high incident TB areas surrounding Tygerberg Hostpital. P4 = Rv0878c_c. P5 = Rv0878c_d. P11 = Rv2356c_a. P12 = Rv2608_a. P14 = Rv2608_c and P16 = Rv2608_g.

4.1.4.2 Distribution of $CD4^+$ T-cell subsets in PPE_MPTR-stimulated peripheral blood

Naïve T-cells (T_N) are released from the thymus with the ability to recognise specific *M. tuberculosis* antigens through interactions with MHC-I ($CD8^+$) or MHC-II ($CD4^+$) molecules (Murphy, 2013). As a result, T_N cells become activated, proliferate and differentiate into different effecter cell subtypes. Differentiation of T-helper (Th) subset is cytokine dependant and each Th subset (Th1, Th2, Th17) releases a specific subset of cytokines that are associated with different effector functions (T_N, T_{CM} T_{EM} T_{TEMRA}), contributing to the immunophenotype of the cell. Intracellular cytokine staining was not in the scope of this project, however the functional marker frequencies and activation states of Th1, Th2 and Th17 T_N, T_{CM} T_{EM} T_{TEMRA} $CD4^+$ cells were investigated.

The proportions of total $CD4^+$ T_N, T_{CM} T_{EM} T_{TEMRA} (Th1, Th2, Th17) in the peripheral blood of TB, LTBI and healthy controls in response to ESAT-6 and CFP-10 did not differ from those observed in unstimulated conditions (**Figure 4.11**, **Figure 4.12** and **Figure 4.13**). Despite the similar distribution of cells between stimulated and unstimulated conditions, the T_N and T_{CM} $CD4^+$ cells in the peripheral blood of LTBI individuals had a higher expression of surface markers $CD183^+$(Th1) **(Figure 4.11)**, $CD193^+$ (Th2) **(Figure 4.12)** and $CD196^+$ (Th17) **(Figure 4.13)** compared to TB and healthy individuals. The percentage $CD4^+$ E_M T-cell subset was the lowest in all individuals in response to ESAT-6 and CFP-10, comparable with measured populations in unstimulated conditions (**Figure 4.11**, **Figure 4.12** and **Figure 4.13**). Noticeable differences in the levels of activated $CD4^+$ cells were measured in the peripheral blood of TB, LTBI and healthy controls in response to ESAT-6 and CFP-10, when compared to unstimulated controls (**Appendix 7.3; Figure 7.1 - Figure 7.4**). As expected, no activated $CD4^+$ T-cells were observed in healthy individuals in response to controls. In response to CFP-10, LTBI and active TB individuals exhibited activated $CD183^+$ (Th1) and $CD193^+$ (Th2) $CD4^+$ T_{CM} cells, with higher levels of activation observed in LTBI individuals (**Appendix 7.3; Figure**

7.2). In response to ESAT-6, only LTBI individuals exhibited activated CD196^{+} (Th17) CD4^{+} T_{CM} T-cells (**Appendix 7.3; Figure 7.2**).

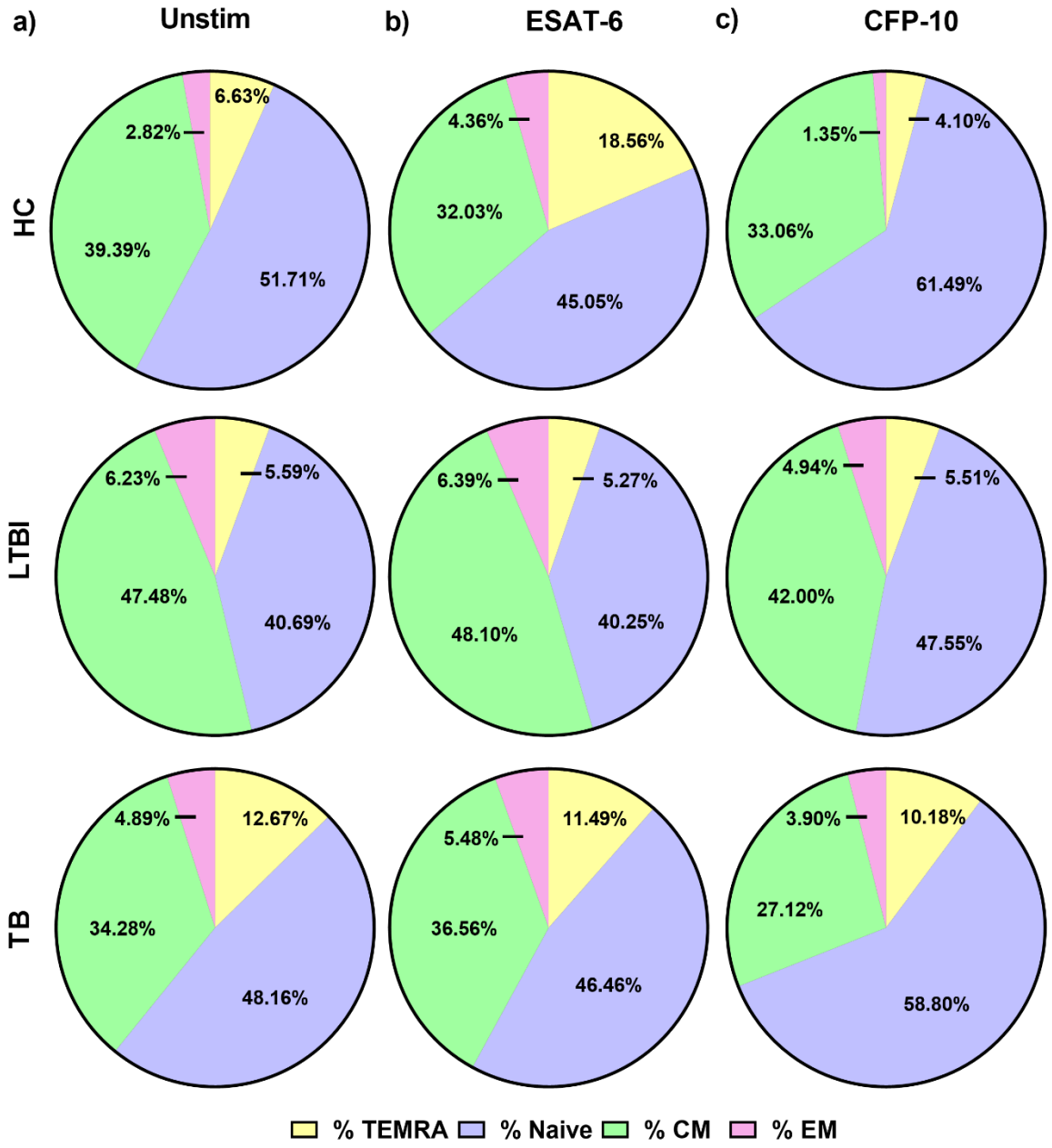

Figure 4.11: Circulating CD183^{+} (Th1) CD4^{+} memory subsets in the peripheral blood of healthy, LTBI and active TB individuals in (a) unstimulated conditions or in response to (b) ESAT-6 and (c) CFP-10. The pie charts represent the proportions of Th1 T_N, T_{CM} T_{EM} T_{TEMRA} as a mean percentage of the total circulating CD4^{+} population in the peripheral blood of TB (n=5), LTBI (n=5) and healthy individuals (n=11) recruited from high incident TB areas surrounding Tygerberg Hostpital. Naïve T-cells = T_N = blue; Central memory T-cells = T_{CM} = green; Effector memory T-cells = T_{EM} = pink; Terminally differentiated T-cells = T_{TEMRA} = yellow. P4 = Rv0878c_a. P5 = Rv0878c_d and P11 = Rv2356c_a.

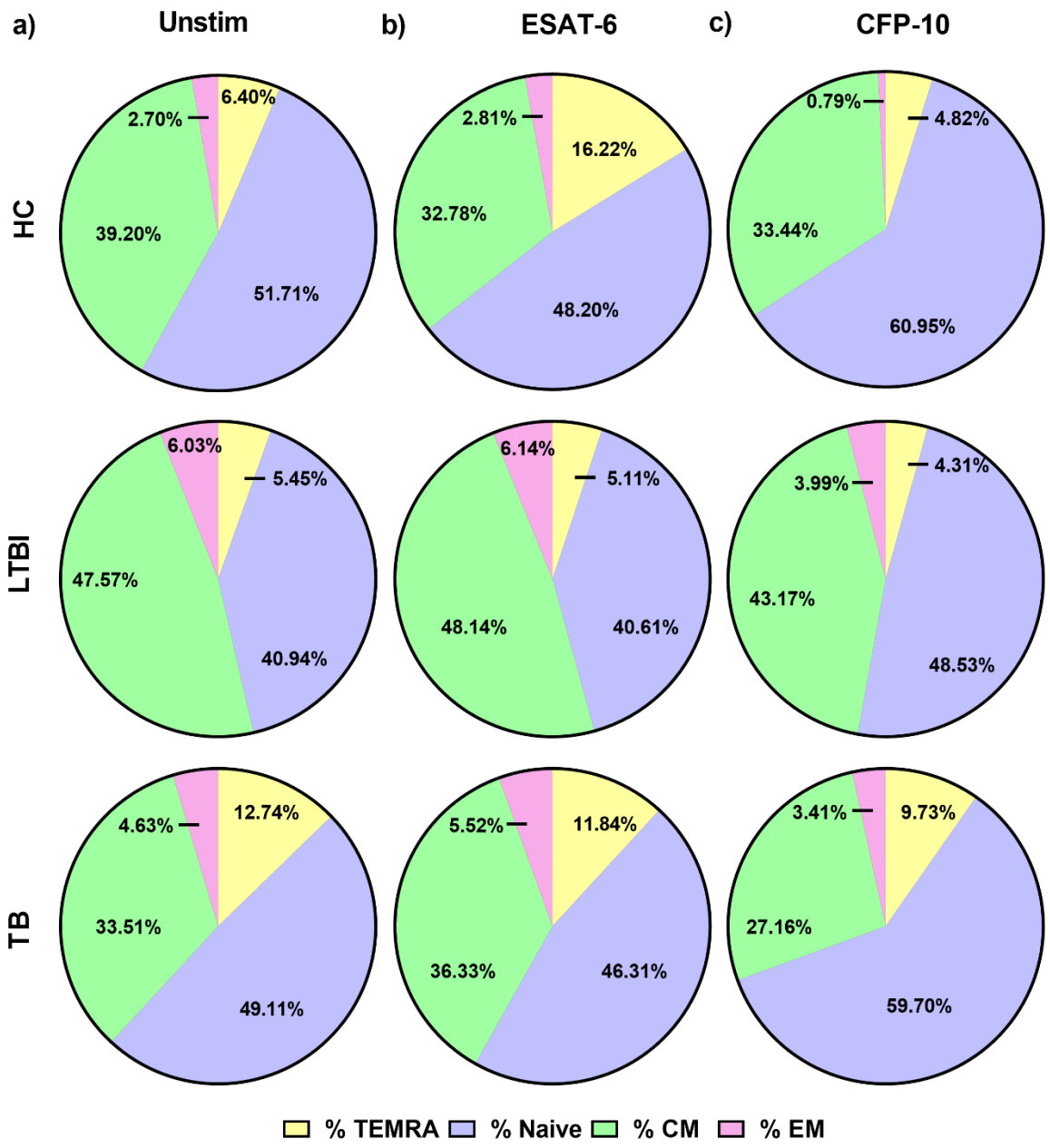

Figure 4.12: Circulating CD193⁺ (Th2) CD4⁺ memory subsets in the peripheral blood of healthy, LTBI and active TB individuals in (a) unstimulated conditions or in response to (b) ESAT-6 and (c) CFP-10. The pie charts represent the proportions of Th1 T_N, T_{CM} T_{EM} T_{TEMRA} as a mean percentage of the total circulating CD4⁺ population in the peripheral blood of TB (n=5), LTBI (n=5) and healthy individuals (n=11) recruited from high incident TB areas surrounding Tygerberg Hostpital. Naïve T-cells = T_N = blue; Central memory T-cells = T_{CM} = green; Effector memory T-cells = T_{EM} = pink; Terminally differentiated T-cells = T_{TEMRA} = yellow. P4 = Rv0878c_a. P5 = Rv0878c_d and P11 = Rv2356c_a.

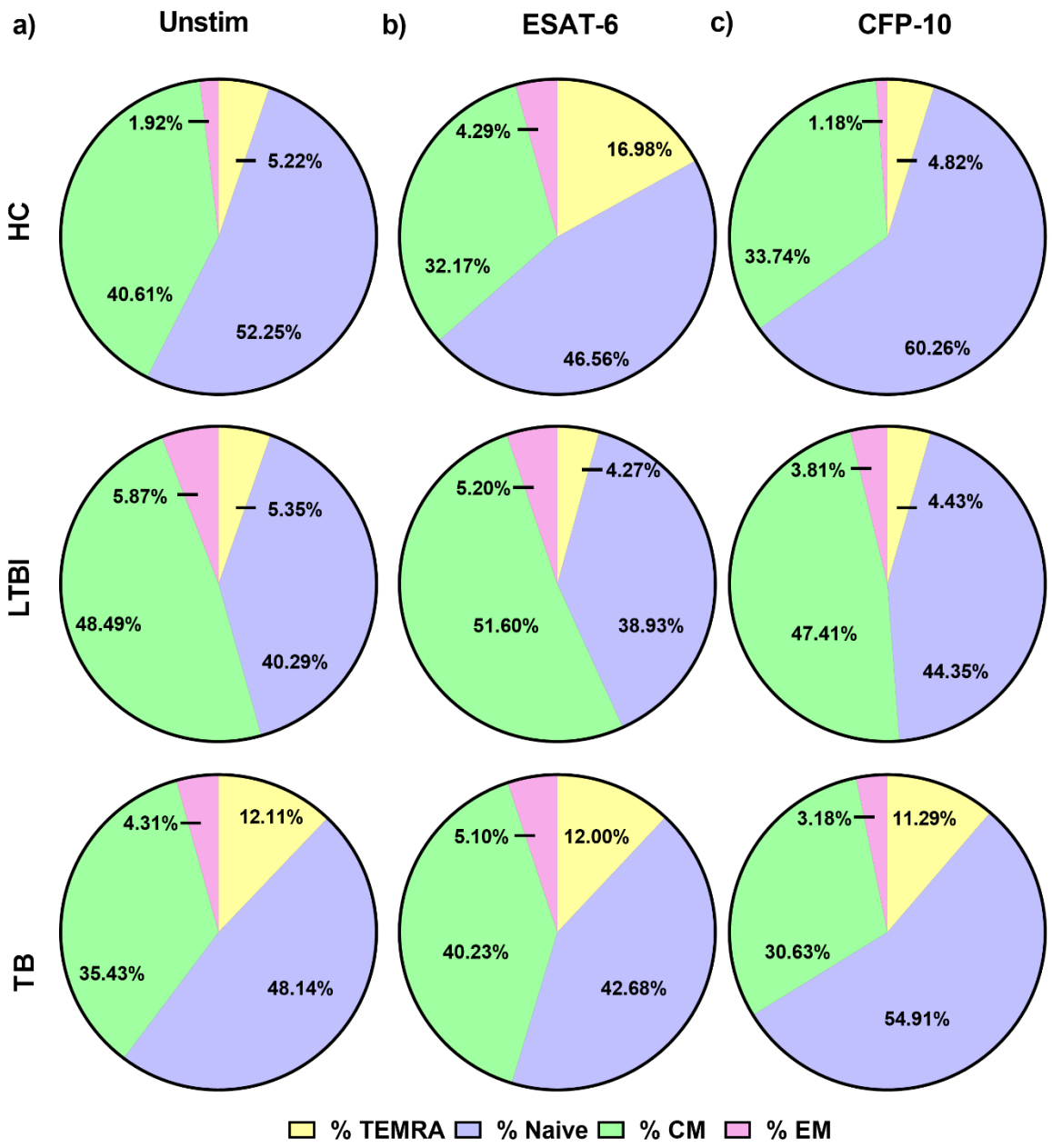

Figure 4.13: Circulating CD196$^+$ (Th17) CD4$^+$ memory subsets in the peripheral blood of healthy, LTBI and active TB individuals in (a) unstimulated conditions or in response to (b) ESAT-6 and (c) CFP-10. The pie charts represent the proportions of Th1 T_N, T_{CM} T_{EM} T_{TEMRA} as a mean percentage of the total circulating CD4$^+$ population in the peripheral blood of TB (n=5), LTBI (n=5) and healthy individuals (n=11) recruited from high incident TB areas surrounding Tygerberg Hostpital. Naïve T-cells = T_N = blue; Central memory T-cells = T_{CM} = green; Effector memory T-cells = T_{EM} = pink; Terminally differentiated T-cells = T_{TEMRA} = yellow. P4 = Rv0878c_a. P5 = Rv0878c_d and P11 = Rv2356c_a.

In response to stimulation with PPE_MPTR peptides, the $CD4^+$ T_N and T_{CM} cells were also the predominant circulating $CD4^+$ memory subtype in healthy, LTBI and TB individuals, with the $CD4^+$ T_{EM} subset comprising the lowest mean proportion of $CD4^+$ memory cells (**Figure 4.14 - Figure 4.16**). The PPE_MPTR peptides induced activated $CD4^+$ T_N, T_{CM}, and T_{EM} T-cells in healthy, LTBI and active TB individuals (**Appendix 7.3; Figure 7.1 - Figure 7.3**), with only marginal levels of activation observed for the $CD4^+$ T_{TEMRA} subset in LTBI individuals (**Appendix 7.3; Figure 7.4**).

$CD3^+CD4^+$ Naïve T-cells

A primary cell mediated immune response is established by the activation of circulating naïve $CD4^+$ T-cells, their proliferation and subsequent differentiation into $CD4^+$ effecter cells. The $CD183^+$ (Th1), $CD193^+$ (Th2) and $CD196^+$ (Th17) naïve T-cell (T_N) subsets were defined as $CD45RA^+CD28^+$ and were the dominant circulating $CD4^+$ memory subset in response to PPE_MPTR-stimulation. The proportion of $CD4^+$ T_N cells was calculated as a percentage of the grandparent Th1, Th2 or Th17 $CD3^+CD4^+$ populations (**Table 4.4**).

Stimulation with P11, P12, P14 and P16 induced more $CD183^+$ (Th1), $CD193^+$ (Th2) and $CD196^+$ (Th17) expressing T_N $CD4^+$ T-cells in TB and healthy controls than observed in unstimulated conditions (**Figure 4.14**, **Figure 4.15** and **Figure 4.16 d, e, f, g**). Similar expression levels were also observed in LTBI individuals, however the expression of $CD183^+$ (Th1) T_N $CD4^+$ T-cells was not influenced by stimulation with P14 and P16 as observed in TB and healthy individuals (**Figure 4.14 f, g**). In healthy controls, the highest proportion of $CD4^+$ T_N cells was observed for $CD193^+$ (Th2) and $CD196^+$ (Th17) T_N $CD4^+$ cells in response to P14 (75%) (**Figure 4.15 f** and **Figure 4.16 f**). In active TB individuals, equally high $CD193^+$ (Th2) and $CD196^+$ (Th17) proportions of T_N $CD4^+$ cells were produced in response to P11 and P14 (**Figure 4.15 d,f** and **Figure 4.16 d,f**) (70%). The highest proportion of $CD4^+$ T_N produced in LTBI individuals were T_N $CD4^+$ cells expressing $CD193^+$ (Th2) in response to P11 and P14 (65%) (**Figure 4.15 d,f**).

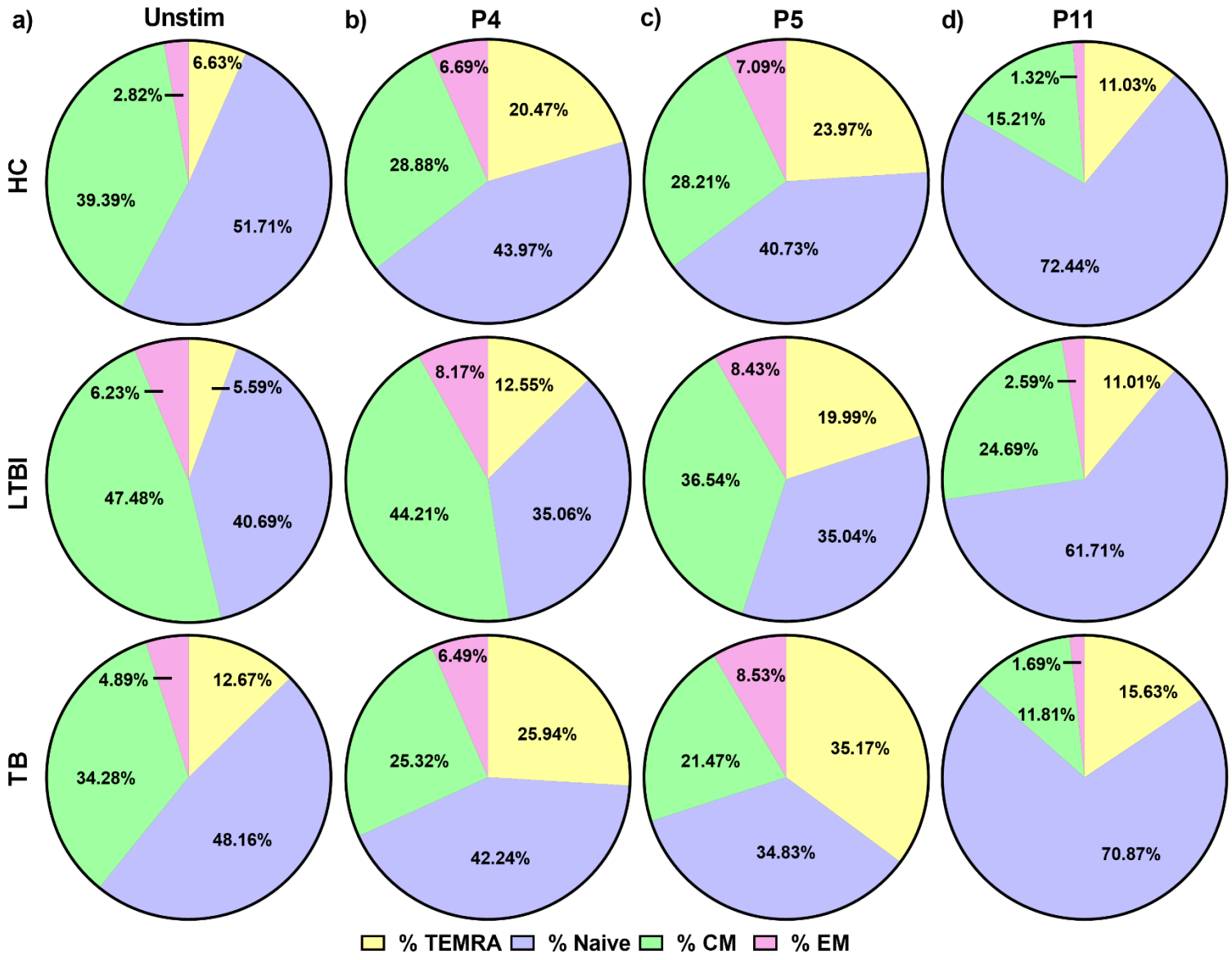

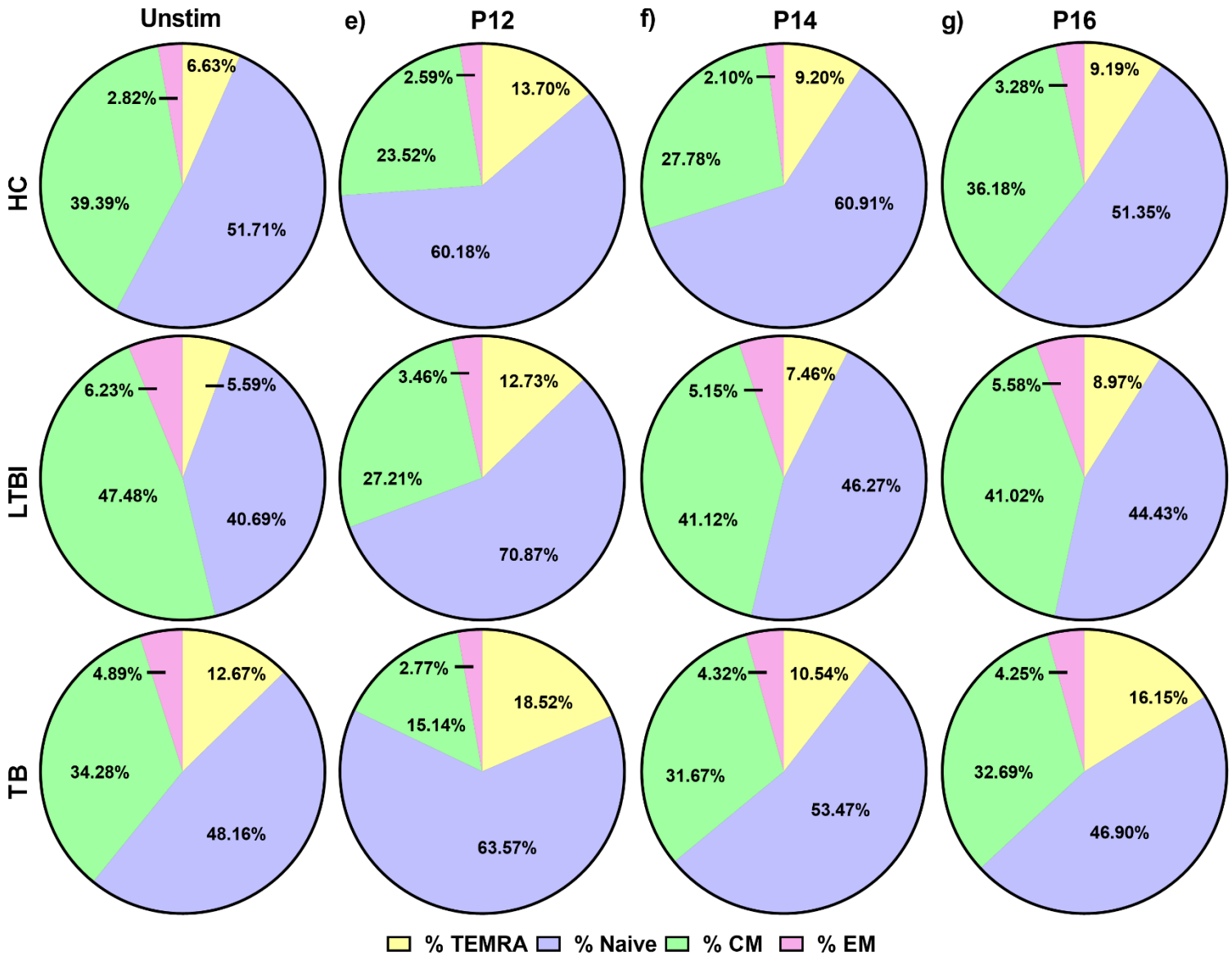

Figure 4.14: Circulating CD183$^+$ (Th1) CD4$^+$ memory subsets in the peripheral blood of healthy, LTBI and active TB individuals in unstimulated conditions or in response to PPE_MPTR peptides. (a) unstimulated **(b)** P4 **(c)** P5 **(d)** P11 **(e)** P12 **(f)** P14 and **(g)** P16. The pie charts represent the proportions of Th1 T_N, T_{CM} T_{EM} T_{TEMRA} as a mean percentage of the total circulating CD4$^+$ population in the peripheral blood of TB (n=5), LTBI (n=5) and healthy individuals (n=11) recruited from high incident TB areas surrounding Tygerberg Hostpital. Naïve T-cells = T_N = blue; Central memory T-cells = T_{CM} = green; Effector memory T-cells = T_{EM} = pink; Terminally differentiated T-cells = T_{TEMRA} = yellow. P4 = Rv0878c_a. P5 = Rv0878c_d and P11 = Rv2356c_a

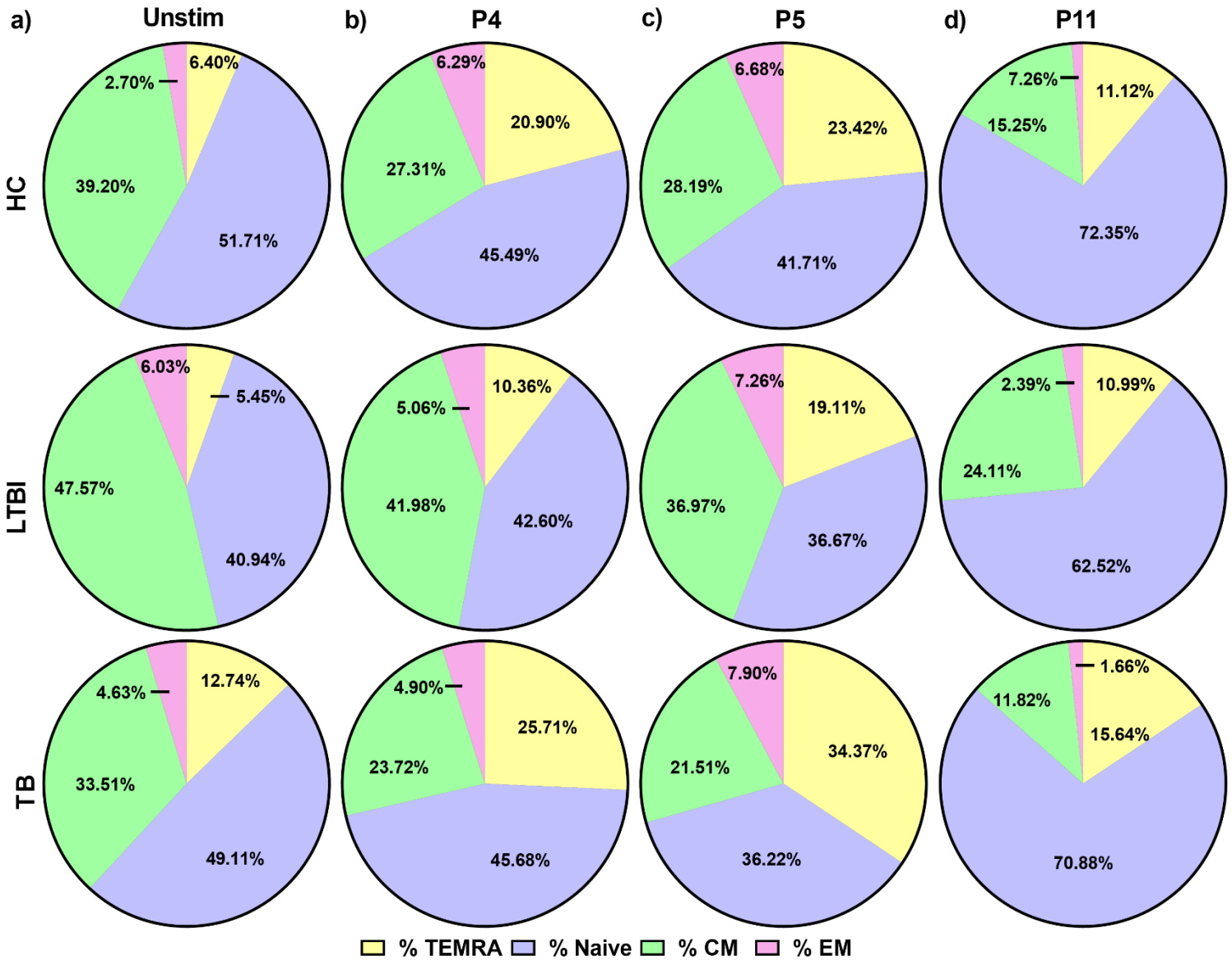

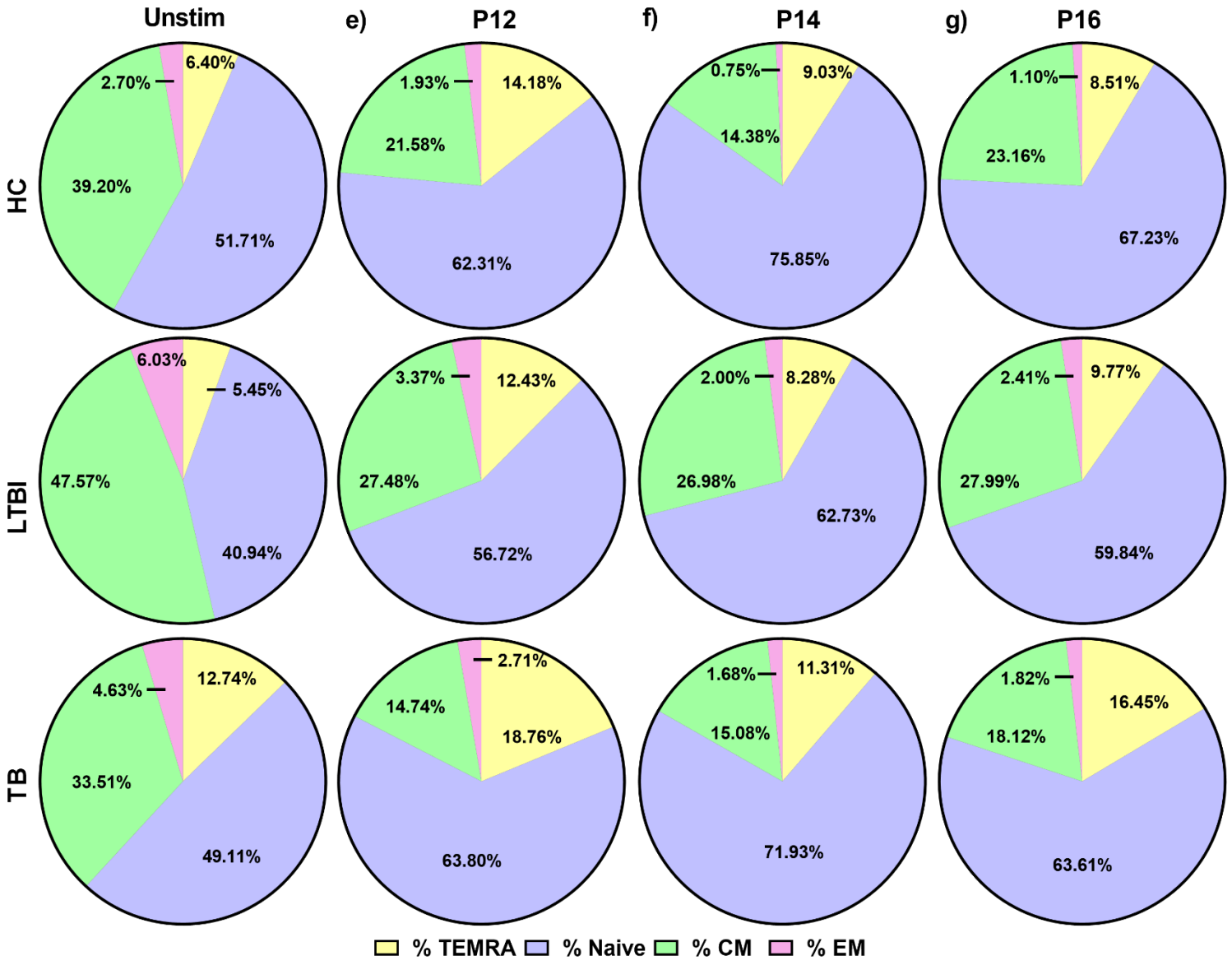

Figure 4.15: Circulating CD193$^+$ (Th2) CD4$^+$ memory subsets in the peripheral blood of healthy, LTBI and active TB individuals in unstimulated conditions or in response to PPE_MPTR peptides. (a) unstimulated **(b)** P4 **(c)** P5 **(d)** P11 **(e)** P12 **(f)** P14 and **(g)** P16. The pie charts represent the proportions of Th2 T_N, T_{CM} T_{EM} T_{TEMRA} as a mean percentage of the total circulating CD4$^+$ population in the peripheral blood of TB (n=5), LTBI (n=5) and healthy individuals (n=11) recruited from high incident TB areas surrounding Tygerberg Hostpital. Naïve T-cells = T_N = blue; Central memory T-cells = T_{CM} = green; Effector memory T-cells = T_{EM} = pink; Terminally differentiated T-cells = T_{TEMRA} = yellow. P4 = Rv0878c_a. P5 = Rv0878c_d and P11 = Rv2356c_a

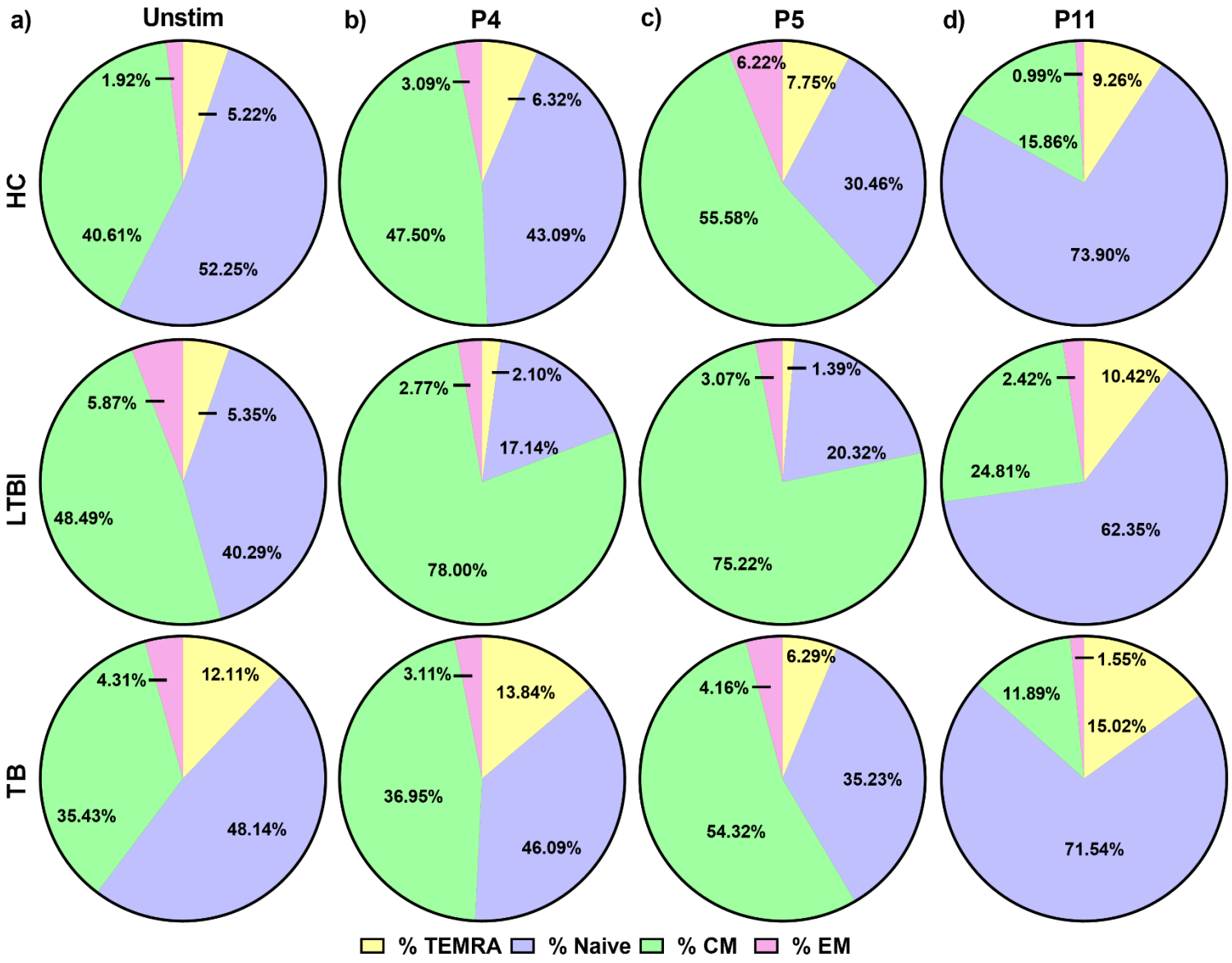

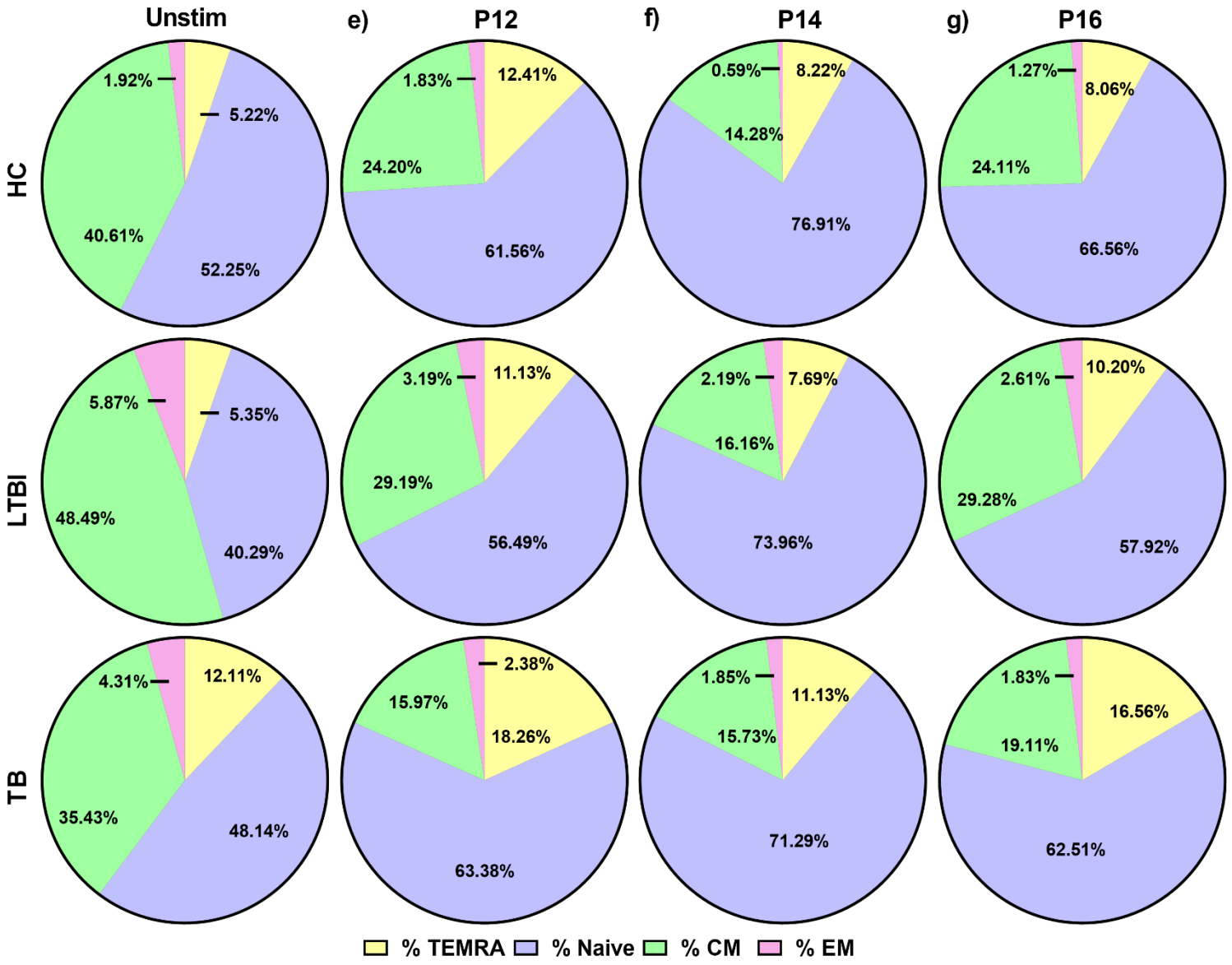

Figure 4.16: Circulating CD196⁺ (Th17) CD4⁺ memory subsets in the peripheral blood of healthy, LTBI and active TB individuals in unstimulated conditions or in response to PPE_MPTR peptides. (a) unstimulated **(b)** P4 **(c)** P5 **(d)** P11 **(e)** P12 **(f)** P14 and **(g)** P16. The pie charts represent the proportions of Th17 T_N, T_{CM} T_{EM} T_{TEMRA} as a mean percentage of the total circulating $CD4^+$ population in the peripheral blood of TB (n=5), LTBI (n=5) and healthy individuals (n=11) recruited from high incident TB areas surrounding Tygerberg Hostpital. Naïve T-cells = T_N = blue; Central memory T-cells = T_{CM} = green; Effector memory T-cells = T_{EM} = pink; Terminally differentiated T-cells = T_{TEMRA} = yellow. P4 = Rv0878c_a. P5 = Rv0878c_d and P11 = Rv2356c_a

In response to stimulation with each PPE_MPTR candidate, $CD183^+$ (Th1), $CD193^+$ (Th2) and $CD196^+$ (Th17) T_N $CD4^+$ T-cells were activated in active TB, LTBI and healthy individuals (**Appendix 7.3; Figure 7.1**). PPE_MPTR peptide, P4, induced the highest level of activated T_N $CD4^+$ T-cells compared to the other peptides and was seen in the $CD183^+$ (Th1) T_N $CD4^+$ T-cell subset of LTBI individuals. Interestingly, the distribution of activated T_N $CD4^+$ T-cells was similar in healthy and active TB individuals. In response to P16, higher levels of activated $CD183^+$ (Th1), $CD193^+$ (Th2) and $CD196^+$ (Th17) $CD4^+$ T_N T-cells were observed in healthy and active TB individuals compared to LTBI individuals. The level of activation in response to P12 in healthy and active TB individuals was similar to what was observed for P16, however, no activated $CD193^+$ (Th2) $CD4^+$ T_N T-cells were observed (**Appendix 7.3; Figure 7.1**).

$CD3^+CD4^+$ Central Memory T-cells

We went on to assess the proportions of different $CD4^+$ memory subsets. Both central- and effector memory cells recognise previously encountered antigens and respond rapidly to secondary infection (Mahnke *et al.*, 2013). Central memory $CD4^+$ T-cells (T_{CM}) migrate through lymph nodes and like T_{EM}, can secrete effector cytokines. T_{CM} T-cells are known to have a substantially higher proliferative capability than T_{EM} T-cells which is vital during secondary antigen encounter (Farber *et al.*, 2014). Effector memory $CD4^+$ T-cells migrate though peripheral tissues and exert rapid effector functions at the site of infection in an attempt to eradicate the pathogen.

In response to stimulation with PPE_MPTR peptides, higher proportions of $CD4^+$ T_{CM} cells were observed in the peripheral blood of active TB, LTBI and healthy individuals compared to $CD4^+$ T_{EM} cells and were defined as $CD45RA^-$ $CD28^+$ (**Figure 3.1**). The proportion of T_{CM} was calculated as a percentage of the grandparent $CD183^+$ (Th1), $CD193^+$ (Th2) and $CD196^+$ (Th17) $CD3^+CD4^+$ populations.

In response to stimulation with P12, P14 and P16, similar proportions of $CD183^+$ expressing (Th1) T_{CM} $CD4^+$ cells were observed in TB, LTBI and healthy individuals as seen in

unstimulated conditions (**Figure 4.14 e, f, g**). In response to P4, P5 and P11, active TB, LTBI and healthy individuals all exhibited increased expression of $CD183^+$ on T_{CM} $CD4^+$ cells (Th1) (**Figure 4.14 b, c, d**) compared to unstimulated levels. One exception to this result was observed in LTBI, where only marginal PPE_MPTR-specific differences in the expression of CD183 was observed on T_{CM} $CD4^+$ cells. The greatest proportion of PPE_MPTR-specific T_{CM} $CD4^+$ cells in LTBI individuals expressed CD196 (**Figure 4.16**). In response to P4 and P5, the proportion of $CD196^+CD4^+$cells increased by 30% and 27%, respectively (**Figure 4.16 b, c**). Only in response to P5, did the proportions of $CD196^+$ T_{CM} $CD4^+$ cells (Th17) increase in active TB (20%) and healthy individuals (15%) (**Figure 4.16 c**).

Similarly to the proportions of activated T_N $CD4^+$ T-cells observed in response to PPE_MPTR peptides, all T_{CM} $CD4^+$ cell subtypes were activated in healthy, LTBI and active TB individuals during stimulation (**Appendix 7.3; Figure 7.2**). PPE_MPTR peptide P4 induced the highest levels of activated $CD183^+$ (Th1), $CD193^+$ (Th2) and $CD196^+$ (Th17) T_{CM} $CD4^+$ T-cells compared to the other peptides, the distribution of which was similar between healthy, active TB and LTBI individuals. In response to P11 and P14, LTBI individuals exhibited higher levels of activated $CD183^+$ (Th1), $CD193^+$ (Th2) and $CD196^+$ (Th17) T_{CM} $CD4^+$ T-cells compared to healthy and active TB individuals. The activated T_{CM} $CD4^+$ T-cell subsets between healthy individuals displayed a large amount of variation, especially in response to P11, P12 and P14 (**Appendix 7.3; Figure 7.2**).

$CD3^+CD4^+$ Effector memory T-cells

Effector memory $CD4^+$ T-cells (T_{EM}) mediate rapid protective responses during *M. tuberculosis* infection by travelling through peripheral tissues to the lung, where they secrete pro-inflammatory cytokines that aid in pathogen clearance (Murphy, 2013). From the four memory subsets investigated, the $CD4^+$ T_{EM} subset comprised the lowest mean proportion of circulating memory cells in response to controls and PPE_MPTR peptides. The T_{EM} cells were defined as $CD45RA^-CD28^-$ and the proportion of T_{EM} in the peripheral blood cells of TB, LTBI and healthy individuals was calculated as a percentage of the grandparent $CD183^+$ (Th1), $CD193^+$ (Th2) and $CD196^+$ (Th17) $CD3^+CD4^+$ populations (**Table 4.4**).

There was no difference in the PPE_MPTR-specific proportions of $CD4^+$ T_{EM} cells expressing CD183 (Th1), CD193 (Th2) or CD196 (Th17) compared to those observed in unstimulated conditions (**Figure 4.14**, **Figure 4.15** and **Figure 4.16**). There were marginal increases, above unstimulated conditions, in the proportions of T_{EM} $CD4^+$ cells expressing $CD183^+$ (Th1) and

$CD193^+$ (Th2) observed in response to P4 and P5 (**Figure 4.14** and **Figure 4.15 b, c**). This occurred in equal distributions between active TB, LTBI and healthy individuals.

Activated T_{EM} $CD4^+$ cells were observed in response to all PPE_MPTR peptides, with higher proportions of $CD183^+$ (Th1) and $CD193^+$ (Th2) expressing T_{EM} $CD4^+$ T-cells than $CD196^+$ (Th17) expressing T_{EM} $CD4^+$ T-cells (**Appendix 7.3; Figure 7.3**). The levels of activated T_{EM} $CD4^+$ T-cells were highest in LTBI and active TB individuals compared to healthy controls. In response to P4, TB individuals produced higher proportions of activated $CD183^+$ (Th1) and $CD193^+$ (Th2) expressing T_{EM} $CD4^+$ T-cells than LTBI individuals, however P4 and P5 activated more $CD196^+$ (Th17) T_{EM} $CD4^+$ T-cells in LTBI individuals compared to active TB individuals (**Appendix 7.3; Figure 7.3**).

$CD3^+$ $CD4^+$ TEMRA T-cells

Highly differentiated effector memory $CD4^+$ cells have been identified in individuals with active TB disease (Arrigucci *et al.*, 2018). These cells can be referred to as terminally differentiated effector memory T-cells re-expressing CD45RA (T_{TEMRA}) and are characterised by low functional and proliferative abilities. The T_{TEMRA} subset was defined as $CD45RA^+CD28^-$ and the proportion of T_{TEMRA} was calculated as a percentage of the grandparent $CD183^+$ (Th1), $CD193^+$ (Th2) and $CD196^+$ (Th17) $CD3^+CD4^+$ populations (**Table 4.4**).

In response to P4, P5 and P12, higher proportions of $CD183^+$ (Th1) and $CD193^+$ (Th2) expressing T_{TEMRA} $CD4^+$ cells were measured in the peripheral blood of active TB, LTBI and healthy individuals and the distribution of these subsets was comparable between the different study groups as compared to unstimulated conditions (**Figure 4.14** and **Figure 4.15 c, d, e**). Only P12 induced higher proportions of $CD196^+$ (Th17) expressing T_{TEMRA} $CD4^+$ cells (**Figure 4.16 e**) above unstimulated conditions in LTBI and healthy individuals.

In response to all PPE_MPTR peptides, activated $CD193^+$ (Th1) T_{TEMRA} $CD4^+$ T-cells were observed in healthy, LTBI and active TB individuals, with the highest level of activated $CD193^+$ T_{TEMRA}'s observed in LTBI individuals in response to P4 (**Appendix 7.3; Figure 7.4**). Overall, $CD196^+$ (Th17) T_{TEMRA} $CD4^+$ T-cell subset in LTBI individuals exhibited the highest level of activation (P4) compared to $CD183^+$ (Th1) and $CD193^+$ (Th2) subsets. Healthy controls exhibited no activated $CD193^+$ (Th2) or $CD196^+$ (Th17) T_{TEMRA} $CD4^+$ T-cell subsets in response to any PPE_MPTR peptides. In TB individuals, no activated $CD193^+$ (Th2) or

$CD196^+$ (Th17) T_{TEMRA} $CD4^+$ T-cells were observed in response to P5 and P12 respectively (**Appendix 7.3; Figure 7.4**).

4.1.4.3 $CD8^+$ T-cells subsets found in PPE_MPTR-stimulated peripheral blood

The precise function of $CD8^+$ T-cells during TB disease is less well characterised than those of $CD4^+$ T-cells, however it has been shown that optimal $CD4^+$ T-cell function requires the presence of $CD8^+$ T-cells (Ling Lin and Flynn, 2005). $CD8^+$ T-cells are also able to secrete pro-inflammatory cytokines such as IFN-γ and TNF-α, but unlike $CD4^+$ T-cells, $CD8^+$ T-cells also release cytotoxic molecules (perforin, granzymes or granulysin) that result in the apoptosis of heavily burdened *M. tuberculosis* cells (Prezzemolo *et al.*, 2014). We included $CD8^+$ T-cells in the analyses of functional marker frequencies to PPE_MPTR peptides to determine if the candidate peptides induce any PPE_MPTR-specific changes.

In response to ESAT-6 and CFP-10, the proportions of $CD183^+$ (Th1) and $CD193^+$ (Th2) T_N $CD8^+$ T-cells in healthy controls was higher compared to what was observed for the unstimulated control (**Figure 4.17** and **Figure 4.18**). No changes in the proportions of $CD183^+$ (Th1) T_N, T_{CM} T_{EM} T_{TEMRA} $CD8^+$ cells were observed in response to ESAT-6 or CFP-10 in LTBI or active TB individuals (**Figure 4.17**). In response to CFP-10, LTBI, active TB and healthy individuals exhibited higher proportions of $CD196^+$ (Th17) T_N $CD8^+$ T-cells compared to the unstimulated control (**Figure 4.19**). This was also observed for $CD193^+$ (Th2) T_N $CD8^+$ T-cells, but only in LTBI and TB individuals (**Figure 4.18**). Only stimulation with ESAT-6 resulted in activation of $CD183^+$, $CD193^+$ and $CD196^+$ T_N $CD8^+$ T-cells in healthy controls. The proportions of activated $CD183^+$, $CD193^+$ and $CD196^+$ T_N $CD8^+$ T-cells observed in healthy controls was greater than seen in TB and LTBI individuals. In response to ESAT-6, active TB and LTBI individuals did not exhibit activated $CD183^+$, $CD193^+$ and $CD196^+$ $CD8^+$ T-cells in proportions greater than observed for unstimulated conditions (**Figure 4.17** and **Figure 4.18** and **Figure 4.19**). No activated $CD183^+$, $CD193^+$ and $CD196^+$ $CD8^+$ T-cells (T_N, T_{CM}, T_{EM}, T_{TEMRA}) were observed in response to ESAT-6 or CFP-10 in healthy controls, LTBI or active TB individuals (**Appendix 7.4; Figure 7.5 - Figure 7.8**).

The functional marker frequencies of the $CD3^+CD8^+$ T-cells in response to stimulation with PPE_MPTR peptides were comparable to unstimulated levels. PPE_MPTR peptides induced marginal levels of activated $CD8^+$ subsets in healthy, LTBI and active TB individuals.

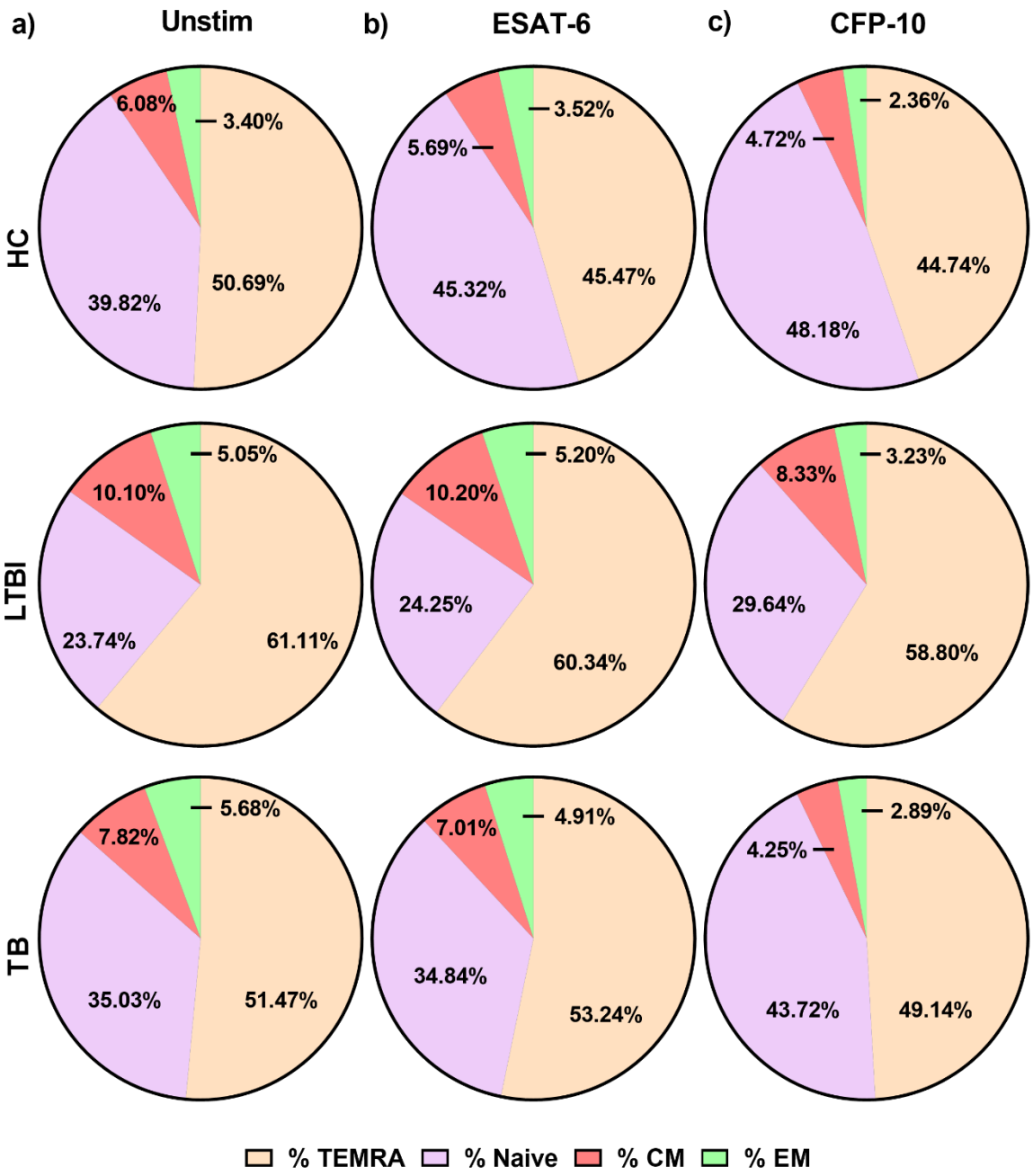

Figure 4.17: Circulating CD183⁺ (Th1) CD8⁺ memory subsets in the peripheral blood of healthy, LTBI and active TB individuals in (a) unstimulated conditions or in response to stimulation with (b) ESAT-6 and (c) CFP-10. The pie charts represent the proportions of Th1 T_N, T_{CM} T_{EM} T_{TEMRA} as a mean percentage of the total CD8⁺ population. HC = healthy controls (n=11). LTBI = latent TB infection (n=5). TB = active TB (n=5). ESAT-6 = Early Secreted Antigen-6. CFP-10 = Culture Filtrate Protein 10. Unstim = Unstimulated (PBS). Naïve T-cells = T_N = pink; Central memory T-cells = T_{CM} = red; Effector memory T-cells = T_{EM} = green; Terminally differentiated T-cells = T_{TEMRA} = orange.

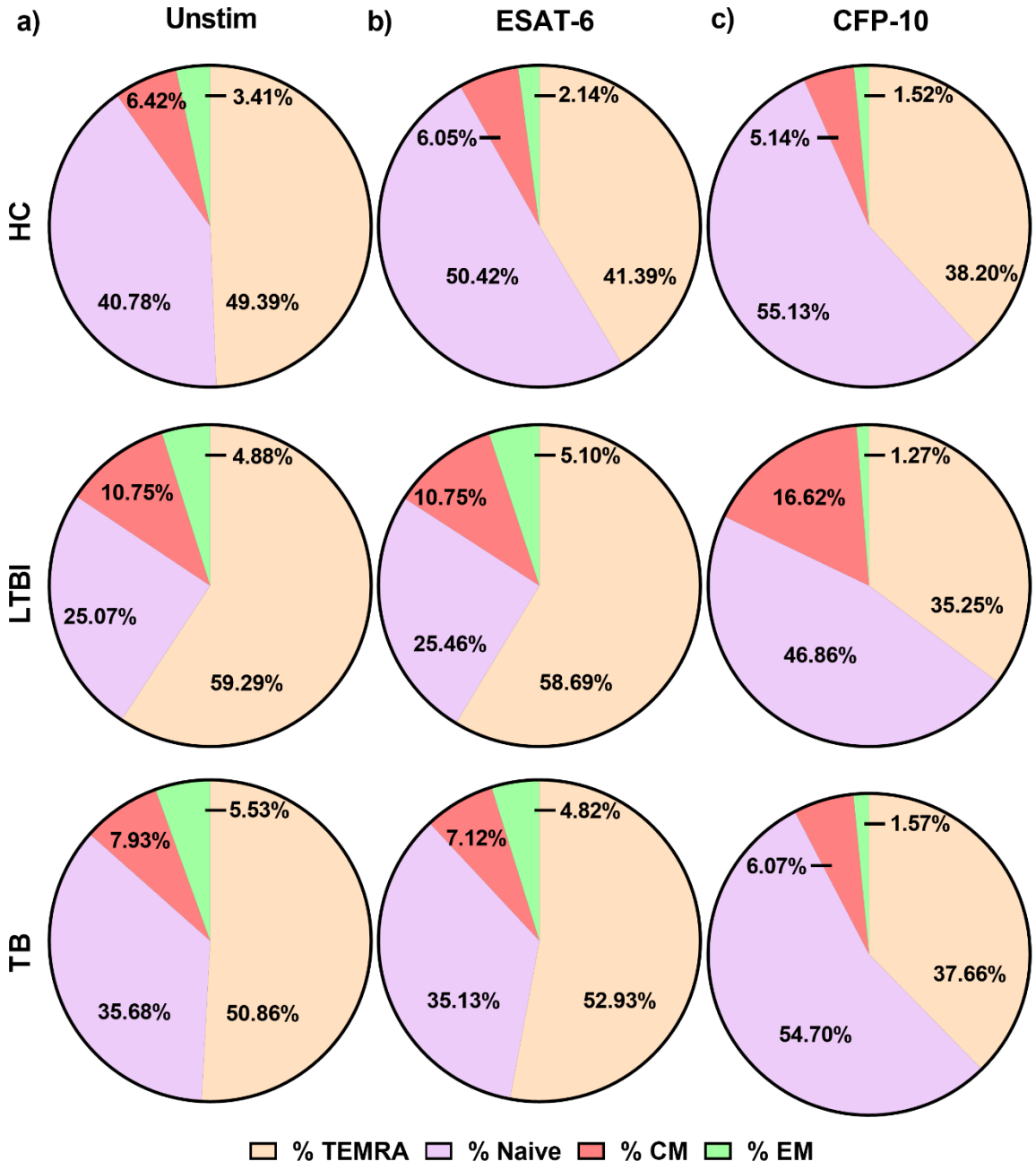

Figure 4.18: Circulating CD193$^+$ (Th2) CD8$^+$ memory subsets in the peripheral blood of healthy, LTBI and active TB individuals in (a) unstimulated conditions or in response to stimulation with (b) ESAT-6 and (c) CFP-10. The pie charts represent the proportions of Th2 T_N, T_{CM} T_{EM} T_{TEMRA} as a mean percentage of the total CD8$^+$ population. HC = healthy controls (n=11). LTBI = latent TB infection (n=5). TB = active TB (n=5). ESAT-6 = Early Secreted Antigen-6. CFP-10 = Culture Filtrate Protein 10. Unstim = Unstimulated (PBS). Naïve T-cells = T_N = pink; Central memory T-cells = T_{CM} = red; Effector memory T-cells = T_{EM} = green; Terminally differentiated T-cells = T_{TEMRA} = orange.

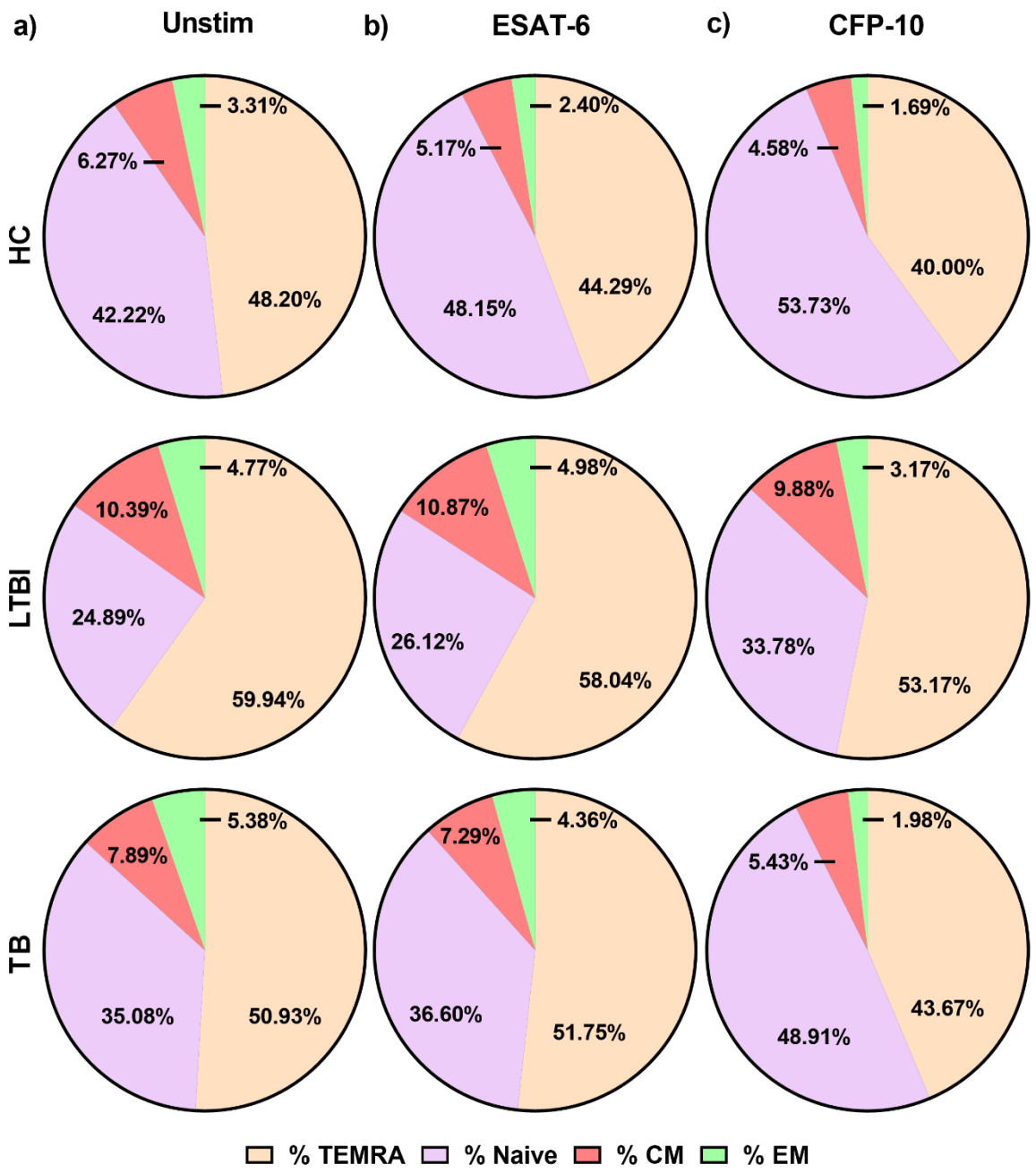

Figure 4.19: Circulating CD196$^+$ (Th17) CD8$^+$ memory subsets in the peripheral blood of healthy, LTBI and active TB individuals in (a) unstimulated conditions or in response to stimulation with (b) ESAT-6 and (c) CFP-10. The pie charts represent the proportions of Th17 T_N, T_{CM} T_{EM} T_{TEMRA} as a mean percentage of the total CD8$^+$ population. HC = healthy controls (n=11). LTBI = latent TB infection (n=5). TB = active TB (n=5). ESAT-6 = Early Secreted Antigen-6. CFP-10 = Culture Filtrate Protein 10. Unstim = Unstimulated (PBS). Naïve T-cells = T_N = pink; Central memory T-cells = T_{CM} = red; Effector memory T-cells = T_{EM} = green; Terminally differentiated T-cells = T_{TEMRA} = orange.

$CD3^+CD8^+$ Naïve T-cells

Naïve $CD8^+$ T-cells circulate in the peripheral blood and become activated in lymphoid tissues following recognition of antigen. Naïve $CD8^+$ undergo expansion and are able to differentiate in various subpopulations, namely central memory (T_{CM}), effector memory (T_{EM}) and terminally differentiated effector (T_{TEMRA}) cells (Geginat *et al.*, 2003). The $CD183^+$ (Th1) $CD193^+$ (Th2), and $CD196^+$ (Th17) naïve $CD8^+$T-cell (T_N) subsets were defined as $CD45RA^+CD28^+$ and the proportion of $CD8^+$ T_N cells was calculated as a percentage of the grandparent Th1, Th2 or Th17 $CD3^+CD4^+$ populations (**Table 4.4**).

Overall, candidate PPE_MPTR peptides caused marginal differences in the proportions of $CD8^+$ T_N cells compared to those observed for unstimulated conditions. No changes in the proportions of T_N $CD8^+$ cells expressing $CD183^+$ (Th1) or $CD193^+$ (Th2) were measured in active TB, LTBI or healthy individuals in response to stimulation with PPE_MPTR peptides (**Figure 4.20** and **Figure 4.21**). In response to stimulation with P4 and P5, active TB, LTBI and healthy individuals all exhibited increased proportions of $CD196^+$ (Th17) T_N $CD8^+$ cells compared to unstimulated conditions (**Figure 4.22 b, c**). The mean highest proportions of $CD196^+$ (Th17) T_N $CD8^+$ cells in response to P4 and P5 was observed in active TB and healthy controls (~58%) compared to LTBI individuals (~43%) (**Figure 4.22 b, c**).

In response to stimulation with PPE_MPTR peptides, no activation of $CD183^+$ T_N $CD8^+$ cells (Th1) were detected in healthy, LTBI or active TB individuals in response to P5 (**Appendix 7.4; Figure 7.5**). The highest proportion of activated T_N $CD8^+$ T-cells was observed for the $CD183^+$ (Th1) subset in TB individuals in response to P14. In response to P11, P12, P14 and P16 similar proportions of activated $CD193^+$ (Th2) and $CD196^+$ (Th17) T_N $CD8^+$ T-cells were observed in healthy, LTBI and active TB individuals (**Appendix 7.4; Figure 7.5**).

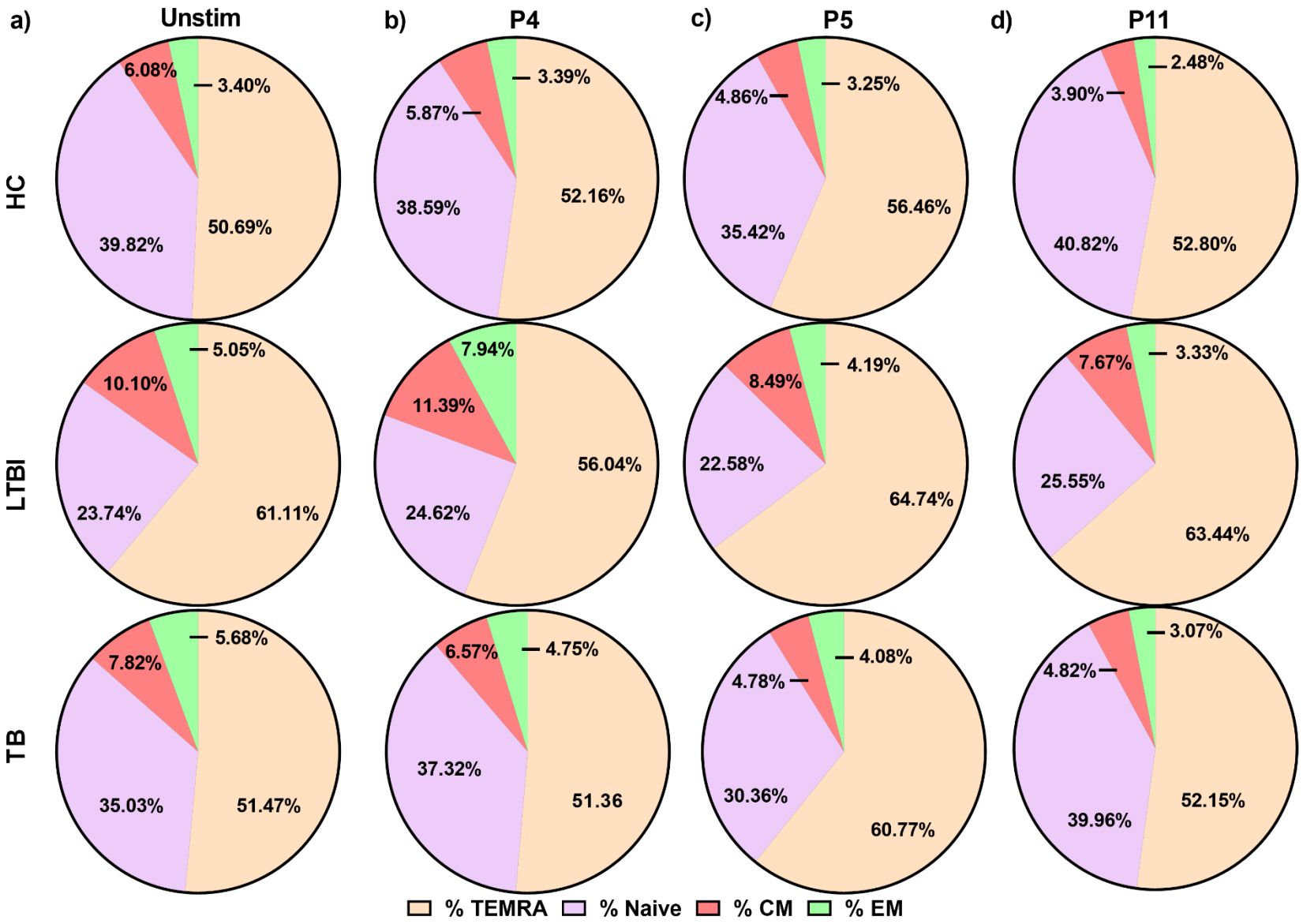

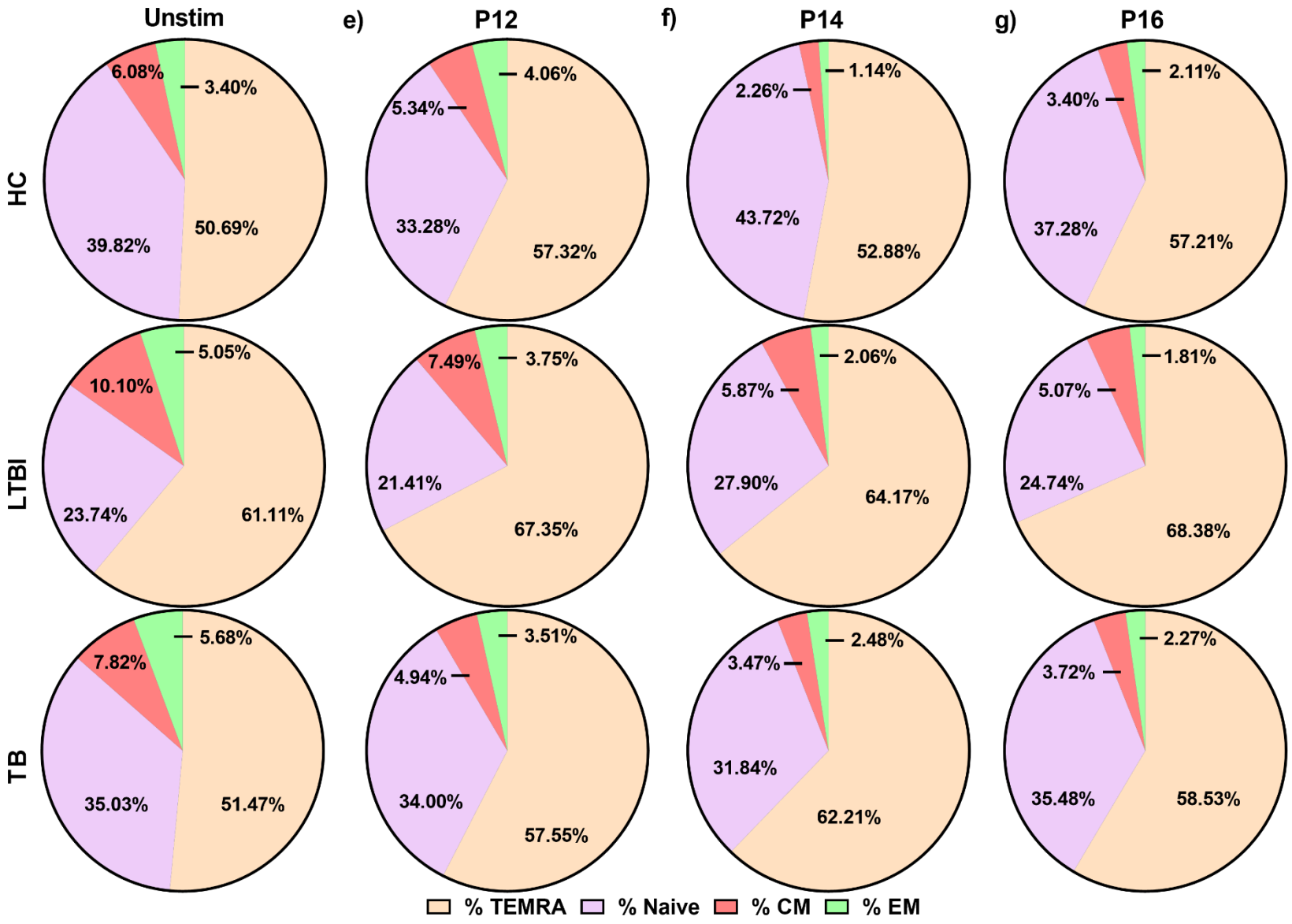

Figure 4.20: Circulating CD183$^+$ (Th1) CD8$^+$ memory subsets in the peripheral blood of healthy, LTBI and active TB individuals in unstimulated conditions or in response to PPE_MPTR peptides. (a) unstimulated **(b)** P4 **(c)** P5 **(d)** P11 **(e)** P12 **(f)** P14 and **(g)** P16. The pie charts represent the proportions of Th1 T_N, T_{CM} T_{EM} T_{TEMRA} as a mean percentage of the total circulating CD8$^+$ population in the peripheral blood of TB (n=5), LTBI (n=5) and healthy individuals (n=11) recruited from high incident TB areas surrounding Tygerberg Hostpital. Naïve T-cells = T_N = pink; Central memory T-cells = T_{CM} = red; Effector memory T-cells = T_{EM} = green; Terminally differentiated T-cells = T_{TEMRA} = orange. P4 = Rv0878c_a. P5 = Rv0878c_d. P11 = Rv2356c_a. P12 =Rv2608_a. P14 = Rv2608c and P16 = Rv2608_g.

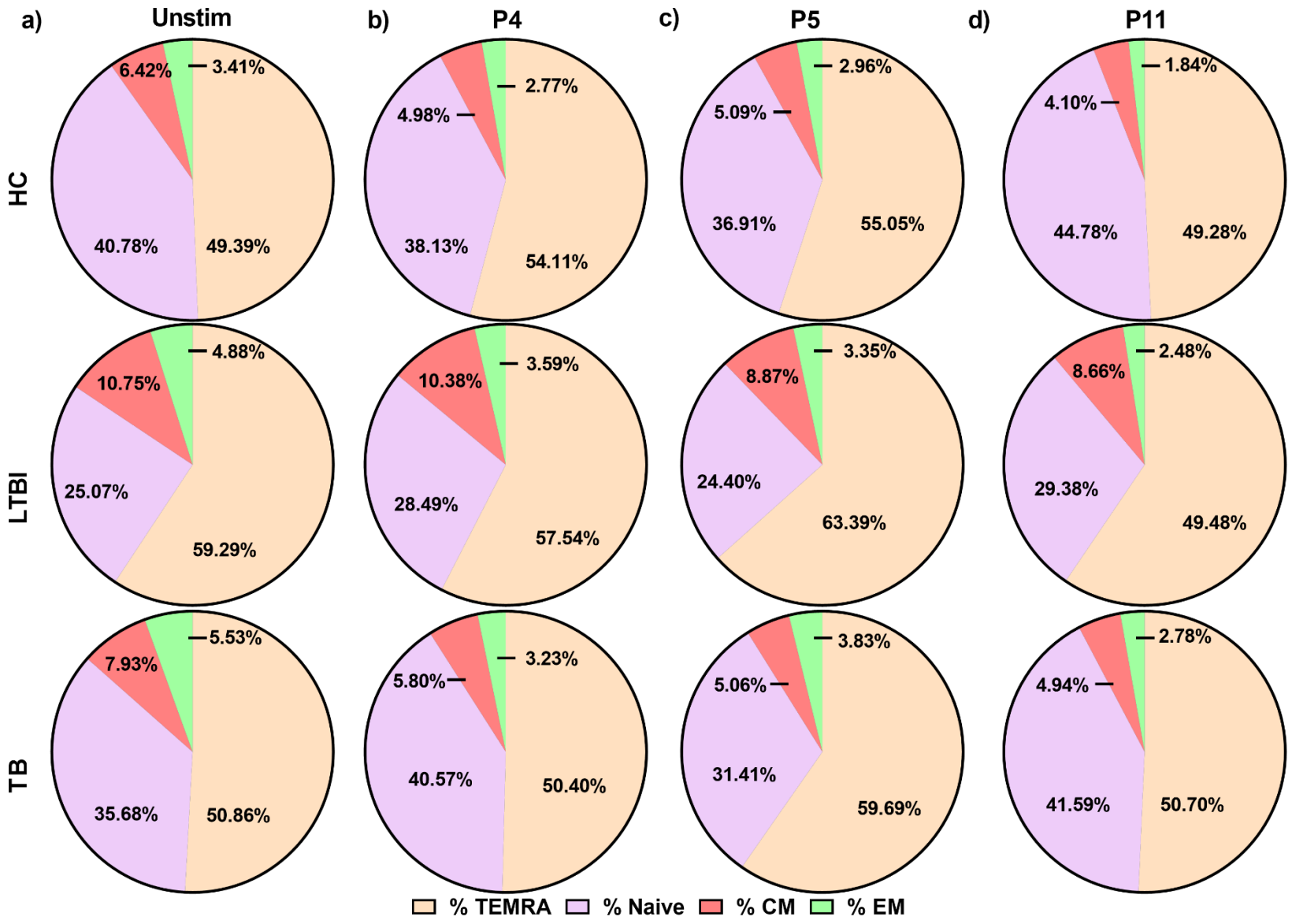

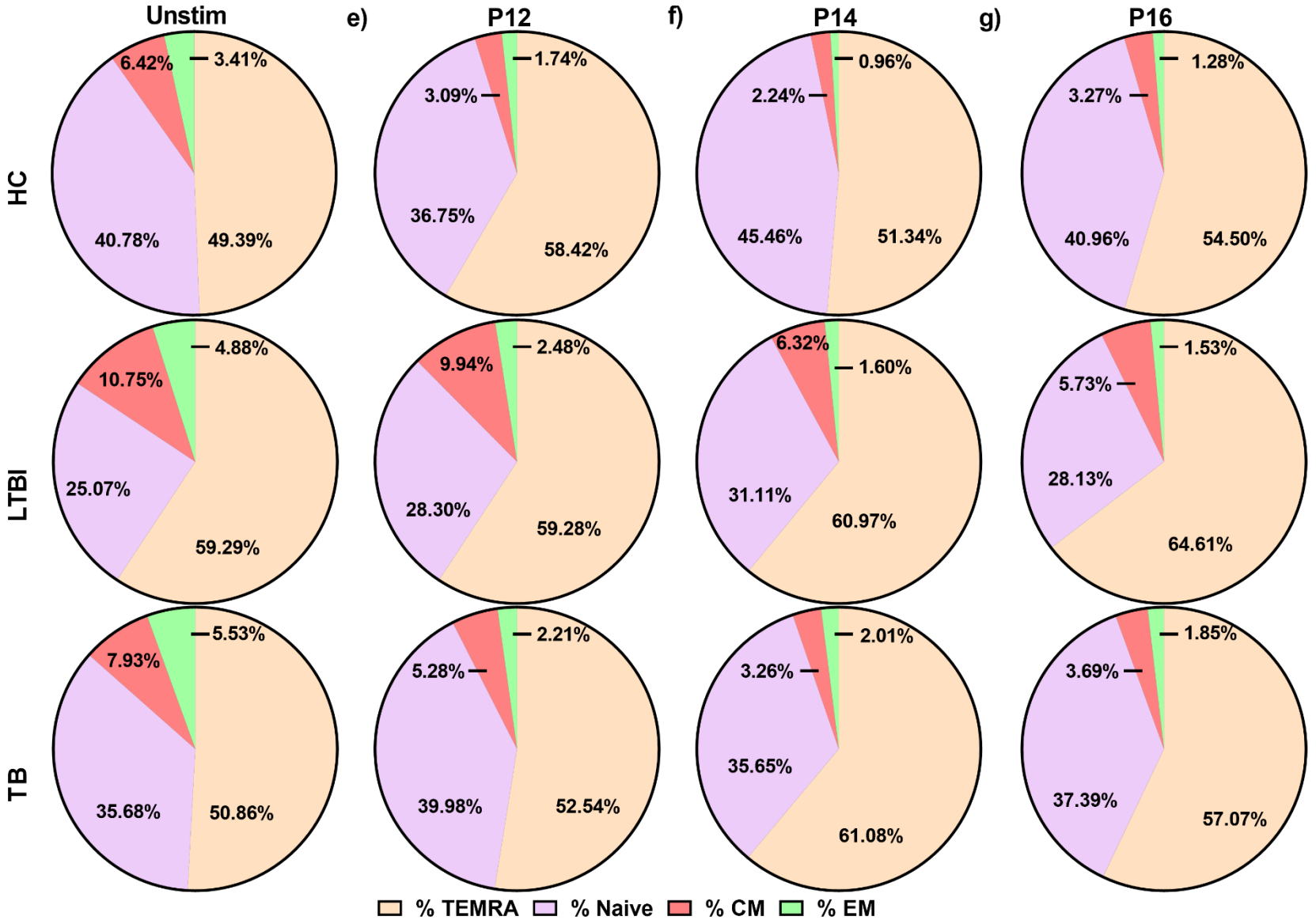

Figure 4.21: Circulating CD193$^+$ (Th2) CD8$^+$ memory subsets in the peripheral blood of healthy, LTBI and active TB individuals in unstimulated conditions or in response to PPE_MPTR peptides. (a) unstimulated **(b)** P4 **(c)** P5 **(d)** P11 **(e)** P12 **(f)** P14 and **(g)** P16. The pie charts represent the proportions of Th2 T_N, T_{CM} T_{EM} T_{TEMRA} as a mean percentage of the total circulating CD8$^+$ population in the peripheral blood of TB (n=5), LTBI (n=5) and healthy individuals (n=11) recruited from high incident TB areas surrounding Tygerberg Hostpital. Naïve T-cells = T_N = pink; Central memory T-cells = T_{CM} = red; Effector memory T-cells = T_{EM} = green; Terminally differentiated T-cells = T_{TEMRA} = orange. P4 = Rv0878c_a. P5 = Rv0878c_d. P11 = Rv2356c_a. P12 =Rv2608_a. P14 = Rv2608c and P16 = Rv2608_g.

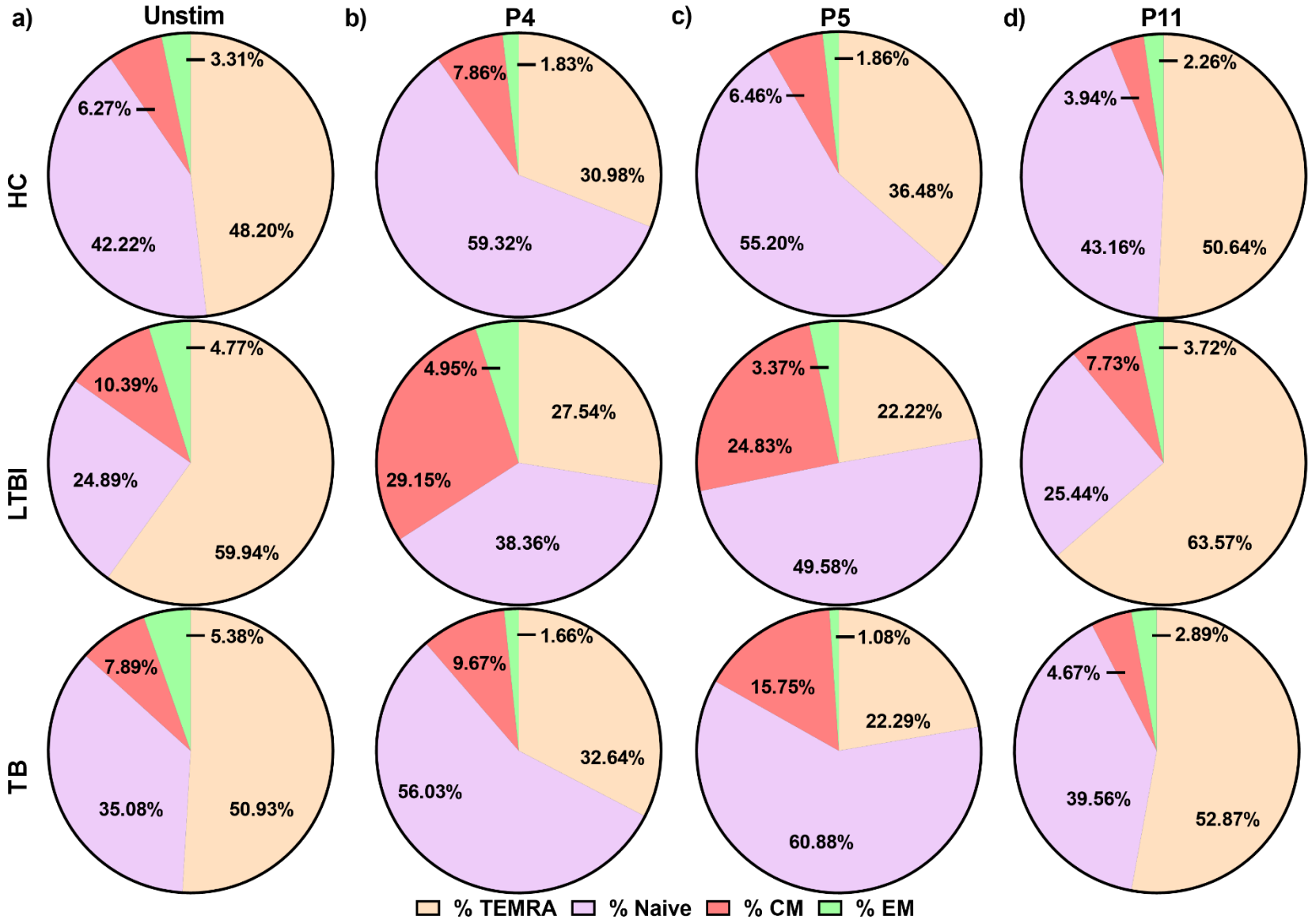

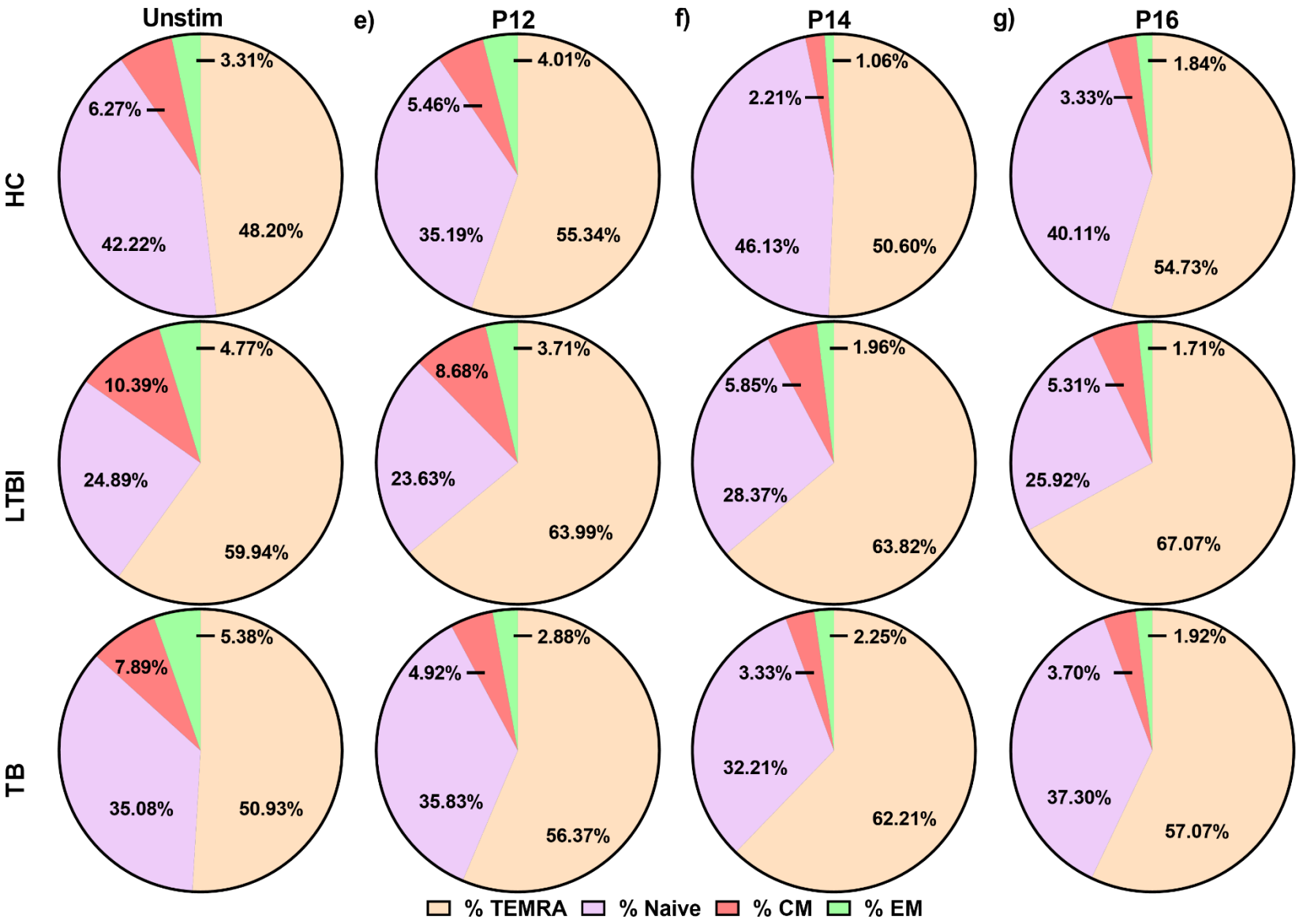

Figure 4.22: Circulating CD196⁺ (Th17) CD8⁺ memory subsets in the peripheral blood of healthy, LTBI and active TB individuals in unstimulated conditions or in response to PPE_MPTR peptides. (a) unstimulated **(b)** P4 **(c)** P5 **(d)** P11 **(e)** P12 **(f)** P14 and **(g)** P16. The pie charts represent the proportions of Th1 T_N, T_{CM} T_{EM} T_{TEMRA} as a mean percentage of the total circulating $CD8^+$ population in the peripheral blood of TB (n=5), LTBI (n=5) and healthy individuals (n=11) recruited from high incident TB areas surrounding Tygerberg Hostpital. Naïve T-cells = T_N = pink; Central memory T-cells = T_{CM} = red; Effector memory T-cells = T_{EM} = green; Terminally differentiated T-cells = T_{TEMRA} = orange. P4 = Rv0878c_a. P5 = Rv0878c_d. P11 = Rv2356c_a. P12 =Rv2608_a. P14 = Rv2608c and P16 = Rv2608_g.

$CD3^+CD8^+$ Central memory T-cells

The subpopulations of circulating memory $CD8^+$ T-cells in response to PPE_MPTR stimulation were also investigated. Like $CD4^+$ memory cells, $CD8^+$ memory T-cell populations are defined as antigen-specific, long-lived lymphocyte populations that provide a more effective immune response following secondary encounter with an antigen (Samji and Khanna, 2017). The $CD183^+$ (Th1), $CD193^+$ (Th2), and $CD196^+$ (Th17) T_{CM} subsets were defined as $CD45RA^-CD28^+$ and the distribution of these populations was calculated as a mean percentage of the $CD3^+CD8^+$ T-cell population.

Akin to what was observed for T_N $CD8^+$ cells in response to PPE_MPTR stimulation, no differences in the proportions of $CD183^+$ (Th1) and $CD193^+$ (Th2) T_{CM} $CD8^+$ cells were observed in active TB, LTBI or healthy controls (**Figure 4.20** and **Figure 4.21**). In response to P4 and P5, the peripheral blood of LTBI individuals exhibited higher proportions of $CD196^+$ (Th17) T_{CM} $CD8^+$ cells compared to what was observed in unstimulated conditions (**Figure 4.22 b, c**). Active TB individuals also exhibited higher proportions of $CD196^+$ (Th17) T_{CM} $CD8^+$ cells above unstimulated conditions, but only in response to P5 (**Figure 4.22 c**).

All PPE_MPTR peptides induced the activation of $CD183^+$ (Th1) and $CD196^+$ (Th17) T_{CM} $CD8^+$ T-cells in healthy, LTBI and active TB individuals (**Appendix 7.4; Figure 7.6**). For both $CD183^+$ (Th1) and $CD196^+$ (Th17) subsets, P11 and P14 induced the highest proportions of activated $CD8^+$ T-cells and was observed in active TB individuals. The $CD193^+$ (Th2) T_{CM} $CD8^+$ subset of healthy, LTBI and active TB individuals exhibited activation in response to P11, P12, P14 and P16, with the highest levels observed in response to P14 in active TB individuals. Interestingly, in response to P12, healthy individuals had more activated $CD183^+$ (Th1) T_{CM} $CD8^+$ T-cells than LTBI or active TB individuals (**Appendix 7.4; Figure 7.6**).

$CD3^+CD8^+$ Effector memory T-cells

Effector memory $CD8^+$ T-cells are responsible for exerting cytotoxic effector functions on *M. tuberculosis*-burdened host cells, ultimately resulting in apoptosis of the target cell (Geginat *et al.*, 2003). The $CD183^+$ (Th1), $CD193^+$ (Th2), and $CD196^+$ (Th17) T_{EM} subsets were defined as $CD45RA^-CD28^-$ (**Figure 3.1**) and the distribution of these subsets was calculated as a mean percentage of the $CD3^+CD8^+$ T-cell population. The distributions of the $CD183^+$ (Th1), $CD193^+$ (Th2), and $CD196^+$ (Th17) T_{EM} $CD8^+$ subsets were comparable between unstimulated conditions and in response to stimulation with PPE_MPTR peptides (**Figure 4.20**, **Figure 4.21** and **Figure 4.22**).

In response to P11, P12 and P14, marginal levels of activation were observed for $CD193^+$ (Th2) T_{EM} $CD8^+$ T-cell subsets in healthy, LTBI and active TB individuals (**Appendix 7.4; Figure 7.7**). None of the PPE_MPTR peptides activated $CD183^+$ (Th1) or $CD196^+$ (Th17) T_{EM} $CD8^+$ T-cells (**Appendix 7.4; Figure 7.7**).

$CD3^+CD8^+$ TEMRA T-cells

Terminally differentiated memory $CD8^+$ T-cells are characterised by the highest effector functionality but are known to lack the ability to recognise antigen on secondary encounter (Larbi and Fulop, 2014). The $CD183^+$ (Th1), $CD193^+$ (Th2), and $CD196^+$ (Th17) T_{TEMRA} subsets were defined as $CD45RA^+CD28^-$ (**Figure 3.1**) and the distribution of these $CD8^+$ subsets was calculated as a mean percentage of the $CD3^+CD8^+$ T-cell population.

Out of the four $CD8^+$ cell subsets, the proportions of the T_{TEMRA} $CD8^+$ cells were the most influenced by stimulation with PPE_MPTR peptides. The proportions of $CD183^+$ (Th1) T_{TEMRA} $CD8^+$ cells in TB individuals increased by 10% following stimulation with P14 (**Figure 4.20 f**). In response to P5, P12, P14 and P16, active TB individuals exhibited increased proportions of $CD193^+$ (Th2) T_{TEMRA} $CD8^+$ cells (**Figure 4.21 c, e, f, g**). Healthy controls showed comparably elevated proportions of $CD193^+$ (Th2) T_{TEMRA} $CD8^+$ cells, however only in response P12 (**Figure 4.21 e**). The proportions of $CD196^+$ (Th17) T_{TEMRA} $CD8^+$ cells in healthy, LTBI and active TB individuals were higher in response to P16 than unstimulated conditions (**Figure 4.22 g**). Only LTBI and active TB individuals exhibited increased proportions of $CD196^+$ (Th17) T_{TEMRA} $CD8^+$ cells in response to P12 (**Figure 4.22 e**), while active TB individuals also showed increased proportions of $CD196^+$ (Th17) T_{TEMRA} $CD8^+$ cells in response to P14 (**Figure 4.22 e, f**).

In healthy, LTBI and active TB individuals, similar levels of activated CD183$^+$ (Th1), CD193$^+$ (Th2), and CD196$^+$ (Th17) T_{TEMRA} CD8$^+$ were observed (**Appendix 7.4; Figure 7.8**). PPE_MPTR peptides, P4 and P5, did not induce activation of CD183$^+$ (Th1) T_{TEMRA} CD8$^+$ T-cells in healthy, LTBI or TB individuals (**Appendix 7.4; Figure 7.8**).

4.1.4.4 B-cells found in PPE_MPTR-stimulated peripheral blood

The role that B-cells play in protection against *M. tuberculosis* requires deeper characterization, however it is known that B-cells contribute to protective immune responses during TB disease (Chan *et al.*, 2014). When activated by *M. tuberculosis* antigens, B-cells produce *M. tuberculosis*-specific antibodies that regulate effector functions that contribute to *M. tuberculosis* clearance. B-cell populations were identified from the CD3$^-$ lymphocyte population and defined by the expression of CD19 (CD19$^+$). The CD3$^-$CD19$^+$ B-cell population was subsequently assessed for the distribution of activated B-cells that express CD25 (CD3$^-$ CD19$^+$CD25$^+$) (**Figure 3.2**). The distribution of B-cell subsets was calculated as a percentage of the parent B-cell population (**Table 4.4**).

CD3$^-$CD19$^+$CD25$^+$ B-cell subsets

Fewer B-cells were detected in response to PPE_MPTR peptides in active TB individuals compared to LTBI and healthy individuals, which produced comparable proportions of B-cells (~20% vs ~10% for TB). The only PPE_MPR peptides that caused activation (CD25$^+$) of B-cells were P11, P12, P14 and P16, all of which produced comparable proportions of activated B-cells between TB, LTBI and healthy individuals (~15%) (**Figure 4.23**).

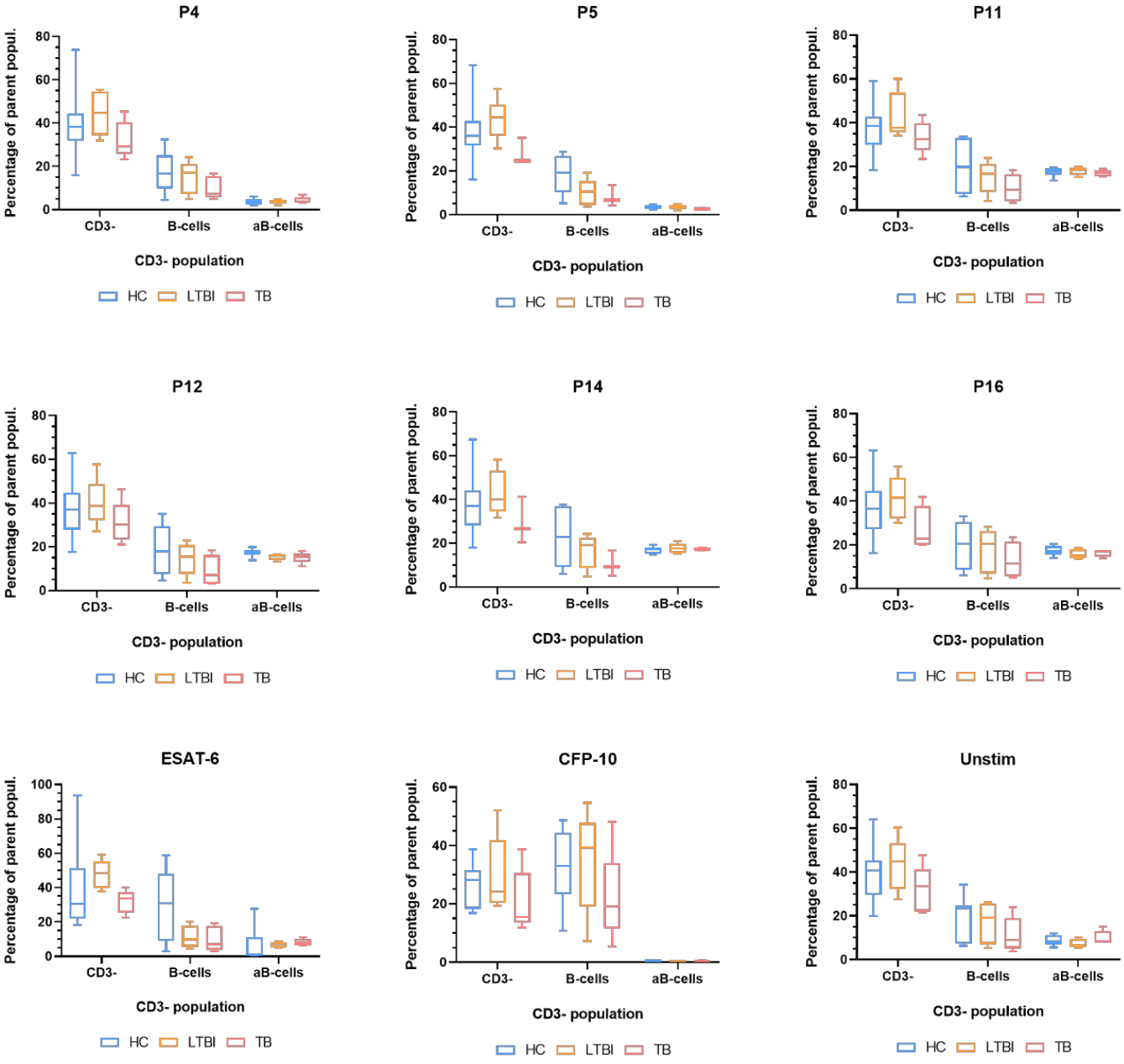

Figure 4.23: Circulating B-cell subsets in the peripheral blood of TB, LTBI and healthy individuals in response to stimulation PPE_MPTR peptides. The box-and-whisker plots represent the distribution of CD3- cells as a mean percentage of the parent population. The whiskers represent the minimum-to-maximum percentages. The box represents interquartile range with the horizontal line at the median. The CD3- population is represented as a percentage of total lympocyte population. The B-cells (CD3-CD19+) are represented a percentage of the CD3- population. The activated B-cells (aB-cells; CD3-CD19+CD25+) are represented a percentage of the B-cell population. HC = healthy controls (n=11) = blue. LTBI = latent TB infection (n=5) = orange. TB = active TB (n=5) = red. ESAT-6 = Early Secreted Antigen-6. CFP-10 = Culture Filtrate Protein 10. Unstim = Unstimulated (PBS). P4 = Rv0878c_a. P5 = Rv0878c_d. P11 = Rv2356c. P12 = Rv2608_a. P14 = Rv2608_c and P16 = Rv2608_g.

Chapter 5

Discussion

Tuberculosis (TB) is one of the most concerning global public health issues and desperately requires the development of new vaccines and improved diagnostic tools for the prevention and detection of disease. For decades the *Mycobacterium bovis* Bacille Calmette Guèrin (BCG) vaccine has been the most widely administered vaccine, worldwide (WHO, 2018). Vaccination during early childhood with *M. bovis* BCG has proven effective, however efficacy has been shown to wane with age (Rodrigues *et al*., 1993; Colditz *et al.*, 1994; Abubakar *et al.*, 2013), rendering the adolescent and adult populations vulnerable to TB infection and active disease (Sterne *et al.*, 1998; Ozeki *et al.*, 2011). Current TB vaccine development focuses on replacing or boosting the BCG vaccine in an attempt to prevent active TB disease in the adult population (Harris *et al.*, 2016) Alternatively, a decrease in the incidence of developing active TB disease may be achieved through the development of improved diagnostic tools that enable the detection of early TB infections (Abu-Raddad *et al.*, 2009). The development of such diagnostic tools has been hindered by our incomplete understanding of the heterogeneous host response to TB infection as well as our ability to detect and genotype low disease burdens without bacterial culture.

The protective efficacy of a vaccine candidate is influenced both by pathogen diversity and the immense variety of Human Leukocyte Antigen (HLA) alleles found in populations of different geographical regions (González-Galarza *et al.*, 2015). *In silico* analyses have proven useful in identifying promising vaccine candidates, by predicting population coverage through evaluating the binding affinity of *M. tuberculosis* epitopes to different HLA alleles (McNamara *et al.*, 2010; Davila *et al.*, 2012), however these predictions still require laboratory characterization to be functionally validated.

In this study, we aimed to validate the immunogenicity of nineteen computationally identified PPE_MPTR epitopes that were predicted to bind to HLA alleles frequently found in South African, Zimbabwean, Congolese and Ethiopian populations (Colic, 2016). We predicted that peptides representing these epitopes would elicit a *M. tuberculosis*-specific immune response, therefore we assessed the cytokine responses to these peptides in QFN+ and QFN- individuals. Further, we went on to investigate the diagnostic potential of these epitopes by comparing the immune responses elicited by these peptides in active TB, LTBI and healthy individuals. This

was complemented by investigating the distribution of functional marker frequencies, memory and activation states of T- and B- lymphocytes in PPE_MPTR-stimulated peripheral blood of active TB, LTBI and healthy individuals.

The functional assays performed in this study successfully validated the immunogenicity of the nineteen computationally identified PPE_MPTR epitopes in individuals from the four African countries stated above. We found that in response to P4, P5, P11, P12, P14 and P16, measurable concentrations of IL-17A, TNF-α and IL-6 were detected in South African, Zimbabwean, Congolese and Ethiopian individuals. In a South African cohort of healthy, LTBI and active TB individuals, P17 and P11 induced significantly more IL-6 and IL-17A, respectively, in active TB individuals than those without active disease. Furthermore, P4, P8, P12 and P17 induced significantly higher concentrations of IL-6 in active TB than LTBI individuals. Only one peptide (P19) induced significantly higher TNF-α in LTBI individuals compared to healthy controls.

The distribution of functional marker frequencies suggest that Th17 $CD4^+$ and $CD8^+$ T-cells are the major circulating cellular populations that govern the PPE_MPTR-induced immune responses in active TB and LTBI individuals, whereas more variability was observed in healthy controls who displayed a combined Th1/Th17 cell-mediated immune response. Activated T_N, T_{CM}, T_{EM} and T_{TEMRA} $CD4^+$ and $CD8^+$ T-cell populations were mainly observed in response to PPE_MPTR peptides P4, P11, P12 and P16, with $CD8^+$ T-cells exhibiting marginal differences in functional marker frequencies compared to $CD4^+$ T-cells. Overall, this pilot study has identified promising PPE_MPTR candidates that are worthy of further immunological investigation and characterization to fully characterize their potential as vaccine candidates for TB disease.

5.1 The immunogenicity of population-tailored PPE_MPTR epitopes

A multiplex cytokine screening assay detected an increase in the production of pro-inflammatory cytokines, IL-6, TNF-α and IL-17A, in peripheral blood of healthy QFN+ individuals in response to positive control (ESAT-6 and CFP-10) and PPE_MPTR candidate peptides. None of the PPE_MPTR peptides induced detectable concentrations of anti-inflammatory cytokine IL-10, thus supporting the identified pro-inflammatory role of the candidates.

Overall, QFN+ individuals exhibited higher cytokine responses to PPE_MPTR peptides than QFN- individuals. Since QFN+ individuals have been previously sensitized to *M. tuberculosis* antigens, this observation confirms that the identified PPE_MPTR peptides elicit an *M. tuberculosis*-specific response as hypothesized (**Section 4.1**). In QFN+ individuals, the cell-mediated immune response was characterized by the production of IL-6 and TNF-α, which is suggestive of a pro-inflammatory Th1 immune response (Mootoo *et al.*, 2009). The precise inflammatory role of IL-6 is unclear as this cytokine has been shown to promote Th2 responses through the induction of IL-4 (Diehl and Rincón, 2002), but has also been shown to potentiate protective Th1 inflammatory responses following BCG vaccination (Leal *et al.*, 1999). Interestingly, there was differential IL-6 production in response to peptides representing different regions of the same PPE_MPTR protein. Of the six peptides (P12, P13, P14, P15, P16 and P17) representing epitopes of PPE_MPTR42, P16 (Rv2608_g) elicited a greater immune response from QFN- individuals than QFN+ individuals, whereas QFN+ individuals responded better to P12, P13, P14 and P15. The greater immune response elicited by peptides from PPE_MPTR42 in QFN+ individuals supports the immunogenicity of PPE_MPTR42, as demonstrated in the recombinant BCG (Bertholet *et al.*, 2010) and ID93 vaccine candidates (Baldwin *et al.*, 2009).

There was a substantial amount of inter-individual variation observed in the detected cytokine responses, particularly for IL-17A, towards stimulation conditions. IL-17A is most well-known for its role during autoimmune and chronic inflammatory disorders where its dysregulation causes extensive pro-inflammatory responses that result in the production of numerous cytokines and tissue damage. (Domingo-Gonzalez *et al.*, 2016). During participant recruitment, information regarding chronic inflammatory disorders (for example, asthma, irritable bowel syndrome or coeliac disease) were not accounted for. From the high IL-17A concentrations observed during unstimulated conditions and the comparable concentrations of IL-17A in response to PPD (QFN+ and QFN-), it seems possible that some individuals included in this study had an underlying source of inflammation, which was exacerbated following stimulation.

The PPE_MPTR peptides that induced the production of three or more cytokines from QFN+ individuals were identified as having the greatest immunogenic potential. From these analyses P4, P5, P11, P12, P14 and P16 were identified as the most promising candidates and induced a pro-inflammatory immune response. PPE_MPTR peptides, P4 and P5 represent epitopes of PPE_MPTR13, P11 of PPE_MPTR40 and P12, P14 and P16 of PPE_MPTR42. The immunogenicity of PPE_MPTR42 has reportedly been associated with inducing Th1 cell-

mediated and humoral responses (Choudhary *et al.*, 2003; Bertholet *et al.*, 2008). The cell-mediated immune response observed in response to PPE_MPTR42 was observed in healthy PPD+ individuals with various HLA types and was characterized by multifunctional $CD4^+$ and $CD8^+$ T-cells, releasing TNF-α and IFN-γ (Bertholet *et al.*, 2008). These findings have supported its inclusion in a leading TB vaccine candidate (Baldwin *et al.*, 2009; Bertholet *et al.*, 2010). We report here for the first time the immunogenicity of PPE_MPTR13 and PPE_MPTR40. The results from our functional assays suggest that, like PPE_MPTR42, PPE_MPTR13 and PPE_MPTR40 also elicit a Th1 immune response from QFN+ individuals as measured by detectable concentrations of IL-6 and TNF-α. Previous vaccine studies have demonstrated that combining multiple *M. tuberculosis* antigens increases vaccine efficacy (Lu *et al.*, 2012), thus it would be interesting to assess the immunogenicity of a PPE_MPTR fusion protein consisting of PPE_MPTR13, PPE_MPTR40 and PPE_MPTR42.

5.2 The diagnostic potential of population-tailored PPE_MPTR epitopes

In collaboration with the *Stop TB Partnership* and the *Global Fund to Fight AIDS, Tuberculosis and Malaria*, the World Health Organisation launched the *Find. Treat. All.* initiative (WHO, 2018). This initiative aims at diagnosing and treating 40 million people with TB between 2018 and 2022, however an improved understanding regarding the interactions between *M. tuberculosis* and the host immune response is desperately needed to accomplish this goal. Research on the correlates of disease and host biomarkers of active and latent TB infection (Walzl *et al.*, 2011; Chegou *et al.*, 2012; Loxton *et al.*, 2012) have highlighted the heterogeneity of immune responses elicited during *M. tuberculosis* infection, a concept which is further complicated when considering understudied *M. tuberculosis* antigens, such as those from the PE/PPE protein family.

In support of our observations made during the immunogenicity assessment, significant differences in Th1 cytokine production were observed between individuals with latent and active TB disease. This was characterized by significantly more IL-6 produced from active TB individuals in response to P4, P8, P12 and P17. These peptides represent epitopes of PPE_MPTR13 (P4), PPE_MPTR28 (P8) and PPE_MPTR42 (P12 and P17). Peptides P12 and P17 showed the most promise as diagnostic antigens but further research is needed to fully characterize their cell-mediated immune response. IL-6 is a pluripotent cytokine that has been shown to play an essential role in the protective immunity against *M. tuberculosis* challenge

(Ladel *et al.*, 1997) and also enhances the Th1 immune responses during BCG vaccination (Leal *et al.*, 1999). In our study, the most significant difference in IL-6 production was observed between *cases* and *controls* in response to P17 (p-value = 0.0088). However, the data suggests that P12 (from the same protein, PPE_MPTR42) may elicit a broader immune response compared to P17, as little to no IL-6 was produced by any LTBI individuals in response to P17. In the case of P12, one LTBI individual produced concentrations of IL-6 comparable to active TB individuals. The ability of this individual to release a comparable concentration of IL-6 in response to P12 could indicate that this individual may be currently living with undiagnosed active TB.

Unlike the Th1 cytokine mediated response to P11 (PPE_MPTR40) observed during the immunogenicity assessment, P11 was shown to induce significant production of IL-17A by active TB individuals compared to healthy controls (p=0.0346). The ability of P11 to induce IL-6, TNF-α and IL-17A suggests P11 could induce a more robust Th1/Th17 immune response. A significant difference in the immune response between LTBI and healthy individuals was also observed and characterized by significantly higher TNF-α production by LTBI individuals. TNF-α is major pro-inflammatory mediator that has been implicated in establishing and maintaining the granuloma during *M. tuberculosis* infection (Mohan *et al.*, 2001; Roach *et al.*, 2002; Mootoo *et al.*, 2009). The higher concentrations of TNF-α observed in LTBI individuals could indicate the successful maintenance of undetected granulomatous structures in LTBI individuals, which is maintaining their latent state of disease.

It should be noted that the observed absolute cytokine concentrations in response to PPE_MPTR peptides produced by active TB, LTBI and healthy individuals were low. This does not necessarily mean the PPE_MPTR peptides investigated are not immunogenic, but rather that these peptides do not induce the production of the analytes investigated. An alternative explanation may be that a 24-hour whole blood assay was not a sufficient stimulation time to see a change in cytokine production.

5.3 The distribution of PPE_MPTR-specific functional marker frequencies and activation states

An effective immune response to *M. tuberculosis* infection has been shown to depend on the production of pro-inflammatory cytokines such as IL-6, IFN-γ and TNF-α from $CD4^+$ and $CD8^+$ Th1 T-cells (Flynn and Chan, 2001). There is also evidence for the crucial role of Th17 T-cells in *M. tuberculosis* infection. Th17 T-cells secrete IL-17A, IL-22 and IL-23 and have

been shown to enhance Th1 immune responses and contribute to adequate granuloma formation (Jin and Dong, 2013). Interestingly, the proportion of Th1/Th17 T-cells has been shown to correlate with severity of active TB disease, with active TB individuals producing higher IL-17A concentrations in response to *M. tuberculosis* whole cell lysate than LTBI individuals (Jurado *et al.*, 2012).

In our study, the distribution of functional marker frequencies was assessed in response to PPE_MPTR peptides that have previously been computationally identified as $CD4^+$ T-cell epitopes having high binding affinity to HLA alleles in individuals from four African populations (Colic, 2016). The distribution of $CD4^+$ T-cell functional marker frequencies showed more variation in response to PPE_MPTR candidates than those of $CD8^+$ T-cells. $CD4^+$ T-cells also displayed higher levels of activation compared to $CD8^+$ T-cells, suggesting that candidate PPE_MPTR peptides are presented to the MHC-II binding groove characteristic of $CD4^+$ T-cells, as hypothesized. To functionally confirm this, MHC-II tetramers specific for the nineteen PPE_MPTR epitopes represented in this study can be used in future studies to assess the specific $CD4^+$ T-cell responses (Nepom, 2012).

Due to persistent exposure to *M. tuberculosis*-antigens during infection, the distribution of functional, memory and activation states observed in active TB individuals has been shown to differ from those observed in healthy or latently infected individuals (Marín *et al.*, 2012). In partial agreement with this, higher proportions of activated ($CD25^+$) $CD4^+$ and $CD8^+$ T-cells were detected in LTBI and active TB individuals compared to healthy individuals, however no noticeable differences were observed between LTBI and TB individuals. All PPE_MPTR peptides were capable of inducing activation of $CD4^+$ T-cell populations in healthy controls. This may be due to environmental sensitization to *M. tuberculosis* antigens as a result of residing in high incident TB communities. The similar functional marker frequencies observed between healthy individuals and active TB individuals only provide information regarding the expression of surface markers on various cell types. To properly assess if the memory states between healthy and active TB individuals differ functionally, future studies could include intracellular cytokine staining to identify the associated cytokine profile of memory populations.

In our study, T_N T-cells were characterised as $CD45RA^+$ and $CD28^+$ ($CD45RA^+$ $CD28^+$) which indicate a high level of functional and proliferative capabilities, respectively. In response to PPE_MPTR peptides, similar distributions of expanded and activated $CD183^+$ (Th1), $CD193^+$ (Th2) and $CD196^+$ (Th17) naïve $CD4^+$ T-cells were observed in healthy, LTBI and active TB

individuals. The expansion of naïve T-cell populations observed in LTBI and active TB individuals may be a consequence of the persistent pro-inflammatory state within these individuals which encourages the proliferation of circulating naïve T-cells. As such, in response to ESAT-6 and CFP-10, active TB individuals have been shown to have expanded naïve T-cell populations that secreted IFN-γ (Orlando *et al.*, 2018). The expanded T_N $CD4^+$ T-cells observed in healthy individuals suggests that there are other sources of inflammation which may be inducing the proliferation of these cells (Orlando *et al.*, 2018). To confirm whether T_N $CD4^+$ T-cells are indeed proliferating, future cytometric analyses could include a proliferative marker, such as Ki67 (Soares *et al.*, 2010).

Immunosurveillance is performed by circulating central memory cells that rapidly proliferate and expand upon antigen encounter (Murphy, 2013). Central memory cells were characterized as $CD45RA^-CD28^+$ which indicated their highly differentiated state ($CD45RA^-$), however still maintaining proliferative capabilities (Shipkova and Wieland, 2012; Larbi and Fulop, 2014). Proliferative capabilities allow expansion of this long-lived cellular population for optimal immunosurveillance to be maintained (Murphy, 2013). The central memory response to stimulation with PPE_MPTR peptides was governed by expanding $CD196^+$ (Th17) T_{CM} $CD4^+$ T-cells in healthy, LTBI and active TB individuals. In response to P4, active TB individuals displayed increased proportions of $CD196^+$ (Th17) $CD4^+$ T_{CM} cells, whereas in healthy and LTBI individuals expanded $CD196^+$ (Th17) $CD4^+$ T_{CM} cell populations were observed in response to both P4 and P5. There were significant differences in the concentrations of IL-17A observed between healthy, TB and LTBI individuals (**Section 5.2; Figure 4.5**), which could suggest that these Th17 T-cell populations contribute to the IL-17A production observed. This is in agreement with reports that demonstrated circulating Th17 T_{CM} $CD4^+$ T-cells to be the main source of IL-17A in response to BCG stimulation in active TB individuals (Scriba *et al.*, 2008). Furthermore, the induction, differentiation and maintenance of $CD196^+$ (Th17) T-cell populations in active TB individuals could, in part, be maintained by the high levels of IL-6 observed (**Section 5.2; Figure 4.5**). Other cytokines such as IL-21, IL-23 and TGF-1β have also been implicated in influencing differentiation of Th17 cells, however, were not investigated in this study. In future studies, the production of these cytokines in response to PPE_MPTRs in peripheral blood could be investigated and complemented with intracellular cytokine staining in order to fully assess immunophenotypes of induced T-cell populations, and identify the source of secreted cytokines (Torrado and Cooper, 2011; Lyadova and Panteleev, 2015).

Overall, the effector memory cells showed the lowest amount of expansion in response to PPE_MPTR peptides, however due to their highly differentiated state they are still able to secrete cytokines in response to antigen (MacLeod *et al.*, 2009; Mahnke *et al.*, 2013).This is consistent with reports which describe the T_{CM} cells as the predominant memory population in peripheral blood (Sallusto *et al*., 2004). Although comparable expansion of $CD183^+$ (Th1) and $CD193^+$ (Th2) memory subsets (T_{CM} and T_{EM}) was observed in healthy and TB individuals, only healthy individuals exhibited expansion of $CD196^+$ (Th17) $CD4^+$ T_{EM} cells. Interestingly, the expansion of $CD196^+$ (Th17) $CD4^+$ T_{EM} T-cells was also absent in LTBI individuals which could suggest that the expansion of this T_{EM} subset is protective against developing TB disease (latent or active).

Terminally differentiated effector memory cells (T_{TEMRA}) have lost their ability to proliferate but have maintained their effector phenotype by re-expressing CD45RA. This allows T_{TEMRA} cells to play a functional role during *M. tuberculosis* infection. Expanded $CD183^+$ (Th1), $CD193^+$ (Th2) and $CD196^+$ (Th17) $CD4^+$ T_{TEMRA} cells were comparable among healthy, LTBI and active TB individuals, except expanded $CD196^+$ (Th17) $CD4^+$ T_{TEMRA} cells were absent from active TB individuals. PPE_MPTR peptides induced the activation of $CD183^+$ (Th1), $CD193^+$ (Th2) and $CD196^+$ (Th17) $CD4^+$ T_{TEMRA} cells in LTBI and active TB individuals, whereas only activated $CD183^+$ (Th1) $CD4^+$ T_{TEMRA} cells were detected in healthy individuals. These results suggest that in response to PPE_MPTR peptides, healthy controls can exhibit a pro-inflammatory Th1/Th17 response characterized by expanded $CD196^+$ (Th17) T_{EM} and activated $CD183^+$ (Th1) T_{TEMRA} $CD4^+$ T-cells. In LTBI and active TB individuals, the cell-mediated immune response is evidently more complex due to the activation of $CD193^+$ (Th2) T_{TEMRA} $CD4^+$ T-cells. Th2-associated cytokines, such as IL-4 and IL-10, have been shown to have a dampening effect on the host immune response during *M. tuberculosis* infection and have been shown to diminish protective Th1 responses (Rook, 2007). Conversely, Th2-associated cytokines have also been shown to facilitate activation of B-cells and antibody production (Diehl and Rincón, 2002). The lack of activated $CD193^+$ (Th2) T_{TEMRA} $CD4^+$ T-cells in healthy individuals may suggest that healthy individuals fail to produce antibodies in response to *M. tuberculosis* antigens. Alternatively, the lack of $CD193^+$ (Th2) T_{TEMRA} $CD4^+$ T-cells in these individuals may be a correlate of protection against TB disease, which facilitates the induction of a more effective Th1 immune response against stimulation with *M. tuberculosis* antigens.

The exact role of B-cells during *M. tuberculosis* infection requires more investigation, however it is known that B-cells aid in controlling the host immune response to *M. tuberculosis* infection through the production of cytokines and *M. tuberculosis*-specific antibodies (Mauri and Bosma, 2012; Loxton, 2019). The importance of B-cells in the immune response during *M. tuberculosis* infection was demonstrated in B-cell deficient mice, which showed increased immunopathology and susceptibility to *M. tuberculosis* Erdman challenge (Vordermeier *et al.*, 1996; Maglione *et al.*, 2007). Furthermore, a reduction in the number and frequency of circulating B-cells has been observed in individuals with active TB disease and was shown to be restored following successful anti-TB treatment (Joosten *et al.*, 2016; Van Rensburg *et al.*, 2017). PPE_MPTR42 has been shown to induce a predominately humoral response in relapsed TB individuals (Chakhaiyar *et al.*, 2004) and has also been identified as a possible serodiagnostic candidate for active TB due to the significantly higher concentrations of PPE_MPTR42 antibodies observed in the sera of active TB individuals compared to healthy controls (Choudhary *et al.*, 2003).

In response to stimulation with PPE_MPTR peptides, active TB individuals had the lowest proportion of circulating B-cells compared to healthy and LTBI individuals. This finding is in support of some literature (Corominas *et al.*, 2004; van Rensburg and Loxton, 2018), however others have also observed an increased frequency of B-cells during active TB (Wu *et al.*, 2009). The distribution of $CD25^{+}$ B-cells (activated B-cells) in response to selected PPE_MPTR candidates in this study was comparable between healthy, LTBI and active TB individuals. It is important to note that the distribution of B-cells and subsequent activation states were not extensively characterized in this study. Future work should include a broader panel of fluorophore-conjugated monoclonal antibodies to adequately characterize B-cell populations in response to PPE_MPTR stimulation.

5.4 Limitations

This pilot study was not large enough to provide enough power to draw conclusions regarding the populations from which the samples were taken. During participant recruitment, the status of chronic inflammatory disorders was not noted, the presence of which may have caused unexpected pro-inflammatory responses, resulting in misleading cytokine responses. Furthermore, the cohort recruited to assess the immunogenicity of candidate peptides included mostly South African individuals, therefore the results observed do not provide an accurate demonstration of Zimbabwean, Congolese or Ethiopian population's immune responses to

peptides. The candidate peptides were predicted to elicit strong immune responses based on their potential to bind the HLA alleles common in individuals of South Africa, Congo, Ethiopia and Zimbabwe (Colic, 2016). However, HLA-typing was not in the scope of this pilot study and could be done in future studies to confirm the HLA subtype of individuals.

The Luminex multiplex screening assays were not sensitive enough to detect very low concentrations of cytokines. Furthermore, inconsistencies were observed between the internal control on different plates of the same kit, suggesting large inter-plate variation. Furthermore, Luminex data analysis would greatly benefit from standardization within the scientific community due to the effects data analysis can have on the interpretation of results (Van Meijgaarden *et al.*, 2018).

In order to properly characterize the immunophenotype of lymphocyte populations, intracellular cytokine staining is usually performed, however was not in the scope of this pilot study. This hampered our ability to provide a PPE_MPTR-specific immunophenotype of circulating T-and B-lymphocytes. In future, candidate PPE-MPTR epitopes identified in this study (P11 and P17) will be investigated using a larger cohort of individuals from African origin. In these follow-up studies, intracellular cytokine staining will be used to assess the ability of PPE_MPTR proteins to induce the production of polyfunctional T-cells, which have been shown to correlate with vaccine-induced protection following *M. tuberculosis* challenge (Lindenstrøm *et al.*, 2009; Derrick *et al.*, 2011).

5.5 Conclusion

The World Health Organisation have deemed the development of new TB vaccines as essential in achieving the goals set out by the '*End TB Strategy'* (WHO, 2018). Currently, the TB vaccine development pipeline includes promising candidates that are already in Phase IIb clinical trials (**Table 1.1).** However due to the lack of immunological correlates of protection against TB disease, identifying promising vaccine candidates has proven challenging. This is further complicated by HLA allele diversity among individuals of different populations that influence the recognition of *M. tuberculosis*-specific antigens. The use of *in silico* methods has provided researchers with a cost-effective way of identifying promising vaccine candidates that are well recognised by individuals from different geographical locations. Members of the PE/PPE protein family have demonstrated immunogenic potential (Vordermeier *et al.*, 2012); however, little is known regarding the immunogenicity of the PPE_MPTR proteins. The results of this study validated the immunogenicity of nineteen computationally identified PPE_MPTR

epitopes in individuals in South Africa, Zimbabwe, Congo and Ethiopia. Furthermore, these PPE_MPTR epitopes also showed potential in differentiating between individuals with and without active TB disease by inducing significantly different cytokine responses. Selected candidate PPE_MPTR peptides were shown to elicit a pro-inflammatory cell-mediated immune response characterized by the production of TNF-α, IL-6 and IL-17A. Functional marker frequencies of $CD4^+$ and $CD8^+$ T-cells also suggest that selected PPE_MPTR peptides could induce the production of memory populations.

Vaccine-induced protection is known to rely on immunological memory that maintains immunity to pathogens (Seder *et al.*, 2008). A balanced, well-orchestrated Th1/Th17 immune response has been shown to be more effective at providing protection against active TB disease, compared with a Th1 response alone. This has been demonstrated by the expanded Th1/Th17 T-cell populations observed in LTBI individuals in response to *M. tuberculosis*-derived antigenic stimulation (Lindestam Arlehamn *et al.*, 2013). The production of IL-17A, IL-6 and TNF-α in response to PPE_MPTR peptides, coupled with PPE_MPTR-induced activation of $CD183^+$ (Th1), $CD193^+$ (Th2) and $CD196^+$ (Th17) T_{CM} and T_{EM} $CD4^+$ and $CD8^+$ T-cells indicates protective potential of these peptides. The presence of complex T-cell profiles, however, does not necessarily correlate with protection (Kagina *et al.*, 2010). As such, we observed significantly higher concentrations of IL-6 and IL-17A in response to PPE_MPTR peptides in active TB individuals, however these cytokines were also detected in LTBI and healthy individuals, albeit in low concentrations. To properly assess the protective capabilities of PPE_MPTR-induced activation T_{CM} and T_{EM} $CD4^+$ and $CD8^+$ T-cells, intracellular cytokine staining should be included in future studies. This should also incorporate proliferation and cytolytic markers so that the kinetics of PPE_MPTR-induced responses can be further understood and any cytolytic functions imposed by PPE_MPTRs can be identified.

The results of this study emphasize the heterogeneity of the host immune response to *M. tuberculosis*-specific antigens in both previously sensitized (active TB or LTBI individuals) and uninfected healthy individuals. In future studies, the existence of pro-inflammatory disorders should be accounted for during participant recruitment and individuals with underlying sources of inflammation should not be included. The combination of *M. tuberculosis*-derived antigens in new TB vaccine candidates have demonstrated improved immunogenicity and protective efficacy (Bertholet *et al.*, 2010; Lu *et al.*, 2012). In support of this, future studies could investigate the combined cell-mediated responses of PPE_MPTR peptides from this study that induced significant production of pro-inflammatory cytokines.

The pro-inflammatory response induced by combining PPE_MPTR peptides may be stronger than that induced by natural immunity, which is an important consideration in TB vaccine development due to the dormant state in which *M. tuberculosis* can persist (Kaufmann, 2007).

Chapter 6

Reference List

Abbas, A. K., Lichtman, A. H. and Pillai, S. (2001) *Basic Immunology: Functions and Disorders of the Immune System*. Forth Edit. Philadelphia: Elsevier Saunders.

Abel, B. *et al.* (2002) 'Toll-Like Receptor 4 Expression Is Required to Control Chronic Mycobacterium tuberculosis Infection in Mice', *The Journal of Immunology*, 169, pp. 3155–3162. doi: 10.4049/jimmunol.169.6.3155.

Abel, B. *et al.* (2010) 'The novel tuberculosis vaccine, AERAS-402, induces robust and polyfunctional CD4+and CD8+T cells in adults', *American Journal of Respiratory and Critical Care Medicine*, 181(12), pp. 1407–1417. doi: 10.1164/rccm.200910-1484OC.

Abu-Raddad, L. J. *et al.* (2009) 'Epidemiological benefits of more-effective tuberculosis vaccines, drugs, and diagnostics', *Pnas*, 106(33), pp. 13980–13985. doi: x.

Abubakar, I. *et al.* (2013) 'Systematic review and meta-analysis of the current evidence on the duration of protection by bacillus Calmette-Guérin vaccination against tuberculosis', *Health Technology Assessment*, 17(37), pp. 1–4. doi: 10.3310/hta17370.

Afkarian, M. *et al.* (2002) 'T-bet is a STATI-induced regulator for IL-12R expression in naïve CD4 + T cells', *Nature Immunology*, 3(6), pp. 549–557. doi: 10.1038/ni794.

Akira, S. and Takeda, K. (2004) 'Toll-like receptor signalling', *Nature Reviews Immunology*, 4(7), pp. 499–511. doi: 10.1038/nri1391.

Akira, S., Uematsu, S. and Takeuchi, O. (2006) 'Pathogen recognition and innate immunity', *Cell*, 124(4), pp. 783–801. doi: 10.1016/j.cell.2006.02.015.

Al-Ashmawy, G. M. Z. (2018) 'Dendritic Cell Subsets, Maturation and Function', in *Dendritic Cells*, p. 13. doi: http://dx.doi.org/10.5772/57353.

Alberts, B., Johnson, A. and Lewis, J. (2002) 'Chapter 24: The Adaptive Immune System', in *Molecular Biology of the Cell*. 4th edn.

Alexander, W. S. (2002) 'Suppressors of cytokine signalling (SOCS) in the immune system', *Nature Reviews Immunology*, 2(6), pp. 410–416. doi: 10.1038/nri818.

Almeida, A. S. *et al.* (2009) 'Tuberculosis Is Associated with a Down-Modulatory Lung Immune Response That Impairs Th1-Type Immunity', *The Journal of Immunology*, 183, pp.

718–731. doi: 10.4049/jimmunol.0801212.

Altare, F. *et al.* (1998) 'Impairment of mycobacterial immunity in human interleukin-12 receptor deficiency', *Science*, 280(5368), pp. 1432–1435. doi: 10.1126/science.280.5368.1432.

Amaral, E. P., Lasunskaia, E. B. and D'Império-Lima, M. R. (2016) 'Innate immunity in tuberculosis: How the sensing of mycobacteria and tissue damage modulates macrophage death', *Microbes and Infection*, 18(1), pp. 11–20. doi: 10.1016/j.micinf.2015.09.005.

Ameixa, C. and Friedland, J. S. (2001) 'Down-Regulation of Interleukin-8 Secretion from Mycobacterium tuberculosis -Infected Monocytes by Interleukin-4 and -10 but Not by Interleukin-13', *Infection and Immunity*, 69(4), pp. 2470–2476. doi: 10.1128/IAI.69.4.2470.

Ancelet, L. and Kirman, J. (2012) 'Shaping the CD4+ memory immune response against tuberculosis: The role of antigen persistence, location and multi-functionality', *Biomolecular Concepts*, 3(1), pp. 13–20. doi: 10.1515/bmc.2011.051.

Arbues, A. *et al.* (2013) 'Construction, characterization and preclinical evaluation of MTBVAC, the first live-attenuated M. tuberculosis-based vaccine to enter clinical trials', *Vaccine*. Elsevier, 31(42), pp. 4867–4873. doi: 10.1016/J.VACCINE.2013.07.051.

Armstrong, A. and Hart, P. D. (1971) 'Response of cultured macrophages to Mycobacterium tuberculosis with observations of fusion of lysosomes with phagosomes', *The Journal of Experimental Medicine*, 134(3), pp. 713–740.

Arrigucci, R. *et al.* (2018) 'Active tuberculosis is characterized by highly differentiated effector memory Th1 cells', *Frontiers in Immunology*, 9(SEP), pp. 1–9. doi: 10.3389/fimmu.2018.02127.

Ates, L. S. *et al.* (2016) 'The ESX-5 System of Pathogenic Mycobacteria Is Involved In Capsule Integrity and Virulence through Its Substrate PPE10', *PLoS Pathogens*, 12(6). doi: 10.1371/journal.ppat.1005696.

Bafica, A. *et al.* (2005) 'TLR9 regulates Th1 responses and cooperates with TLR2 in mediating optimal resistance to Mycobacterium tuberculosis', *The Journal of Experimental Medicine*, 202(12), pp. 1715–1724. doi: 10.1084/jem.20051782.

Baldwin, S. L. *et al.* (2009) 'Intradermal Immunization improves protective efficacy of a novel TB vaccine candidate', *Vaccine*, 27(23), pp. 3063–3071. doi: 10.1016/j.vaccine.2009.03.018.Intradermal.

Balkhi, M. Y., Sinha, A. and Natarajan, K. (2004) 'Dominance of CD86 , Transforming Growth Factor – b 1 , and Interleukin-10 in Mycobacterium tuberculosis Secretory Antigen – Activated Dendritic Cells Regulates T Helper 1 Responses to Mycobacterial Antigens', *The Journal of Infectious Diseases*, 189, pp. 1598–1609.

Banchereau, J. and Steinman, Ralph, M. (1998) 'Dendritic cells and the control of immunity.', *Nature*, 392(6673), pp. 245–252. Available at: http://dx.doi.org/10.1038/32588.

Bansal, K. *et al.* (2010) 'Src Homology 3-interacting Domain of Rv1917c of Mycobacterium tuberculosis Induces Selective Maturation of Human Dendritic Cells by Regulating PI3K-MAPK-NF-kB Signaling and Drives Th2 Immune Responses', *Journal of Biological Chemistry*, 285(47), pp. 36511–36522. doi: 10.1074/jbc.M110.158055.

Basset, C. *et al.* (2003) 'Innate immunity and pathogen-host interaction', *Vaccine*, 21(SUPPL. 2), pp. 12–23. doi: 10.1016/S0264-410X(03)00195-6.

Basu, S. *et al.* (2007) 'Execution of Macrophage Apoptosis by PE_PGRS33 of Mycobacterium tuberculosis Is Mediated by Toll-like Receptor 2-dependent Release of Tumor Necrosis Factor-a', *Journal of Biological Chemistry*, 282(2), pp. 1039–1050. doi: 10.1074/jbc.M604379200.

Bertholet, S., Ireton, Gregory C., *et al.* (2008) ' Identification of Human T Cell Antigens for the Development of Vaccines against Mycobacterium tuberculosis ', *The Journal of Immunology*, 181(11), pp. 7948–7957. doi: 10.4049/jimmunol.181.11.7948.

Bertholet, S., Ireton, Gregory C, *et al.* (2008) 'Identification of human T cell antigens for the development of vaccines against Mycobacterium tuberculosis.', *Journal of immunology*. American Association of Immunologists, 181(11), pp. 7948–7957. doi: 10.4049/JIMMUNOL.181.11.7948.

Bertholet, S. *et al.* (2010) 'A Defined Tuberculosis Vaccine Candidate Boosts BCG and Protects Against Multidrug Resistant Mycobacterium tuberculosis', *Science Translational Medicine*, 2(53). doi: 10.1371/journal.pone.0178059.

Beveridge, N. E. R. *et al.* (2007) 'Immunisation with BCG and recombinant MVA85A induces long-lasting, polyfunctional Mycobacterium tuberculosis-specific CD4 + memory T lymphocyte populations', *European Journal of Immunology*, 37(11), pp. 3089–3100. doi: 10.1002/eji.200737504.

Bhat, K. H. *et al.* (2012) 'Proline-proline-glutamic acid (PPE) protein Rv1168c of Mycobacterium tuberculosis augments transcription from HIV-1 long terminal repeat

promoter', *Journal of Biological Chemistry*, 287(20), pp. 16930–16946. doi: 10.1074/jbc.M111.327825.

Bodnar, K. A., Serbina, N. V. and Flynn, J. L. (2001) 'Fate of Mycobacterium tuberculosis within murine dendritic cells', *Infection and Immunity*, 69(2), pp. 800–809. doi: 10.1128/IAI.69.2.800-809.2001.

Brennan, M. J. (2017) 'The Enigmatic PE/PPE Multigene Family of Mycobacteria and Tuberculosis Vaccination', *Infection and Immunity*, 85(6). doi: 10.1128/IAI.

Brennan, M. J. and Delogu, G. (2002) 'The PE multigene family: a "molecular mantra" for mycobacteria', *Trends in Microbiology*, 10(5), pp. 246–249.

Cardona, P. J. (2006) 'RUTI: A new chance to shorten the treatment of latent tuberculosis infection', *Tuberculosis*, 86(3-4 SPEC. ISS.), pp. 273–289. doi: 10.1016/j.tube.2006.01.024.

Caruso, A. M. *et al.* (1999) 'Mice deficient in CD4 T cells have only transiently diminished levels of IFN-gamma, yet succumb to tuberculosis.', *Journal of immunology*, 162(9), pp. 5407–16. Available at: http://www.ncbi.nlm.nih.gov/pubmed/10228018.

Chackerian, A. A. *et al.* (2002) 'Dissemination of Mycobacterium tuberculosis is influenced by host factors and precedes the initiation of T-cell immunity.', *Infection and immunity*, 70(8), pp. 4501–9. doi: 10.1128/IAI.70.8.4501.

Chakhaiyar, P. *et al.* (2004) 'Regions of high antigenicity within the hypothetical PPE major polymorphic tandem repeat open-reading frame, Rv2608, show a differential humoral response and a low T cell response in various categories of patients with tuberculosis.', *The Journal of infectious diseases*, 190(7), pp. 1237–1244. doi: 10.1086/423938.

Chan, J. *et al.* (2014) 'The role of B cells and humoral immunity in Mycobacterium tuberculosis infection', *Seminars in Immunology*. Elsevier Ltd, 26(6), pp. 588–600. doi: 10.1016/j.smim.2014.10.005.

Chegou, N. N. *et al.* (2012) 'Potential of novel Mycobacterium tuberculosis infection phase-dependent antigens in the diagnosis of TB disease in a high burden setting', *BMC Infectious Diseases*. BioMed Central Ltd, 12(1), p. 10. doi: 10.1186/1471-2334-12-10.

Chensue, S. W. *et al.* (1994) 'Cytokine Responses During Mycobacterial and Schistosomal Antigen-Induced Pulmonary Granuloma Formation Production of Th 1 and Th2 Cytokines and Relative Contribution of Tumor Necrosis Factor', *American Journal of Pathology*, 145(5), pp. 1105–1113.

Choudhary, R. K. *et al.* (2003) 'PPE Antigen Rv2430c of Mycobacterium tuberculosis Induces a Strong B-Cell Response', *Infection and Immunity*, 71(11), pp. 6338–6343. doi: 10.1128/IAI.71.11.6338.

Codarri, L. *et al.* (2011) 'RORγt drives production of the cytokine GM-CSF in helper T cells, which is essential for the effector phase of autoimmune neuroinflammation', *Nature Immunology*, 12(6), pp. 560–567. doi: 10.1038/ni.2027.

Colditz, G. A. *et al.* (1994) 'Efficacy of BCG Vaccine in the Prevention of Tuberculosis: Meta-analysis of the Published Literature', *JAMA*, 271(9), pp. 698–702. doi: 10.1001/jama.1994.03510330076038.

Cole, S. T. *et al.* (1998) 'Deciphering the biology of mycobacterium tuberculosis from the complete genome sequence', *Nature*, 393(6685), pp. 537–544. doi: 10.1038/31159.

Colic, A. D. (2016) *Computational analysis of the immunogenicity and sequence diversity of Mycobacterium tuberculosis PPE _ MPTR proteins*, *Unpublished Data*.

Cooper, A. M. *et al.* (1993) 'Disseminated Tuberculosis in Interferon y Gene-disrupted Mice', *Journal of Experimental Medicine*, 178, pp. 2243–2247.

Cooper, A. M. (2009) 'Cell-Mediated Immune Responses in Tuberculosis', *Annual Review of Immunology*, 27(1), pp. 393–422. doi: 10.1146/annurev.immunol.021908.132703.

Corominas, M. *et al.* (2004) 'B-lymphocytes and co-stimulatory molecules in Mycobacterium tuberculosis infection', *International Journal of Tuberculosis and Lung Disease*, 8(1), pp. 98–105.

Couper, K. N., Blount, D. G. and Riley, E. M. (2008) 'IL-10: The Master Regulator of Immunity to Infection', *The Journal of Immunology*, 180(9), pp. 5771–5777. doi: 10.4049/jimmunol.180.9.5771.

Daim, S. *et al.* (2011) 'Expression of the Mycobacterium tuberculosis PPE37 protein in Mycobacterium smegmatis induces low tumour necrosis factor alpha and interleukin 6 production in murine macrophages', *Journal of Medical Microbiology*, 60, pp. 582–591. doi: 10.1099/jmm.0.026047-0.

Dalton, D. K. *et al.* (1993) 'Multiple defects of immune cell function in mice with disrupted Interferon-y Genes', *Science*, 259(March), pp. 1739–1742.

Davila, J., McNamara, L. A. and Yang, Z. (2012) 'Comparison of the predicted population

coverage of tuberculosis vaccine candidates Ag85b-ESAT-6, Ag85B-TB10.4, and Mtb72f via a bioinformatics approach', *PLoS ONE*, 7(7), pp. 1–11. doi: 10.1371/journal.pone.0040882.

Day, C. L. *et al.* (2013) 'Induction and regulation of T-cell immunity by the novel tuberculosis vaccine M72/AS01 in South African adults', *American Journal of Respiratory and Critical Care Medicine*, 188(4), pp. 492–502. doi: 10.1164/rccm.201208-1385OC.

Derrick, S. C. *et al.* (2011) 'Vaccine-induced anti-tuberculosis protective immunity in mice correlates with the magnitude and quality of multifunctional CD4 T cells', *Vaccine*. Elsevier Ltd, 29(16), pp. 2902–2909. doi: 10.1016/j.vaccine.2011.02.010.

Desjardins, M. *et al.* (1994) 'Biogenesis of phagolysosomes proceeds through a sequential series of interactions with the endocytic apparatus', *Journal of Cell Biology*, 124(5), pp. 677–688. doi: 10.1083/jcb.124.5.677.

Dheenadhayalan, V., Delogu, G. and Brennan, M. J. (2006) 'Expression of the PE_PGRS 33 protein in Mycobacterium smegmatis triggers necrosis in macrophages and enhanced mycobacterial survival', *Microbes and Infection*. Elsevier Masson, 8(1), pp. 262–272. doi: 10.1016/J.MICINF.2005.06.021.

Diedrich, C. R., O'Hern, J. and Wilkinson, R. J. (2016) 'HIV-1 and the Mycobacterium tuberculosis granuloma: A systematic review and meta-analysis', *Tuberculosis*. Elsevier Ltd, 98, pp. 62–76. doi: 10.1016/j.tube.2016.02.010.

Diehl, S. and Rincón, M. (2002) 'The two faces of IL-6 on Th1/Th2 differentiation', *Molecular Immunology*, 39(9), pp. 531–536. doi: 10.1016/S0161-5890(02)00210-9.

van Dissel, J. T. *et al.* (2010) 'Ag85B-ESAT-6 adjuvanted with IC31® promotes strong and long-lived Mycobacterium tuberculosis specific T cell responses in naïve human volunteers', *Vaccine*, 28(20), pp. 3571–3581. doi: 10.1016/j.vaccine.2010.02.094.

van Dissel, J. T. *et al.* (2014) 'A novel liposomal adjuvant system, CAF01, promotes long-lived Mycobacterium tuberculosis-specific T-cell responses in human', *Vaccine*. Elsevier Ltd, 32(52), pp. 7098–7107. doi: 10.1016/j.vaccine.2014.10.036.

Djuretic, I. M. *et al.* (2007) 'Transcription factors T-bet and Runx3 cooperate to activate Ifng and silence Il4 in T helper type 1 cells', *Nature Immunology*, 8(2), pp. 145–153. doi: 10.1038/ni1424.

Domingo-Gonzalez, R. *et al.* (2016) 'Cytokines and Chemokines in Mycobacterium tuberculosis Infection.', *Microbiology spectrum*, 4(5), pp. 1–58. doi:

10.1128/microbiolspec.TBTB2-0018-2016.

Doz, E. *et al.* (2009) 'Mycobacterial Phosphatidylinositol Mannosides Negatively Regulate Host Toll-like Receptor 4, MyD88-dependent Proinflammatory Cytokines, and TRIF-dependent Co-stimulatory Molecule Expression', *Journal of Biological Chemistry*, 284(35), pp. 23187–23196. doi: 10.1074/jbc.m109.037846.

Drennan, M. B. *et al.* (2004) 'Toll-Like Receptor 2-Deficient Mice Succumb to Mycobacterium tuberculosis Infection', *American Journal of Pathology*, 164(1), pp. 49–57. doi: 10.1016/S0002-9440(10)63095-7.

East, L. and Isacke, C. M. (2002) 'The mannose receptor family', *Biochimica et Biophysica Acta - General Subjects*, 1572(2–3), pp. 364–386. doi: 10.1016/S0304-4165(02)00319-7.

Essone, P. N. *et al.* (2019) 'M. tuberculosis infection and antigen specific cytokine response in healthcare workers frequently exposed to tuberculosis', *Scientific Reports*, 9(1), pp. 1–13. doi: 10.1038/s41598-019-44294-0.

Farber, D. L., Yudanin, Naomi, A. and Restifo, Nicholas, P. (2014) 'Human memory T-cells: generation, compartmentalization and homeostatsis', *Nature Reviews Immunology*, 14(1), pp. 24–35. doi: 10.1038/nri3567.Human.

Ferguson, J. S. *et al.* (1999) 'Surfactant Protein D Binds to Mycobacterium tuberculosis Bacilli and Lipoarabinomannan via Carbohydrate-Lectin Interactions Resulting in Reduced Phagocytosis of the Bacteria by Macrophages', *The Journal of Immunology*, 163, pp. 312–321. doi: 10.4049/jimmunol.170.2.711.

Ferguson, J. S. *et al.* (2006) 'Surfactant protein D increases fusion of Mycobacterium tuberculosis- containing phagosomes with lysosomes in human macrophages', *Infection and Immunity*, 74(12), pp. 7005–7009. doi: 10.1128/IAI.01402-06.

Fine, P. (1995) 'Variation in protection by BCG: implications of and for heterologous immunity', *The Lancet*, 346, pp. 1339–1345. Available at: https://ac-els-cdn-com.ez.sun.ac.za/S0140673695923489/1-s2.0-S0140673695923489-main.pdf?_tid=d20db316-a570-4be8-982b-51f47f286ab2&acdnat=1521026498_dfc10615903970840de20fcb39e27798 (Accessed: 14 March 2018).

Flynn, J. L. *et al.* (1993) 'An essential role for interferon gamma in resistance to Mycobacterium tuberculosis infection', *Journal of Experimental Medicine*, 178(6), pp. 2249–

2254. doi: 10.1084/jem.178.6.2249.

Flynn, J. L. and Chan, J. (2001) 'Immunology of tuberculosis', *Annu. Rev. Immunol*, 19, pp. 93–129.

Fratti, R. A. *et al.* (2003) 'Mycobacterium tuberculosis glycosylated phosphatidylinositol causes phagosome maturation arrest', *PNAS*, 100(9), pp. 5437–5442.

Fulton, S. A. *et al.* (2004) 'Inhibition of Major Histocompatibility Complex II Expression and Antigen Processing in Murine Alveolar Macrophages by Mycobacterium bovis BCG and the 19-Kilodalton Mycobacterial Lipoprotein', *Infection and Immunity*, 72(4), pp. 2101–2110. doi: 10.1128/IAI.72.4.2101-2110.2004.

Gantner, B. N. *et al.* (2003) 'Collaborative Induction of Inflammatory Responses by Dectin-1 and Toll-like Receptor 2', *The Journal of Experimental Medicine*, 197(9), pp. 1107–1117. doi: 10.1084/jem.20021787.

von Garnier, C. *et al.* (2005) 'Anatomical location determines the distribution and function of dendritic cells and other APCs in the respiratory tract.', *Journal of immunology (Baltimore, Md. : 1950)*, 175(3), pp. 1609–18. doi: 10.4049/jimmunol.175.3.1609.

Gaynor, C. D. *et al.* (1995) 'Pulmonary surfactant protein A mediates enhanced phagocytosis of Mycobacterium tuberculosis by a direct interaction with human macrophages', *The Journal of Immunology*, 155(0022–1767), pp. 5343–5351. doi: 10.1007/s13238-014-0077-5.

Geginat, J. *et al.* (2003) 'Proliferation and differentiation potential of human CD8', *Blood*, 101(June), pp. 4260–4266. doi: 10.1182/blood-2002-11-3577.Supported.

Gehring, A. J. *et al.* (2004) 'Mycobacterium tuberculosis LprG (Rv1411c): A Novel TLR-2 Ligand That Inhibits Human Macrophage Class II MHC Antigen Processing', *The Journal of Immunology*, 173(4), pp. 2660–2668. doi: 10.4049/jimmunol.173.4.2660.

Geijtenbeek, T. B. H. *et al.* (2003) 'Mycobacteria Target DC-SIGN to Suppress Dendritic Cell Function', *The Journal of Experimental Medicine*, 197(1), pp. 7–17. doi: 10.1084/jem.20021229.

Geldmacher, C., Zumla, A. and Hoelscher, M. (2012) 'Interaction between HIV and Mycobacterium tuberculosis: HIV-1-induced CD4 T-cell depletion and the development of active tuberculosis', *Current Opinion in HIV and AIDS*, 7(3), pp. 268–275. doi: 10.1097/COH.0b013e3283524e32.

Gong, J. *et al.* (1996) 'Interleukin-10 Downregulates Mycobacterium tuberculosis - Induced Th1 Responses and CTLA-4 Expression', *Infection and Immunity*, 64(3), pp. 913–918.

González-Galarza, F. F. *et al.* (2015) 'Allele frequency net 2015 update: New features for HLA epitopes, KIR and disease and HLA adverse drug reaction associations', *Nucleic Acids Research*, 43(D1), pp. D784–D788. doi: 10.1093/nar/gku1166.

Gordon, S. *et al.* (1992) 'Antigen Markers of Macrophage Differentiation in Murine Tissues', in *Macrophage Biology and Activation. Current Topics in Microbiology and Immunology*. doi: 10.1007/978-3-642-77377-8_1.

Grode, L. *et al.* (2005) 'Increased vaccine efficacy against tuberculosis of recombinant Mycobacterium bovis bacille Calmette-Guerin mutants that secrete listeriolysin', *Journal of Clinical Investigation*, 115(9), pp. 2472–2479. doi: 10.1172/JCI24617.2472.

Gupta, D. *et al.* (2010) 'Suppression of TLR2-Induced IL-12, Reactive Oxygen Species, and Inducible Nitric Oxide Synthase Expression by Mycobacterium tuberculosis Antigens Expressed inside Macrophages during the Course of Infection', *The Journal of Immunology*, 184(10), pp. 5444–5455. doi: 10.4049/jimmunol.0903283.

Harris, R. C. *et al.* (2016) 'Systematic review of mathematical models exploring the epidemiological impact of future TB vaccines', *Human Vaccines and Immunotherapeutics*. Taylor & Francis, 12(11), pp. 2813–2832. doi: 10.1080/21645515.2016.1205769.

Hazenberg, M. D. *et al.* (2000) 'T cell depletion in HIV-1 infection: How CD4+ T cells go out of stock', *Nature Immunology*, 1(4), pp. 285–289. doi: 10.1038/79724.

Hemmi, H. *et al.* (2000) 'A Toll-like receptor recognizes bacterial DNA', *Nature*, 408(6813), pp. 740–745. doi: 10.1038/35047123.

Henderson, R. A., Watkins, S. C. and Flynn, J. L. (1997) 'Activation of human dendritic cells following infection with Mycobacterium tuberculosis.', *The Journal of Immunology*, 159(2), pp. 635 LP – 643. Available at: http://www.jimmunol.org/content/159/2/635.abstract.

Hertz, C. J. *et al.* (2001) 'Microbial Lipopeptides Stimulate Dendritic Cell Maturation Via Toll-Like Receptor 2', *The Journal of Immunology*, 166(4), pp. 2444–2450. doi: 10.4049/jimmunol.166.4.2444.

Hoshino, K. *et al.* (1999) 'Cutting edge: Toll-like receptor 4 (TLR4)-deficient mice are hyporesponsive to lipopolysaccharide: evidence for TLR4 as the Lps gene product.', *Journal of immunology*, 162(7), pp. 3749–52. Available at:

http://www.ncbi.nlm.nih.gov/pubmed/10201887.

Hwang, E. S. *et al.* (2005) 'T helper cell fate specified by kinase-mediated interaction of T-bet with GATA-3', *Science*, 307(5708), pp. 430–433. doi: 10.1126/science.1103336.

Indrigo, J., Hunter, R. L. and Actor, J. K. (2003) 'Cord factor trehalose 6,69-dimycolate (TDM) mediates trafficking events during mycobacterial infection of murine macrophages', *Microbiology*, 149, pp. 2049–2059. doi: 10.1099/mic.0.26226-0.

Ito, T., Schaller, M., Hogaboam, Cory M., *et al.* (2007) 'TLR9 activation is a key event for the maintenance of a mycobacterial antigen-elicited pulmonary granulomatous response', *European Journal of Immunology*, 37(10), pp. 2847–2855. doi: 10.1002/eji.200737603.

Ito, T., Schaller, M., Hogaboam, Cory M, *et al.* (2007) 'TLR9 activation is a key event for the maintenance of a mycobacterial antigen-elicited pulmonary granulomatous response', *European Journal of Immunology*, 37, pp. 2847–2855. doi: 10.1002/eji.200737603.

Ito, T., Schaller, M., Hogaboam, C. M., *et al.* (2009) 'TLR9 regulates the mycobacteria-elicited pulmonary granulomatous immune response in mice through DC-derived Notch ligand delta-like 4', *The Journal of Clinical Investigation*, 119(1), pp. 33–46. doi: 10.1172/JCI35647DS1.

Ito, T., Schaller, M., Raymond, T., *et al.* (2009) 'Toll-like Receptor 9 Activation Is a Key Mechanism for the Maintenance of Chronic Lung Inflammation', *American Journal of Respiratory and Critical Care Medicine*, 180(12), pp. 1227–1238. doi: 10.1164/rccm.200906-0892oc.

Ivanov, I. I. *et al.* (2006) 'The Orphan Nuclear Receptor RORγt Directs the Differentiation Program of Proinflammatory IL-17+ T Helper Cells', *Cell*, 126(6), pp. 1121–1133. doi: 10.1016/j.cell.2006.07.035.

Jakob, T. *et al.* (1998) 'Activation of Cutaneous Dendritic Cells by CpG-Containing Oligodeoxynucleotides: A Role for Dendritic Cells in the Augmentation of Th1 Responses by Immunostimulatory DNA', *The Journal of Immunology*, 161(6), pp. 3042–3049. doi: 10.4049/jimmunol.0902925.

Janeway, C. A. J. *et al.* (2001) 'The Humoral Immune Response', in *Immunobiology: The Immune System in Health and Disease*. Garland Science. Available at: https://www.ncbi.nlm.nih.gov/books/NBK10752/ (Accessed: 22 May 2019).

Jin, W. and Dong, C. (2013) 'IL-17 cytokines in immunity and inflammation', *Emerging Microbes and Infections*, 2. doi: 10.1038/emi.2013.58.

Joosten, S. A. *et al.* (2010) 'Mycobacterium tuberculosis peptides presented by HLA-E molecules are targets for human CD8+ T-cells with cytotoxic as well as regulatory activity', *PLoS Pathogens*, 6(2). doi: 10.1371/journal.ppat.1000782.

Joosten, S. A. *et al.* (2016) 'Patients with Tuberculosis Have a Dysfunctional Circulating B-Cell Compartment, Which Normalizes following Successful Treatment', *PLoS Pathogens*, 12(6), pp. 1–24. doi: 10.1371/journal.ppat.1005687.

Jurado, J. O. *et al.* (2012) 'IL-17 and IFN- expression in lymphocytes from patients with active tuberculosis correlates with the severity of the disease', *Journal of Leukocyte Biology*, 91(6), pp. 991–1002. doi: 10.1189/jlb.1211619.

Kagina, B. M. N. *et al.* (2010) 'Specific T cell frequency and cytokine expression profile do not correlate with protection against tuberculosis after bacillus Calmette-Guérin vaccination of newborns', *American Journal of Respiratory and Critical Care Medicine*, 182(8), pp. 1073–1079. doi: 10.1164/rccm.201003-0334OC.

Kang, P. B. *et al.* (2005) 'The human macrophage mannose receptor directs Mycobacterium tuberculosis phagosome biogenesis', *The Journal of Experimental Medicine*, 202(7), pp. 987–999. doi: 10.1084/jem.20051239.

Kaplan, M. H. *et al.* (1996) 'Impaired IL-12 responses and enhanced development of TH2 cells in Stat4-deficient mice', *Nature*, 382, pp. 174–177.

Kaufmann, S. H. E. (2007) 'The contribution of immunology to the rational design of novel antibacterial vaccines', *Nature Reviews Microbiology*, 5(7), pp. 491–504. doi: 10.1038/nrmicro1688.

Khader, S. A. *et al.* (2007) 'IL-23 and IL-17 in the establishment of protective pulmonary CD4+ T cell responses after vaccination and during Mycobacterium tuberculosis challenge', *Nature Immunology*, 8(4), pp. 369–377. doi: 10.1038/ni1449.

Khader, S. A., Gaffen, S. L. and Kolls, J. K. (2009) 'Th17 cells at the crossroads of innate and adaptive immunity against infectious diseases at the mucosa', *Mucosal Immunology*, 2(5), pp. 403–411. doi: 10.1038/mi.2009.100.

Khoo, K.-H. *et al.* (1995) 'Structural definition of acylated phosphatidylinositol mannosides from Mycobacterium tuberculosis: definition of a common anchor for lipomannan and lipoarabinomannan', *Glycobiology*, 5(1), pp. 117–127. doi: 10.1093/glycob/5.1.117.

Khubaib, M. *et al.* (2016) 'Mycobacterium tuberculosis Co-operonic PE32/PPE65 Proteins

Alter Host Immune Responses by Hampering Th1 Response', *Frontiers in Microbiology*, 7(May), pp. 1–10. doi: 10.3389/fmicb.2016.00719.

Kim, A. *et al.* (2017) 'Protective vaccine efficacy of the complete form of PPE39 protein from mycobacterium tuberculosis Beijing/K strain in mice', *Clinical and Vaccine Immunology*, 24(11), pp. 1–12. doi: 10.1128/CVI.00219-17.

Kobayashi, T. *et al.* (1998) 'A lipid associated with the antiphospholipid syndrome regulates endosome structure and function', *Nature*, 392(March), pp. 193–197.

Koh, K. W., Lehming, N. and Seah, G. T. (2009) 'Degradation-resistant protein domains limit host cell processing and immune detection of mycobacteria', *Molecular Immunology*, 46(7), pp. 1312–1318. doi: 10.1016/j.molimm.2008.11.008.

Koning, F. (1997) 'Enhancement of HLA class II restricted antigen presentation by mannose-receptor-mediated uptake', *Biochemical Society Transactions*, 25(2), pp. 664–665. doi: 10.1042/bst0250664.

Kozakiewics, L. *et al.* (2013) 'The Role of B Cells and Humoral Immunity in Mycobacterium tuberculosis Infection', in *Divangahi M. (eds), The New Paradigm of Immunity to Tuberculosis. Advances in Experimental Medicine and Biology*, pp. 225–250. doi: 10.3389/fimmu.2013.00386.

Ladel, C. H. *et al.* (1997) 'Lethal tuberculosis in interleukin-6-deficient mutant mice', *Infection and Immunity*, 65(11), pp. 4843–4849.

Ladel, C. H., Daugelat, S. and Kaufmann, S. H. (1995) 'Immune response to Mycobacterium bovis bacille Calmette Guérin infection in major histocompatibility complex class I- and II-deficient knock-out mice: contribution of CD4 and CD8 T cells to acquired resistance', *European journal of immunology.* Weinheim : Wiley-VCH, 25(2), pp. 377–384.

Larbi, A. and Fulop, T. (2014) 'From "truly naïve" to "exhausted senescent" T cells: When markers predict functionality', *Cytometry Part A*, 85(1), pp. 25–35. doi: 10.1002/cyto.a.22351.

Latchumanan, V. K. *et al.* (2002) 'Mycobacterium tuberculosis Antigens Induce the Differentiation of Dendritic Cells from Bone Marrow', *The Journal of Immunology*, 169(12), pp. 6856–6864. doi: 10.4049/jimmunol.169.12.6856.

Lazarevic, V. *et al.* (2011) 'Transcription factor T-bet represses Th17 differentiation by preventing Runx1-mediated activation of the RORγt gene', *Nat. Immunol.*, 12(1), pp. 96–104. doi: 10.1038/ni.1969.Transcription.

Leal, I. S., Smedegård, B. and Andersen, P. (1999) 'Interleukin-6 and Interleukin-12 Participate in Induction of a Type 1 Protective T-Cell Response during Vaccination with a Tuberculosis Subunit Vaccine', *American society for Microbiology*, 67(11), pp. 5747–5754.

LeibundGut-Landmann, S. *et al.* (2007) 'Syk- and CARD9-dependent coupling of innate immunity to the induction of T helper cells that produce interleukin 17', *Nature Immunology*, 8(6), pp. 630–638. doi: 10.1038/ni1460.

Li, H. *et al.* (2016) 'Mycobacterium tuberculosis PE13 (Rv1195) manipulates the host cell fate via p38-ERK-NF-jB axis and apoptosis', *Apoptosis*, 21, pp. 795–808. doi: 10.1007/s10495-016-1249-y.

Lighvani, A. A. *et al.* (2002) 'T-bet is rapidly induced by interferon- in lymphoid and myeloid cells', *Proceedings of the National Academy of Sciences*, 98(26), pp. 15137–15142. doi: 10.1073/pnas.261570598.

Lindenstrøm, T. *et al.* (2009) 'Tuberculosis Subunit Vaccination Provides Long-Term Protective Immunity Characterized by Multifunctional CD4 Memory T Cells', *The Journal of Immunology*, 182(12), pp. 8047–8055. doi: 10.4049/jimmunol.0801592.

Lindestam Arlehamn, C. S. *et al.* (2013) 'Memory T Cells in Latent Mycobacterium tuberculosis Infection Are Directed against Three Antigenic Islands and Largely Contained in a CXCR3+CCR6+ Th1 Subset', *PLoS Pathogens*, 9(1). doi: 10.1371/journal.ppat.1003130.

Ling Lin, P. and Flynn, J. L. (2005) 'CD8 T cells and Mycobacterium tuberculosis infection', *Seminars in Immunopathology*, 37(3), pp. 239–249. doi: 10.1016/j.physbeh.2017.03.040.

Longmate, J. *et al.* (2001) 'Population coverage by HLA class-I restricted cytotoxic T-lymphocyte epitopes', *Immunogenetics*. Springer-Verlag, 52(3–4), pp. 165–173. doi: 10.1007/s002510000271.

Lopez, M. *et al.* (2003) 'The 19-kDa Mycobacterium tuberculosis Protein Induces Macrophage Apoptosis Through Toll-Like Receptor-2', *The Journal of Immunology*, 170(5), pp. 2409–2416. doi: 10.4049/jimmunol.170.5.2409.

Loxton, A. G. *et al.* (2012) 'Heparin-binding hemagglutinin induces IFN-y + IL-2 + IL-17 + multifunctional CD4 + T cells during latent but not active tuberculosis disease', *Clinical and Vaccine Immunology*, 19(5), pp. 746–751. doi: 10.1128/CVI.00047-12.

Loxton, A. G. (2019) 'Bcells and their regulatory functions during Tuberculosis: Latency and active disease', *Molecular Immunology*. Elsevier, 111(March), pp. 145–151. doi:

10.1016/j.molimm.2019.04.012.

Loxton, A. G., Hondalus, M. K. and Sampson, S. L. (2015) 'Chapter 5: TB Vaccine Assessment', in *Drug Delivery Systems for Tuberculosis Prevention and Treatment*, pp. 91–110.

Lu, Y. *et al.* (2012) 'Novel Recombinant BCG Coexpressing Ag85B, ESAT-6 and Rv2608 Elicits Significantly Enhanced Cellular Immune and Antibody Responses in C57BL/6 Mice', *Scandinavian Journal of Immunology*, 76(3), pp. 271–277. doi: 10.1111/j.1365-3083.2012.02726.x.

Luckheeram, R. V. *et al.* (2011) 'CD4 +T cells: Differentiation and functions', *Clinical and Developmental Immunology*, 2012. doi: 10.1155/2012/925135.

Lyadova, I. V. and Panteleev, A. V. (2015) 'Th1 and Th17 Cells in Tuberculosis: Protection, Pathology, and Biomarkers', *Mediators of Inflammation*. Hindawi, 2015, pp. 1–13. doi: 10.1155/2015/854507.

MacGurn, J. A. and Cox, J. S. (2007) 'A genetic screen for Mycobacterium tuberculosis mutants defective for phagosome maturation arrest identifies components of the ESX-1 secretion system', *Infection and Immunity*, 75(6), pp. 2668–2678. doi: 10.1128/IAI.01872-06.

MacLeod, M. . K. . *et al.* (2009) 'CD4 memory T cells: what are they and what can they do?', *Seminars in Immunology*, 21(2), pp. 53–61. doi: 10.1016/j.smim.2009.02.006.

Maeda, N. *et al.* (2003) 'The Cell Surface Receptor DC-SIGN Discriminates between Mycobacterium Species through Selective Recognition of the Mannose Caps on Lipoarabinomannan', *Journal of Biological Chemistry*, 278(8), pp. 5513–5516. doi: 10.1074/jbc.c200586200.

Maglione, P. J. and Chan, J. (2009) 'How B cells shape the immune response against Mycobacterium tuberculosis', *European Journal of Immunology*, 39(3), pp. 676–686. doi: 10.1002/eji.200839148.

Maglione, P. J., Xu, J. and Chan, J. (2007) ' B Cells Moderate Inflammatory Progression and Enhance Bacterial Containment upon Pulmonary Challenge with Mycobacterium tuberculosis ', *The Journal of Immunology*, 178(11), pp. 7222–7234. doi: 10.4049/jimmunol.178.11.7222.

Mahnke, Y. D. *et al.* (2013) 'The who's who of T-cell differentiation: Human memory T-cell subsets', *European Journal of Immunology*, 43(11), pp. 2797–2809. doi: 10.1002/eji.201343751.

Malik, B. Z. A., Denning, G. M. and Kusner, D. J. (2000) 'Inhibition of Ca2+ Signaling by Mycobacterium tuberculosis Is Associated with Reduced Phagosome – Lysosome Fusion and Increased Survival within Human Macrophages', *The Journal of Experimental Medicine*, 191(2), pp. 287–302.

Malik, Z. A. *et al.* (2003) 'Mycobacterium tuberculosis Blocks Ca 2+ Signaling and Phagosome Maturation in Human Macrophages Via Specific Inhibition of Sphingosine Kinase', *The Journal of Immunology*, 170, pp. 2811–2815. doi: 10.4049/jimmunol.170.6.2811.

Manicassamy, S. *et al.* (2009) 'TLR2 dependent induction of vitamin A metabolizing enzymes in dendritic cells promotes T regulatory responses and inhibits Th-17 mediated autoimmunity', *Nature Medicine*, 15(4), pp. 401–409. doi: doi:10.1038/nm.1925.

Marín, N. D. *et al.* (2012) 'Reduced frequency of memory T cells and increased Th17 responses in patients with active tuberculosis', *Clinical and Vaccine Immunology*, 19(10), pp. 1667–1676. doi: 10.1128/CVI.00390-12.

Mauri, C. and Bosma, A. (2012) 'Immune Regulatory Function of B Cells', *Annual Review of Immunology*, 30(1), pp. 221–241. doi: 10.1146/annurev-immunol-020711-074934.

Mayo, R. E. P. and Stanford, J. L. (2000) 'Double-blind placebo-controlled trial of Mycobacterium vaccae immunotherapy for tuberculosis in KwaZulu, South Africa, 1991-97', *Transactions of the Royal Society of Tropical Medicine and Hygiene*, 94(5), pp. 563–568. doi: 10.1016/S0035-9203(00)90088-9.

McBride, J. A. and Striker, R. (2017) 'Imbalance in the game of T cells: What can the CD4/CD8 T-cell ratio tell us about HIV and health?', *PLoS Pathogens*, 13(11), pp. 1–7. doi: 10.1371/journal.ppat.1006624.

McNamara, L. A., He, Y. and Yang, Z. (2010) 'Using epitope predictions to evaluate efficacy and population coverage of the Mtb72f vaccine for tuberculosis', *BMC Immunology*, 11. doi: 10.1186/1471-2172-11-18.

Van Meijgaarden, K. E. *et al.* (2018) 'Cross-laboratory evaluation of multiplex bead assays including independent common reference standards for immunological monitoring of observational and interventional human studies', *PLoS ONE*, 13(9), pp. 1–17. doi: 10.1371/journal.pone.0201205.

Meyer, F. *et al.* (2003) 'Cutting Edge: Cyclooxygenase-2 Activation Suppresses Th1 Polarization in Response to Helicobacter pylori', *The Journal of Immunology*, 171(8), pp.

3913–3917. doi: 10.4049/jimmunol.171.8.3913.

Mills, C. D. (2015) 'Anatomy of a discovery: M1 and M2 macrophages', *Frontiers in Immunology*, 6(MAY), pp. 1–12. doi: 10.3389/fimmu.2015.00212.

Mohan, V. P. *et al.* (2001) 'Effects of Tumor Necrosis Factor Alpha on Host Immune Response in Chronic Persistent Tuberculosis: Possible Role for Limiting Pathology', *American S*, 69(3), pp. 1847–1855. doi: 10.1128/IAI.69.3.1847.

Mootoo, A. *et al.* (2009) 'TNF-α in tuberculosis: A cytokine with a split personality', *Inflammation and Allergy - Drug Targets*, 8(1), pp. 53–62. doi: 10.2174/187152809787582543.

Murphy, K. P. (2012) *Janeway's Immunobiology*. 8th edn. New York: Garland Science, Taylor & Francis Group, LLC.

Murphy, K. P. (2013) *Janeway's Immunobiology 8th Edition*. 8th Editio, *Garland Science, Taylor & Francis Group*. 8th Editio. Edited by J. Scobie et al. New York, USA: Garland Science, Taylor & Francis Group, LLC. Available at: http://ir.obihiro.ac.jp/dspace/handle/10322/3933.

Nair, S. *et al.* (2009) 'The PPE18 of Mycobacterium tuberculosis Interacts with TLR2 and Activates IL-10 Induction in Macrophage', *The Journal of Immunology*, 183(10), pp. 6269–6281. doi: 10.4049/jimmunol.0901367.

Nair, S., Pandey, A. D. and Mukhopadhyay, S. (2011) 'The PPE18 Protein of Mycobacterium tuberculosis Inhibits NF- B/rel-Mediated Proinflammatory Cytokine Production by Upregulating and Phosphorylating Suppressor of Cytokine Signaling 3 Protein', *The Journal of Immunology*, 186(9), pp. 5413–5424. doi: 10.4049/jimmunol.1000773.

Natarajan, K. *et al.* (2003) 'Down-Regulation of T Helper 1 Responses to Mycobacterial Antigens Due to Maturation of Dendritic Cells by 10-kDa Mycobacterium tuberculosis Secretory Antigen', 187.

Nepom, G. T. (2012) 'MHC Class II Tetramers', *Journal of immunology*, 188(6), pp. 2477–2482. doi: 10.1038/jid.2014.371.

Nigou, J. *et al.* (2001) 'Mannosylated Lipoarabinomannans Inhibit IL-12 Production by Human Dendritic Cells: Evidence for a Negative Signal Delivered Through the Mannose Receptor', *The Journal of Immunology*, 166(12), pp. 7477–7485. doi: 10.4049/jimmunol.166.12.7477.

Noss, E. H. *et al.* (2001) 'Toll-Like Receptor 2-Dependent Inhibition of Macrophage Class II MHC Expression and Antigen Processing by 19-kDa Lipoprotein of Mycobacterium tuberculosis', *The Journal of Immunology*, 167(2), pp. 910–918. doi: 10.4049/jimmunol.167.2.910.

O' Leary, S., Sullivan, M. P. O. and Keane, J. (2011) 'IL-10 Blocks Phagosome Maturation in Mycobacterium tuberculosis – Infected Human Macrophages', *American Journal of Respiratory Cell and Molecular Biology*, 45, pp. 172–180. doi: 10.1165/rcmb.2010-0319OC.

O'Shea, J. J. *et al.* (2011) 'Genomic views of STAT function in CD4+ T helper cell differentiation: new technology brings new insights and new questions', *Nature Reviews Immunology*, 11(4), pp. 239–250. doi: 10.1038/nri2958.Genomic.

Orlando, V. *et al.* (2018) 'Human CD4 T-cells with a naive phenotype produce multiple cytokines during Mycobacterium tuberculosis infection and correlate with active disease', *Frontiers in Immunology*, 9(MAY). doi: 10.3389/fimmu.2018.01119.

Orme, I. M. *et al.* (1997) 'Interleukin 12 Is Crucial to the Development of Protective Immunity in Mice Intravenously Infected with Mycobacterium tuberculosis', *The Journal of Experimental Medicine*, 186(1), pp. 39–45. doi: 10.1084/jem.186.1.39.

Ottenhoff, T. H. M. (2012) 'New pathways of protective and pathological host defense to mycobacteria', *Trends in Microbiology*. Elsevier Ltd, 20(9), pp. 419–428. doi: 10.1016/j.tim.2012.06.002.

Ozeki, Y. *et al.* (2011) 'Loss of anti-mycobacterial efficacy in mice over time following vaccination with Mycobacterium bovis bacillus Calmette-Guérin', *Vaccine*. Elsevier Ltd, 29(40), pp. 6881–6887. doi: 10.1016/j.vaccine.2011.07.051.

Pagan, A. J. and Ramakrishnan, L. (2015) 'Immunity and immunopathology in the tuberculous granuloma', *Cold Spring Harbor Perspectives in Medicine*, 5(9), pp. 1–19. doi: 10.1101/cshperspect.a018499.

Pagán, A. J. and Ramakrishnan, L. (2015) 'Immunity and immunopathology in the tuberculous granuloma', *Cold Spring Harbor Perspectives in Medicine*, 5(9), pp. 1–19. doi: 10.1101/cshperspect.a018499.

Pasquinelli, V. *et al.* (2013) 'Phosphorylation of mitogen-activated protein kinases contributes to interferon γ production in response to mycobacterium tuberculosis', *Journal of Infectious Diseases*, 207(2), pp. 340–350. doi: 10.1093/infdis/jis672.

Pasula, R. *et al.* (1997) 'Surfactant Protein A (SP-A) Mediates Attachment of Mycobacterium tuberculosis to Murine Alveolar Macrophages', *American Journal of Respiratory Cell and Molecular Biology*, 17(2), pp. 209–217. doi: 10.1165/ajrcmb.17.2.2469.

Pathak, S. K. *et al.* (2007) 'Direct extracellular interaction between the early secreted antigen ESAT-6 of Mycobacterium tuberculosis and TLR2 inhibits TLR signaling in macrophages', *Nature Immunology*, 8(6), pp. 610–618. doi: 10.1038/ni1468.

Pecora, N. D. *et al.* (2004) 'Mycobacterium tuberculosis LprA Is a Lipoprotein Agonist of TLR2 That Regulates Innate Immunity and APC Function', *The Journal of Immunology*, 177(1), pp. 422–429. doi: 10.4049/jimmunol.177.1.422.

Perreau, M. *et al.* (2013) 'Lack of Mycobacterium tuberculosis-specific interleukin-17A-producing CD4+ T cells in active disease', *European Journal of Immunology*, 43(4), pp. 939–948. doi: 10.1002/eji.201243090.

Poltorak, A. *et al.* (1998) 'Defective LPS signaling in C3H/HeJ and C57BL/10ScCr mice: mutations in Tlr4 gene', *Science*, 282(5396), pp. 2085–2088. doi: 10.1126/science.282.5396.2085.

Pompei, L. *et al.* (2007) 'Disparity in IL-12 Release in Dendritic Cells and Macrophages in Response to Mycobacterium tuberculosis Is Due to Use of Distinct TLRs', *The Journal of Immunology*, 178(8), pp. 5192–5199. doi: 10.4049/jimmunol.178.8.5192.

Prezzemolo, T. *et al.* (2014) 'Functional Signatures of Human CD4 and CD8 T Cell Responses to Mycobacterium tuberculosis', *Frontiers in Immunology*, 5(April), pp. 1–13. doi: 10.3389/fimmu.2014.00180.

Prigozy, T. I. *et al.* (1997) 'The Mannose Receptor Delivers Lipoglycan Antigens to Endosomes for Presentation to T Cells by CD1b Molecules', *Immunity*, 6(February), pp. 187–197.

Pym, A. S. *et al.* (2003) 'Recombinant BCG exporting ESAT-6 confers enhanced protection against tuberculosis', *Nature Medicine*, 9(5), pp. 548–553. doi: 10.1038/nm.

Qureshi, R. *et al.* (2019) 'PPE65 of M . tuberculosis regulate pro-in fl ammatory signalling through LRR domains of Toll like receptor-2', *Biochemical and Biophysical Research Communications*, 508, pp. 152–158. doi: 10.1016/j.bbrc.2018.11.094.

Rajaram, M. V. S. *et al.* (2010) 'Mycobacterium tuberculosis Activates Human Macrophage Peroxisome Proliferator-Activated Receptor g Linking Mannose Receptor Recognition to

Regulation of Immune Responses', *The Journal of Immunology*, 185, pp. 929–942. doi: 10.4049/jimmunol.1000866.

Rajaram, M. V. S. *et al.* (2014) 'Macrophage immunoregulatory pathways in tuberculosis', *Seminars in Immunology*. Elsevier Ltd, 26(6), pp. 471–485. doi: 10.1016/j.smim.2014.09.010.

Ramakrishnan, L., Federspiel, N. A. and Falkow, S. (2000) 'Granuloma-Specific Expression of Mycobacterium Virulence Proteins from the Glycine-Rich PE-PGRS Family', *Science*, 288, pp. 1436–1439. Available at: http://science.sciencemag.org.ez.sun.ac.za/content/sci/288/5470/1436.full.pdf (Accessed: 22 May 2018).

Reid, S. D., Penna, G. and Adorini, L. (2000) 'The control of T cell responses by dendritic cell subsets', *Current Opinion in Immunology*, 12(1), pp. 114–121. doi: 10.1016/S0952-7915(99)00059-X.

Reiling, N. *et al.* (2002) 'Cutting Edge: Toll-Like Receptor (TLR)2- and TLR4-Mediated Pathogen Recognition in Resistance to Airborne Infection with Mycobacterium tuberculosis', *The Journal of Immunology*, 169(7), pp. 3480–3484. doi: 10.4049/jimmunol.169.7.3480.

Reiling, R. *et al.* (2001) 'Complex Encounters at the Macrophage-Mycobacterium Interface : Studies on the Role of the Mannose Receptor and CD14 in Experimental Infection Models with Mycobacterium', *Immunobiology*, 204, pp. 558–571.

Van Rensburg, I. C. *et al.* (2017) 'B-cells with a FasL expressing regulatory phenotype are induced following successful anti-tuberculosis treatment':, *Immunity, inflammation and disease*, 5(1), pp. 57–67. doi: 10.1002/iid3.140.

van Rensburg, I. C. and Loxton, A. G. (2018) 'Killer (FASL regulatory) B cells are present during latent TB and are induced by BCG stimulation in participants with and without latent tuberculosis', *Tuberculosis*. Elsevier, 108(June 2017), pp. 114–117. doi: 10.1016/j.tube.2017.11.010.

Roach, D. R. *et al.* (2002) 'TNF Regulates Chemokine Induction Essential for Cell Recruitment, Granuloma Formation, and Clearance of Mycobacterial Infection', *The Journal of Immunology*, 168, pp. 4620–4627. doi: 10.4049/jimmunol.168.9.4620.

Robinson, J. *et al.* (2015) 'The IPD and IMGT/HLA database: Allele variant databases', *Nucleic Acids Research*, 43, pp. D423–D431. doi: 10.1093/nar/gku1161.

Rodrigues, L. C., Diwan, V. K. and Wheeler, J. G. (1993) 'Protective Effect of BCG against

Tuberculous Meningitis and Miliary Tuberculosis: A Meta-Analysis', *International Journal of Epidemiology*, 22(6), pp. 1154–1158. doi: 10.1093/ije/22.6.1154.

Rohde, K. *et al.* (2007) 'Mycobacterium tuberculosis and the environment within the phagosome', *Immunological Reviews*, 219, pp. 37–54. Available at: https://www.researchgate.net/profile/Roisin_Owens/publication/265114430_Mycobacterium_tuberculosis_and_the_Four-Minute_Phagosome/links/5552fbbb08aeaaff3bf0061b.pdf%5Cnpapers3://publication/uuid/8A985647-F0C9-4C0C-BD4F-C8E0CD5DFD21.

Rook, G. W. (2007) 'Th2 Cytokines in Susceptibility to Tuberculosis', *Current Molecular Medicine*, 7(3), pp. 327–337. doi: 10.2174/156652407780598557.

Rothfuchs, A. G. *et al.* (2007) 'Dectin-1 Interaction with Mycobacterium tuberculosis Leads to Enhanced IL-12p40 Production by Splenic Dendritic Cells', *The Journal of Immunology*, 179(6), pp. 3463–3471. doi: 10.4049/jimmunol.179.6.3463.

Rozot, V. *et al.* (2013) 'Mycobacterium tuberculosis-specific CD8+T cells are functionally and phenotypically different between latent infection and active disease', *European Journal of Immunology*, 43(6), pp. 1568–1577. doi: 10.1002/eji.201243262.

Saini, N. K. *et al.* (2016) 'Suppression of autophagy and antigen presentation by Mycobacterium tuberculosis PE_PGRS47', *Nature Microbiology*, 1(9). doi: 10.1097/CCM.0b013e31823da96d.Hydrogen.

Sakaguchi, S. *et al.* (2003) 'Essential role of IRF-3 in lipopolysaccharide-induced interferon -b gene expression and endotoxin shock', *Biochemical and Biophysical Research Communications*, 306, pp. 860–866. doi: 10.1016/S0006-291X(03)01049-0.

Sallusto, F., Geginat, J. and Lanzavecchia, A. (2004) 'Central Memory and Effector Memory T Cell Subsets: Function, Generation, and Maintenance', *Annual Review of Immunology*, 22(1), pp. 745–763. doi: 10.1146/annurev.immunol.22.012703.104702.

Samji, T. and Khanna, K. M. (2017) 'Understanding Memory CD8+ T cells', *Immunology Letters*, 185, pp. 32–39. doi: 10.1016/j.physbeh.2017.03.040.

Sampson, S. L. (2011) 'Mycobacterial PE/PPE proteins at the host-pathogen interface', *Clinical and Developmental Immunology*, 2011(Figure 1). doi: 10.1155/2011/497203.

Sánchez, D. *et al.* (2009) 'Role of TLR2- and TLR4-mediated signaling in Mycobacterium tuberculosis-induced macrophage death', *Cellular Immunology*. Elsevier Inc., 260(2), pp. 128–

136. doi: 10.1016/j.cellimm.2009.10.007.

Sayes, F., Sun, L., Di Luca, M., *et al.* (2012) 'Strong immunogenicity and cross-reactivity of Mycobacterium tuberculosis ESX-5 type VII secretion-encoded PE-PPE proteins predicts vaccine potential', *Cell Host and Microbe*. Elsevier Inc., 11(4), pp. 352–363. doi: 10.1016/j.chom.2012.03.003.

Sayes, F., Sun, L., Di Luca, M., *et al.* (2012) 'Strong Immunogenicity and Cross-Reactivity of Mycobacterium tuberculosis ESX-5 Type VII Secretion -Encoded PE-PPE Proteins Predicts Vaccine Potential', *Cell Host & Microbe*. Cell Press, 11(4), pp. 352–363. doi: 10.1016/J.CHOM.2012.03.003.

Schnappinger, D. *et al.* (2003) 'Transcriptional Adaptation of *Mycobacterium tuberculosis* within Macrophages', *The Journal of Experimental Medicine*, 198(5), pp. 693–704. doi: 10.1084/jem.20030846.

Schneberger, D. *et al.* (2013) 'Expression of Toll-like receptor 9 in mouse and human lungs', *Journal of Anatomy*, 222(5), pp. 495–503. doi: 10.1111/joa.12039.

Schnettger, L. *et al.* (2017) 'A Rab20-Dependent Membrane Trafficking Pathway Controls M . tuberculosis Replication by Regulating Phagosome Spaciousness and Integrity', *Cell Host and Microbe*. Elsevier Inc., 21(5), pp. 619–628. doi: 10.1016/j.chom.2017.04.004.

Scriba, T. J. *et al.* (2008) 'Distinct, Specific IL-17- and IL-22-Producing CD4+ T Cell Subsets Contribute to the Human Anti-Mycobacterial Immune Response', *The Journal of Immunology*, 180(3), pp. 1962–1970. doi: 10.4049/jimmunol.180.3.1962.

Scriba, T. J., Coussens, A. K. and Fletcher, H. A. (2016) 'Human Immunology of Tuberculosis', *Microbiology spectrum*, 4(4), pp. 1–23. doi: 10.1128/microbiolspec.TBTB2-0016-2016.Correspondence.

Seder, R. A., Darrah, P. A. and Roederer, M. (2008) 'T-cell qualty in memory and protection: implications for vaccine design', *Nature Reviews Immunology*, 8(April), pp. 247–258.

Shipkova, M. and Wieland, E. (2012) 'Surface markers of lymphocyte activation and markers of cell proliferation', *Clinica Chimica Acta*. Elsevier B.V., 413(17–18), pp. 1338–1349. doi: 10.1016/j.cca.2011.11.006.

Sia, J. K., Georgieva, M. and Rengarajan, J. (2015) 'Innate Immune Defenses in Human Tuberculosis: An Overview of the Interactions between Mycobacterium tuberculosis and Innate Immune Cells', *Journal of Immunology Research*. Hindawi Publishing Corporation,

2015. doi: 10.1155/2015/747543.

Sinha, A. *et al.* (2006) 'Impaired Generation of Reactive Oxygen Species during Differentiation of Dendritic Cells (DCs) by Mycobacterium tuberculosis Secretory Antigen (MTSA) and Subsequent Activation of MTSA-DCs by Mycobacteria Results in Increased Intracellular Survival', *The Journal of Immunology*, 177(1), pp. 468–478. doi: 10.4049/jimmunol.177.1.468.

Slack, J. L. *et al.* (2000) 'Identification of Two Major Sites in the Type I Interleukin-1 Receptor Cytoplasmic Region Responsible for Coupling to Pro-inflammatory Signaling Pathways', *Journal of Biological Chemistry*, 275(7), pp. 4670–4678. doi: 10.1074/jbc.275.7.4670.

Soares, A. *et al.* (2010) 'Novel application of Ki67 to quantify antigen-specific in vitro lymphoproliferation', *Journal of Immunological Methods*. Elsevier B.V., 362(1–2), pp. 43–50. doi: 10.1016/j.jim.2010.08.007.

Sparwasser, T *et al.* (1998) 'Bacterial DNA and immunostimulatory CpG oligonucleotides trigger maturation and activation of murine d ...', *European Journal of Immunology*, 28, pp. 2045–2054. doi: 10.1002/(SICI)1521-4141(199806)28.

Spertini, F. *et al.* (2015) 'Safety of human immunisation with a live-attenuated Mycobacterium tuberculosis vaccine: A randomised, double-blind, controlled phase I trial', *The Lancet Respiratory Medicine*, 3(12), pp. 953–962. doi: 10.1016/S2213-2600(15)00435-X.

Srivastava, V. *et al.* (2009) 'Toll-like Receptor 2 and DC-SIGNR1 Differentially Regulate Suppressors of Cytokine Signaling 1 in Dendritic Cells during Mycobacterium tuberculosis Infection', *The Journal of Biological Chemistry*, 284(38), pp. 25532–25541. doi: 10.1074/jbc.M109.006221.

Stahl, P. *et al.* (1980) 'Receptor-mediated pinocytosis of mannose glycoconjugates by macrophages: Characterization and evidence for receptor recycling', *Cell*, 19(1), pp. 207–215. doi: 10.1016/0092-8674(80)90402-x.

Steinman, L. (2007) 'A brief history of TH17, the first major revision in the T H1/TH2 hypothesis of T cell-mediated tissue damage', *Nature Medicine*, 13(2), pp. 139–145. doi: 10.1038/nm1551.

Sterne, J. A. C., Rodrigues, L. C. and Guedes, I. N. (1998) 'Does the efficacy of BCG decline with time since vaccination?', *International Journal of Tuberculosis Lung Disease*, 2(3), pp. 200–207.

Su, H. *et al.* (2015) 'PPE26 induces TLR2-dependent activation of macrophages and drives Th1-type T-cell immunity by triggering the cross-talk of multiple pathways involved in the host response', *Oncotarget*, 6(36), pp. 38517–38537. doi: 10.18632/oncotarget.5956.

Sullivan, J. T. *et al.* (2012) 'The Mycobacterium tuberculosis SecA2 System Subverts Phagosome Maturation To Promote Growth in Macrophages', *Infection and Immunity*, 80(3), pp. 996–1006. doi: 10.1128/IAI.05987-11.

Sun, J. *et al.* (2010) 'Mycobacterial Nucleoside Diphosphate Kinase Blocks Phagosome Maturation in Murine Raw 264 . 7 Macrophages', *PLoS ONE*, 5(1), pp. 1–12. doi: 10.1371/journal.pone.0008769.

Szabo, S. J. *et al.* (1997) 'Regulation of the interleukin (IL)-12R beta 2 subunit expression in developing T helper 1 (Th1) and Th2 cells.', *The Journal of experimental medicine*, 185(5), pp. 817–24. Available at: http://www.ncbi.nlm.nih.gov/pubmed/9120387%0Ahttp://www.pubmedcentral.nih.gov/articlerender.fcgi?artid=PMC2196166.

Tailleux, L. *et al.* (2003) 'Constrained Intracellular Survival of Mycobacterium tuberculosis in Human Dendritic Cells', *The Journal of Immunology*, 170(4), pp. 1939–1948. doi: 10.4049/jimmunol.170.4.1939.

Tailleux, Ludovic *et al.* (2003) 'DC-SIGN Is the Major Mycobacterium tuberculosis Receptor on Human Dendritic Cells', *The Journal of Experimental Medicine*, 197(1), pp. 121–127. doi: 10.1084/jem.20021468.

Team, R. C. (no date) *R: A Language and Environment for Statistical Computing*. Available at: https://www.r-project.org.

Thoma-Uszynski, S. *et al.* (2000) 'Activation of Toll-Like Receptor 2 on Human Dendritic Cells Triggers Induction of IL-12, But Not IL-10', *The Journal of Immunology*, 165(7), pp. 3804–3810. doi: 10.4049/jimmunol.165.7.3804.

Tiwari, B., Soory, A. and Raghunand, T. R. (2014) 'An immunomodulatory role for the Mycobacterium tuberculosis region of difference 1 locus proteins PE35 (Rv3872) and PPE68 (Rv3873)', *FEBS Journal*, 35, pp. 1556–1570. doi: 10.1111/febs.12723.

Torrado, E. and Cooper, A. M. (2011) 'IL-17 and Th17 cells in TB', *Cytokine Growth Factor Rev*, 21(6), pp. 455–462. doi: 10.1016/j.cytogfr.2010.10.004.IL-17.

Trunz, B. B., Fine, P. and Dye, C. (2006) 'Effect of BCG vaccination on childhood tuberculous

meningitis and miliary tuberculosis worldwide: a meta-analysis and assessment of cost-effectiveness', *The Lancet*, 367(9517), pp. 1173–1180. doi: 10.1016/S0140-6736(06)68507-3.

Tshabalala, M. *et al.* (2015) 'Human Leukocyte Antigen Diversity: A Southern African Perspective', *Journal of Immunology Research*, 2015(class I), pp. 1–11. doi: 10.1155/2015/746151.

Udgata, A. *et al.* (2015) 'Transduction of Functionally Contrasting Signals by Two Mycobacterial PPE Proteins Downstream of TLR2 Receptors', *BioMed Research International*, 2015, p. Article ID 483150, 16 pages. doi: 10.4049/jimmunol.1501816.

Umemura, M. *et al.* (2007) 'IL-17-Mediated Regulation of Innate and Acquired Immune Response against Pulmonary Mycobacterium bovis Bacille Calmette-Guerin Infection', *The Journal of Immunology*, 178(6), pp. 3786–3796. doi: 10.4049/jimmunol.178.6.3786.

Underhill, D. M. *et al.* (1999) 'Toll-like receptor-2 mediates mycobacteria-induced proinflammatory signaling in macrophages', *Pnas*, 96(25), pp. 14459–14463. doi: 10.1073/pnas.96.25.14459.

Underhill, D. M. and Ozinsky, A. (2002) 'Phagocytosis of Microbes: Complexity in Action', *Annual Review of Immunology*, 20(1), pp. 825–852. doi: 10.1146/annurev.immunol.20.103001.114744.

Valadas, E. (2004) 'Nontuberculous Mycobacteria: Clinical Importance and Relevance to Bacille Calmette-Guérin Vaccination', *Clinical Infectious Diseases*, 39, pp. 457–478. Available at: https://watermark.silverchair.com/39-4-457.pdf?token=AQECAHi208BE49Ooan9kkhW_Ercy7Dm3ZL_9Cf3qfKAc485ysgAAAbIwggGuBgkqhkiG9w0BBwagggGfMIIBmwIBADCCAZQGCSqGSIb3DQEHATAeBglghkgBZQMEAS4wEQQMUvJeE3xDlL-w5iVgAgEQgIIBZaPfhxl7UkGGgLOdBtISzqzWJ0pOAryzG-z0EAYbwKROyZ (Accessed: 14 March 2018).

Veerdonk, F. L. Van De *et al.* (2010) 'Mycobacterium tuberculosis induces IL-17A responses through TLR4 and dectin-1 and is critically dependent on endogenous IL-1', *Journal of Leukocyte Biology*, 88(August), pp. 227–232. doi: 10.1189/jlb.0809550.

Velez, D. R. *et al.* (2010) 'Variants in toll-like receptors 2 and 9 influence susceptibility to pulmonary tuberculosis in Caucasians, African-Americans, and West Africans', *Human Genetics*, 127(1), pp. 65–73. doi: 10.1007/s00439-009-0741-7.Variants.

Vergne, I., Chua, J. and Deretic, V. (2003) 'Tuberculosis Toxin Blocking Phagosome Maturation Inhibits a Novel Ca2+ / Calmodulin-PI3K hVPS34 Cascade', *The Journal of Experimental Medicine*, 198(4), pp. 653–659. doi: 10.1084/jem.20030527.

Via, L. E. *et al.* (1997) 'Arrest of Mycobacterial Phagosome Maturation Is Caused by a Block in Vesicle Fusion between Stages Controlled by rab5 and rab7 *', *The Journal of Biological Chemistry*, 272(20), pp. 13326–13331.

Vordermeier, H. M. *et al.* (1996) 'Increase of tuberculous infection in the organs of B cell-deficient mice', *Clinical and Experimental Immunology*, 106(2), pp. 312–316. doi: 10.1046/j.1365-2249.1996.d01-845.x.

Vordermeier, H. M. *et al.* (2001) 'Use of Synthetic Peptides Derived from the Antigens ESAT-6 and CFP-10 for Differential Diagnosis of Bovine Tuberculosis in Cattle', *Clinical and Diagnostic Laboratory Immunology*, 8(3), pp. 571–578. doi: 10.1128/CDLI.8.3.571–578.2001.

Vordermeier, H. M. *et al.* (2012) 'Conserved Immune Recognition Hierarchy of Mycobacterial PE/PPE Proteins during Infection in Natural Hosts', *PLoS ONE*, 7(8). doi: 10.1371/journal.pone.0040890.

Voskuil, M. I. *et al.* (2004) 'Regulation of the Mycobacterium tuberculosis PE/PPE genes.', *Tuberculosis (Edinburgh, Scotland)*. Elsevier, 84(3–4), pp. 256–62. doi: 10.1016/j.tube.2003.12.014.

Walburger, A. *et al.* (2004) 'Protein kinase G from pathogenic mycobacteria promotes survival within macrophages', *Science*, 304(5678), pp. 1800–1804. doi: 10.1126/science.1099384.

Walker, J. A. and McKenzie, A. N. J. (2018) 'TH2 cell development and function', *Nature Reviews Immunology*, 18(2), pp. 121–133. doi: 10.1038/nri.2017.118.

Walzl, G. *et al.* (2011) 'Immunological biomarkers of tuberculosis', *Nature Reviews Immunology*, 11(5), pp. 343–354. doi: 10.1038/nri2960.

WHO (2018) *Global Tuberculosis Report 2018*.

Wickam, H. (2017) *tidyverse: Easily Install and Load the 'Tidyverse'. R package version 1. https://CRAN.R-project.org/package=tidyverse*. Available at: https://cran.r-project.org/package=tidyverse (Accessed: 21 November 2019).

Wileman, T. E., Lennartz, M. R. and Stahl, P. D. (1986) 'Identification of the macrophage mannose receptor as a 175-kDa membrane protein', *Proc*, 83(April), pp. 2501–2505.

Wolf, A. J. *et al.* (2007) 'Mycobacterium tuberculosis Infects Dendritic Cells with High Frequency and Impairs Their Function In Vivo', *The Journal of Immunology*, 179(4), pp. 2509–2519. doi: 10.4049/jimmunol.179.4.2509.

Wolf, A. J., Linas, B., *et al.* (2008) 'Initiation of the adaptive immune response to Mycobacterium tuberculosis depends on antigen production in the local lymph node, not the lungs', *The Journal of Experimental Medicine*, 205(1), pp. 105–115. doi: 10.1084/jem.20071367.

Wolf, A. J., Desvignes, L., *et al.* (2008) 'Initiation of the adaptive immune response to *Mycobacterium tuberculosis* depends on antigen production in the local lymph node, not the lungs', *The Journal of Experimental Medicine*, 205(1), pp. 105–115. doi: 10.1084/jem.20071367.

Wu, Y. E. *et al.* (2009) 'Changes in lymphocyte subsets in the peripheral blood of patients with active pulmonary tuberculosis', *Journal of International Medical Research*, 37(6), pp. 1742–1749. doi: 10.1177/147323000903700610.

Xu, Y. *et al.* (2007) 'Toll-like receptor 4 is a sensor for autophagy associated with innate immunity', *Immunity*, 27(1), pp. 135–144. doi: 10.1016/j.immuni.2007.05.022.Toll-like.

Xu, Y. *et al.* (2015) 'PPE57 induces activation of macrophages and drives Th1-type immune responses through TLR2', *Journal of Molecular Medicine*. Springer Berlin Heidelberg, 93(6), pp. 645–662. doi: 10.1007/s00109-014-1243-1.

Yonekawa, A. *et al.* (2014) 'Dectin-2 Is a Direct Receptor for Mannose-Capped Lipoarabinomannan of Mycobacteria', *Immunity*. Elsevier Inc., 41, pp. 402–413. doi: 10.1016/j.immuni.2014.08.005.

Zambrano-Zaragoza, J. F. *et al.* (2014) 'Th17 Cells in Autoimmune and Infectious Diseases', *International Journal of Inflammation*, 2014, pp. 1–12. doi: 10.1155/2014/651503.

Zenaro, E., Donini, M. and Dusi, S. (2009) ' Induction of Th1/Th17 immune response by Mycobacterium tuberculosis : role of dectin-1, mannose receptor, and DC-SIGN ', *Journal of Leukocyte Biology*, 86(6), pp. 1393–1401. doi: 10.1189/jlb.0409242.

Zhu, J. *et al.* (2012) 'The transciptional factor T-bet is induced by multiple pathaways anmd prevents an endogenous T helper-2 program during T helper-1 responses', *Immunity*, 37(4), pp. 660–673. doi: 10.1016/j.immuni.2012.09.007.The.

Chapter 7

Appendices

7.1 Ethics Approval Letter

UNIVERSITEIT
STELLENBOSCH
UNIVERSITY

Approval Letter
Progress Report

05/08/2019

Project ID: 4107

Ethics Reference No: N16/05/070

Title: Evaluation of host biomarker-based point-of-care tests for targeted screening for active TB (Screen TB)

Dear Miss Stephanie Alexander,

Your request for extension/annual renewal of ethics approval dated 04/07/2019 08:51 refers.

The Health Research Ethics Committee reviewed and approved the annual progress report you submitted through an expedited review process.

The approval of this project is extended for a further year.

Approval date: 05 August 2019

Expiry date: 04 August 2020

Kindly be reminded to submit progress reports two (2) months before expiry date.

Where to submit any documentation

Kindly note that the HREC uses an electronic ethics review management system, *Infonetica*, to manage ethics applications and ethics review process. To submit any documentation to HREC, please click on the following link: https://applyethics.sun.ac.za.

Please remember to use your **Project ID [4107]** and ethics reference number **[N16/05/070]** on any documents or correspondence with the HREC concerning your research protocol.

Yours sincerely,

Mr. Francis Masiye,

HREC Coordinator,

Health Research Ethics Committee 2 (HREC2).

National Health Research Ethics Council (NHREC) Registration Number:
REC-130408-012 (HREC1)·REC-230208-010 (HREC2)

Federal Wide Assurance Number: 00001372
Office of Human Research Protections (OHRP) Institutional Review Board (IRB) Number:
IRB0005240 (HREC1)·IRB0005239 (HREC2)

The Health Research Ethics Committee (HREC) complies with the SA National Health Act No. 61 of 2003 as it pertains to health research. The HREC abides by the ethical norms and principles for research, established by the World Medical Association (2013). Declaration of Helsinki; Ethical Principles for Medical Research Involving Human Subjects; the South African Department of Health (2006).Guidelines for Good Practice in the Conduct of Clinical Trials with Human Participants in South Africa (2nd edition); as well as the Department of Health (2015). Ethics in Health Research: Principles, Processes and Structures (2nd edition).

The Health Research Ethics Committee reviews research involving human subjects conducted or supported by the Department of Health and Human Services, or other federal departments or agencies that apply the Federal Policy for the Protection of Human Subjects to such research (United States Code of Federal Regulations Title 45 Part 46); and/or clinical investigations regulated by the Food and Drug Administration (FDA) of the Department of Health and Human Services.

7.2 Informed Consent Recruitment Form

UNIVERSITEIT•STELLENBOSCH•UNIVERSITY
jou kennisvennoot • your knowledge partner

PPE_MPTR proteins: Elucidating population-specific immune responses

Caitlyne Young, MSc candidate

Supervisors: Prof Sampson, Dr Kriel, Dr Loxton

The aim of this work is to determine the immune response elicited by population-tailored PPE_MPTR peptides in an African cohort. We will assess if there are T-cell responses to these peptides by assessing the resultant cytokine production following stimulation of whole blood with these peptides.

The study is conducted with Ethics number: N16/05/070

I understand the proposed study and hereby give consent for my blood to be drawn and screened against the mentioned antigens.

Please provide the following information about your QuantiFeron® status.

Please note, this information will be kept 100% confidential.

POSITIVE **NEGATIVE** **UNKNOWN**

.....	.....	M/F	.....
Name of participant	Date of birth	Sex	Date

Molecular Biology and Human Genetics • Department Biomedical Sciences • Faculty of Health Sciences • Stellenbosch University

Molekulêre Biologie en Menslike Genetika • Departement Biomediese Wetenskappe • Fakulteit Gesondheidswetenskappe • Universiteit Stellenbosch

PO Box/Posbus 19063 • Tygerberg, 7505 • South Africa/Suid-Afrika • Fax/Faks: +27 (0) 21 938 9476

7.3 Distribution of PPE_MPTR-induced activation states of CD4+ T-cells

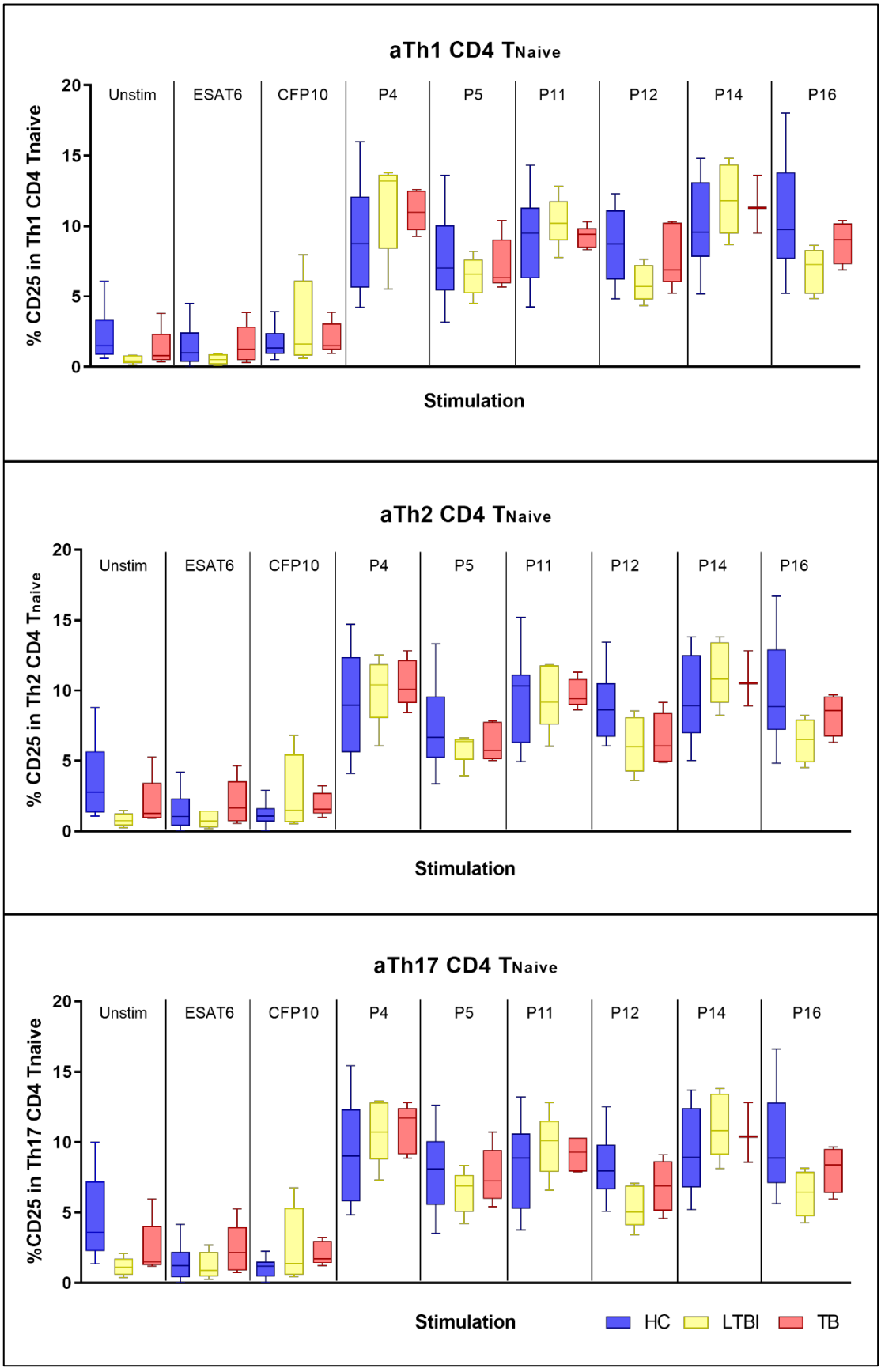

Figure 7.1: Distribution of activated naïve $CD4^+$ T-cells ($CD25^+$) in the peripheral blood of TB, LTBI and healthy individuals. The box-and-whisker plots represent the proportions of activated Th1, Th2 and Th17 T_N $CD4^+$ T-cell subsets as a mean percentage of the total Th1, Th2 or Th17 T_N $CD4^+$ T-cell populations. Blue = HC = healthy controls (n=11). Yellow = LTBI = latent TB infection (n=5). Red = TB = active TB (n=5). ESAT-6 = Early Secreted Antigen-6. CFP-10 = Culture Filtrate Protein 10. Unstim = Unstimulated (PBS). P4 = Rv0878c_c. P5 = Rv0878c_d. P11 =Rv2356c_a. P12 = Rv2608_a. P14 = Rv2608_c. P16 =Rv2608_g.

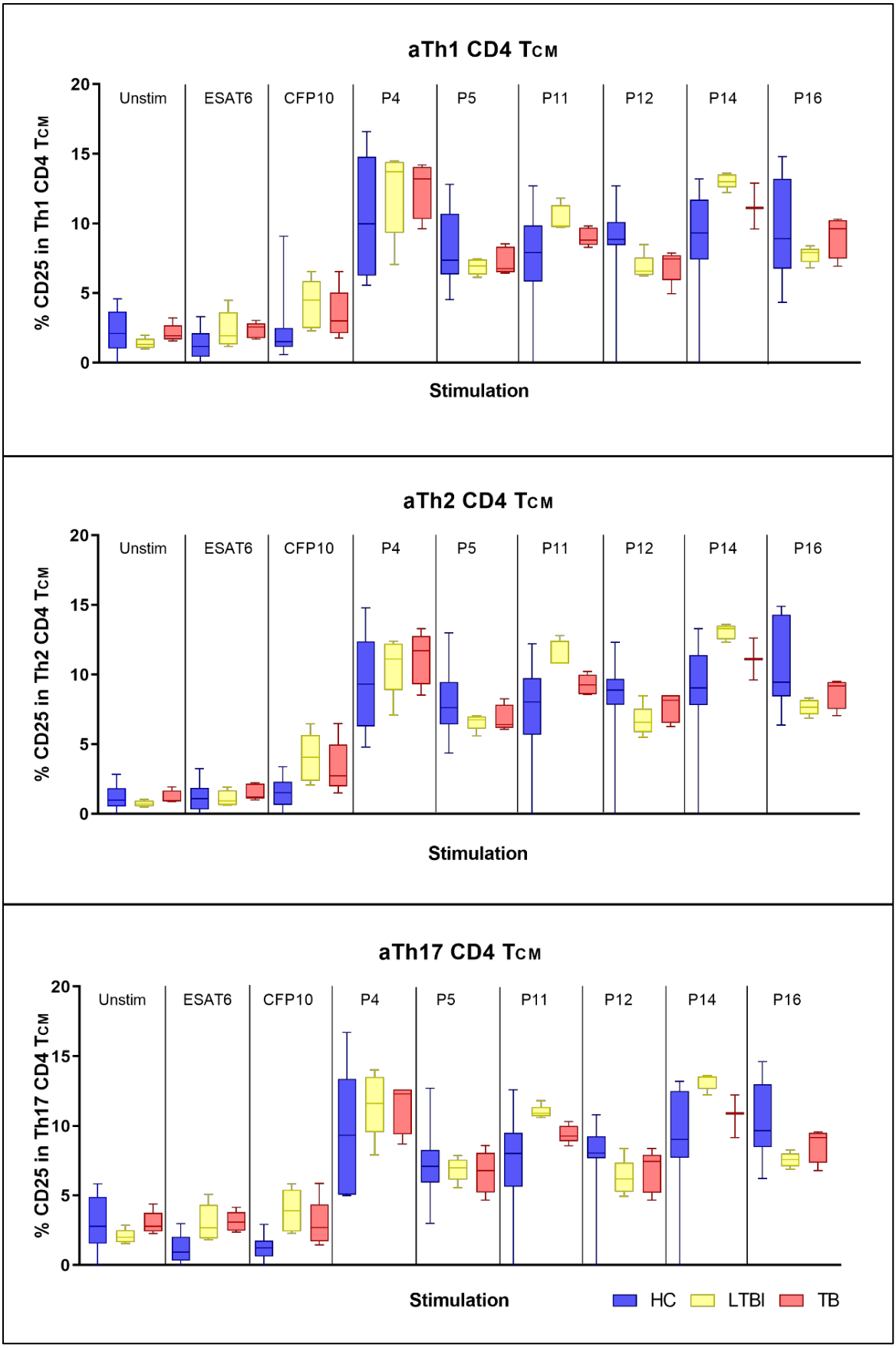

Figure 7.2: Distribution of activated central memory $CD4^+$ T-cells ($CD25^+$) in the peripheral blood of TB, LTBI and healthy individuals. The box-and-whisker plots represent the proportions of activated Th1, Th2 and Th17 T_{CM} $CD4^+$ T-cell subsets as a mean percentage of the total Th1, Th2 or Th17 T_{CM} $CD4^+$ T-cell populations. Blue = HC = healthy controls (n=11). Yellow = LTBI = latent TB infection (n=5). Red = TB = active TB (n=5). ESAT-6 = Early Secreted Antigen-6. CFP-10 = Culture Filtrate Protein 10. Unstim = Unstimulated (PBS). P4 = Rv0878c_c. P5 = Rv0878c_d. P11 =Rv2356c_a. P12 = Rv2608_a. P14 = Rv2608_c. P16 =Rv2608_g.

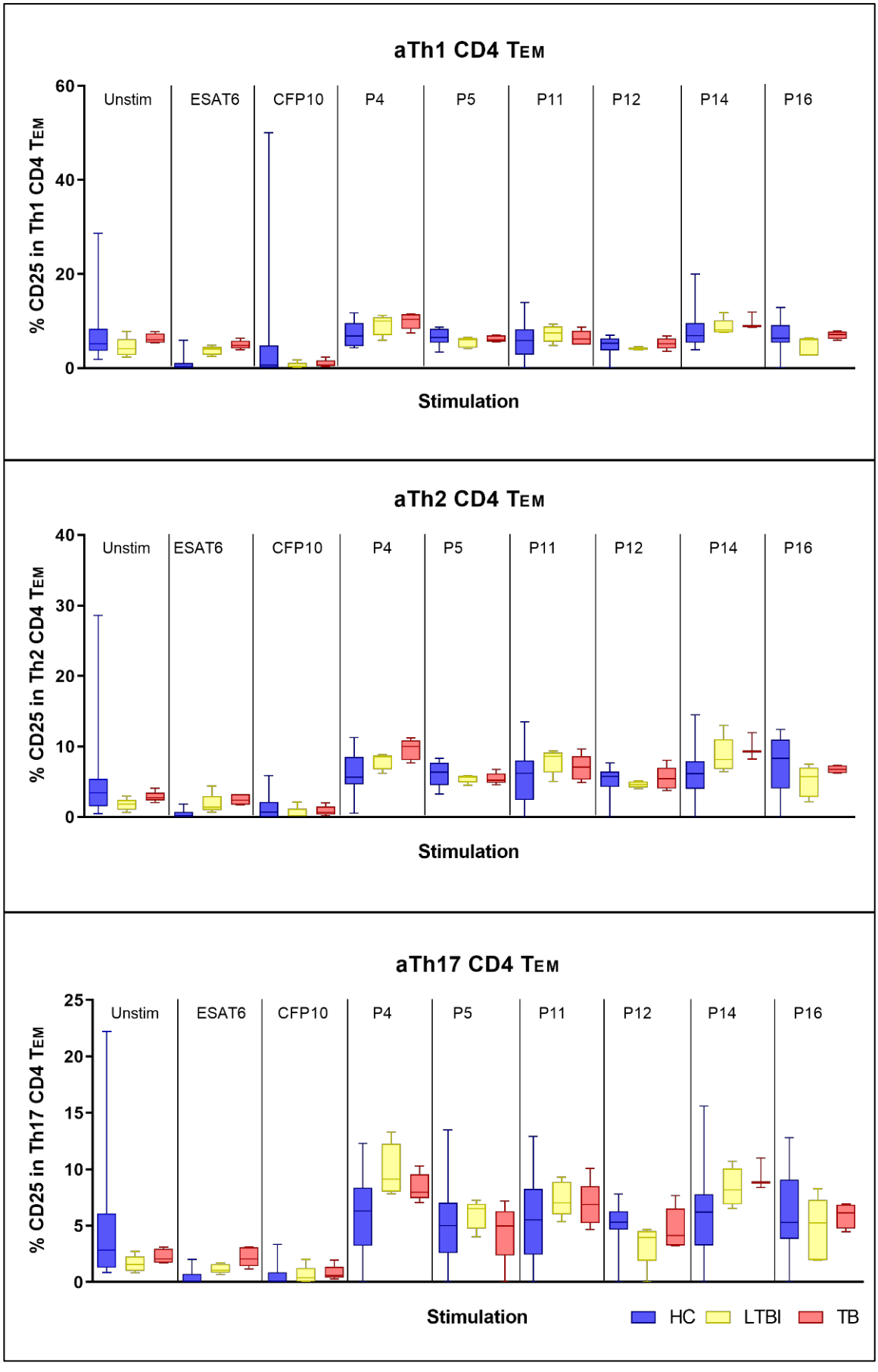

Figure 7.3: Distribution of activated effector memory $CD4^+$ T-cells ($CD25^+$) in the peripheral blood of TB, LTBI and healthy individuals. The box-and-whisker plots represent the proportions of activated Th1, Th2 and Th17 T_{EM} $CD4^+$ T-cell subsets as a mean percentage of the total Th1, Th2 or Th17 T_{EM} $CD4^+$ T-cell populations. Blue = HC = healthy controls (n=11). Yellow = LTBI = latent TB infection (n=5). Red = TB = active TB (n=5). ESAT-6 = Early Secreted Antigen-6. CFP-10 = Culture Filtrate Protein 10. Unstim = Unstimulated (PBS). P4 = Rv0878c_c. P5 = Rv0878c_d. P11 =Rv2356c_a. P12 = Rv2608_a. P14 = Rv2608_c. P16 =Rv2608_g.

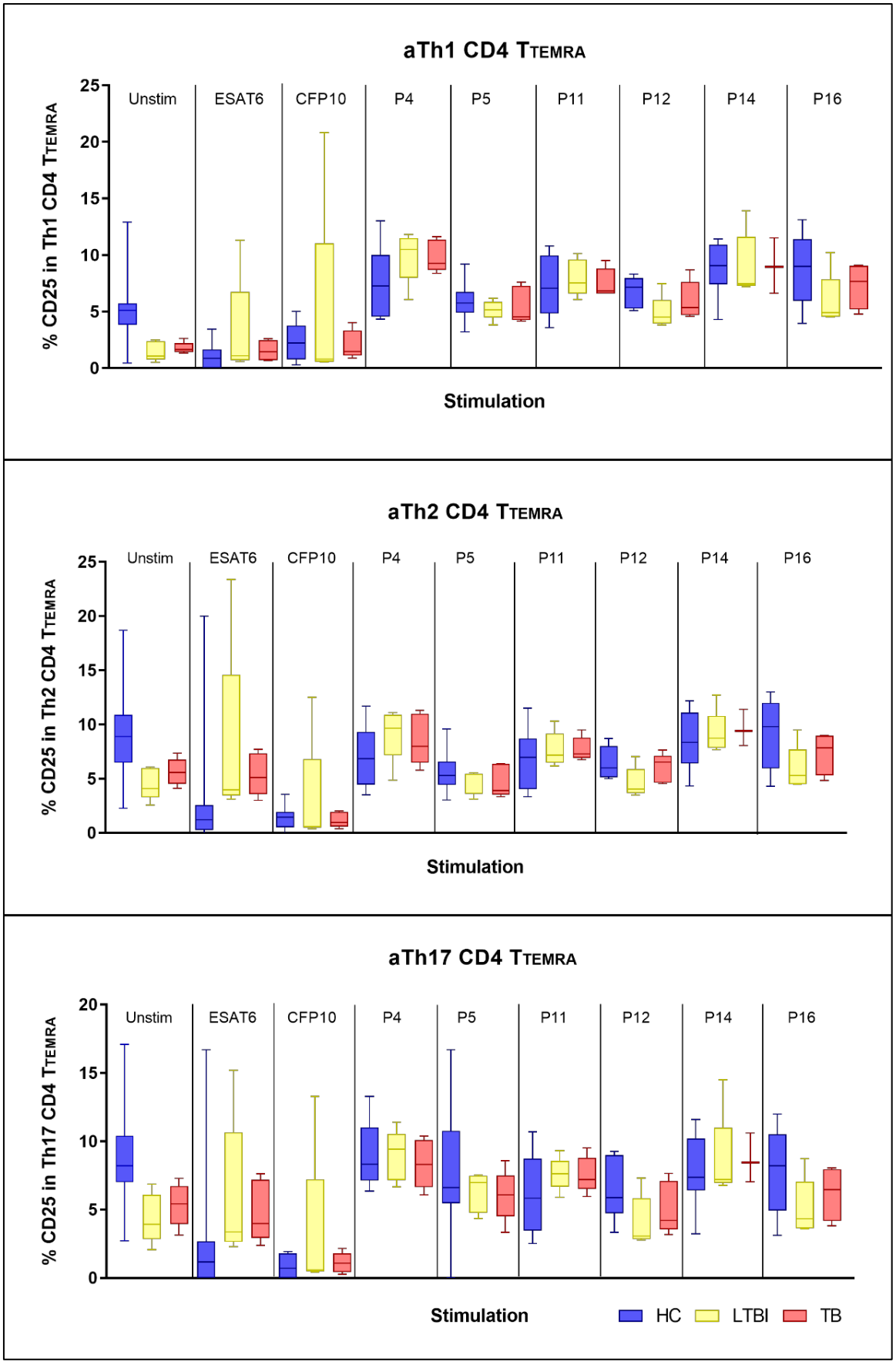

Figure 7.4: Distribution of activated terminally differentiated effector memory $CD4^+$ T-cells ($CD25^+$) in the peripheral blood of TB, LTBI and healthy individuals. The box-and-whisker plots represent the proportions of activated Th1, Th2 and Th17 T_{TEMRA} $CD4^+$ T-cell subsets as a mean percentage of the total Th1, Th2 or Th17 T_{TEMRA} $CD4^+$ T-cell populations. Blue = HC = healthy controls (n=11). Yellow = LTBI = latent TB infection (n=5). Red = TB = active TB (n=5). ESAT-6 = Early Secreted Antigen-6. CFP-10 = Culture Filtrate Protein 10. Unstim = Unstimulated (PBS). P4 = Rv0878c_c. P5 = Rv0878c_d. P11 =Rv2356c_a. P12 = Rv2608_a. P14 = Rv2608_c. P16 =Rv2608_g.

7.4 Distribution of PPE_MPTR-induced activation states of $CD8^+$ T-cells

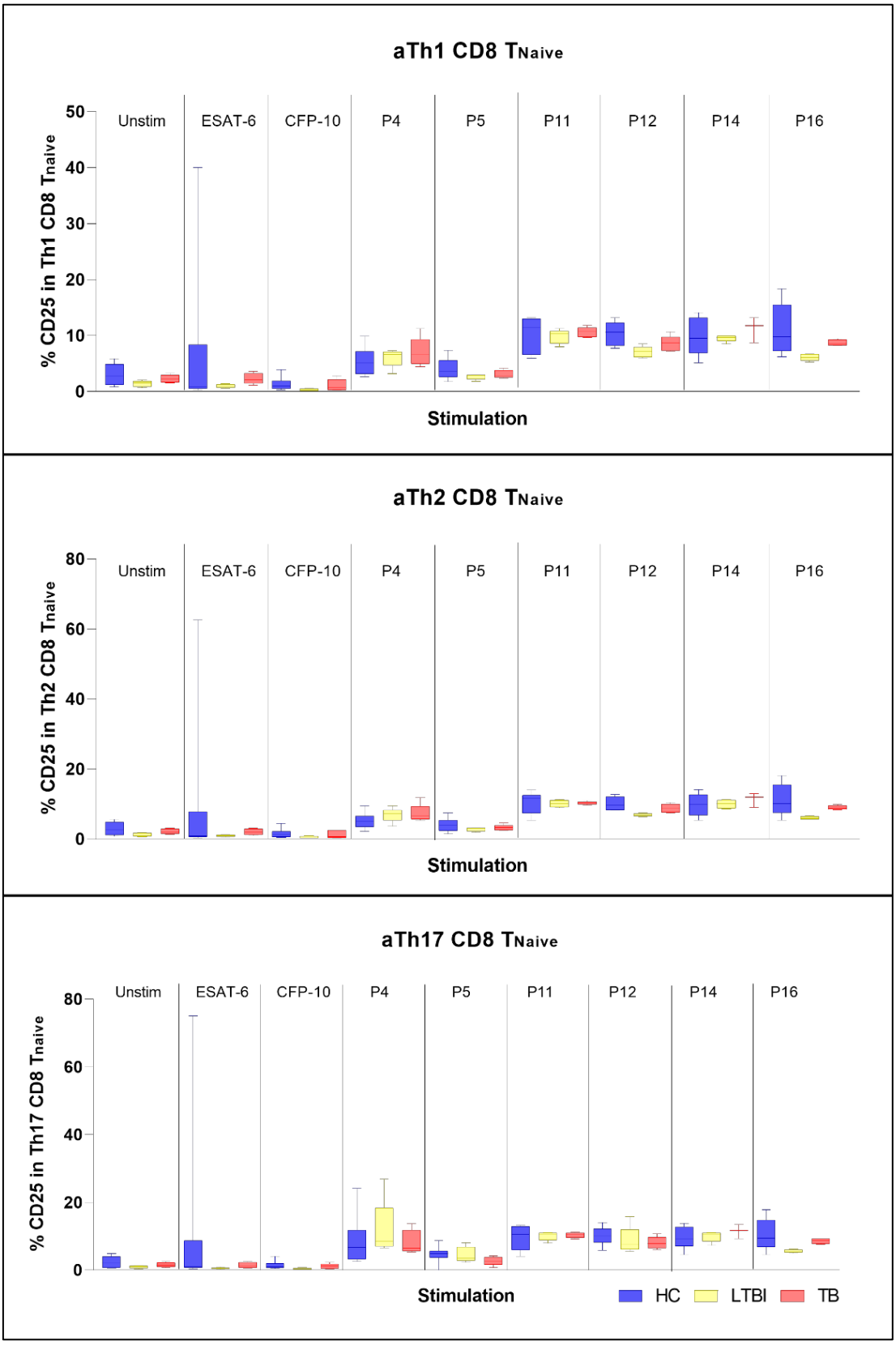

Figure 7.5: Distribution of activated naïve $CD8^+$ T-cells ($CD25^+$) in the peripheral blood of TB, LTBI and healthy individuals. The box-and-whisker plots represent the proportions of activated Th1, Th2 and Th17 T_N $CD8^+$ T-cell subsets as a mean percentage of the total Th1, Th2 or Th17 T_N $CD8^+$ T-cell populations. Blue = HC = healthy controls (n=11). Yellow = LTBI = latent TB infection (n=5). Red = TB = active TB (n=5). ESAT-6 = Early Secreted Antigen-6. CFP-10 = Culture Filtrate Protein 10. Unstim = Unstimulated (PBS). P4 = Rv0878c_c. P5 = Rv0878c_d. P11 =Rv2356c_a. P12 = Rv2608_a. P14 = Rv2608_c. P16 =Rv2608_g.

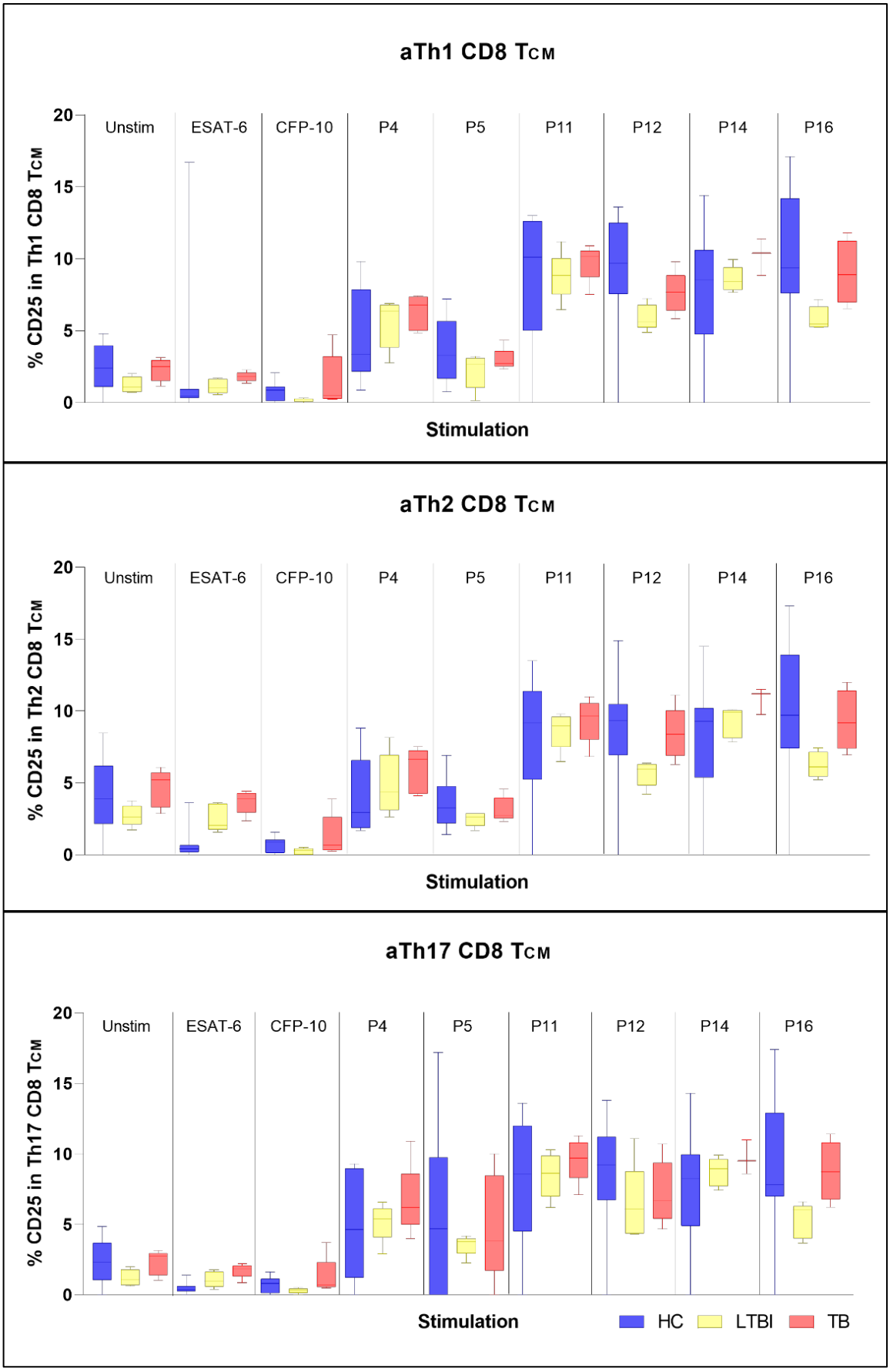

Figure 7.6: Distribution of activated central memory $CD8^+$ T-cells ($CD25^+$) in the peripheral blood of TB, LTBI and healthy individuals. The box-and-whisker plots represent the proportions of activated Th1, Th2 and Th17 T_{CM} $CD8^+$ T-cell subsets as a mean percentage of the total Th1, Th2 or Th17 T_{CM} $CD8^+$ T-cell populations. Blue = HC = healthy controls (n=11). Yellow = LTBI = latent TB infection (n=5). Red = TB = active TB (n=5). ESAT-6 = Early Secreted Antigen-6. CFP-10 = Culture Filtrate Protein 10. Unstim = Unstimulated (PBS). P4 = Rv0878c_c. P5 = Rv0878c_d. P11 =Rv2356c_a. P12 = Rv2608_a. P14 = Rv2608_c. P16 =Rv2608_g.

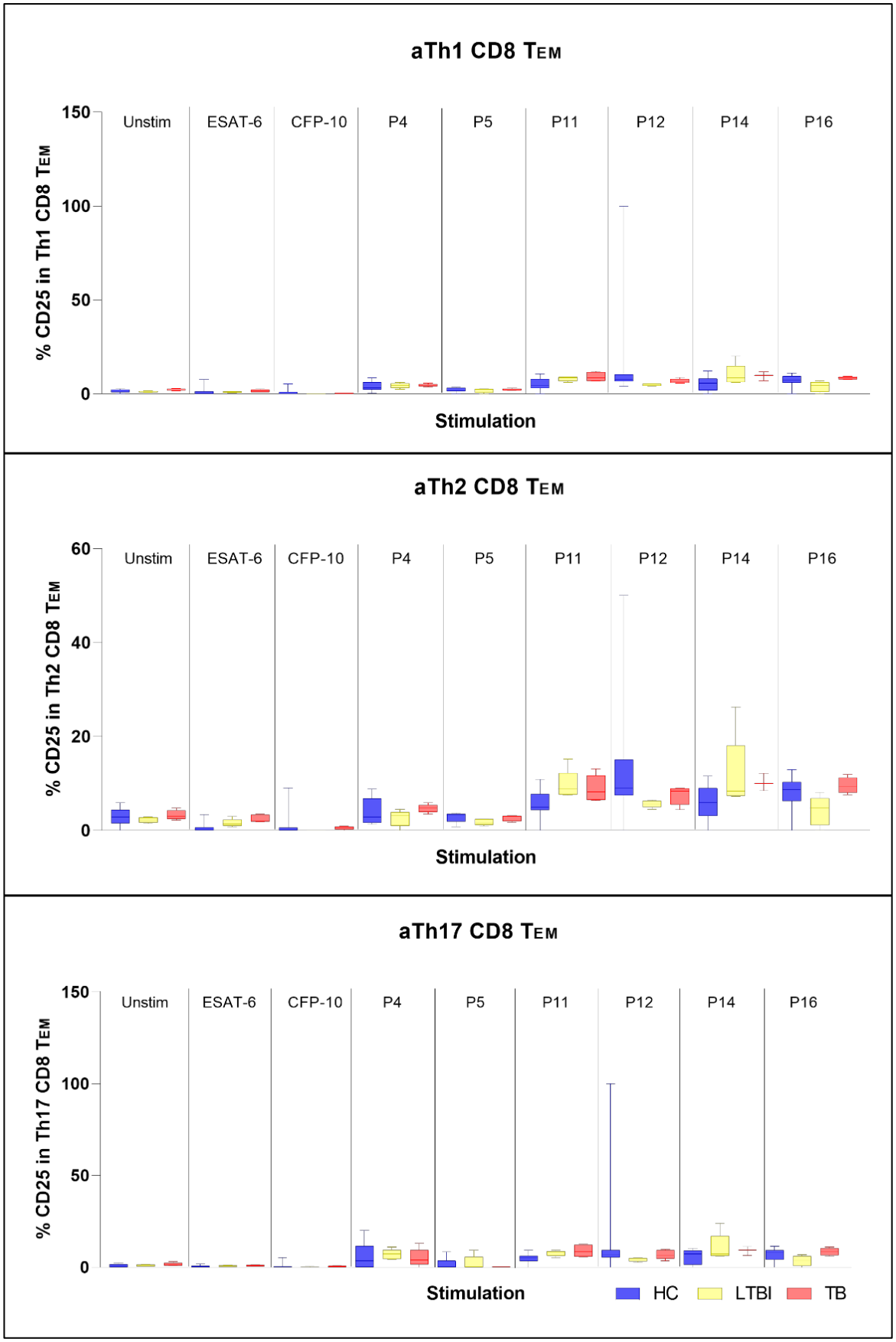

Figure 7.7: Distribution of activated effector memory $CD8^+$ T-cells ($CD25^+$) in the peripheral blood of TB, LTBI and healthy individuals. The box-and-whisker plots represent the proportions of activated Th1, Th2 and Th17 T_{EM} $CD8^+$ T-cell subsets as a mean percentage of the total Th1, Th2 or Th17 T_{EM} $CD8^+$ T-cell populations. Blue = HC = healthy controls (n=11). Yellow = LTBI = latent TB infection (n=5). Red = TB = active TB (n=5). ESAT-6 = Early Secreted Antigen-6. CFP-10 = Culture Filtrate Protein 10. Unstim = Unstimulated (PBS). P4 = Rv0878c_c. P5 = Rv0878c_d. P11 =Rv2356c_a. P12 = Rv2608_a. P14 = Rv2608_c. P16 =Rv2608_g.

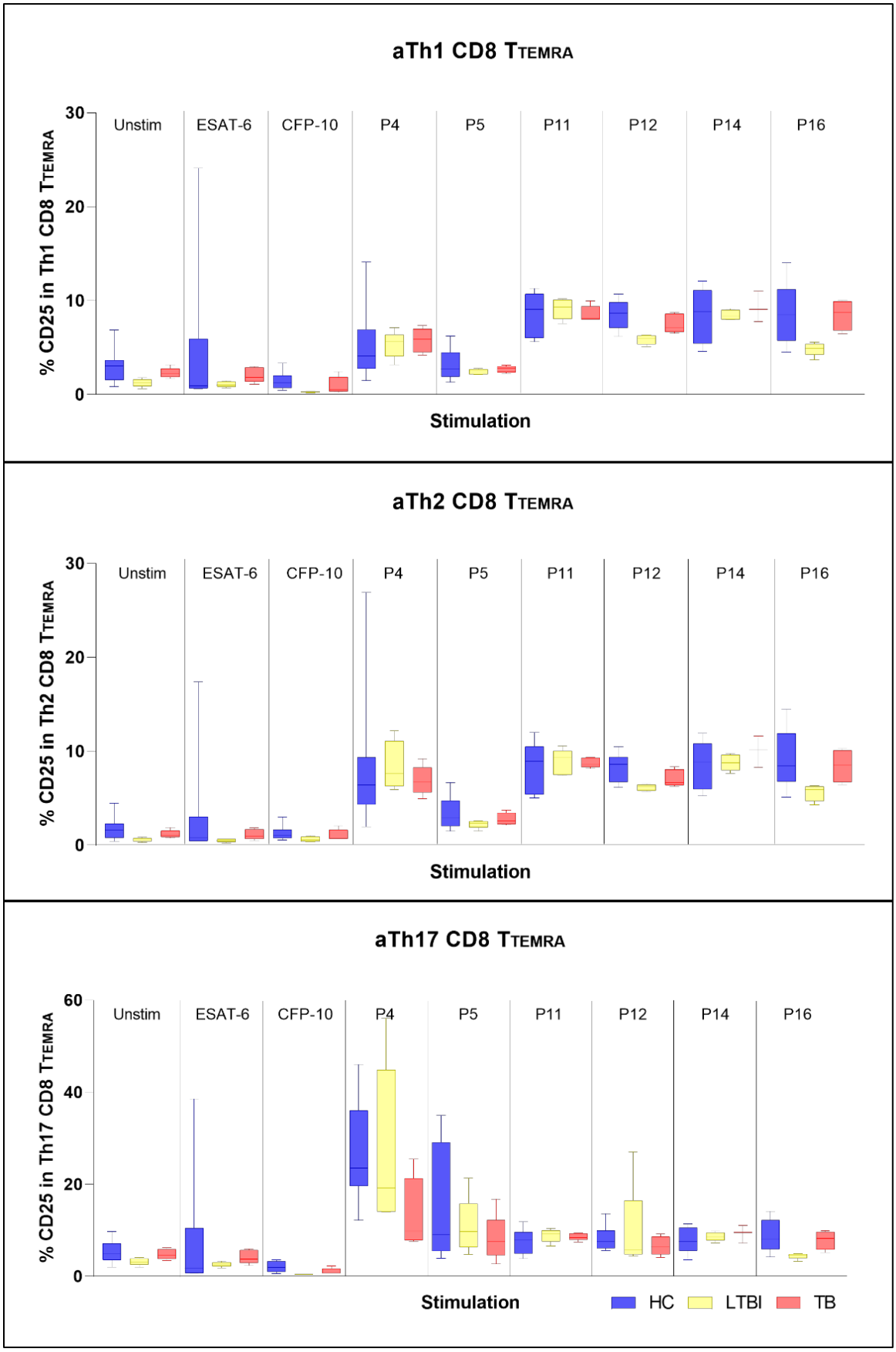

Figure 7.8: Distribution of activated terminally differentiated effector memory $CD8^+$ T-cells ($CD25^+$) in the peripheral blood of TB, LTBI and healthy individuals. The box-and-whisker plots represent the proportions of activated Th1, Th2 and Th17 T_{TEMRA} $CD8^+$ T-cell subsets as a mean percentage of the total Th1, Th2 or Th17 T_{TEMRA} $CD8^+$ T-cell populations. Blue = HC = healthy controls (n=11). Yellow = LTBI = latent TB infection (n=5). Red = TB = active TB (n=5). ESAT-6 = Early Secreted Antigen-6. CFP-10 = Culture Filtrate Protein 10. Unstim = Unstimulated (PBS). P4 = Rv0878c_c. P5 = Rv0878c_d. P11 =Rv2356c_a. P12 = Rv2608_a. P14 = Rv2608_c. P16 =Rv2608_g.